Studying the Links Between the Loss of POU4F2/BRN-3B and Inflammatory Changes that Contribute to Cardiovascular Disease

Norfazlina Mohd Nawi

Molecular Biology Development and Disease (MBDD)

Institute of Cardiovascular Science (ICS)

Faculty of Population Health

University College London

This dissertation is submitted for the degree of Doctor of Philosophy

February 2025

DECLARATION

I, Norfazlina Mohd Nawi, confirm that the work presented in this thesis is my own. Where information has been derived from other sources, I confirm that this has been indicated in the thesis.

Norfazlina Mohd Nawi

Sunday, 23 February 2025

ABSTRACT

Chronic diseases such as cardiovascular disease (CVD) and Type 2 Diabetes Mellitus (T2DM) are intricately linked to inflammatory responses, with gene expression changes governed by transcription factors playing a crucial role. This thesis delves into the potential association between the Brn-3b transcription factor and inflammatory response, and its possible link to vascular dysfunction. Initial investigations utilizing human THP-1 and Jurkat cells unveiled an upregulation of Brn-3b protein post-vitamin D3 treatment in THP-1 cells and in PMA+IL4 differentiated THP-1 cells, contrasting with non-significant changes in activated and non-activated human Jurkat cells. Employing a Brn-3b knock-out (Brn-3b KO) mouse model, I observed that the cellular immune cell profile, specifically CD44- immune-related cells in T and non-T cell lineages including monocytes, B lymphocytes, and granulocytes in Brn-3b KO bone marrow and blood, did not significantly change compared to wild-type (WT) controls. Furthermore, I explored the inflammatory status of the Brn-3b KO mouse model by analysing soluble protein mediators in bone marrow conditional medium and blood plasma. The data showed no significant alteration of protein biomarkers tumor necrosis factor alpha (TNFα), IL-1β, and IL-6 in bone marrow supernatant, while interestingly, IL-1β was significantly reduced in Brn-3b KO blood plasma, but not TNFα and IL-6. In the final chapter, I investigated the potential link between immune response and alterations in vascular proteins in the aorta of Brn-3b KO mice. The analysis showed no significant changes in immune markers (CD3, CD45R/B220, CD11b, CD44) or vascular proteins (alpha smooth muscle actin (αSMA), smooth muscle protein 22 (SM22)) and proliferative marker Ki67 in Brn-3b KO samples. An additional work on spleen also showed these immune markers CD3, CD4, CD8, CD44, CD11b, B220 and Thy-1 in Brn-3b KO mice mirrored those in WT controls. Overall, the findings suggest that the loss of Brn-3b may not substantially impact immune regulatory responses in bone marrow, blood, aorta, and spleen tissue of the Brn-3b KO mouse model.

KEYWORDS: T2DM, CVD, Transcription Factors, Brn-3b, Inflammation, Vascular Dysfunction, Bone Marrow (BM)

IMPACT STATEMENT

The research presented in my thesis, *"Studying the Links Between Loss of POU4F2/Brn-3b and Inflammatory Changes that Contribute to Cardiovascular Disease,"* offers insights into how the Brn-3b transcription factor may influence vascular function independently of immune-related inflammation. While not all of my findings reached statistical significance, this work nonetheless opens up questions about the role of Brn-3b in maintaining vascular integrity. The broader relevance of these findings, both within academia and beyond, lies in exploring alternative mechanisms of vascular disease development that do not rely solely on inflammatory pathways.

Academic Impact

Within academic research, the thesis contributes to the understanding of non-inflammatory mechanisms in vascular dysfunction, particularly by investigating how Brn-3b affects the expression of vascular proteins such as SM22+CD44, SM22+αSMA, and Ki67. Though the data did not conclusively establish the full scope of Brn-3b's role, the study provides a foundation for further research to explore transcriptional regulation in cardiovascular health. Future researchers may build on these preliminary findings to refine our understanding of Brn-3b's function and potentially investigate its effects in other tissues or disease models. The methodologies employed, including deep immunophenotyping and vascular protein analysis, could also inform future studies in related fields. These approaches can contribute to a more nuanced understanding of the interactions between transcription factors and vascular biology, potentially influencing future research methods or coursework in cardiovascular biology and molecular medicine.

Impact Outside Academia

While my research highlights the potential of Brn-3b as a target for therapeutic intervention, more extensive studies are needed before concreting clinical applications can be established. If validated through further work, targeting Brn-3b could offer a new therapeutic approach for managing vascular dysfunction in patients who do not respond to anti-inflammatory treatments. However, at this

stage, the translational impact remains speculative, requiring additional research to confirm its clinical relevance. In terms of public health and therapeutic development, this work underscores the importance of investigating non-inflammatory pathways in cardiovascular diseases. If future research builds on these findings, there could be gradual changes in how we approach disease prevention and treatment strategies. By providing a different perspective on disease mechanisms, this study may contribute to broader public health discussions on cardiovascular risk factors.

Broader Impacts and Dissemination

The insights gained from this research, while not fully conclusive, offer a starting point for further exploration in the field. Disseminating these findings through academic journals, scientific conferences, and collaborative discussions with clinical researchers can facilitate dialogue on how transcription factors like Brn-3b might influence vascular biology. Over time, this may contribute to shaping research directions, particularly as new data becomes available. Overall, while the results of my thesis did not lead to definitive conclusions, they raise important questions about non-inflammatory drivers of vascular dysfunction. The incremental impact of this work may emerge as part of a broader research effort, helping to inform both future academic inquiries and potential clinical applications down the line.

ACKNOWLEDGEMENTS

First and foremost, I would like to express my deepest gratitude to my supervisors, Professor Derek Gilroy, Dr Reddy Venkat, and Professor Andrew Cook, for their unwavering support, guidance, and encouragement throughout this journey. Your insights and expertise have been invaluable, and I am incredibly fortunate to have had the opportunity to work under your mentorship. Thank you for continually providing me with moral support, especially during the times when I felt like giving up. Your encouragement kept me going. I am particularly grateful to have learned such good science from Professor Derek Gilroy and Dr Reddy Venkat, whose knowledge and passion for research have deeply inspired me. I would also like to thank my supervisor, Professor Shanie Budhram Mahadeo, for teaching me to express my feelings and to distinguish the good from the bad, not only in science but also in life. You have helped shape me into a stronger person.

To my family, especially my mom, thank you for constantly asking when I would finish my PhD. Your daily questions motivated me to finally reach the end of this journey. Your endless love, encouragement, and patience were my greatest source of strength, even when I doubted myself. I am forever grateful for the sacrifices you've made to support my education and dreams. To my late father, Mohd Nawi Ibrahim, thank you for raising me and being a strong figure in my life. I will carry your name in all of my research publications, ensuring that people will know you even though you are no longer here. Thank you to my siblings, Mohd Irwan, Noor Baizura, Norliana, and Mohd Shahmi, and to all my nieces and nephews for always praying for my success.

A special thanks to my dear friend Fatimah Zachariah Ali, who kept pushing me to meet deadlines. Thank you for being such a good partner, listening to my struggles both mentally and physically. Without you, I would not have completed my PhD. You are the main person that helped me throughout this journey, after my supervisors, and I am forever grateful for your unwavering belief in me. In terms of science, thank you for asking me the "weird" questions that made me think deeper—without your genius questions, I would never have challenged myself in the same way. A heartfelt thank you to Dr Sofea Aljffri, Naqibah Rais,

Nuraisha Azmi, and Dr Nuraini Daud, for always reminding me not to give up and reassuring me that I would make it through.

Thank you, Dr Premkamon Chaipanichkul, for always arguing about science with me. After my supervisors, you were the friend who challenged my scientific knowledge the most. I would also like to extend my thanks to Tan Xu, for being such a good supporter and even a fortune teller for my future. Your presence in my life has been invaluable.

A special thank you goes to my lab members, Vaishali Yogendran, Dr Laura Mele, and Dr Parisa Samangouei, for the stimulating discussions, troubleshooting assistance, and camaraderie that made the challenging days easier. Your friendship and support have made this journey more fulfilling, and I am grateful for the countless ways you've contributed, both scientifically and personally. To my friend Chloe, thank you so much for checking in on me every day—it kept me going through this challenging journey.

To the most important person in this journey, Jaquie Mitchell, thank you for saving me from the hardships I faced during my PhD. I am also deeply grateful to Dr Jigisha Patel, for always being there for me and being one of my biggest supporters throughout this journey.

To my friends Nada Alhindi, Nada Mabrouk, Huda Alnufei, and Milena Ribera, thank you for being with me throughout this journey. I would also like to thank Mek Kelate London for successfully supporting me financially during this process.

Lastly, I would like to acknowledge the funding agencies and institutions that made this research possible, including MARA, for their financial support and resources, without which this work could not have been completed.

This thesis represents the culmination of years of hard work, and it would not have been possible without the support, guidance, and encouragement of all those mentioned above. Thank you.

CONTENTS

LIST OF TABLES

LIST OF FIGURES

List of Abbreviations and Acronyms

αSMA – α-smooth muscle actin

ACK – Ammonium-chloride-potassium

AGE – Advanced glycation end-product

AngII – Angiotensin-II

AP1 – Activator protein 1

APC – Antigen presenting cell

BCL2 – B-cell lymphoma 2

BCR – B cell receptor

BCZ – B cell zone

BM – Bone marrow

CCL – Chemokine ligand

CCR – C-C chemokine receptor

CD –Cell differentiation

CLP – Common lymphoid progenitor

CNN1 – Calponin 1

CMP – Common myeloid progenitor

CTLs – Cytotoxic T lymphocytes

CVD – Cardiovascular disease

CXCR – C-X-C chemokine receptor

DBD – DNA binding domain

DC – Dendritic cell

DLEU2 - Deleted in Lymphocytic Leukaemia 2 (DLEU2)

DN – Double negative

DP – Double positive

DZ – Dark zone

ETP – Early T cell progenitor

EC – Endothelium cells

ECM – Extracellular matrix

ER – Endoplasmic reticulum

ERK – Extracellular signal-regulated kinase

eNOS – Endothelial nitric oxide synthase

FACS – Flow cytometry staining

FBS – Foetal bovine serum

FMO – Fluorescence minus one

FSC – Forward scatter

GC – Germinal center

GLUT 4 – Glucose transporter type 4

GM-CSF – Granulocytes-macrophages colony-stimulating factor

GMP – Granulocyte-macrophage progenitor

GPx – Glutathione peroxidases

Grx – Glutaredoxin

GSKβ – Glycogen synthase kinase-beta

H&E – Haemoxylin and eosin

HDL – High density lipoprotein

HFSD – High in fat and sugar

HSC – Hematopoietic stem cell

HSP 27 – Heat shock protein 27

ICAM – Intercellular adhesion molecule

IFNγ – Interferon-gamma

IKKβ – Inhibitory kappa kinase beta

IL – Interleukin

ILC – Innate lymphoid cells

Iono – Ionomycin

IRS1 – Insulin receptor substrate 1

JAKS – Janus kinases

JNK – Jun N-terminal kinase

JNK/SPK - Jun amino-terminal kinase/stress-activated protein kinases

Ki-67 – Antigen kiel 67

KO – Knock-out

LDL – Low-density lipoprotein

LDL-R – Low-density lipoprotein receptor

LNs – Lymph nodes

LPS – Lipopolysaccharide

LSK – Lin-Sca1+cKIT+

LZ – Light zone

mAb – Mouse antibody

MAPK – Mitogen-activated protein kinase

MCP-1 – Monocyte chemotactic protein-1

MDSC – Myeloid-derived suppressor cells

MIP-1 alpha – Macrophage inflammatory protein-1 α

miR-214 – microRNA-214

MMPs – Metalloproteinases

MHC – Myosin heavy chain

MHC – Major histocompatibility complex

MPP – Multipotent progenitor

MSC – Mesenchymal stem cell

MTT – 3-(4,5-Dimethylthiazol-2-yl)-2,5-diphenyltetrazolium bromide

MZ – Marginal zone

MZB – Marginal zone B cell

NADPH – Nicotinamide adenine dinucleotide phosphate

NFAT – Nuclear factor of activated T cells

NK – Natural killer cell

NO – Nitric oxide

NFκB – Nuclear factor kappa B

NVRM – Neonatal rat ventricular myocytes

OD – Optical density

OPG – Osteoprotegerin

OVA – Ovalbumin

oxLDL – oxidised low-density lipoprotein

PBMC – Peripheral blood mononuclear cell

PBS – Phosphate-buffered saline

PCNA – Proliferating cell nuclear antigen

PCR – Polymerase chain reaction

Pim1 – Serine/threonine-protein kinase 1

PMA – Phorbol 12-myristate 13-acetate

PRR – Pattern recognition receptors

PVAT – Perivascular adipose tissue

RA – Rheumatoid arthritis

RBC – Red blood cell

RhoA – Ras homolog family member A

RT – Room temperature

ROI – Region of interest

ROS – Reactive oxygen species

RP – Red pulp

rRNA – ribosomal RNA

S – Short

SLE – Systemic lupus erythematosus

SP – Single positive

SP4 – Single positive CD4

SP8 – Single positive CD8

SM22 – Smooth muscle protein 22

Smad – Mothers against decapentaplegic homolog 3

SSC – Side scatter

STAT - Signal transducer and activator of transcription

T2DM – Type 2 diabetes mellitus

TA – Tunica adventitia

TCR – T cell receptor

TCZ – T cell zone

TEC – Thymic epithelial cells

Tfh – T follicle Helper

TGFβ – Transforming growth factor beta

Th – T helper

TI – Tunica intima

TM – Tunica media

TNF-α –Tumor necrosis factor-α

Treg – Regulatory T cells

tRNA – transfer RNA

UC – Untreated control

VCAM - Vascular cell adhesion molecule

VDR – Vitamin D receptor

VITD3 – Vitamin D3

VSMC – Vascular smooth muscle cells

WBC – White blood cells

WT – Wild-type

WP – White pulp

XO – Xanthine oxidase

LIST OF APPENDICES

1 INTRODUCTION

1.1 Cardiovascular disease (CVD)

Cardiovascular disease (CVD) remains a major health problem with high mortality rates (Azuaje *et al.,* 2011). Although there have been some reductions from 1990 to 2013 in the United Kingdom (UK), it remains the second main cause of death in 2014 and is estimated to further increase in the future (Bhatnagar *et al.,* 2016; Kelly & Fuster., 2010). According to the World Health Organization (WHO), an estimated 17.9 million people died from CVDs in 2019, accounting for 32% of all global deaths. Of these fatalities, 85% were due to heart attack and stroke. CVD encompasses a group of disorders affecting the heart and blood vessels, including coronary heart disease, cerebrovascular disease, rheumatic heart disease, congenital heart disease, peripheral arterial disease, deep vein thrombosis and pulmonary embolism. It is a chronic disease that develops over a prolonged period, adversely affecting general health such as fatigue, physical and mental distress and significantly deteriorating quality of life (Grover and Joshi, 2015; Newland et al, 2017; Adam et al., 2020). The pathogenesis of CVD is intricate, involving a multifaceted interplay of genetic, environmental, and lifestyle factors (WHO, 2021).

The mechanisms underlying CVD are complex, involving the deterioration of the vasculature construction that compromises the integrity and structure of the vascular wall. The precise gene expression and cellular signalling are required to meticulously orchestrate vascular wall components including smooth muscle

cells (SMC), endothelial cells (EC) and fibroblast, extracellular matrix (ECM) and lamella, to protect the morphology and homeostasis of the blood vessel, as illustrated in Figure 1 (Mazurek et al., 2017).

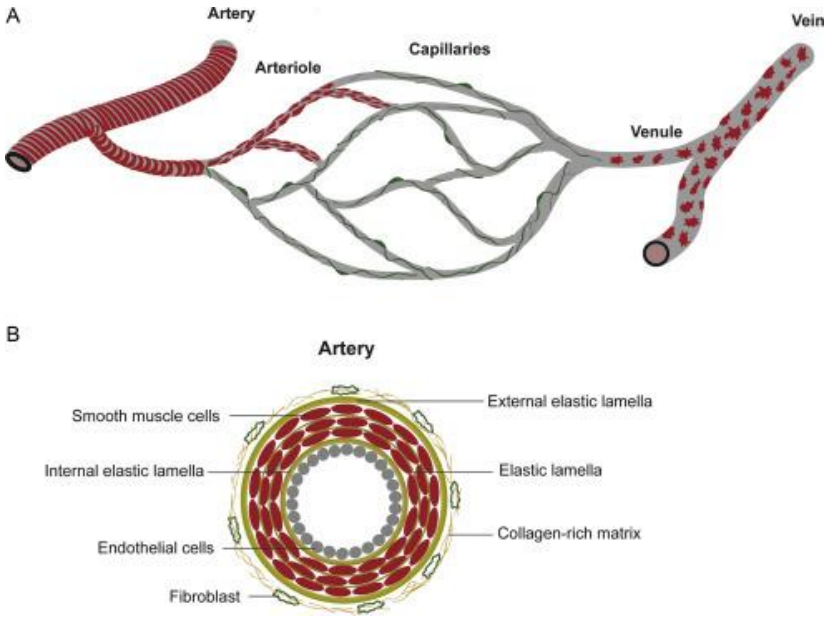

Figure 1: Structural components and functional homeostasis of the vascular wall. The vascular walls comprise various vascular components including smooth muscle cell (SMC), endothelial cell (EC), fibroblast, extracellular matrix (ECM) and lamella. The strong link of these components is required to protect the blood vessel integrity and functionality (Mazurek et al., 2017).

Changes in the signalling pathways in blood vessel components such as vascular ECs and vascular smooth muscle cells (VSMCs) are key mechanisms which cause vascular dysfunction and promote the progression of CVD (Ma et al., 2023). Specifically, the most well-known vascular dysfunction in the blood vessels is arteriosclerosis and atherosclerosis which cause hypertension that can lead to hypertrophy and heart failure (Park and Avolio, 2023); or atherosclerosis in the coronary vasculature that contributes to injury e.g. myocardial infarction (Palasubraniam et al., 2019). Atherosclerosis is also known as a primary cause of aneurysms and aortic dissection that develops the false lumen in the blood vessel wall (Ashley and Niebauer, 2004).

Arteriosclerosis is a Greek origin term that brings the meaning “hardening of the arteries’’ means the arteries thicken and lose flexibility (Fishbein and Fishbein,

2009). Atherosclerosis is not the same as it develops from fatty plaque buildup, however, it is a common type of arteriosclerosis. Atherosclerosis is a classic inflammatory disease that involves T cells and macrophages, smooth SMC highly proliferate and migrate, and the ECs are highly damaged. In contradiction, arteriosclerotic disease mainly involves SMCs, whereas immune cells seem to play a minor role. Calcification of vascular cells could be observed in atherosclerotic and arteriosclerotic disease at the end stage of both entities, however, in atherosclerosis it is found in the intima, whereas in arteriosclerosis, the calcification is in the media of the vessel wall (Tolle *et al*., 2015). Thus, atherosclerosis and arteriosclerosis are diagnostically different processes that often coexist, share common risk factors and are independently correlated with increased CVD risk (Figure 2).

ATHERO 	Modifications	 ARTERIO
	LOCALIZATION	
+++ +	Intimal Medial	(+) +++
	CELLS	
+++ +++ +++ +++ ++	VSMC EC Platelets Monocytes/macrophages Lymphocytes	+++ (+) (+) (+) (+)
	EXTRACELLULAR MATRIX	
+++ +	Collagen Elastin	+ ++
	MINERALIZATION	
++ +	Intimal Medial	(+) +++
	INFLAMMATION	
+/++ +++	Innate Acquired	(+) (+)

Figure 2: Comparative pathophysiology of atherosclerosis and arteriosclerosis in vascular dysfunction. Different pathophysiologies of atherosclerosis and arteriosclerosis within the vascular wall contribute to vascular dysfunction. The '+'assesses the role: +++ high impact, ++ moderate impact, + low impact, (+) unknown impact (Tolle et al., 2015).

The key mechanisms underlying arteriosclerosis and atherosclerosis that contribute to CVD involve complex structural, cellular and mechanical changes. The process begins with endothelial dysfunction, where damage to the ECs due to factors like hypertension, oxidative stress, and inflammation leads to increased

lipid permeability, immune cell infiltration such as monocytes, macrophages and T lymphocytes and reduced nitric oxide (NO) bioavailability (Egashira, 2002). This dysfunction changes VSMC phenotype by facilitating the migration and proliferation of VSMCs, driven by growth factors such as platelet-derived growth factor (PDGF) and transforming growth factor (TGFβ) and cytokines such as tumour necrosis factor alpha (TNFα), interleukin 1 (IL-1) and IL-4. PDGF regulates microRNA-214 (miR-214) and serine/threonine-protein kinase 1 (Pim-1), inducing mesenchymal-like traits that enhance mobility and invasiveness, while activating extracellular signal-regulated kinase 1/2 (ERK1/2) and Jun N-terminal kinase (JNK) pathways to promote growth by increasing Deleted in Lymphocytic Leukaemia 2 (DLEU2) and proliferating cell nuclear antigen (PCNA) expression and downregulating α-smooth muscle actin (α-SMA) and Calponin 1 (CNN1). TGF-β modulates VSMC phenotypic changes through mothers against decapentaplegic homolog 3 (Smad) signalling, promoting the expression of contractile genes. Meanwhile, TNF-α released from damaged endothelial cells drives VSMC proliferation and migration via the Akt/ activator protein 1 (Akt/AP-1) and Ras homolog family member A (RhoA) pathways (Xin et al., 2024).

Concurrently, these VSMCs produce ECM components, including collagen, elastin and glycosaminoglycans contributing to the thickening of the arterial wall. The ECM remodelling is regulated by matrix metalloproteinases (MMPs) such as MMP-2, MMP-9 and membrane-type MMP, maintaining a balance between matrix deposition and degradation. Upregulation of MMP-2 production and induction of other gelatinase, MMP-9, occur rapidly following mechanical injury (Rudijanto, 2007).

In addition to these changes, calcification occurs within the arterial wall, where calcium salts deposit in the media, intima or other site of the wall leading to increased stiffness and reduced arterial compliance. In the tunica media (TM), loss of elastin is coupled with medial calcification, and the degradation of elastin is believed to further contribute to the osteogenic process in aortic tissue. SMCs differentiate into osteoblast-like cells in media where it is like bone formation, and it is related to genes such as BMP2, msh homeobox 2 (MSX2), and alkaline phosphatase (ALP). On the other side of the wall, which is intima, calcification is closely associated with lipid deposits, and the clinically related to infiltration of inflammatory cells, with disruptive arterial disease, whereas in the end is more

obvious by transformation into osteoblast-like cells from SMCs (Lee et al., 2020). Collectively, these mechanisms underscore the pathophysiological basis of arteriosclerosis and atherosclerosis, however, atherosclerosis is distinct by forming the plaque on the intimal wall due to lipid deposition, foam cells and apoptotic body and arteriosclerosis is more toward the stiffness of the wall due to the calcification in the media (Tolle et al., 2015).

These mechanisms cause changes in blood vessel structure and function that directly or indirectly affect cardiac function, due to abnormal pressure of vascular blood. Thus, controlling the blood vessel's health is the main strategy to prevent the lateral pressure exerted on the walls of blood vessels per unit area during the flow of blood, which also represent a crucial global public health strategy in the effort to reduce premature mortality from CVDs (Ma et al., 2023).

1.1.1 The interplay of immune mechanism in CVD

Plaque formation and the arterial stiffening process in the two main features of vascular dysfunctional; Arteriosclerosis and atherosclerosis are both closely linked to inflammation (Goncalves et al., 2024). In the vessel wall, the intima and adventitia are normally involved in the disease process, with luminal and microvascular ECs performing a critical role in the recruitment and activation of leukocytes (Tellides and Pober, 2015). The dysfunction of ECs causes dysregulation of immune cells and increased secretion of inflammatory cytokines (Dal et al., 2019; Rengarajan et al., 2024). In the TM, the VSMCs are capable of inducing robust proinflammatory cytokines such as IL-1, IL-6, chemokine ligand 2 (CCL2), and CCL10 in response to various cues including hypertension, microbial infection, sentinel resident leukocytes or infiltrates of innate immunocytes (Tellides and Pober, 2015). Collectively, the vascular dysfunction due to the build-up of plaque and increased vessel stiffness is fundamentally involved in complex cellular crosstalk between VSMCs, EC and immune cells, such as macrophages (Mϕs) and T cells which promote vascular inflammation (Wiejak et al., 2023).

In addition, atherosclerosis, ischemic/hypoxic injury, and chronic stress are interconnected in the development of CVD. Dysregulation of immune cells, such as monocytes, dendritic cells (DCs), and T cells, within plaques plays a critical role in the development of ischemic injury or myocardial infarction, which occurs

due to stenosis or plaque rupture, ultimately reducing myocardial blood flow or oxygen supply (Zhao et al., 2023). Chronic stress compounds these conditions by promoting systemic inflammation and increasing blood pressure, which accelerates atherosclerosis and makes blood vessels more prone to injury. Stress further exacerbates ischemic injury by worsening endothelial dysfunction and increasing the risk of plaque rupture (Yao et al., 2019). These three factors, atherosclerosis, ischemic injury, and chronic stress create a vicious cycle, where each condition exacerbates the others, contributing to vascular and cardiac dysfunction.

Innate and adaptive immune response has been piloted as the pathological feature of arteriosclerosis/atherosclerosis. It is evidenced by the high accumulation of inflammatory cells within the plaque tissue and the association with increased plasma levels of inflammatory markers. This inflammatory onset is mostly due to modified lipids (Goncalves et al., 2024).

The general information on the immune cells phenotypes and their response in the innate and adaptive immune systems are collectively compiled and elaborated in the next section.

1.1.1.1 Innate and adaptive immune systems

The immune system consists of two elementary lines of defence which are innate and adaptive immunity. Innate and adaptive immune response are two branches of the immune system that are critical for the beginning and progression of chronic inflammatory diseases, including atherosclerosis (Sun et al., 2020). Innate immunity is the rapid, first-line defense against pathogens such as bacteria, fungi, parasites, viruses, cancer cells, and toxins. It involves immune cells, including phagocytes (macrophages and neutrophils) and DCs, which respond through mechanisms like phagocytosis, cytokine release, and antigen-independent recognition, within minutes to hours after exposure (Marshall et al., 2018). On the other hand, the adaptive immune response is antigen-dependent and antigen-specific, with a slower initial reaction but a strong memory capacity. This enables the host to mount a more rapid and efficient immune response through T and B cells after exposure to an antigen. The response involves mechanisms such as cytokine release by T cells and antibody production by B cells, as described in Table 1. leThere is a great relationship between innate and

adaptive immune systems, where they can be mirror to each other, however its defects can provoke illness or disease, such as inappropriate inflammation, autoimmune diseases, immunodeficiency disorders and hypersensitivity reactions (Marshall et al., 2018).

In the innate and adaptive immune systems, the response was driven by different types of immune cellular phenotypes. These immune cells were phenotypically characterised based on the cellular markers known as cell differentiated (CD) markers as elaborated in Table 1. In response to intruder/cue, the Innate and adaptive immune systems initiate the local inflammation and immune cell recruitment by producing cytokines such as IL-1, IL-6, TNFα, IL-4 and C-X-C chemokine receptors such as CXCR2, CXCR10. Through cytokines and chemokines, different cell phenotypes can communicate between cells (Marshall et al., 2018). In the immunity response, cytokines may act on the cells that secrete them which is called autocrine action, on nearby cells known as paracrine action, or in some instances on distant cells known as endocrine action. The recruited cells either cause/enhance the inflammation where it's induced by pro-inflammatory cytokines or resolves the inflammation where it is activated by anti-inflammatory cytokines (Zhang and An, 2007).

Typically, in acute inflammatory responses, cellular and molecular events interact effectively to minimize impending injury or infection.

This improvement process contributes to repairing the tissue and resolving the acute inflammation. However, uncontrolled acute inflammation may become chronic, leading to a variety of chronic inflammatory diseases such as cardiovascular and bowel diseases, diabetes, arthritis, and cancer (Chen et al., 2018). In these inflammatory responses, pro-and anti-inflammatory mechanisms are involved for maintaining homeostasis and the health of disease. The detail function of the pro and anti-inflammatory mechanisms in maintaining the haemodynamic of the tissue/organ, especially the vascular system was elaborated further in the next section.

Table 1: Markers and immunological stimuli of the innate and adaptive immune system. Summary of characterisation markers and immunology stimuli induced/secreted by macrophages and lymphocytes cells in the innate and adaptive immune system (Nagasawa, 2006; Jenkins et al., 2011; Aristizabal and Gonzalez, 2013; Ying et al., 2013; Zhou et al., 2017; Wager and Wormley, (2014); Yang et al., 2014; Moganti et al., 2017; Zhu and Zhu, 2020).

Inflammatory Immune Response					
Innate			Adaptive		
Host First Line Defence			Take over after Innate Immune Response		
Non-specific mechanism			Specific mechanism		
Fast reaction (minutes to hours)			Slow reaction (days to weeks)		
Immune cells	Markers	Inflammatory Cytokines	Immune cells	Markers	Inflammatory Cytokines
Monocytes	Mouse LY6C^{+}	TNFα, IL-1, IFNγ - matured into M1 macrophages	Lymphocytes	Naïve T-cells	IFNγ, IL-4, IL-1β, IL-2, IL6, IL-12. IL21, IL-23, TGFβ (Mature into B cell, T helper 1, T helper 2 and T helper 17, T reg)
	LY6C^{-}	IL-10, IL-4, IL-13 - matured into M2 macrophages		CD4, CD8	IFNγ (Mature into T helper 1)
	Human CD14^{++} CD16^{+}	IL-1 and TNFα - matured into M1 macrophages		B cells B220	
	CD14^{++} CD16^{-}	IL-10 - matured into M2 macrophages		T reg FOXP3, CD25	
Macrophages	non-specific macrophages - CD11b			T Helper 1 (T h1) T bet	IL-1β, IL-6, IFNγ (Pro-Inflammatory)
	M1 Macrophages - CD68 - CD80 - CD86	IFNγ, IL-1, IL6, TNFα, IL12, CXCL9, CXCL10, CXCL11 (Activates T helper 1, CD8 T-cells)		T Helper 2 (T h2) GATA3	IL-4 (Anti-Inflammatory)
	M2 Macrophages - CD163 - CD206	IL-4, IL-10, IL-13, CCL18, IL1Rα (Activates T-helper 2 cells)		T Helper 17 (T h17) RORγt	IL-21, IL-23

1.1.1.1.1 Pro and anti-inflammatory responses in maintaining vascular homeostasis and their defective effects

In inflammatory diseases such as autoimmune disease, diabetes mellitus, arthritis, cancer and heart disease, the pro and anti-inflammatory effects in both innate and adaptive immune systems determine the occurrence and outcome of inflammation. These pro-inflammatory and anti-inflammatory responses are driven mainly by the monocytes, macrophages and T cells through cytokines as the communication signal (Chen et al., 2018). The specific cytokines and their roles in the pro- and anti-inflammatory responses were described in Table 2.

Their role is primarily to maintain cellular or tissue homeostasis and health, by exerting an appropriate immune activation to challenge malignant/infectious agents and essentially applying mechanisms to resolve the inflammation. Failure to diminish an ‘alert alarm' stimuli or activate an appropriate immune mechanism leads to pathological inflammation and disrupts tissue homeostasis characterised by the progressive development of immune disease features such as fibrosis, cirrhosis, tumour, organ failure and ultimately death (Robinson et al., 2016). This chronic pathological inflammation occurred due to excessive inflammatory cytokine production (Chen et al., 2018).

Table 2: Cytokines involved in inflammatory immune response. The summary of cytokines released by the immune cells that contribute to pro and anti-inflammatory responses (Chen et al., 2018)

Cytokine	Family	Main sources	Function
IL-1β	IL-1	Macrophages, monocytes	Pro-inflammation, proliferation, apoptosis, differentiation
IL-4	IL-4	Th-cells	Anti-inflammation, T-cell and B-cell proliferation, B-cell differentiation
IL-6	IL-6	Macrophages, T-cells, adipocyte	Pro-inflammation, differentiation, cytokine production
IL-8	CXC	Macrophages, epithelial cells, endothelial cells	Pro-inflammation, chemotaxis, angiogenesis
IL-10	IL-10	Monocytes, T-cells, B-cells	Anti-inflammation, inhibition of the pro-inflammatory cytokines
IL-12	IL-12	Dendritic cells, macrophages, neutrophils	Pro-inflammation, cell differentiation, activates NK cell
IL-11	IL-6	Fibroblasts, neurons, epithelial cells	Anti-inflammation, differentiation, induces acute phase protein
TNF-α	TNF	Macrophages, NK cells, CD4+lymphocytes, adipocyte	Pro-inflammation, cytokine production, cell proliferation, apoptosis, anti-infection
IFN-γ	INF	T-cells, NK cells, NKT cells	Pro-inflammation, innate, adaptive immunity anti-viral
GM-CSF	IL-4	T-cells, macrophages, fibroblasts	Pro-inflammation, macrophage activation, increase neutrophil and monocyte function
TGF-β	TGF	Macrophages, T cells	Anti-inflammation, inhibition of pro-inflammatory cytokine production

Inflammation can occur in various tissues and organs that contribute to various diseases. Specifically, focusing on the pathological inflammation in the blood vessel wall, the vascular system is known as a key to the inflammatory response because most of the inflammatory response components circulate through the blood and vessels. The disruption of the immune mechanism to preserve the homeostasis of the vasculature health may affect the normal structure and function of the vessel wall. The main feature of the pathological inflammation in the vasculature system is atherosclerosis/arteriosclerosis which affects the integrity/stiffness of the blood vessel wall and reduces the lumen size by lipid plague that leads to hypertension and eventually causes cardiac failure (Zanoli et al., 2020).

In immune-related pathological conditions of blood vessels, the innate immune system is the first defense activated in response to the inflammatory trigger. Various humoral, physical and mechanical factors are included in the activation of the inflammatory response in the blood vessel shown in Figure 3. The earliest immune mechanism in innate immunity that response to these inflammatory factors involves the increase of endothelial adhesion molecules expression including vascular cell adhesion molecule 3 (VCAM3), intercellular adhesion molecule 1 (ICAM −1), and platelets endothelial cell adhesion molecule 1 (PECAM −1) on the EC surface (Zanoli et al., 2020; Mohmmad et al., 2021). The increased expression of these molecules recruits immune system cells towards ECs.

The Immune cells that are recruited during the innate immune response in the pathological vessel wall such as atherosclerosis including monocytes and macrophages (M1 and M2), neutrophils, mast cells, natural killer (NK) cells and DCs (Mohmmad et al., 2021). These immune cells exert pro and anti-inflammatory cytokines during the pathological condition. Their role in protecting or pro-atherogenic is shown in Table 3.

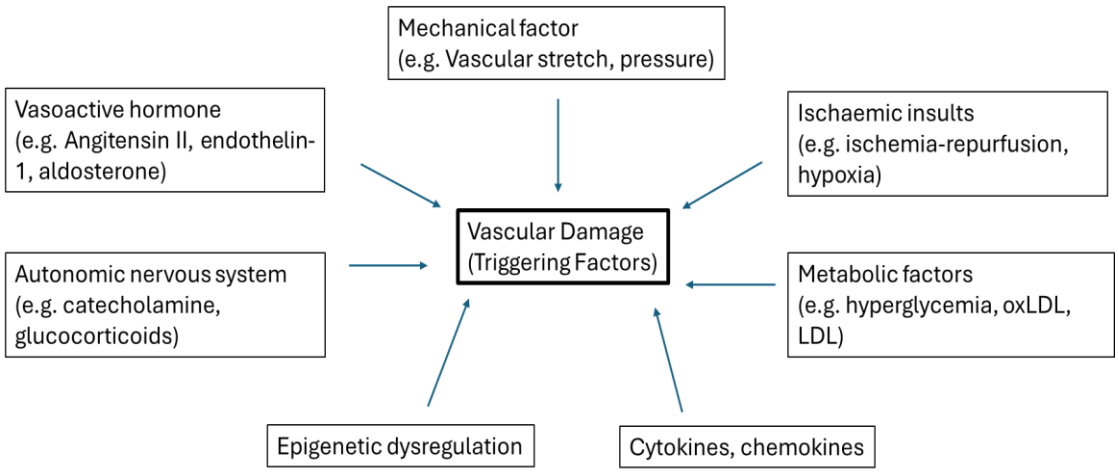

Figure 3: Biological basis and redox biology of inflammation in vascular disease. The humoral, physical and mechanical risk factors trigger inflammatory responses in the blood vessels that lead to vascular damage (Zanoli et al., 2020).

M1 and M2 macrophages are the core of the immune system (Mills, 2015). M1 functions as proinflammatory immune cells or host defence, while M2 functions as immune suppressors (Chen et al., 2023). Activated innate immune cells promote tissue inflammation by secreting pro-inflammatory mediators, such as TNFα, IL-6, and reactive oxygen species (ROS). Alongside or following innate immune responses, infiltration of adaptive immune cells such as T and B cells that regulate antigen-specific immune responses occurred (Miteva et al., 2018). During the inflammation process, T cells differentiate into effector T cells such as T helper 1 (Th1), Th2, Th17 and CD8 T cells that produce pro- or anti-inflammatory cytokine, and B cells differentiate into plasma cells with specific antibody production (Sun et al., 2020; Rizzoni et al., 2022).

In detail mechanism of action, activated Th1 cells secrete interferon-gamma (IFN-γ) promoting atherosclerosis and inflammation as IFN-γ is a major inducer of atherosclerosis development. IFN-γ enhances monocyte infiltration, macrophage activation, foam-cell formation, lesion formation, accumulation of lipids and destabilization of the plaque *via* weakening of endothelial function, lessening of the collagen content and intensification of the inflammatory cell's penetration. While Th2 cells function as athero-protective cells by inhibiting Th1 cells and IFNγ function by secreting IL-4. On the other hand, CD8 T cells act as both athero-protective and pro-atherogenic functions in vascular dysfunctional mechanisms. Moreover, B cells such as B1 cells exhibit athero-protective effects, and B2 cells promote atherosclerosis by secreting inflammatory cytokines, which

consequently trigger Th1 cells and monocyte/macrophage activation (Miteva et al., 2018).

The end -outcome of the vascular dysfunctional (e.g. coronary artery disease) due to the obstructive of innate and adaptive immune response cause the hypertension due to obstruction of blood flow. This obstacle then causes complications to the heart (e.g. cardiac infarction, left ventricular hypertrophy) as the obstruction of blood flow leads to an insufficient supply of the nutrient of oxygen to the cardiac cells. In the long run, the heart can no longer withstand the persistent hemodynamic stress which leads to heart failure. Vascular dysfunction especially atherosclerosis extremely impacts the regular heart function, nominate it as the main cause of cardiovascular diseases (Masenga and Kirabo, 2023).

Table 3: Immune cells' roles during the innate immune response in atherosclerosis of blood vessels. The immune cells exert pro /and anti-inflammatory responses during the pathological condition. Different types of innate immune cells including macrophages, monocytes, neutrophils, mast cells, natural killer (NK) cells and dendritic cells (DCs) involve in the immune-related atherosclerosis condition (Mohmmad et al., 2021).

Innate immune cells	Function during atherosclerosis	Atheroprotective or pro-atherogenic

Macrophage	• Transformed into foam cells and form atherosclerotic plaque
	• Imbalance between macrophage: Atherosclerosis progress
	  ○ Classic or M1 macrophages
	• Acute-phase proteins (APPs) leads to formation of M1 macrophages and progression of atherosclerotic plaque
	• Destruction of fibrous layer, plaque rupture, and eventually myocardial infarction through production of collagenase (MMP1) and stromelysin (MMP-10)
	  ○ Alternative or M2 macrophages
	• M2 macrophages predominate in the early stages of atherosclerosis
	• May play an atheroprotective role
	• M2 macrophages are categorized into four subclasses, including M2a, M2b, M2c, and M2d
	  ○ Other types of macrophages in atherosclerosis plaque include M4, Mox, M(Hb), and Mhem
		Pro-atherogenic
		Atheroprotective and pro-atherogenic

Monocyte	• Two subgroups of mouse monocytes have been identified • $Gr1^{+}Ly6C^{high}CCR2^{+}CX3CR^{low}$(inflammatory) • $Gr1^{-}Ly6C^{low}CCR2^{-}CX3CR1^{high}$ • $Ly\text{-}6C^{high}$ monocytes is raised in the first days following acute myocardial infarction • $Ly\text{-}6C^{low}$ monocytes is raised following acute myocardial infarction and can boost wound healing and regeneration of blood vessels • $Ly6C^{low}$ and $Ly6C^{high}$ monocytes become macrophages M2 and M1, respectively • Monocyte subtypes may play a vital role in inhibition and progression of atherosclerosis ○ Monocytes in the humans are classified into three subgroups including • Non-classical ($CD14^{+}$ $CD16^{++}$) • Intermediate ($CD14^{++}$ $CD16^{+}$) • Classical ($CD14^{++}$ $CD16^{-}$) • $CD14^{+}CD16^{high}$ monocytes promote atherosclerosis by the increased production of TNF-α	Pro-atherogenic
Neutrophil	• Elevated cholesterol levels: Increase release of neutrophils and size of atherosclerotic plaque • Direct relationship between the number of peripheral neutrophils and size of the atherosclerotic lesion • Inflammatory activity in atherosclerotic plaques via secretion of various mediators ○ Pentraxin 3, ROS, neutrophil clastases, MPO, leukotriene B4, neutrophil extracellular traps (NET), connexin, IFN-γ, and MMPs • Neutrophils are also involved in development of atherosclerosis by secreting azurocidin, proteinase 3, and defensin.	Pro-atherogenic
Mast cell	• Inactivation of mast cells by FcεR1: decrease the number of inflammatory cells like macrophages and T cells in atherosclerotic plaque • Activation of mast cells by TLR4 induces apoptosis in vascular smooth muscle cells of atherosclerotic plaques • Mast cells cause plaque instability and exposing of necrotic nucleus through secretion of various mediators: ○ Histamine, heparin, proteases (tryptase and chymase), and multiple cytokines (such as IL-6, IL-8, MCP1, TNF-α, and IFN-γ)	Pro-atherogenic
Natural killer cell	• NK cells are leading sources for production of IFN-γ: decrease in the IFN-γ levels significantly reduces atherosclerotic plaques in mice • Overall, the function of NK cells in atherosclerosis has not been identified	Has not been identified
Dendritic cells	• DCs have a pivotal role in both innate and adaptive immune systems • Decreased number of DCs reduces lipid accumulation and number of foam cells and ultimately reduces size of atherosclerotic plaques • Interactions of DCs with NK cells enhance production of IL-12 and IFN-γ: may have a role in formation and progression of atherosclerosis plaques • The interaction between mDC, pDC, and other immune cells activates other immune cells, rupture plaques, and eventually leads to atherosclerosis • Regulatory DCs interfere with anergy and depletion of inflammatory T cells and production and proliferation of atheroprotective Tregs	Atheroprotective and pro-atherogenic

During the innate and adaptive immune response, the immune cell phenotypes resident/ recruited to the affected tissue or organ such as the blood vessel wall are derived/developed from the primary and secondary immune organs including bone marrow, thymus and spleen. These cells circulate through the blood before infiltrating the targeted organ/tissues (Shi and Pamer, 2011). In the next section, the development of various immune cell phenotypes in the immune organ was elaborated in further detail.

1.1.1.2 Development of different populations of immune cell phenotype

Immune cells referred to as the leukocytes or white blood cells (WBC) are important in the immune system and responsible for regulating the immune responses to pathogens and injury (Tigner et al., 2020). In summary, all leukocytes share a common ancestor which is the hematopoietic stem cell (HSC). HSCs differentiate into common lymphoid progenitors (CLP) and common myeloid progenitors (CMP) before developing into lymphoid and myeloid cells (Figure 4) (Kondo, 2010). HSCs derived in the primary immune organ; bone marrow, circulate, and develop in the blood and other immune organs e.g., thymus, spleen, and liver. Certain immune cells can also mature in the bone marrow (Janeway et al., 2001).

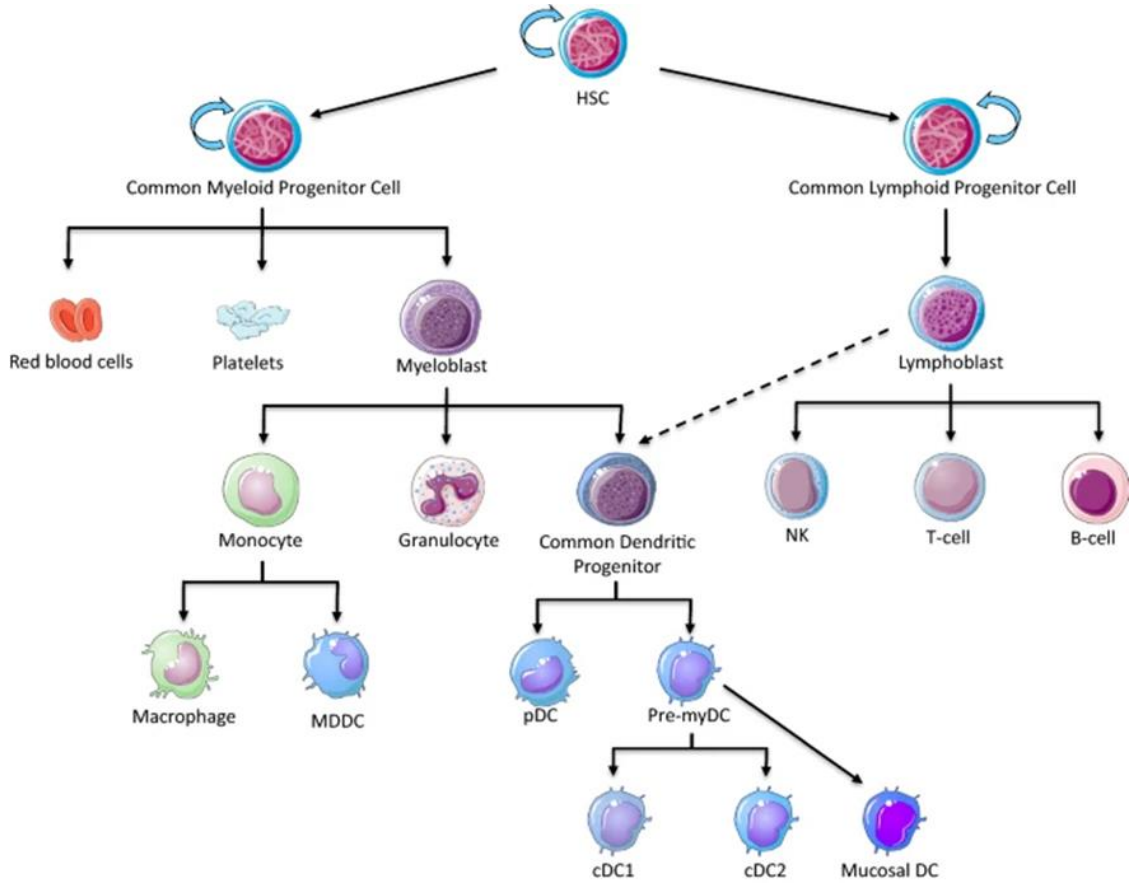

Figure 4: Classic pathways of immune cell development from hematopoietic stem cells (HSC). In Myeloid divergence, common myeloid progenitors (CMP)-derived HSC differentiated into red blood cells (RBC), platelets and myeloblast. Myeloblasts further differentiate into myeloid lineage including monocytes, granulocytes and common dendritic progenitor (CDP). Among these myeloid lineages, monocytes polarised to macrophage and monocytes derived dendritic cells (MDDC) and dendritic cells (DCs) derived from CDP. While granulocytes develop into various effector cells including neutrophils. In lymphoid cell development, HSCs differentiate into common lymphoid cell (CLP) and become lymphoblast, which further develop into natural killer (NK) cells, T and B cells. Lymphoblast also can differentiate into CDP, where it further develops into dendritic cells (DCs) (Rocamonde et al., 2019).

1.1.1.2.1 Immune cell development in bone marrow

Bone marrow is the primary site for immune cells' production, proliferation, and selective retainment of innate and adaptive immune cells. Bone marrow is a primary hematopoietic organ and consists of various immune cells, including regulatory T (Treg) cells, conventional T cells, B cells, DCs, natural killer T (NKT) cells, neutrophils, monocytic lineage, myeloid-derived suppressor cells (MDSC) and mesenchymal stem cells (MSC) (Zhou et al., 2015). Therefore, bone marrow

which consists of various immune cells can find immunity tuning and makes it suitable as an immune regulatory model for immune response research.

In the immune cell development process, the bone marrow-stem cell-derived (HSCs) develop into progenitors that gradually lose certain lineage differentiation potential before committing to the specific cell lineages. During the early stage of cell differentiation in response to cell differentiation signal, HSCs slowly lose self-renewal ability, which is the capacity to proliferate, though able to fully sustain the differentiation potential of the parental cells, whereas it is the unique features possessed by all types of stem cells. HSCs' self-renewal ability is divided into long-term (LT) and short-term (ST) HSCs, whereas LT-HSCs have life-long self-renewal ability while ST-HSCs have limited self-renewal ability and can only support modification of the hematopoietic cells for 6 weeks. LT-HSCs contribute to long-term multi-lineage reconstitution, while ST-HSCs enable to develop into multipotent progenitors (MPPs) whereas it can support the generation of all types of blood cells with no obvious self-renewal capacity that leads the MPP can only support haematopoiesis transiently. Specifically, HSCs are immature stem cells that form a sequential developmental lineage from LT-HSCs to ST-HSCs and it then develop into MPPs, as illustrated in Figure 5. These cells are included in the population of $cKIT^{hi}$Lineage−Sca-1+ (KLS) bone marrow fraction (Kondo, 2010). KLS cells are considered primitive HSCs and likely play a role in maintaining stem/progenitor cell quiescence, thereby preventing stem cell exhaustion (Hirabayashi et al., 2008).

1.1.1.2.1.1 Myeloid cell development

ST-HSC will develop into MPP1 to MPP4 and these MPPs will attain myeloid and lymphoid lineage. Myeloid-derived cells are heterogeneous populations consisting of myeloid progenitors, immature myeloid cells, and macrophages. Myeloid cells such as monocytes are derived from MPP2 and 3 that further differentiate into CMPs. Furthermore, CMP will differentiate into monocytes and granulocytes through CMP-derived granulocyte-macrophage progenitors (GMPs) or eosinophil and basophil progenitor (EoBP), as illustrated in Figure 5 (Singh and Cancelas, 2020). DCs and monocytes also can be derived from CMP-derived monocytes-dendritic cell progenitors (MDPs) (Yanez et al., 2017). These

pathways not only produce monocytes/macrophages but also neutrophils, eosinophils, basophils and DCs.

To relate with myeloid cell development, certain myeloid cells develop distinctly during normal and abnormal physiology conditions. For example, in a normal mouse, immature myeloid cells differentiate into mature granulocytes/macrophages or leukocyte progenitors and express the Gr-1+CD11b+ phenotype. However, under pathological conditions (e.g., tumour), immature myeloid cells become MDSCs and express CD11b+Ly6G+Ly6Clow (M2 macrophages) or CD11b+Ly6G-Ly6Chi (M1 macrophages). MDSCs may be defined as cells with CD14−CD11b+HLA-DRdim phenotype in humans (Zhao et al., 2012; Ghasemlou et al., 2015; Lu et al., 2018). Therefore, the differentiation pattern of the myeloid cells may be different depending on the physiological condition of the tissue/organs.

Moreover, to relate the myeloid cell development in the bone marrow and its immunity response, the mechanism of myeloid cell development in bone marrow during inflammation is further elaborated. To be re-emphasized, myeloid cells are important immune cells for innate immune response. Therefore, during inflammation such as systemic infection, the innate immune response is activated. The alarm signal activates pattern recognition receptors (PRR) on the myeloid surface including GMP and GDP, monocytes and macrophages and these cells rapidly travel to the injury site/ targeted tissue through the peripheral blood. Besides that, some myeloid cells such as GMP and GDP bypass the periphery blood but travel to lymph nodes (LNs) to undergo maturation before spreading to the injury site to suppress the inflammation or remove the inflammatory agent (Serrano et al., 2021; Ratajczak and Kucia, 2022). Overall, the bone marrow organ is involved to recognise and respond to infection by rapidly generating myeloid immune cells and quickly released into the blood/lymphatic circulation to replace those that are used in the periphery.

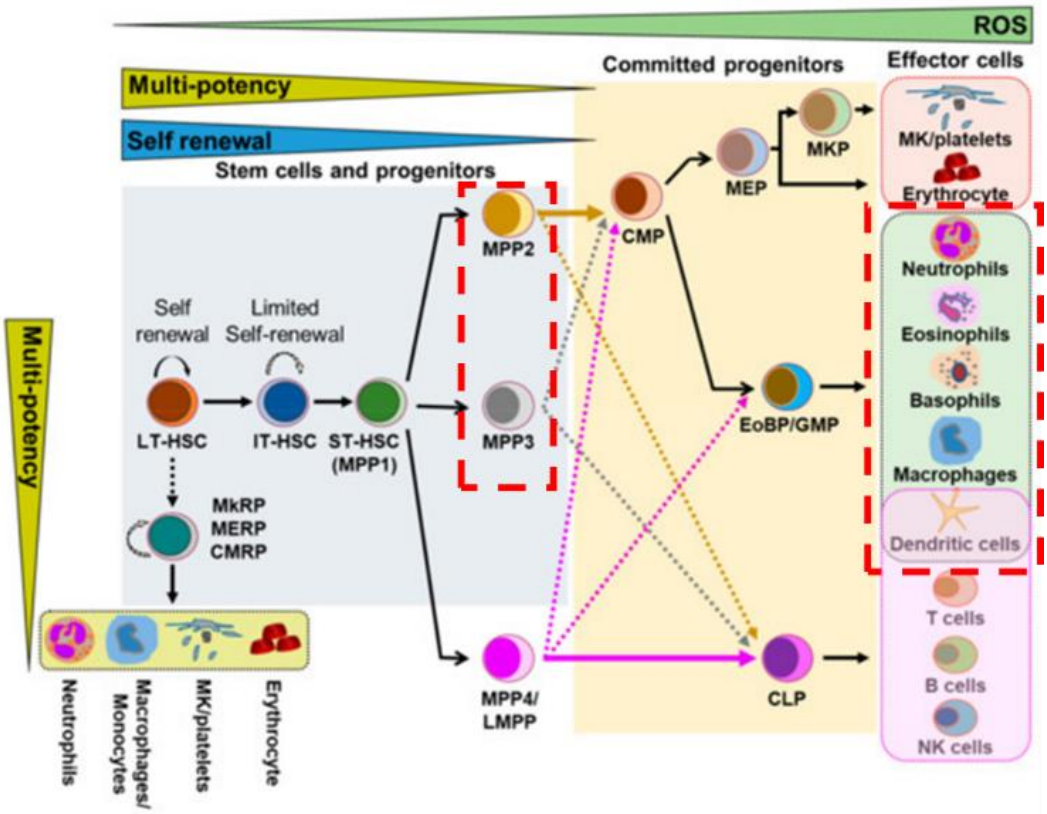

Figure 5: Detailed illustration of myeloid cell development. The multipotent progenitor (MPP) and myeloid cells were denoted in the red box. Long-term hematopoietic stem cells **(**LT-HSCs) are at the top of the hierarchy for all cell lineages. LT-HSCs differentiate into short-term hematopoietic stem cells (ST-HSCs), and afterwards into MPPs (MPP1 to MPP4) with reduced self-renewal ability. Downstream of MPPs, myeloid lineage is derived from MPP2 and MPP3 (red box), which develop into common myeloid progenitors (CMPs), the first step in myeloid lineage commitment. CMPs then can generate granulocyte-monocyte progenitors (GMPs) which afterwards produce granulocytes (e.g., neutrophils, eosinophils and basophils), macrophages, and dendritic cells (DCs) (red box) (Singh and Cancelas, 2020).

1.1.1.2.1.2 Lymphoid cell development

Furthermore, lymphoid stem cells are the primary cells that develop into B, T, and NK. It is derived from MPP4/LMPP which afterwards develops into CLP, as shown in Figure 5. The representative of T cell surface markers that are usually studied in immunology research is summarised in Table 4.

Statistically, approximately 8–20% of bone marrow mononuclear cells are lymphocytes, with a 5:1 ratio of T cell/B cell. Moreover, 1% of the bone marrow population are plasma cells, which can produce antibodies. Approximately 1–5% of CD3+ T cells in the bone marrow are composed of CD4+ T cells, CD8+ T cells and CD4+CD25+Treg cells. CD4/CD8 ratio in the bone marrow is 1:2 as

compared to both peripheral LNs and the blood. Two-thirds of bone marrow T cells express surface markers indicating antigen experience (e.g., CD44hi and CD122+), while T cells in the spleen and LNs exhibit naive phenotypes (Zhao et al., 2012). These lymphoid cells are important for regulating immune response, especially adaptive immune response.

In the next section, how these cell populations, specifically B and T cells undergo the development process is comprehensively elaborated for a deep understanding of their development process. In addition, the link between their development process and their immunity response is further highlighted.

Table 4: Surface markers representing T and B lymphocytes. The table summarised the representative marker for total lymphocyte cells, T cells and type of T cells, B cells and the cellular activation status (Tchilian et al., 2004; Rumfelt et al., 2006; Zhao et al., 2012; Sauls et al., 2018).

Surface Markers	Representative
CD45	Lymphocytes
TCR	T cells
CD3	Pan-T cells
CD45	Lymphocytes
CD4	T helper cells
CD8	Cytotoxic T cells
CD4+CD25	T regulator cells (Treg)
CD19, CD20, CD24, B220	B cells
CD44+	Activator/Effector Cells
CD62L+	Naïve Cells

1.1.1.2.1.3 B cell development in bone marrow and transition in the blood before localising to secondary lymphoid organ

Lymphoid cell development can be divided into B and T cell lineage. The illustration of B cell development is shown in Figure 6. B cells are derived from MPPs (MPP4/LMPP) and undergo several differentiation checkpoints (Singh and Cancelas, 2020). B lymphocytes develop from HSCs in the fetal liver before birth, and then in the bone marrow after birth (Hardy and Hayakawa, 2001; Montecino-Rodriguez and Dorshkind, 2012). In adult mouse bone marrow, B cell progenitors

differentiate into pro-B and pre-B cells before developing into immature B cells. The immature B cells then infiltrate and circulate in the blood, differentiating into transitional 1 (T1) B cells. These T1 B cells further differentiate into T2 and T3 B cells before maturing into B cells (Zhou et al., 2020).

The percentage of transitional B cells that develop into mature B cells decreases significantly, from 10% entering the circulation to only 1-3% reaching maturity. Mature B cells then give rise to short-lived plasma cells or migrate to the germinal center (GC) to form GC B cells (Zhou et al., 2020). Differentiation of B cells in the GC predominantly occurs in lymph nodes, spleen, and Peyer's patches (Young and Brink, 2021). In the GC, B cells can undergo selection to differentiate into long-lived plasma blasts or memory B cells (Zhou et al., 2020; Shiraz et al., 2022). Mature B Cells can be segregated into several subsets based on their location, cell surface phenotype, Ag specificity, and activation routes, as illustrated in Table 5.

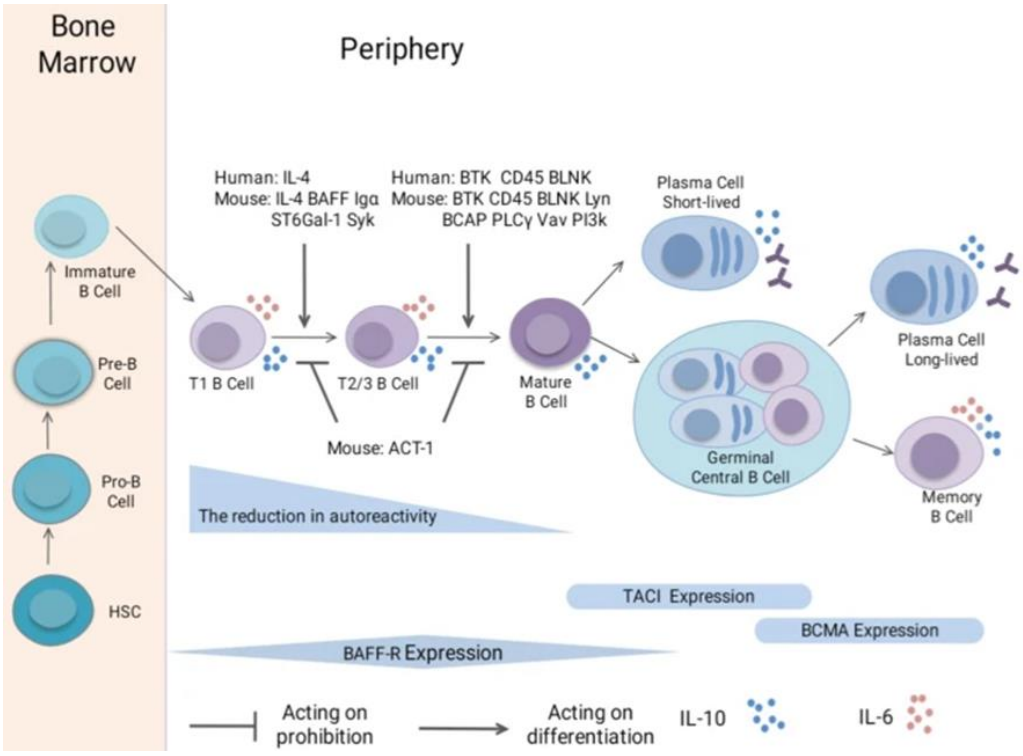

Figure 6: Illustration of B cell development in bone marrow and blood. The B cell develops in the bone marrow and the naïve B cells exit the bone marrow and develop into several subsets of B cells including transition B cells (T B cells) in the blood, then become mature B cells and differentiate into short-lived plasma membrane or/and germinal center (GC) B cells in the GC region of a lymphoid organ. The GC B cells then further develop into long-lived plasma cells and memory B cells that function to release antibodies, cytokines or both (Zhou et al., 2020).

In adaptive immune response, naïve B cells exit bone marrow and are activated through specific antigens binding to the B cell receptor (BCR) and PRR ligands weakening the infection by producing low-specificity antibodies. This early immune response is driven by short-lived plasma cells. Besides that, regulatory B cells also have been induced and cause an immunosuppressive function by excretion of IL-10, IL-17, IL-35 and TGFβ, which suppress Th cell and innate immune cell responses.

Further cross-linking of surface antibodies and antigens leads to further differentiation and selection in GC of lymphoid organs which involves the interaction with T cells (Figure 7). This occurs through cytokine signalling such as IL-21 and IL-4, which are released by follicular T cells and DCs, furthermore, B cells present major histocompatibility complex class II (MHC II) epitope complex on its surface, which can be recognized by cognate T cells. Th2 recognised the MHCII epitope complex on B cell surface using T cell receptor (TCR) and CD4 which permits Th2 cell to activate B cell to proliferate and differentiate into B memory cells and plasma cells. B cells proliferation and differentiation are facilitated by the IL-4, IL-5 and IL-6 secreted by Th2, while IL-10 inhibits the proliferation of Th1 cells. Antibodies bind to either inactivate the antigens or mark them for destruction by macrophages. (Gartner and Hiat, 2011; Nothelfer et al., 2015).

Table 5: Description of B cell subsets. The B Cells are divided into several subsets based on their location, cell surface phenotype, antigen (Ag) specificity, and activation routes (Cano and Lopera, 2013).

Type of B cells	**Characterisation**
Transitional B cells (T B cell)	The earlier B-cell
Follicular B cells (FoB) or B-2	Generated in the bone marrow, infiltrate to the follicles of secondary lymphoid organs through blood
Marginal zone B cells (MZB)	Localised at sentinel in the marginal zone (MZ) of the spleen
B1 B cells	B Cells form in the fetal liver
Plasmocyte or Ab-secretory cells	Activated B Cell derived, expressed IL-2 and IL-10, without CD19, CD20, CD22, HLA class II molecules, and BCR
Short-lived cells	Located in the medulla of the ganglia and, rapidly leaving enters the circulation and then obtains the site where the Ag enters to initiate
Long-lived cells	Migrate to the bone marrow following SDF-1 expression by the stromal cells
Memory B Cells	Classified based on CD27, and m Ig. Found in spleen, GC and intestine lamina propria
Regulatory B cells (Bregs)	Release a variety of cytokines
Innate B cell helpers	Obtain help from other cells besides the T-helper cells

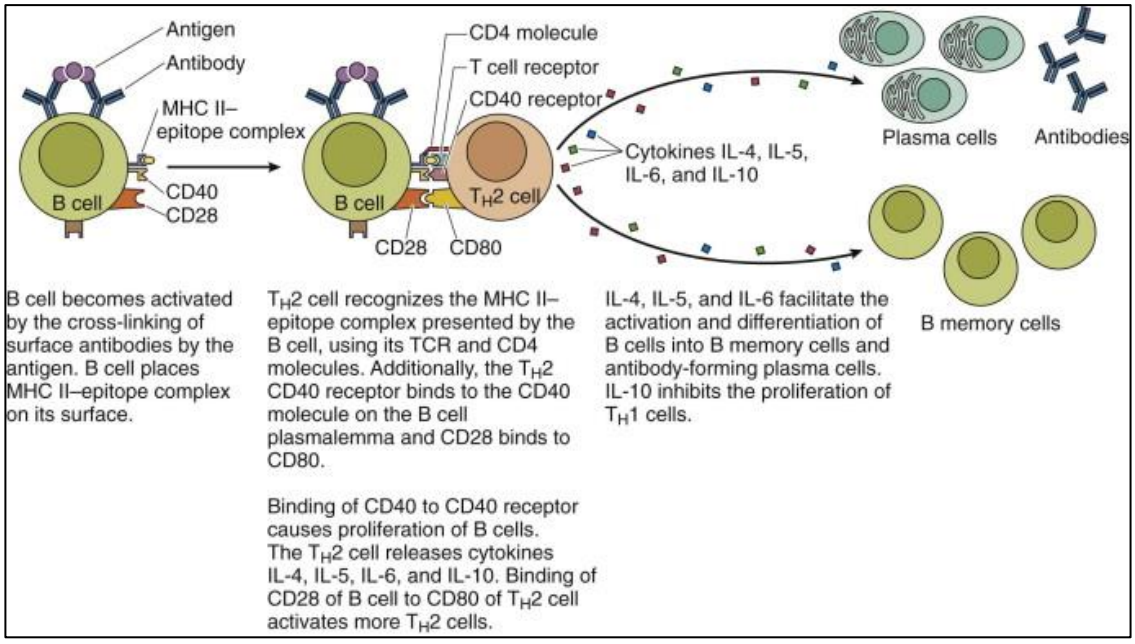

Figure 7: Mechanisms of germinal center (GC) B cell activation and differentiation. Mechanism of activation of B cells in GC following the antigen stimulation. Activation involves the interaction with T cells i.e., T helper 2 (Th2), through major histocompatibility complex II (MHCII) and CD40 receptor-CD40 molecule complex binding on B cells surface. The binding with Th cells promotes the proliferation and differentiation of the B cells into plasma and memory B cells that are facilitated by various cytokines (interleukin 4 (IL-4), IL-5 and IL-6) (Gartner and Hiat, 2011).

1.1.1.2.2 T cell development in bone marrow

Furthermore, T cells are also derived from ST-HSC and the progenitor in the bone marrow, before it continued the development of T cell lineage in the thymus, as illustrated in Figure 8 (Brugman and Staal, 2016). The bone marrow progenitor such as CLP are well known generated in bone marrow (Lancrin et al., 2002; Kawano et al., 2018), however, the intermediate steps leading to T cell commitment are still lacking information. In this section, I elaborate on the process of the T cell development that occurs in bone marrow and thymus.

The nature of early T lineage progenitors in the thymus or bone marrow is still unknown. Therefore, in this thesis, I described the T cell lineage development in the bone marrow from HSC differentiated into CLP (Singh and Cancelas, 2020). CLP was then developed into early T cell progenitor (ETP)/double negative 1 (DN1). ETP derived from bone marrow was reported to express in the thymus and is known as the earliest progenitor for T cell lineage. However, ETP also can develop into other cell lineage including NK cells (Oh et al., 2023). The

extrathymic progenitors depend on the expression of P-selectin-PSGL-1 interactions, P-selectin, C-C chemokine receptor 9 (CCR9) to homing into the thymus. These adhesion proteins were found to express on Lin-Sca1+cKIT + (LSK), CLP, and ETP cells (Krueger and Von, 2007).

In the thymus, the progenitors develop into a DN population (CD44 and CD25 (IL-2 receptor alpha chain)), progressing through stages DN1 to DN4. Subsequently, DN4 cells form a double-positive population expressing both CD4 and CD8 through the rearrangement of the αβ-TCR chain. These double positive (DP) cells then undergo a positive selection process to form immature single positive (SP) CD4 or CD8 cells. They are then translocated into the blood, continuing their maturation into fully functional CD4 and CD8 T cells. Negative selection cells are discarded through apoptosis (Thapa and Farber, 2019).

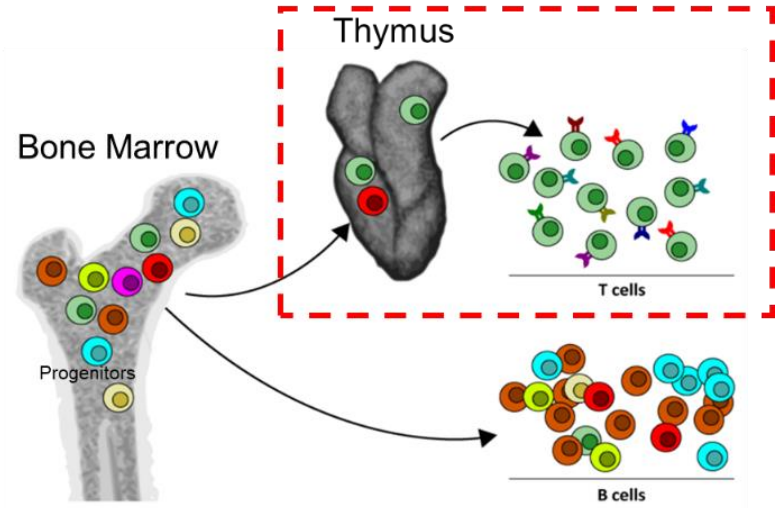

Figure 8: T cell development from hematopoietic stem cells (HSC) derived from bone marrow to mature T cells in the thymus. The stem cells and progenitor are derived from the bone marrow and seedling of the thymus (red box) for further the development of T cell lineage and becoming T immunocompetent cells (Brugman and Staal, 2016).

In general, naive CD4 and CD8 cells further develop into functional T cells to promote and inhibit inflammation, as illustrated in Figure 9. Specifically, CD4 develop into Th cells, either Th1 or Th2, depending on the physiological condition. On the other hand, naive CD8 cells develop into cytotoxic CD8 T cells that destroy the pathogen/foreign antigen by releasing cytolytic enzymes and/or cytokines (Seder and Ahmed, 2003).

In detail, upon antigen stimulation, naïve CD4+ T cells activated by antigen-presenting cells (APCs) through MHC II complex binding, costimulatory stimulation, and cytokine signalling such as IFNy, IL-1 and IL-6, that differentiate the naïve cells into several cell subsets including Th1, Th2, Treg, follicular helper T (Tfh), Th17, Th9, Th22, and CD4+ cytotoxic T lymphocytes (CTLs). While naïve CD8 T cells undergo robust clonal to give rise to effector and memory T cells (Sun et al., 2023). In terms of CD4 and CD8 T cells' role in immune response, Th1 is known to function as pro-inflammatory cells that contribute to inflammation, while Th2 and T regulator cells function as anti-inflammatory immune cells. On the other hand, Tfh cells are specialized CD4+ Th cells that function in supporting humoral immune responses by promoting B cell proliferation and differentiation in GC, and high-affinity antibody production (Sun et al., 2023).

On the other hand, effector CD8+ T cells (CD8+ CTLs) directly induce target cell death by the interaction between Fas/Fas ligand and release the cytolytic mediator perforin that causes pores creation on the target cells which allows the delivery of granule serine proteases (granzymes) to induce apoptosis. Moreover, memory CD8+ T cells provide rapid and strong protection against antigens, which is important for efficient and long-term immunity (Sun et al., 2023).

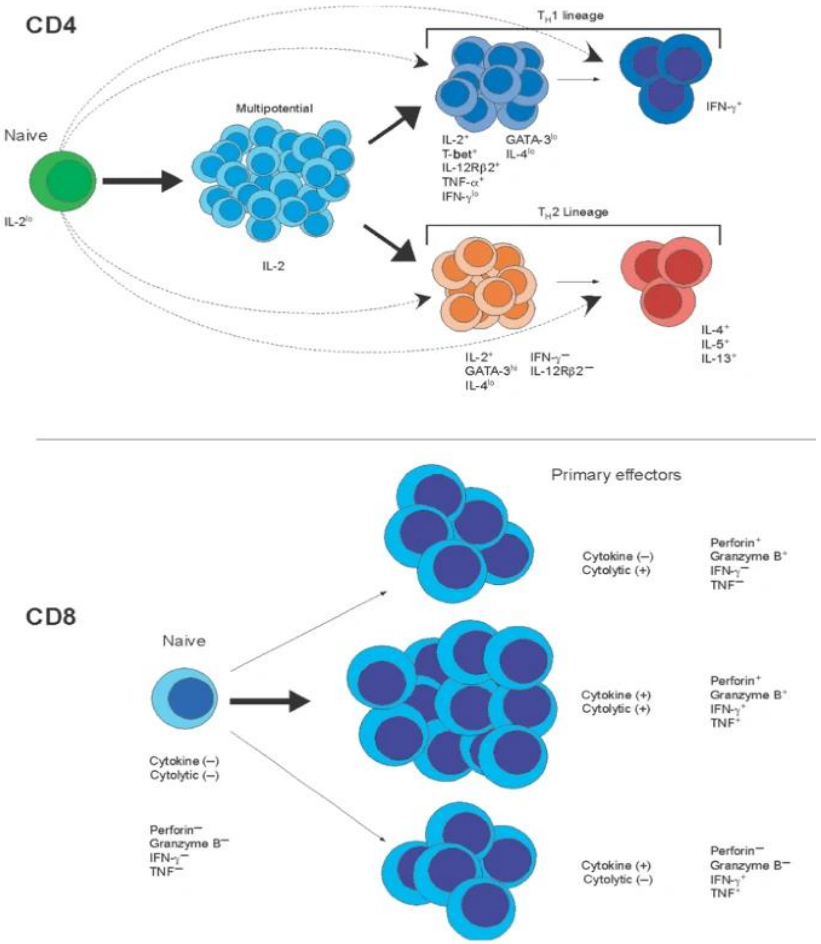

Figure 9: Polarisation of naive CD4 and CD8 T cells into effector subsets. T helper 1 (Th1) and Th2 cells polarised from naive CD4 cells toward becoming interferon gamma (IFN-γ) or interleukin 4 (IL-4)-producing cells. After activation, there is notable heterogeneity at the single-cell level in terms of cells producing IFN-γ or IL-4. Naive CD8 T cells efficiently develop into effector cells called cytotoxic CD8 T cells with cytolytic and/or cytokine-producing capacity after primary stimulation (Seder and Ahmed, 2003).

The purity of the T cell lineage in T cell development can be identified based on the expression of the Thy-1 marker. As cited by Yang et al. (2020), this novel protein was named Thy-1 because it was first discovered on thymocytes. It is abundant on T cells (Furlong et al., 2018). Thy-1 is more than just a T cell marker; it can at least partially substitute for TCR-induced signal 1 during T cell activation and can stimulate T cells (Haeryfar and Hoskin, 2004). Thy-1 provides a TCR-like signal to control CD4+ T cell proliferation and differentiation into effector cells following costimulatory signals by syngeneic lipopolysaccharide (LPS)-matured bone marrow-derived DCs (Furlong et al., 2018).

Therefore, in this study, I employed the Thy-1 marker to identify the purity of the T cell lineage and to separate the non-T cell lineage.

1.1.1.2.3 Immunological function in spleen

The spleen is a secondary lymphoid organ and hosts a various immunological function together with its roles in haematopoiesis and RBC clearance (Lewis et al., 2019). As previously mentioned, naïve T cells from the thymus translocate into the spleen (Janeway et al., 2001; Bonilla and Oettgen, 2010). Besides that, other immune cells (e.g., monocytes, macrophages, and B cells) that circulate through the blood also enter the spleen to direct the immune response.

The Spleen structure consists of red pulp (RP), white pulp (WP) and MZ exist between both regions (Figure 10). WP regions make up the spleen less than a quarter, while RP makes up most of the tissue. Even though WP cover a smaller region than RP, WP plays the primary immunologic role in the spleen of both human and rodent species, while RP plays a different immune function than WP. Different from LNs, the spleen absences of afferent lymphatic vessels which all cells and antigens infiltrate into the spleen through blood circulation (Lewis et al., (2019)).

These splenic architectures make it compatible to play an important role as the secondary immune organ that regulates the immune response. Specifically, RP functions to discard aged, dead cells and cellular debris from the circulation, while concurrently scanning for pathogens and tissue damage. Numerous leukocytes with innate immunity roles inhabit the RP, including neutrophils, monocytes, DCs, gamma delta (γδ) T cells and macrophages, make RP primarily for innate immunity (Lewis et al., 2019; Hu et al., 2020).

Moreover, the blood entering MZ engaged with the macrophage population in the MZ region. These two populations of macrophages which are metallophilic macrophages (MMMs) and marginal zone macrophages (MZMs) retained by CCL21 chemokine. Then both macrophage populations form a barrier that helps to filter the blood and lymphocytes to release into the MZ. A link that exists between the RP and WP is called the bridging zone/channel (BC). Besides that, CCL21 also known as T cell attracting chemokine. Thus, naïve and activated lymphocytes (e.g. T cells) enter or exit the WP through MZ BC (Pabst and Westermann, 1991; Lewis et al., 2019; Sixt and Lammermann, 2020).

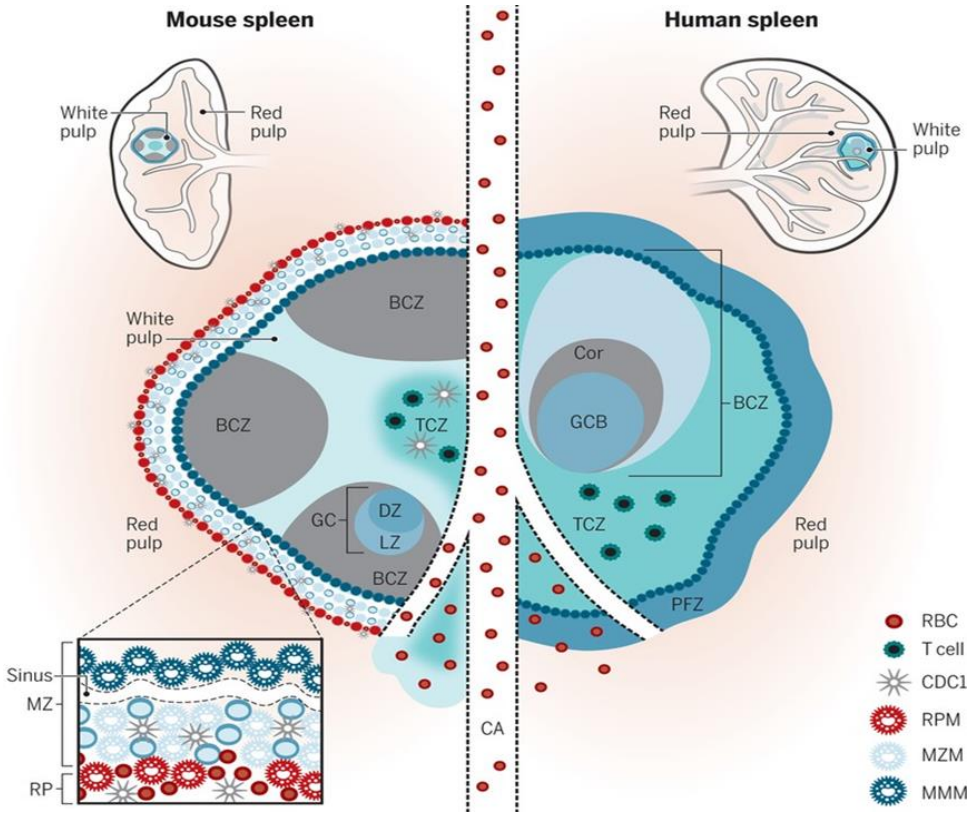

Figure 10: Splenic structure and function at steady states. The splenic architecture is divided into red pulp (RP) (major region), white pulp (WP) (less than a quarter part) and marginal zone (MZ) dividing both RP and WP. WP areas consist of the T-cell zone (TCZ), known as the periarteriolar lymphoid sheath (PALS), arterioles and B-cell zone (BCZ). The WP also consist of germinal center (GC) that can be categorised as dark zone (DZ) and light zone (LZ) in BCZ. The Innate immune cells including monocytes, macrophages, neutrophils, and natural killer (NK) cells are major components in RP, while T and B lymphocytes (adaptive immune response) are the components of WP (Lewis et al., 2019).

During the innate immune response, the monocyte population (e.g., Ly6C^{lo} and Ly6C^{hi}) encounter the bacteria in the blood and then exits into MZ to induce T cell-independent MZB cell response. Besides that, monocytes also help to remove apoptotic bodies and secrete anti-inflammatory factors (e.g., TGFβ and IL-10). Besides that, during the inflammation response, monocytes in MZ secrete CCR2 to recruit and migrate Ly6C^{hi} monocytes from the bone marrow into the spleen for the development of several myeloid cell types (e.g., DC and macrophages). There are highly inflammatory monocytes (CD11c+nTIP (TNF-iNOS)–DCs), producing TNFα and NO. They are also capable of reactivating effector or memory T and NK cells, however, not powerful enough to activate

naïve T cells. Moreover, the spleen also functions as a basin for undifferentiated monocytes such as monocytes marked by the CX3CR1 marker and variable amounts of Ly6C, and it mobilises into the other organs when the signal alarm is received for inflammatory response (Lewis et al., 2019).

On the other hand, the adaptive immune response is driven by T and B cells. In the steady state, naïve follicular B cells inhabit WP follicles, but during the inflammatory state, B cells in BCZ rapidly cycle between the LZ by CXCR5 and the DZ by CXCR4. Following the GC reaction, some B cells leave into the BC and RP to become antibody-secreting cells while some become long-lived plasma cells in the RP. On the other hand, in the steady state, CD4+ and CD8+ T cells are set apart within the TCZ (or PALS) of the murine WP. CD4+ T cells support B cells to produce high-affinity antibodies through cytokine production (e.g., IL-21) and direct co-stimulation (e.g., ICOS-ICOS ligand). During the active immune response, Tfh cells upregulate CXCR5 to reach the T-B border while B cells upregulate CCR7 to move from the BCZ to the T-B border (Lewis et al., 2019). In comparison to CD4 T cells, naïve CD8+ T cells populate in the central TCZ (or PALS) of WP during the steady state waiting for APCs. Following the immune activation, activated CTLs translocate to MZ and RP through the BC to clear the infection in the RP. Moreover, some memory CD8+ T cells return to the PALS and CD62L-CXCR3+ memory CD8+ T cells remain in the RP (Lewis et al., 2019).

Altogether, it indicates that immune cells developed in primary immune organs either continue their development in the spleen for immune regulatory responses or are recruited into organs for immunological functions. The development of these immune cell profiles or the activation/enhancement of the immune response in the organ might be controlled by a master regulator behind the mechanism. Therefore, further understanding of the mechanism of the immune regulatory response at transcriptional regulation levels has been explored in the literature. The mechanism of the immune regulatory response at transcriptional levels is elaborated in the end part of this chapter.

Before further interrogation of the molecular pathway of the inflammation, I explore another influential risk factor of CVD, which is the metabolic dysfunctional factor. Besides inflammation, which is well-known to be an important player and risk factor in CVD, metabolic dysfunction is also a key pathophysiological factor

contributing to CVD. Therefore, in the next section, I have compiled various literature on metabolic disorder as a risk factor for CVD and their interrelationship with inflammation, which can lead to complications such as heart disease or heart failure.

1.1.2 Metabolic dysfunction as a CVD risk factor

Metabolic dysfunction e.g., obesity and type (II) diabetes mellitus (T2DM) are known to significantly increase the risk of CVD (Biglu and Biglu., 2016; Haybar *et al.,* 2019). It is proven that patients with T2DM in addition to a history of Myocardial Infarction (MI) display higher death rates compared to nondiabetic patients (Einarson et al., 2018).

Chronic hyperglycaemia is a primary factor in promoting vascular complications in T2DM (Figure 11) (Rask-Madsen & King., 2013). The degree of vascular damage is linked with the hyperglycaemic-induce production of ROS and consequently, oxidative stress that stimulates the inflammatory response in the vascular wall (Oguntibeju, 2019). The production of pro-inflammatory cells and cytokines drives vascular changes, which are the hallmarks of CVD. The phenotypic changes distort the normal regulation of blood flow and pressure, consequently, contributing to pathological vascular disease e.g., hypertension, myocardial infarction, atherosclerosis, and heart failure (Heinecke, 2006; Chatterjee, 2016; Daryabor et al., 2020).

Overall, there is a strong correlation between metabolic disorders, such as hyperglycaemia, and the activation/enhancement of the inflammatory response in the vascular wall, which consequently contributes to vascular dysfunction (e.g. atherosclerosis) and disease.

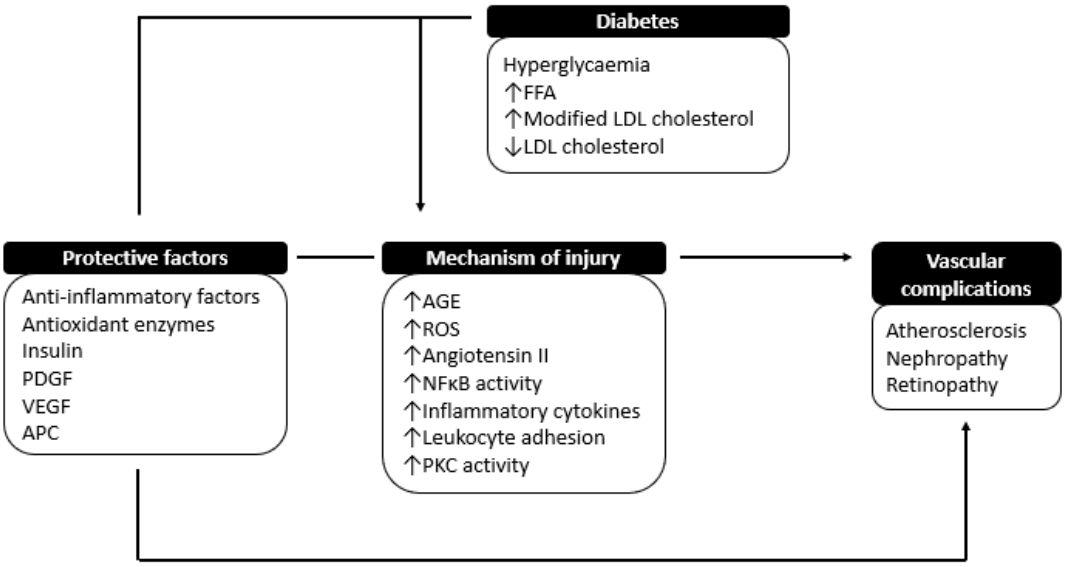

Figure 11: Hyperglycaemia-diabetes metabolic disorder as a risk factor for vascular disease. Metabolic disorders (e.g. diabetes mellitus) diagnosed due to hyperglycaemia lead to increased levels of free fatty acid (FFA), modified low-density lipoprotein (LDL) and reduced high-density lipoprotein (HDL) in the blood. These conditions cause the occurrence of injury mechanisms that involve the obstruction of pro- and anti-inflammatory strategies in immune response (e.g. excessive inflammatory cytokines and leukocytes), an increase of reactive oxygen species (ROS) production, angiotensin II (Ang II), advanced glycation end products (AGE), and the failure of anti-inflammatory and anti-oxidation activity to maintain the homeostasis of the vascular tissue. Prolong period of injury leads to vascular complications including atherosclerosis, nephropathy, and retinopathy (Rask-Madsen & King., 2013).

1.1.2.1 Correlation between metabolic dysfunction, inflammation and CVD

In this section, I elaborate on endoplasmic reticulum (ER) stress as one potential mechanism that links hyperglycaemia to inflammation, which may lead to vascular dysfunction and eventually cause CVD. Accumulated data show a strong connection between inflammatory changes and the risk of CVD. How inflammation contributes to CVD is a hot topic in research (Katsiari et al., 2019). In detail, the molecular mechanisms of inflammatory responses stimulated by metabolic dysfunction (e.g., hyperglycaemia and insulin resistance) are shown in Figure 12. This figure illustrates how metabolic dysfunction (e.g. high glucose) contributes to the inflammatory response by activating ER stress, enhancing the hyperglycaemia condition and promoting insulin resistance at the transcription level. In brief, hyperglycaemia triggers ER stress and activates Inhibitory kappa

kinase beta (IKKβ), which phosphorylates Iκβα and promotes its degradation in proteasome. This causes nuclear factor kappa beta (NFκB) to translocate into the nucleus and induce the transcription of pro-inflammatory genes. IKKβ also inhibits insulin signalling pathways *via* the phosphorylation of insulin receptor substrate 1 (IRS-1) serine residues in adipocytes and promotes insulin resistance (Berbudi et al., 2020).

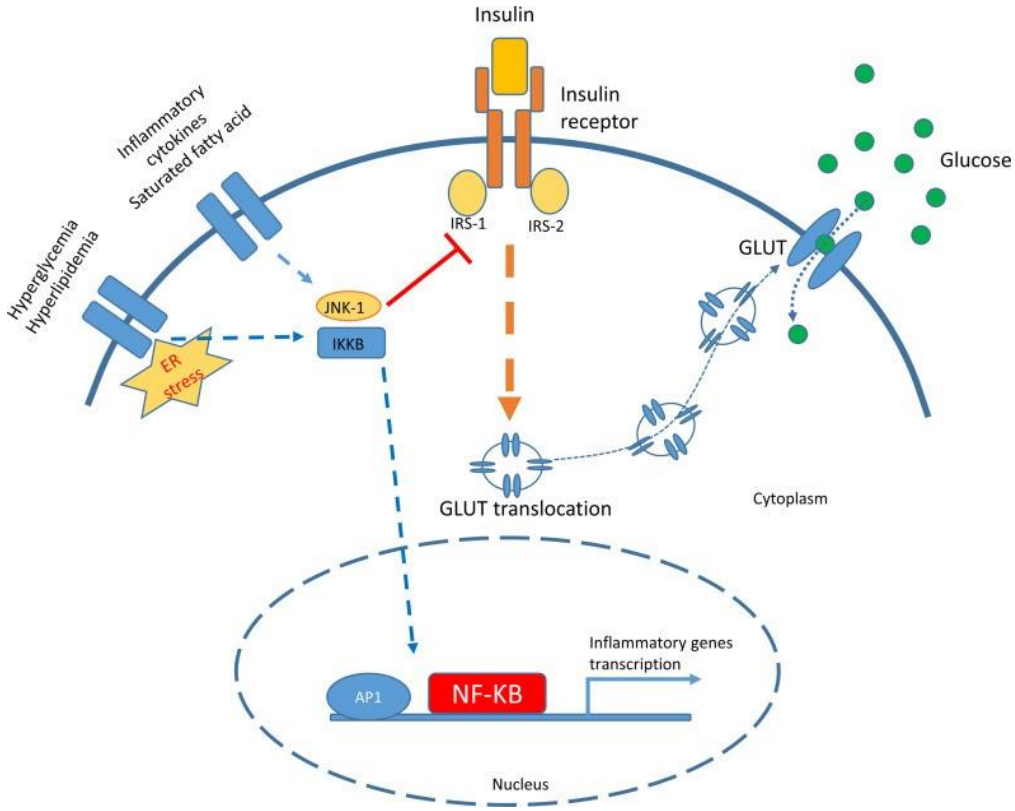

Figure 12: The link between endoplasmic reticulum (ER) stress and inflammatory gene transcription synthesis, insulin resistance and hyperglycaemia. ER stress is a potential mechanism linking hyperglycaemia to inflammation. Both hyperglycaemia and hyperlipidaemia activate ER stress, which promotes the transcription of inflammatory genes through the modulation of Inhibitory kappa B kinase beta (IKKβ) protein molecules. This leads to the translocation of nuclear factor kappa B (NFκB) to the nucleus, initiating the transcription of inflammatory proteins. Additionally, Jun N-terminal kinase 1 (JNK-1), activated by excessive inflammatory cytokines and saturated fatty acids, along with IKKβ, inhibits insulin receptor (IR) function by blocking insulin receptor substrate 1 (IRS1). This blockage prevents glucose from entering cells *via* glucose transporters, resulting in elevated glucose levels (Berbudi et al., 2020).

Hyperglycaemia stimulates stress in organelles and cells, such as the mitochondria and the ER, leading to the production of excessive ROS. These ROS cause oxidative stress (Van Niekerk et al., 2019; Berbudi et al., 2020). In normal physiology, ROS functions to regulate vascular contraction and relaxation, and they are produced by mitochondria at low concentrations (Koju et al., 2019). However, excessive ROS produced by activation of mitochondrial respiratory chain enzymes (e.g., nicotinamide adenine dinucleotide phosphate (NADPH) oxidase, uncoupled endothelial nitric oxide synthase (eNOS), cyclooxygenase, and xanthine oxidase (XO) during hyperglycaemia cause cells and tissues experience high oxidation stress. Moreover, the failure of the antioxidant defence system inhibits the normal roles of antioxidant enzymes (e.g., catalase, peroxiredoxins, glutaredoxin (Grx), and glutathione peroxidases (GPx)), making them unable to mitigate the damaging effect of oxidative stress in the cells and tissues (Nedosugova et al., 2022).

In pathological vascular dysfunction, the high glucose or free fatty acid (FFA) induces excessive accumulation of ROS directly causes damage to the ECs by oxidising the macromolecule including DNA, proteins, and lipids (Koju et al., 2019). Besides that, ROS also cause indirect effects, which as excessive ROS elevate the oxidative stress which then activates stress-sensitive intracellular signalling pathways including NFκB, p38 mitogen-activated protein kinase (MAPK), JNK/SAPK and hexosamines. NFκB plays are well known to play a crucial role in mediating immune and inflammatory responses and apoptosis, while JNK/SAPK is involved in the apoptosis mechanism of EC. On the other hand, activation of the p38 pathway increased phosphorylation of heat shock protein 25, the cell injury functionally related protein. Moreover, high glucose or FFAs result in activation of the hexosamine biosynthetic pathway, which in turn leads to insulin resistance (Figure 13) (Evan et al., 2003).

In addition, free-reducing sugar (e.g. glucose) in hyperglycaemia cause increases the production of advanced glycation end-product (AGE) and FFA in hyperlipidaemia increases the production of oxidised low-density lipoprotein (oxLDL), which is known that both can induce the endothelial dysfunction (Evan et al., 2003; Nedosugova et al., 2022). They cause endothelial dysfunction because the glycation process causes loss of protein function and impaired

elasticity of tissues such as blood vessels, skin, and tendons. The glycation process is known as the non-enzymatic reaction that occurs between free reducing sugars and free amino groups of proteins, DNA, and lipids to form AGEs. This reaction highly accelerates in the presence of high glucose and tissue oxidative stress (Kim et al., 2017).

Moreover, high levels of FFA and low-density lipoprotein (LDL) during hyperlipidaemia undergo a chemical reaction with excessive ROS, producing oxLDL. While LDL in its natural state is not atherogenic, in its oxidised state, it is taken up by macrophages, causing them to undergo phenotype modulation to become foam cells. This process is a pivotal point for the developing atherosclerotic plaque (Leopold and Loscalzo, (2008).

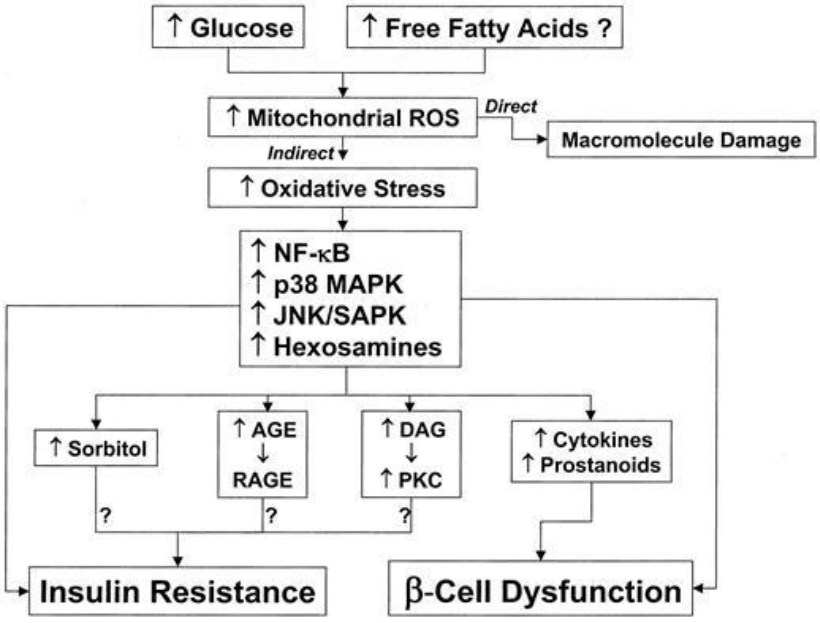

Figure 13: Mechanism of hyperglycaemia and hyperlipidaemia induce-reactive oxygen species (ROS) and vascular damage. Hyperglycaemia and hyperlipidaemia induce excessive ROS secretion, directly and indirectly, affecting the pathophysiological condition of vasculature wall tissue. The excessive ROS produced during hyperglycaemia/hyperlipidaemia directly cause macromolecule damage (eg. DNA, protein and lipid) on the vascular wall. Moreover, high ROS activate stress-sensitive intracellular signalling pathways (e.g. nuclear factor kappa B (NFκB), p38 mitogen-activated protein kinase (MAPK), Jun amino-terminal kinase/stress-activated protein kinases (JNK/SAPK) and hexosamines) due to elevation of oxidation stress, which consequently leads to vascular damage by the inflammatory responses, and glycation process (e.g. advanced glycation end (AGE) product), insulin resistance and β-cell dysfunction (Evan et al., 2003).

EC damage/injury due to the oxidation stress mechanism mentioned above allows a high level of small-density LDL to translocate into tunica intima (TI) and react with excessive ROS to generate more oxLDL. oxLDL aids in recruiting inflammatory mediators by inducing endothelial and VSMC-secreting chemokines (monocyte chemotactic protein-1 (MCP-1)) and causing the infiltration of monocytes into TI (Leopold and Loscalzo, 2008; Rask-Madsen & King., 2013; Reijirink et al., 2022). Monocytes including Ly6C+ (mouse) and CD14 +(human) are the driving force of inflammation that contributes to vascular dysfunction (Italiani and Boraschi, 2014; Reijirink et al., 2022). High levels of Monocytes (eg. Ly6C) differentiated into the M1 macrophages, engulf the oxLDL and produce lipid-laden foam cells (Gui et al., 2012). These foam cells release cytokines and chemokines, causing the trafficking of monocytes and T lymphocytes to the subendothelial space (Batty et al*.,* 2022). The accumulation of foam cells leads to the development of plaque, which is a pathological condition characteristic of vascular disease (Javadifar et al., 2021).

The severity of vascular dysfunction diseases such as coronary artery disease (CAD) is associated with the lymphocyte-to-monocyte ratio. High monocytes and low lymphocyte count were composite markers of inflammation that may provide additional information in the assessment of CVD (Gong et al*.,* 2018; Oh et al*.,* 2022).

Collectively, the literature review reveals an impressive correlation between metabolic disorder, inflammation and vascular dysfunctional disease. In the next section, specific pathological conditions that demonstrate the strong three-way relationship between metabolic disorders, inflammatory immune and CVD are further explored.

1.1.2.1.1 Metabolic disorder versus inflammatory immune response

There is a fascinating link between the metabolic disorder and the inflammatory response that happens in the tissue. Metabolic disorders such as T2DM are thought to stimulate the de-regulation of innate and adaptive immune responses, causing uncontrol infiltration of monocytes into the TI of the vasculature (Tan et al., 2022). The general function of innate and adaptive immune response is summarised in Table 1.

During normal and pathological conditions, regulatory factors in both immune systems are believed to modulate the anti/pro-inflammatory response by different immune cell phenotypes and inflammatory cytokines. The metabolic disorders such as the glycolytic metabolic shift in T2DM, lead to elevated ROS-induced oxidation stress, which induces the differentiation of monocytes (Evan et al., 2003: Nedosugova et al., 2022). Monocytes which are the specialised innate immunity player (Zhang et al., 2021), possess binary M1/M2 macrophage polarisation settings, depending on numerous environmental conditions that fuel polarisation (Chen et al., 2023).

In hyperglycaemia environmental conditions, high glucose causes repression of M2 macrophages and skewed differentiation of monocytes into M1 phenotype to drive pro-inflammation that contributes to vascular dysfunction (Torres et al., 2016). Therefore, M1 macrophages are denoted as the key players in diabetes progression and inflammation effects (Tan et al., 2022). M1 macrophages utilized glucose as an energy substrate (Vats et al., 2006; Moganti et al., 2017), therefore, high glucose condition would recruit a high volume of M1 macrophages into the injury site and glucose-utilizing tissue (e.g., Damaged vascular endothelium tissue, adipose tissue, and liver) (Xia et al., 2017). Therefore, further damage caused by T2DM (e.g., vascular dysfunction) can be prevented by reducing hyperglycemia-induced M1 cytokine profiles (Moganti et al., 2017).

Moreover, T-lymphocytes which are part of the adaptive immune system also act as important regulators of T2DM-associated inflammation (Donath and Shoelson, 2011; Kologrivova et al., 2016; Xia et al., 2017). The adaptive immune response begins with the activation of naïve T cells, which differentiate into Th1, Th2, Th17 or Treg from naïve CD4 T cells, and into CD8 T cytotoxic cells from naïve CD8 T cells (Figure 9 and Figure 14). The polarisation of these cells is influenced by various environmental factors, particularly cytokines. Th1 cells are induced by IFNγ, Th2 cells by IL-4, Th17 cells by IL-6, IL-21, IL-23, IL-1β or TGFβ and Treg cells by TGFβ. These cytokines are typically released by innate immune cells when an infection persists, and the activation of adaptive immunity is required. Additionally, CD8 T cells are developed to directly kill or destroy pathogens through the expression of MHCI (Figure 14) (Netea et al., 2019; Zhu and Zhu, 2020).

In the pathological condition (e.g., T2DM and hyperglycemia), CD8+ T cells and Th1 cells are elevated in the adipose tissue to cause insulin resistance, while Treg cells and Th2 cells tend to counter the pathological condition (Donath and Shoelson, 2011; Xia et al., 2017). Th1 and Th2 responses are closely related to M1/M2 polarisation and play a critical role in T2DM-associated inflammation (Xia et al., 2017). Macrophages function to initiate and direct T-cell responses, indicating that the adaptive immune response requires activation and guidance from innate immunity (Mills and Ley, 2014; Italiani and Boraschi, 2014). Pro-inflammatory cytokines secreted by M1 macrophages increased CD4 T cells/Th1 and cytotoxic CD8 T cells, as illustrated in Figure 14 (Mills and Ley, 2014; Xia et al., 2017; Zhu and Zhu, 2020). Th1 and CD8 T secrete pro-inflammatory cytokines such as IFNy and TNFα to polarize more M1 macrophages, and M1 secreted pro-inflammatory cytokines including TNFα, IL-1 and IL-6 to trigger the inflammatory response (Delprat et al., 2020). Other than insulin-dependent diabetes mellitus, activation of T polarisation cell subsets especially Th1 cells, also contributes the other autoimmune diseases including gastritis, inflammatory bowel diseases, atherosclerosis, and sarcoidosis (Zhu and Zhu, 2020).

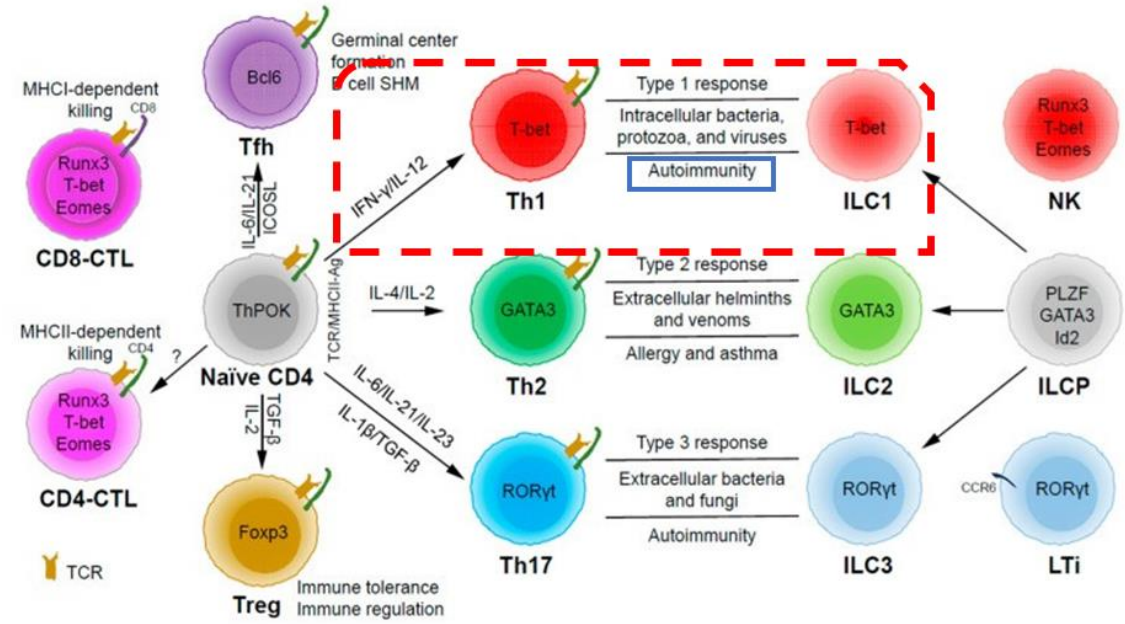

Figure 14: Mechanisms of T cell polarisation and differentiation in response to cytokine stimulation. Naïve CD4 T cells differentiate into specific T cell subsets depending on cytokine stimulation; T helper 1 (Th1) cells develop under the influence of interferon gamma (IFNγ), Th2 cells by interleukin 4 (IL-4), Th17 cells by IL-6, IL-21, IL23, IL-1β or transforming growth factor beta (TGFβ) and T regulator (Treg) cells by TGFβ and IL-1β. Additionally, effector CD8 T cells differentiate to directly kill the pathogen or intruder cells by expressing major histocompatibility complex class I (MHCI). Pathological conditions, such as hyperglycaemia (an auto-immune disease (blue box)) are associated with elevated levels of Th1 cells (red box), which function as pro-inflammatory cells (Zhu and Zhu, 2020).

In addition, the diagnosis of the metabolic disorder (e.g., insulin resistance and Hyperglycaemia) is associated with inflammation, which can be visualised through the expression of cytokines produced by the innate and adaptive immune cells. The role of cytokines in promoting pro and/or anti-inflammatory response is detailed in Table 2. In metabolic pathological conditions such as insulin resistance and obesity, adipose tissue exhibits high levels of IL-1β, IL-6 and TNFα, produced by M1 macrophages, while the expression of IL-4 and IL-10, cytokines produced by M2 macrophages, is reduced. This imbalance inhibits the expression of CD4+ Th2 cells and Treg cells, which secrete IL-4 and IL-13 to polarize M2 macrophages and mitigate inflammation. Altogether, the imbalance in pro and anti-inflammatory cytokine levels reflects the progression of insulin resistance and obesity, contributing to inflammation (Xia et al., 2017). These pathological findings suggest a bidirectional relationship between innate and adaptive immune responses in maintaining normal physiological conditions. In Table 1, I

summarise the immune cell profiles based on cell differentiation (CD) markers and their functions in innate and adaptive immune responses to facilitate understanding and evaluation for further investigation in this research.

1.1.2.1.2 Metabolic disorder versus inflammatory response that contributes to structural vascular dysfunction

In the previous sub-section, I elaborated on the example of pathological metabolic disorders versus their inflammatory effects. In this section, I describe examples of structural vascular dysfunction as a pathological condition that develops due to immune regulatory effects activated or enhanced by metabolic disorders.

Based on the morphology structure, the vasculature wall consists of ECs, VSMCs, fibroblasts, pericytes, and structural ECM components (e.g., elastin and collagen). ECs are the barrier to the blood-carrying lumen and vessel wall. ECs are surrounded by the TI and TM that consist of VSMCs and medial VSMCs function to facilitate vessel dilation and constriction. The outer layer of the vessel wall is known as tunica adventitia (TA) and consists of ECM which contains fibroblasts, blood and lymphatic vessels, nerves, and progenitor of MSC cells and immune cells, making the adventitia the most complex and heterogeneous compartment of the vessel wall. All components of the vessel wall are required to maintain structural integrity and preserve vascular health (Stenmark et al., 2013; Jaminon et al., 2019).

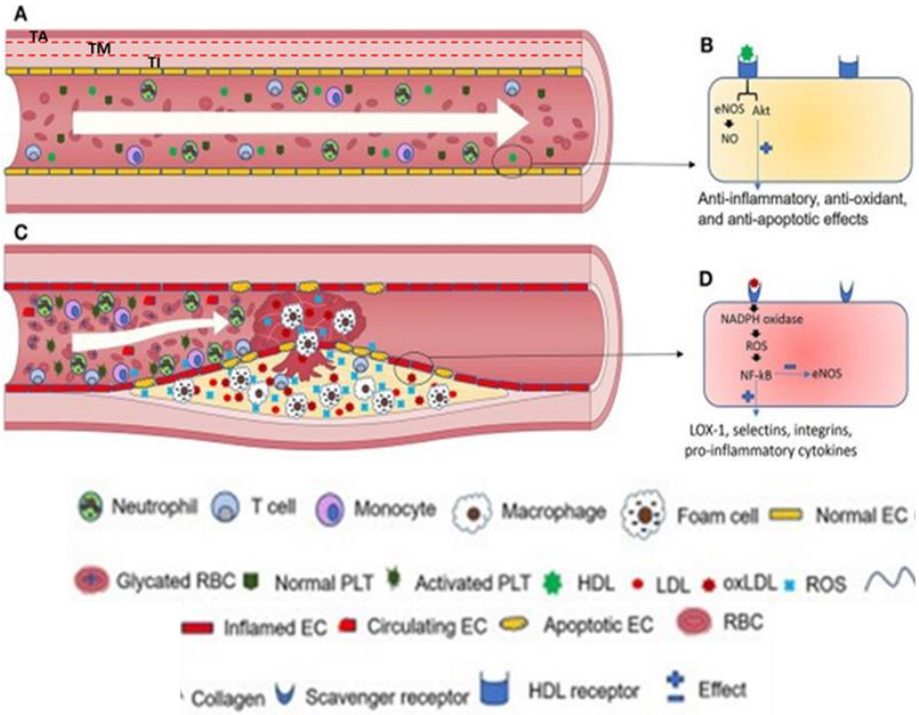

Figure 15: Comparison of blood vessels in healthy individuals and type 2 diabetes mellitus (T2DM) patients. (A) Normal blood flow of healthy individuals. (B) Illustration of high-density lipoprotein (HDL) binding to its receptors on endothelial cells (ECs) that results in the activation of anti-inflammatory cascades. (C) Abnormal blood vessels in T2DM patients (D) interactions of oxidised low-density lipoprotein (oxLDL) with its receptor aggravate reactive oxygen species (ROS) generation (Daryabor et al., 2020).

In the healthy TM, VSMCs are characterised by actively “contractile” and differentiated phenotype to maintain contractile function and consist of αSMA, smooth muscle myosin heavy chain (MHC) and h1-calponin (Casella et al., 2015). Effective vascular contractility depends on the elongation of actin filaments, however, during metabolic shift conditions such as high glucose, it stimulates the filamentous actin (F-actin) reorganisation which is associated with limited elongation of actin filaments (Rachubik et al., 2020). VSMC cytoskeletal reorganization leads to the prevalence of the synthetic phenotype which displays alterations in organelle distribution, aberrant matrix metabolism, and increased proliferation and migration (Casella et al., 2015).

The ECM is composed of various structural glycoproteins, including collagen-I, elastin, fibronectin and vitronectin. In the healthy vascular wall, such as the aorta, collagen-I and elastin are the primary structural ECM proteins that maintain aortic integrity. However, during vascular dysfunction, ECM remodelling occurs, which is further exaggerated when VSMC dedifferentiate into synthetic phenotype. This

phenotype is associated with increased collagen-I accumulation, elastin degradation and enhanced MMP enzymes including collagenases, gelatinases, stromelysins, matrilysins, membrane-type (MT) and other non-classified MMPs. The activation of MMPs degrades the elastic ECM and connective tissue, leading to VSMC migration. This migration results in uncontrolled collagen expression and thickening of the arterial wall, ultimately reducing aortic compliance (Afewerki et al., 2019).

The synthetic condition of VSMCs in the vascular wall can result from metabolic disorders of T2DM such as high glucose level. High glucose stimulates high ROS production by organelles/cells which create oxidation stress that causes injury to the EC (Evan et al., 2003; Koju et al., 2019). Injury not only increases the permeability of the leukocytes and oxLDL into the TI but also causes VSMC migration to the injury sites where they proliferate, produce ECM and undergo lipid uptake. Not only immune cells, but VSMC also produce inflammatory cytokines such as IL1β, TNFα and IL-6, and adhesion molecules (e.g. MCP-1) in response to high glucose environment to promote monocyte recruitment, survival and differentiation into foam cells, stimulate VSMC migration through a reorganization of the cytoskeleton, and soluble cytokines activate MMPs activity. Anti-inflammatory cytokines such as IL-4 and IL-10 function to counteract this process and preserve vascular integrity (Figure 15). However, an imbalance between pro and anti-inflammatory cytokines ultimately leads to the progression of vascular complications, including atherosclerosis and restenosis (Cecchettini et al., 2011; Reddy et al., 2016; Daryabor et al., 2020; Tsioufis et al., 2022).

Altogether, VSMCs undergo a ‘switching’ from a quiescent, actively contractile and differentiated phenotype to a synthetic phenotype in response to metabolic disorders (e.g. high glucose) and inflammatory cytokines. This switch is characterised by a reduction in contractile proteins such as smooth muscle-1 (SM-1) and smooth muscle-2 (SM-2), MHC, an increase in collagen deposition in the ECM, high migration and proliferation (Heinecke, 2006; Rask-Madsen and King, 2013). Therefore, VSMC dysfunction induced by pro-inflammatory cytokines produced either by inflammatory cells or by VSMCs themselves in response to abnormal physiological conditions that affect the vascular wall may be one of the key factors driving vascular changes in the blood vessel wall.

The major effects of phenotypic changes in VSMCs can lead to adverse outcomes, including promoting intimal thickening, the development of plaque bulges, and alterations in blood vessel stiffness. These changes consequently contribute to the progression of vascular diseases (Spagnoli et al., 2007; Rask-Madsen & King, 2013; Rafieian-Kopaei et al., 2014; Bacakova et al., 2018).

1.1.2.1.3 Metabolic dysfunctions shift the immune cell composition in other tissues/organ

In addition to vascular implications, metabolic disorders also significantly alter immune cell composition in various other organs. This section assesses the impact of abnormal metabolic conditions on different organs/tissues especially immune organs, predicting immune status through analysis of immune cell profiles. As previously mentioned, pathological conditions such as high glucose and high FFA, elevate the ROS level and increase the oxidative stress in the tissue leading to the inflammatory response (Figure 13) (Evan et al., 2003). This immune response is mainly driven by the immune cell phenotype, therefore, pathological conditions such as high glucose may affect the normal development of the immune cells in each organ. In detail, high glucose condition in T2DM increased pro-inflammatory myeloid cells (M1 macrophages) recruitment in the tissue which skewed the expansion of lymphocyte subsets (Th1 cells) that promote pro-inflammation (Nikolajczyk et al., 2011; Mills and Ley, 2014; Xia et al., 2017; Zhu and Zhu, 2020). Therefore, hyperglycaemia is suggested to alter immune cell phenotype composition into an inflammatory phenotype that contributes to the progression of the disease, ultimately causing organ failure.

Specifically, in the bone marrow, conditions like hyperglycaemia associated with diabetes can significantly impact HSCs and MPP cells (Hematopoietic stem and progenitor cells (HSPCs)). Glucose dysregulation has been observed to enhance the proliferation of GMPs and CMPs within the bone marrow. This increased proliferation leads to elevated levels of monocytes, specifically Ly6C^{hi} cells, which are released into the bloodstream and can migrate to atherosclerotic lesions. The influx of these inflammatory cells, characterised by monocytosis (elevated monocyte levels) and neutrophilia (elevated neutrophil levels), has been shown to impair the regression of atherosclerotic lesions (Nagareddy et al., 2013). This phenomenon highlights how metabolic shifts associated with conditions like

diabetes can influence the immune cell dynamics in the bone marrow and their subsequent impact on vascular health.

Besides that, the bone marrow of mice with hyperglycaemia shows elevated levels of proinflammatory cytokines, including IL-1β and TNF-α. This is one of the implications of glucose dysregulations that induced ROS overproduction, ER stress alterations, and production of AGEs (Vinci et al., 2020). These cytokines are crucial in the polarisation of macrophages towards the M1 pro-inflammatory phenotype (Batra *et al.,* 2018). Therefore, metabolic dysfunctions such as hyperglycaemia can foster the development of pro-inflammatory M1 macrophages within the bone marrow environment.

In the thymus, T cell development occurs in the peripheral cortex and a central medulla, where most of the T cell development takes place in the cortex and only mature SP T cells can be seen in the medulla (Thapa and Farber, 2019). During pathophysiology conditions such as glucose dysregulation, the normal structure of the thymus can be disrupted, thereby affecting immune cell development such as T cells within this organ. For instance, streptozotocin (STZ)-induced hyperglycaemia has been shown to cause degeneration of the thymic structure in mice. Thymus tissue from hyperglycaemic-induced mice exhibits characteristics such as giant vacuoles, increased connective tissue and mast-cell infiltration, and mitochondrial crystals (Elmas et al., 2008).

The normal T-cell development in the thymus needs extensive apoptosis to eliminate self-reactive and non-functional T cells. More than 95% of lymphocytes undergo apoptosis within the thymus, resulting in only 2–4% leaving as mature SP CD4+ and CD8+ T cells. However, in abnormal conditions such as in ovalbumin (OVA)-specific TCR transgenic mice, the hyperglycaemic condition has been observed to increase lymphocyte survival within the thymic tissue. This phenomenon occurs because glucose stimulates anti-apoptotic factors such as NADPH and B-cell Lymphoma 2 (BCL2) *via* the NFκB p65 pathway, thereby activating thymocyte metabolism. This metabolic activation results in a decrease in thymocyte apoptosis by inhibiting caspase activity. Consequently, the apoptotic process of T lymphocyte cells is suppressed in the thymus of STZ-induced mice (Ramakrishnan et al., 2011).

In the spleen, The RP and WP regions are occupied by various innate and adaptive immune cells, such as monocytes and macrophages of innate immune cells that mainly occupy RP and, T and B cells can be found in WP (Figure 10). These immune cells develop into effector immune cells when required and promote innate and/ or adaptive immune responses (Lewis et al., 2019). Changes in physiological conditions such as hyperglycaemia, obesity, and insulin resistance disrupt the normal regulation of immune cell development and immune responses in the spleen. Diets high in fat and sugar (HFSD) have been linked to elevated levels of proinflammatory serum markers like IL-6 and increased inflammation in peripheral tissues. Regarding the spleen's structure, obesity and diabetic pathologies are associated with enlarged spleen size, known as splenomegaly. These conditions also lead to the expansion of the RP and WP areas within the spleen (Buchan et al., 2018). WP in the spleen consists of immune cells that target blood-borne pathogens, while RP is involved in erythrophagocytosis (Elmor, 2006). HFSD have been shown to increase cellularity in the RP and elevate macrophage numbers (Buchan et al., 2018). The other study showed that hyperglycaemia modestly increased cytotoxic T-cells (CD8+CD3+ cells), reduced T-helper cells (CD4+CD3+ cells) and significantly increased Treg cells (FoxP3+CD4+cells) in STZ-treated mice spleen (Muller-Graff et al., 2018).

The relationship between inflammation and metabolic disorders within organs is indeed intricate. Changes in the composition of immune cell profiles can significantly impact the normal physiological functions of organs. This suggests a strong correlation between metabolic disorders and inflammation, where the development of pathological diseases can depend on the specific location of inflammation.

In detail, metabolic disorders have the potential to disrupt the normal development or recruitment of immune cells within organs, leading to alterations in their composition. A thorough understanding of immune cell development and recruitment in immune organs is essential to diagnose the tissue/organ physiology and correlate with the progress of the immune-related disease. Besides that, the functional macromolecule target that underlies the progression and development of the metabolic-associated disease is also valuable to understand. The involvement of the targets that regulate metabolic mechanisms

has been extensively explored over the past decades, where they aim to terminate the progression of metabolic diseases such as immune-related cardio-vascular disease, diabetes and obesity. Among these targets, transcription factors are important for maintaining metabolic homeostasis, which is transcription factor allows cells/organs to respond to a variety of intracellular/extracellular signals, thus playing vital roles in metabolism occurring in various organs or controlled by inter-organ communication. In the next section, I elaborates in more detail on the roles of transcription factors controlling the cellular function in immune regulation.

1.1.3 Mechanism of the gene transcription by transcription factor

Gene expression is tightly controlled at various levels by intrinsic and extrinsic factors including chromatin remodelling, gene transcription, post-transcriptional modification, translation and post-translational gene transcriptions. Regulation of gene expression at these multiple levels is a key factor to control cell functions (Ralston and Shaw, 2008).

Transcription regulation is the central of the gene transcription process that is controlled by the combination of cis-acting elements and trans-acting factors that cooperate to initiate and regulate gene expression (Figure 16). Cis-acting elements are located at various positions relative to the transcriptional start site of a gene, and include promoters, enhancers, silencers, and insulators, each plays a distinct role in the transcription regulation. Promoters of protein-encoding genes often comprise a “core promoter”, a region that can be found ∼40 bp upstream of the transcriptional initiation site and encompass the TATA box. Upstream of the core promoter region are the proximal and distal regions of promoters. Moreover, trans-acting factors are proteins that bind to cis-acting elements which include transcription factors, co-activators, co-repressor, RNA polymerase II and the other proteins that modulate the transcriptional complex activity. (Hernandez and Hiner, 2014; Ohnmacht et al., 2020).

The primary regulators of gene expression are transcription factors, which can be divided into general and tissue-specific transcription factors (Hernandez and Hiner, 2014; Ohnmacht et al., 2020). Cell-specific transcription activation is fundamentally regulated by the interaction between transcriptional co-activators

and transcription factors, as illustrated in Figure 16 (Mitsis et al., 2020; Ray and Spivakov, 2021; Talukdar and Chatterji, 2023).

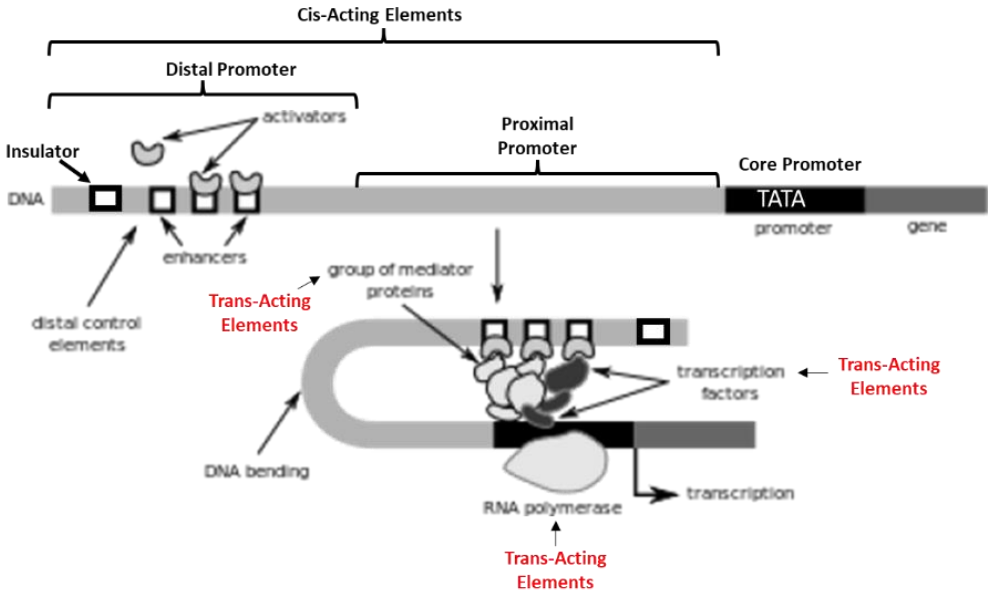

Figure 16: Transcription regulation of genes that control cell function. The process involves the cooperation between the cis and trans elements to initiate and regulate the gene expression. Dynamic regulation of gene transcription, participating in the structure of chromatin and folding of the distal promoter sequences to become proximal to the transcriptional complex (Hernandez and Hiner, 2014; Samanthi, 2018; Ohnmacht et al., 2020).

1.1.3.1 Transcription factors modulate metabolic dysfunctional immune-related disease

Gene transcription regulates key processes such as cell proliferation, differentiation, development, ageing, responses to stimuli, and various diseases. Dysregulation of transcriptional programming, including transcriptional machinery, transcription factors, co-factors, DNA-binding elements, mRNA processing, stability, transport, and translation, disrupts cellular homeostasis, contributing to pathophysiological effects (Hawkins et al., 2018).

Specifically, in pathological conditions such as metabolic disorders, inflammation, and vascular diseases (e.g., atherosclerosis, coronary artery disease, and myocardial infarction), transcription factors play a crucial role in transcriptional regulation, as illustrated in Figure 17 (Dandona et al., 2005; Song et al., 2019;

Luo et al., 2022). Consequently, these transcription factors often emerge as key contributors to the pathogenesis of these diseases.

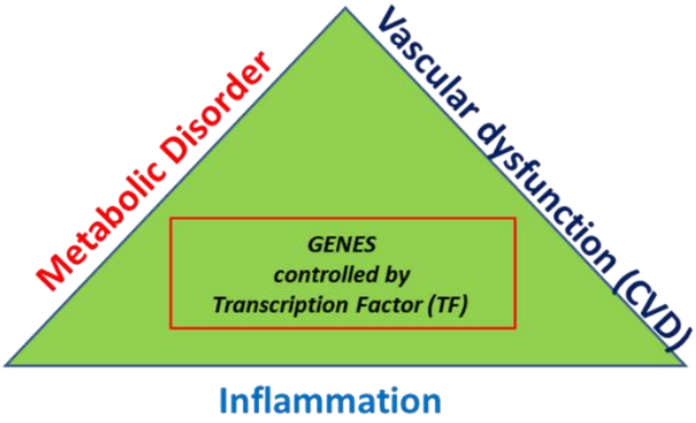

Figure 17: Transcription factor as a master regulator of metabolic disorder, inflammation and vascular disease. Extrinsic factors such as metabolic disorders (e.g. hyperglycaemia and hyperlipidemia) initiate the gene transcription that promotes inflammatory gene synthesis, which disrupts the immune regulation and ultimately causes the disease progression such as atherosclerosis in blood vessels. (Dandona et al., 2005; Song et al., 2019; Luo et al., 2022).

Studies have identified several transcription factors, including NFκB, AP1, signal transducer and activator of transcription (STAT), and nuclear factor of activated T cells (NFAT), that regulate inflammatory gene expression and immune cell phenotypes (Figure 18) (Adcock and Caramari, 2002). Mechanistically, NFκB is a key mediator of pro-inflammatory gene induction and functions in both innate and adaptive immune cells. The canonical NFκB pathway responds to diverse stimuli, including cytokine, PRRs, TNF, TCR and B-cell receptors. Stimuli activate IKK, which phosphorylates IκBα, leading to the nuclear translocation of canonical NFκB. NFκB then drives the transcription of genes, including pro-inflammatory factors that influence immune cell phenotypes (e.g., MIP-1α, MCP-1, GM-CSF) and cytokines/chemokines (e.g., IL-1β, TNF-α, CXCL8). It also regulates adhesion molecules like VCAM-1 and ICAM-1, essential for recruiting inflammatory cells (Adcock and Caramari, 2002; Redhu et al., 2011).

NFκβ also often co-regulates with other transcription factors, such as AP-1. AP-1 is activated through Fos (c-Fos, FosB, Fra-1, Fra-2) and Jun (c-Jun, v-Jun,

JunB, JunD) signal transduction pathway. Both AP-1 and NFκβ binding sites have been identified in the pro-inflammatory promoter region including IL-6 and CXCL8 (Khalaf et al., 2010).

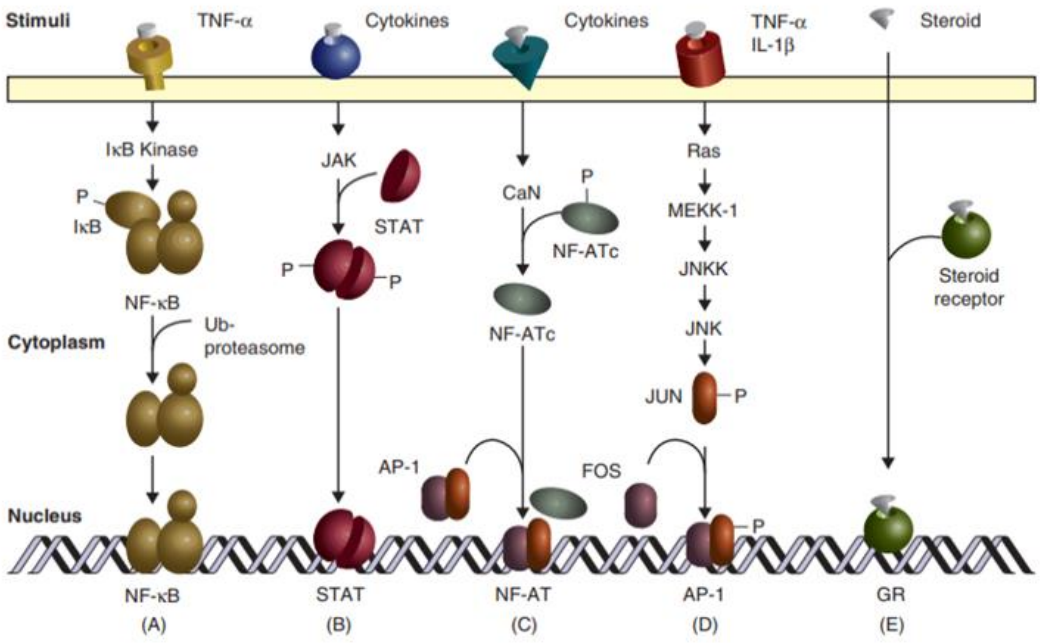

Figure 18: Transcription factors controlling immune response and cellular immune phenotypes. The binding of cytokines, growth factors, chemokines, or ligands to the cellular receptors activates A) nuclear factor-kappa B (NFκB) (B) signal transducer and activator of transcription (STAT) (C) nuclear factor of activated T-cells (NFAT) and (D) activator protein-1 (AP1) to enhance/repress the transcription of the inflammatory response (e.g., pro-, or anti-inflammatory) and immune phenotypic cell genes *via* modulation of signal transduction pathways (e.g., tyrosine kinases, mitogen-activated protein kinases (MAPK) and STAT pathway) (Adcock and Caramari, 2002).

Moreover, AP1 is also an important transcription factor that controls various cellular processes, including proliferation, apoptosis, differentiation, survival, migration and transformation. AP1 consists of Jun, Fos, Maf and ATF (Schnoegl et al., 2023). In transcription regulation, AP1 is activated by various stimuli including TNFα and IL-1β in turn, activates MAPK pathways. AP-1 is in a structure that consists of jun and fos, where jun forms homodimers or heterodimers with Fos through their leucine zipper domains. AP-1 dimers recognize specific response elements in the promoters and enhancers of target genes and transactivates or represses them. This transcription process produces various

genes, including those involved in the regulation of cytokines, chemokines, lymphocyte development, cell proliferation, differentiation, apoptosis, and migration. Dysregulation of AP1 expression can lead to pathogenic processes, such as cellular transformation, angiogenesis, metastasis, and immune or inflammatory disorders (Figure 18 and Figure 19) (Trop and Azar, 2017).

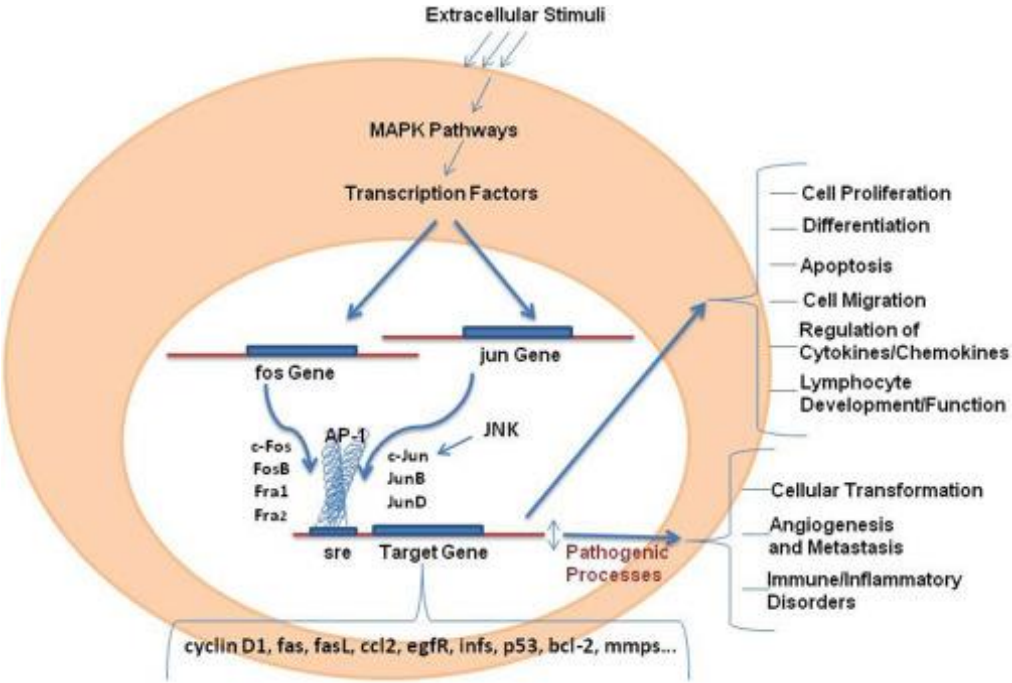

Figure 19: The role of activator protein 1 (AP1) in cellular processes and pathological conditions. During cellular homeostasis, the AP1 is activated to transcript various genes that control cell proliferation, cell differentiation, apoptosis, cell migration, production of cytokines and chemokines and lymphocyte development. Obstruction of the AP1 transcription regulation process causes pathological conditions such as angiogenesis, immune disorder, and cellular transformation (Trop and Azar, 2017).

On the other hand, STAT, protein regulators that control the immune regulatory system also has been studied extensively. STAT is composed of STAT1, STAT2, STAT3, STAT4, STAT5a, STAT5b, and STAT6 employed by more than 50 cytokines and growth factors. The signalling mechanism that begins with extrinsic factors such as cytokines or growth factors facilitates the trans-activation of receptor-bound Janus kinases (JAKS). Activated JAKS then causes STAT phosphorylation by tyrosine, commanding dimerisation into homodimers or

heterodimers, nuclear translocation and DNA binding. STAT binds to DNA sequence and then regulates the transcription that synthesises various genes including immune-related and non-immune-related genes (Villarino et al., 2015). Particularly, STAT 6 is the transcription factor that regulates the anti-inflammatory pathway and is activated by IL-4 and IL-13. IL-4 induces the Th2 cells to regulate the anti-inflammatory pathway in adaptive immune response (Shaheen and Broxmeyer, 2018). Moreover, in T lymphocytes, TGFβ inhibited IL-12-induced JAK2 and TYK2 tyrosine phosphorylation and STAT3 and STAT4 activation, resulting in diminished T-cell proliferation and reduced IFN-γ production. Therefore, in this case study, STAT3 and STAT4 are important transcription factors for T lymphocyte activation and differentiation (Hu et al., 2021).

Furthermore, the immune cell phenotype and immune response also has been driven by NFAT. NFAT modulate immune responses by driving the transcriptional regulation for the synthesis of numerous cytokines, chemokines, and growth factors in immune cells. Specifically, NFAT is crucial for shaping humoral immunity and immune tolerance and plays a different role in the different T cells. In stimulated TCR and co-stimulatory receptors of T cells, NFAT activated and bound on the specific DNA sequence target together with AP-1 (Jun/Fos). NFAT: AP-1 machinery complexes increase the synthesis of cytokines, chemokines and short NFAT2/αA isoform that enhances T-cell activation. Moreover, in Tfh cells, the stimulation of TCR and co-stimulatory receptors on T cells, activate and contribute to NFAT: AP-1 machinery complexes form on the promoter controls the expression of many genes such as IRF4 and BATF that regulate the differentiation of Tfh cells, and also regulate various other immune-related genes such as CXCR5, PD1, ICOS, CD40L, IL-21, IL4 and NFAT2/αA. Moreover, the other T cell phenotype controlled by NFAT includes peripherally induced Treg (iTreg) cells, natural Treg (nTreg) cells in the thymus, and anergic and exhausted T cells, as illustrated in Figure 20 (Vaeth and Feske, 2018). Collectively, these T cells' phenotypes and immune response are tightly regulated by NFAT directly or indirectly by co-regulating with the other Transcription factors and co-factors.

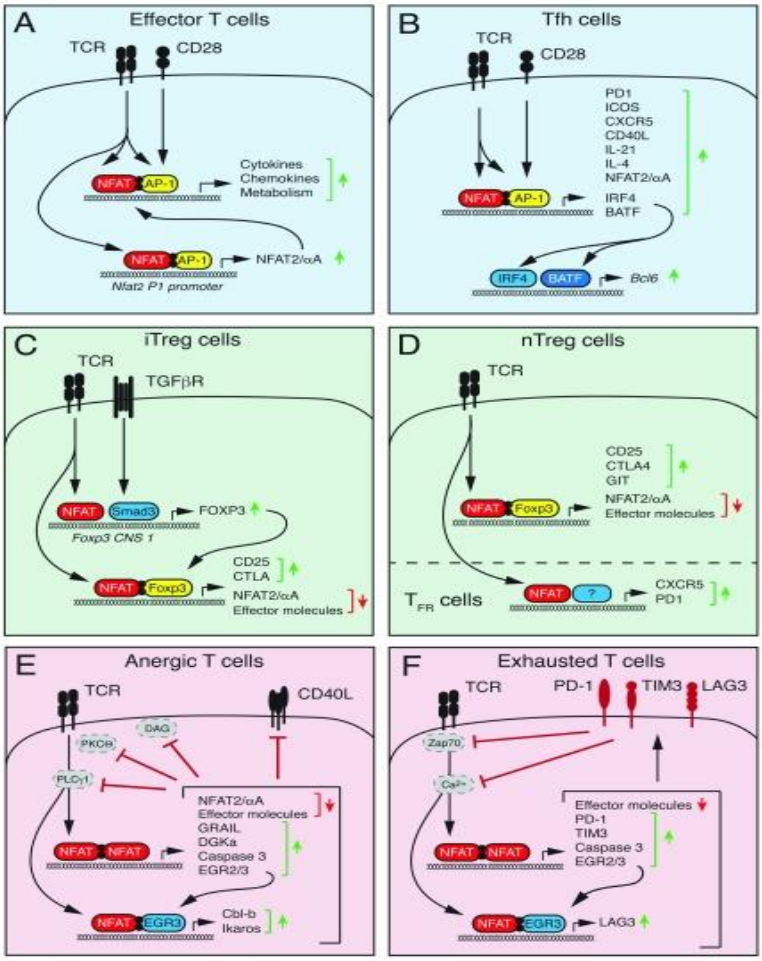

Figure 20: The different roles of nuclear factor of activated T cells (NFAT) in effector, follicular, regulatory, and tolerised T cells. NFAT can co-regulate with the same transcription factor (NFAT: NFAT) or with the other transcription factor (e.g. activator protein-1 (AP1), mothers against decapentaplegic homolog 3 (Smad3) and forkhead box P3 (Foxp3)) to enhance/repress the gene transcription that controls the function and differentiation of T cells including effector T cells, T follicular helper (Tfh) cells, induced T regulator (iTreg) cells, natural T regulator (nTreg) cells, anergic and exhausted T cells (Vaeth and Feske, 2018).

1.1.3.2 Overview of POU4F2/ Brn-3b transcription factor

Brn-3b is the important transcription factor that controls the functional of various tissues by regulating gene expression. In immune cells, Brn-3b has been shown to express in Jurkat cells (Bhagrava et al., 1993), peripheral blood mononuclear cells (PBMCs) (Ripley et al., 2005) and THP-1 cells (Nurminen et al., 2015). Besides that, Brn-3b also has been found in non-immune cells such as neurons of the developing and adult nervous system, breast epithelium, heart, aorta, testis, ovary and skeletal muscle (Budhram-Mahadeo et al., 2021).

In detail of Brn-3b background, it is the transcription factor that derives from the POU domain family. This transcription factor is composed of 2 subunits of the DNA binding domain, while their subunits are separated by a flexible link with variable lengths of amino acids. These helix-turn-helix (HTH) subunits are called POU-specific (POUs) domain (N-terminal) that binds to DNA with high specificity but low affinity and C-terminal homeodomain (POU_H) that binds to DNA with low specificity but high affinity. These POUs and POU_H domains are tied together by a poorly conserved linker and these domains work together to confer high specificity and high-affinity DNA binding to sites in gene promoters (Budhram-Mahadeo et al., 2021). The POU pronounced as a POW is derived from the original family members Pituitary- Pit-1, Octomer-1, Octomer-2, and Unc-86 of Caenorhabditis elegans. The POU-specific and homeodomain region that consists of 70 to 75 amino acids can be found upstream of the homeobox domain of some transcription factors (Herr and Cleary, 1995).

The POU domain is a well-conserved homeodomain and can be classified into 6 classes, POU1, POU2, POU3, POU4, POU5 and POU6 (Gold et al., 2014). Brn-3b transcription factor is derived from the Class IV PitOct-Unc (POU) - domain family together with Brn3a and Brn3c. These proteins share the DNA binding domain but different transcription factors where transcription factor 1 (POU4F1) is denoted for Brn3a, transcription factor 2 (POU4F2) for Brn3b and transcription factor 3 (POU4F3) for Brn3c, and these proteins encoded by different genes (Pan et al., 2005; Ounzain et al., 2011).

Brn-3b is encoded by two exons separated by an intron. Alternative splicing of exons 1 and 2 produces the longer ~43 kDa Brn-3b (L) isoform, while the shorter ~30 to 35 kDa Brn-3b (S) isoform is encoded solely by exon 2 (Figure 21) (Irshad et al., 2004; Mele et al., 2019; Budhram-Mahadeo et al., 2021). Research suggests that Brn-3b isoforms may have distinct roles. Findings by DeCarvalho et al., (2004) highlight differences in their expression in the lateral line and visual system zebrafish. The Brn-3b (L) was detected at 18 hours post-fertilization (hpf), whereas the Brn-3b (S) appeared later, at 36 hpf, and lower levels. Both isoforms were subsequently observed in the functional larval retina (72 hpf) and the adult retina and tectum. These findings provide evidence supporting the distinct functions of the protein isoform in cell development.

The binding site sequence for the Brn-3b POU domain is GCATGCGTAATGC, whereas the Brn-3b protein binds with lower affinity (Xiang et al., 1995). The DNA binding sites can be found in gene promoters (Budhram-Mahadeo et al., 2021). Brn-3b/POU4F2 transcription factor can, directly and indirectly, regulate the gene synthesis. The direct mechanism involves the Brn-3b transcription factor binding to BRNF DNA binding sites of the promoters or enhancers and either activating or repressing transcription of target genes, depending on cell/tissue type (Yogendran et al., 2023). While Brn-3b controls gene expression indirectly by co-regulating with the other proteins to regulate the target genes (Budhram-Mahadeo et al., 2021). Thus, Brn-3b can drive complex effects on gene expression and control cell functions and diseases depending on interaction and co-expression with other regulators. The direct and indirect effects regulated by tissue specific-Brn-3b transcription factor are elaborated further in the next section for a more extensive understanding of Brn-3b role in controlling the cellular mechanism or functions.

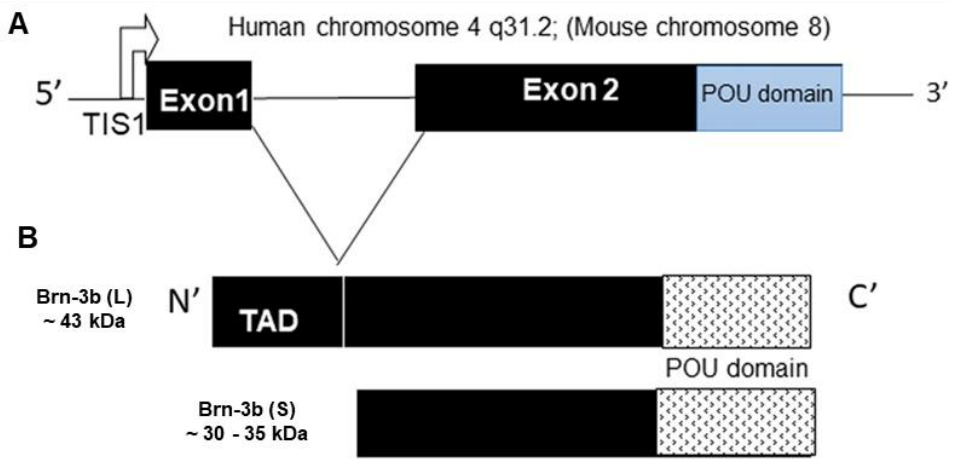

Figure 21: Schematic overview of Brn-3b protein structure and isoforms with exon splicing variants. The schematic diagram shows (A) the Brn-3b protein structure, which is encoded by two exons, and (B) the Brn-3b protein isoforms. Splicing of exons 1 and 2 gives rise to the longer Brn-3b (L) isoform (~43 kDa), while the shorter Brn-3b (S) protein (~30–35 kDa) is encoded by exon 2 (Irshad et al., (2004), Mele et al., 2019; Budhram-Mahadeo et al., 2021).

1.1.3.2.1 POU4F2/Brn-3b transcription factor controls the cell functions

As previously mentioned, the POU4F2/Brn3b transcription factor can control the cellular process either directly or indirectly in different cells/tissues. In the direct mechanism of gene transcription, Brn-3b regulates the transcription of various target genes directly including Hedgehog (SHH), glucose transporter type 4 (GLUT4), Pax6, naCHR2, heat shock protein 27 (HSP-27), Cyclin D1, CDK4, BRCA-1, Dxl1/2, neuronal genes, plakoglobin and ACE following by RNA Pol (II) following its specific binding on the BRNF DNA binding sites (Figure 22) (Budhram-Mahadeo et al., 2021). In cellular processes, Brn3b serves as a critical protein regulator, maintaining cellular or tissue homeostasis; its absence can lead to pathological consequences. For example, in glucose and insulin homeostasis, which is primarily regulated by glycogen synthase kinase-beta (GSKβ) and GLUT4. GLUT4 functions as a channel for glucose transport. Insulin stimulates the translocation of GLUT4, resulting in a 10- to 20-fold increase in glucose transport (Gupta, 2022). Moreover, in response to insulin, GSKβ is phosphorylated and inactivated, permitting the activation of glycogen synthase (GS) and subsequent glucose storage as glycogen (Wang et al., 2022).

However, Brn3b deficiency has been associated with the dysregulation of these proteins. Specifically, the absence of Brn3b leads to an increase in GSKβ and a decrease in GLUT4 in insulin-responsive tissues such as skeletal muscle and adipose tissue (Bitsi et al., 2016). Mechanistically, Brn3b may directly regulate the synthesis of the GLUT4 gene in these tissues, enhancing glucose transport. Additionally, Brn3b may suppress GSKβ activity to inhibit glucose production, thereby controlling blood glucose levels. Consequently, a reduction in Brn3b may cause metabolic disorders linked with these target genes such as hyperglycaemia and insulin resistance.

Further investigation by Bitsi et al., (2016), using co-transfection assay has validated the data by showing that GLUT4 is directly transactivated by the Brn-3b transcription factor at promoter binding sites in C2C12 cells. This finding provides additional validation that Brn-3b is an important regulator required to prevent metabolic dysfunction (e.g., hyperglycaemia, obesity, and insulin resistance).

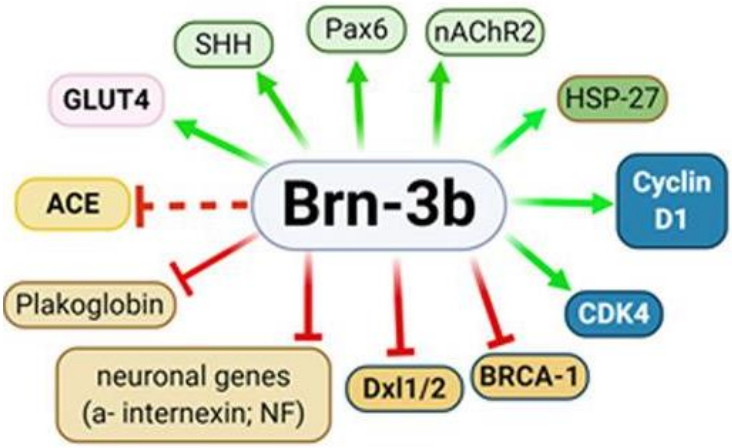

Figure 22: Brn-3b target genes in the regulation of cellular processes. Brn-3b can directly mediate cellular effects by regulating the expression of a diverse set of genes that control many cellular processes including proliferation, metabolism and apoptosis (Budhram-Mahadeo et al., 2021).

Besides that, Brn-3b transcription factor allows cell cycle progression and promotes proliferation in breast cancer and neuroblastoma cells by directly activating Cyclin D1 and CDK4 (Samady et al., 2004; Budhram-Mahadeo et al., 2008). Brn-3b has directly repressed the tumour suppressor gene, BRCA1 in breast cancer tissue, which then promotes tumour development. The sample group with low Brn-3b caused elevated BRCA-1 (Budhram-Mahadeo et al., (1999). On the other hand, western blot analysis shows an increase of cyclin D1 protein in neuroblastoma cells (IMR32) overexpressing Brn-3b (Brn-3b+) and decrease in cells with reduced Brn-3b (3b α-sense) compared with LTR1 (vector) control (Budhram-Mahadeo et al., 2008).

In addition, Brn-3b can cause drug resistance and migration by strongly transactivating the HSP-27 promoter in MCF-7 cells and human breast biopsies, while the loss of Brn-3b reduces HSP-27 expression (Lee et al., 2005). Besides that, Brn-3b also upregulates the HSP27 protein in the ovarian cancer cell, SKOV3 cell lines. Knockdown of Brn-3b resulted in the loss of HSP27 protein expression, hence proving that Brn-3b can directly activate HSP27 gene transcription in ovarian cancer (Maskell et al., (2018). This finding indicates that in cancer cells (e.g., Breast cancer, neuroblastoma and ovarian cancer), the Brn-3b transcription factor can be an important biomarker target to prevent the proliferation and migration of the cancer cells.

Furthermore, the Brn-3b transcription factor is also a crucial regulator in maximizing the transcription of the apoptosis-related genes (e.g., P53 and BAX). Mechanistically, the P53 protein has been shown to trans-activate the BAX promoter, for apoptotic genes synthesis. Brn-3b enhances this process by direct contact with the P53 protein *via* its DNA binding domain (DBD) on the BAX promoter, thereby increasing apoptotic gene expression in neuronal cells (ND7). In contrast, the direct binding of Brn-3b on the BAX promoter without P53 protein results in little effect. This finding underscores the essential role of Brn-3b as a transcription factor in promoting programmed cell death (apoptosis) through its co-regulation with the P53 protein (Budhram-Mahadeo et al., 2006).

Further validation of this role was demonstrated by Budhram-Mahadeo et al., 2014, who studied the co-regulation of P53 and Brn-3b in other cells/tissues, such as cardiomyocytes cells. In this study, cardiac infarction was induced in the heart to investigate the co-expression between P53 and Brn-3b in the infarct zone of the injured tissue. The finding illustrated that Brn-3b expressed in the non-infarct zone, where P53 protein was undetectable, however, its expression was maximised in the injured myocardium that expressed high P53. The co-expression of POU4F2/Brn-3b with P53 appears to be crucial for controlling apoptosis in the injured heart region.The apoptosis mechanism was confirmed by the expression of pro-apoptotic genes, including BAX, PUMA, NOXA and cleavage caspase 3. The interaction between Brn-3b and P53 was further validated using shRNA-mediated Brn-3b gene silencing. Knockdown of Brn-3b in neonatal rat ventricular myocytes (NRVM) or rat cardiomyoblasts (H9c2) cell lines significantly reduced BAX and NOXA protein levels, while P53 expression remained unchanged. Since reducing Brn-3b was sufficient to decrease pro-apoptotic proteins such as BAX, despite unchanged P53 expression, these findings suggest that Brn-3b is required for the maximal expression of pro-apoptotic target genes in the injured myocardium (Budhram-Mahadeo et al., 2014). However, its interaction with P53 in regulating apoptotic gene expression in NRVM and H9c2 cells still requires validation by analysing the Brn-3b binding sites at the target promoters.

1.1.3.2.2 POU4F2/Brn-3b prevent metabolic dysfunction in metabolic tissue and heart

Diabetes is a metabolic disease that is caused by metabolic changes including hyperglycaemia which develops by insulin resistance in insulin-sensitive tissues (Lima et al., 2022). Mechanistically, β cells of the pancreas secrete insulin following the expression of GLUT2 on the pancreatic surface that facilitates glucose transport into the pancreas (Sun et al., 2023). Moreover, insulin enhances GLUT4 transporter for the glucose uptake into metabolic tissue (e.g., Skeletal muscle and adipose tissue) to ensure homeostatic control of blood glucose levels (Czech, 2017). In the liver, hepatocytes respond to insulin by inhibiting gluconeogenesis and promoting glycogenesis, thereby, maintaining blood glucose homeostasis. When blood glucose levels are low, the pancreas releases glucagon, which stimulates hepatocytes to increase gluconeogenesis and glycogenogenesis, thus raising blood glucose levels to their homeostatic range. However, dysregulation of this process leads to hyperglycaemia and contributes to T2DM. Uncontrolled hyperglycaemia can promote inflammation and vascular changes that contribute to cardiovascular, renal, and neuropathic diseases (Figure 23) (Roder et al., 2016; Galicia-Garcia et al., 2020).

POU4F2/Brn-3b functions to control normal metabolic processes, and the deficiency of Brn-3b leads to dysregulation of metabolic functions such as hyperglycaemia, insulin resistance and hemodynamic stress (Bitsi et al*.,* 2016; Mele et al*.,* 2019). In pathological conditions such as hyperglycaemia that are observed in the global Brn-3b KO mouse blood, it is accompanied by the increased insulin level in the blood serum. It shows that the Brn-3b transcription factor is an important regulator in preventing insulin resistance and hyperglycaemia. Besides that, Brn-3b expression is also diminished in skeletal muscle and adipose tissues of obese mice (high-saturated-fat diet mice). The consequence of obesity, hyperglycaemia and insulin resistance in the Brn-3b KO mice indicated that the loss of Brn-3b may promote metabolic dysfunction (Bitsi et al., 2016).

Further validation of the importance of the Brn-3b transcription factor to prevent metabolic dysfunction has been shown in *in vitro* studies using skeletal myoblast-

derived cells, and C2C12 cells. In this experiment, C2C12 cells were grown in a non-glucose (NG) medium or NG medium supplemented with 25 mmol glucose in the absence of insulin (NG-GLU) or with added insulin (NG-GLU-INS). Control cells were grown in full growth medium (FGM). The finding shows that Brn-3b mRNA and proteins are reduced in cells grown in NG media or the presence of insulin but increased following the addition of glucose (25 mM). These effects may be mediated at the transcription level, as NG or insulin can repress the Brn-3b promoter, while the addition of glucose stimulates promoter activity. The tight regulation of Brn-3b observed following insulin and glucose treatments suggests that this transcription factor will have an important role(s) in regulating genes associated with glucose uptake. It is validated when further investigation shows that the loss of Brn-3b in skeletal muscle affects the expression of key metabolic genes including GSK3β and GLUT4. Loss of Brn-3b reduced GLUT4 glucose transporter and increased GSK3β (Bitsi et al., 2016). Dysregulation of these genes is associated with the metabolic disorder including insulin resistance and glucose tolerance.

The regulation of these genes also has been study in C2C12 cells. The potential of Brn-3b binding sites has been identified by bioinformatic analysis and co-transfection studies combined with reporter assays. The finding shows the increase in exogenous Brn-3b highly transactivates the GLUT4 promoter in C2C12 cells. Moreover, Genomatix Transfect analysis illustrated that the GLUT4 gene promoter contains multiple Brn-3b binding sites and ChIP analysis demonstrated that Brn-3b binds directly to the proximal sites in the GLUT4 promoter in intact myoblast cells (*in vivo*) (Bitsi et al., 2016). These findings show strong evidence for a significant correlation between Brn-3b and GLUT4 expression from *in vivo* and *in vitro* studies.

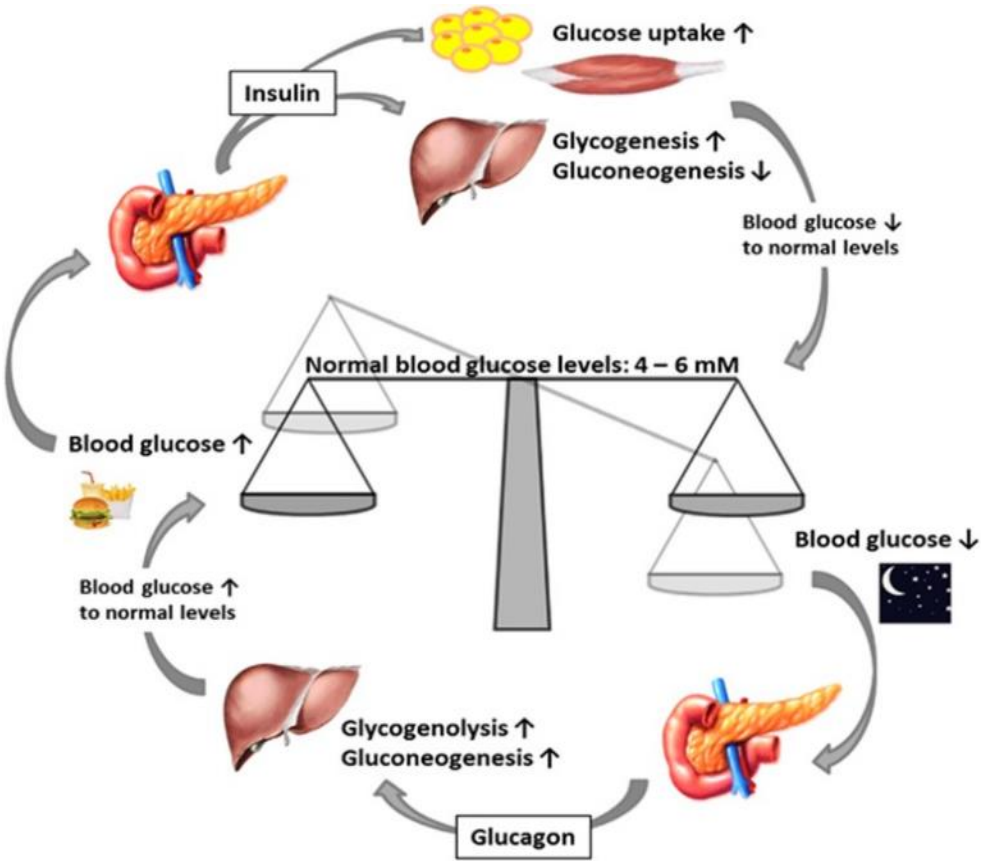

Figure 23: Mechanism of blood glucose homeostasis involving insulin and glucagon regulation. When the blood glucose rises above the normal range, this stimulates insulin secretion from the pancreas. Insulin then promotes glucose uptake by metabolic tissues such as adipose tissue and skeletal muscle. Insulin also acts on the liver by inhibiting gluconeogenesis and increasing glycogenesis, thereby reducing the blood glucose level to its homeostatic range. Conversely, when blood glucose levels fall below the normal range, the pancreas releases glucagon, which plays an important role in elevating glycogenolysis and gluconeogenesis in the liver, thus raising blood glucose levels to their homeostatic range (Roder et al., 2016).

1.1.3.2.3 POU4F2/Brn-3b transcription factor is an important regulator for adaptative to stress and injury in heart

The processes of growth (hypertrophy), angiogenesis, and metabolic plasticity are important for maintaining cardiac homeostasis (Shimizu and Minamino, 2016). Hypertrophic growth, which is the process of an increase in the size of an organ or part, particularly muscle is believed to have a compensatory role that reduces wall stress. However, a continual hypertrophic response can cause adverse re-modelling and cardiac decompensation/deterioration, and contribute to left ventricular dysfunction, dilated cardiomyopathy, ischemic heart disease,

heart failure and sudden death. Pathological hypertrophy can be induced by hypertension, valvular disease or myocardial infarction. Cardiac hypertrophy is categorised by the changes in shape of the heart such as concentric hypertrophy and eccentric hypertrophy. Concentric hypertrophy is identified by the shape change due to pressure overload in conditions such as aortic stenosis or hypertension and it is characterised by an increased cardiomyocyte diameter, due to an increase in wall thickness and decrease of left ventricular lumen. Eccentric hypertrophy occurs due to volume overload in conditions such as chronic aortic regurgitation, mitral regurgitation or myocardial infarction and is characterised by an increase in cardiomyocyte length and dilated left ventricle with thinning of its wall (Van et al., 2008).

Adult hearts undergo hypertrophic growth in response to the increased workload (e.g. prolonged stress or injury). During this process, early adaptive responses by cardiac tissue (e.g. cardiomyocytes) are crucial to maintain the cardiac output. The latter stages of pathological responses (e.g. cardiomyocyte apoptosis and fibrosis) can cause adverse remodelling which ultimately leads to heart failure (Mele et al., 2019). Cardiomyocyte functions are influenced by the re-expression of foetal genes including atrial alpha or beta-type natriuretic peptides (ANP, BNP), *β*-MHC and *α*-skeletal actin (*α*-SKA), and down-regulation of adult cardiac genes such as sarcoendoplasmic reticulum Ca^{2+} ATPase (SERCA) and *α*-MHC (Du, 2007). In the adult, cardiomyocyte cells are unable to proliferate in response to the cardiac stressor, however, re-expression of foetal genes can maintain the cardiac output and function (Zhang et al*.,* 2003; Ponnusamy and Wang, 2017). In addition, the other characteristic of adaptive changes such as cellular growth and metabolic switching arises from the extensive expression of genes including cell cycle genes (e.g. cyclin D1/CDK4) (Glaviano et al., 2024) and glucose transporter genes (e.g. GLUT4) (Sticka et al., 2018). Therefore, the strategy for adaptation changes response is by re-expression of the foetal genes and expression of metabolic and cell growth/cell cycle genes.

Following this, Brn-3b can be recognized as an important regulator to control the expression of foetal genes following pathological stress in adult mice. Originally, Brn-3b is highly expressed in developing hearts and reduced in adult hearts. However, Brn-3b expression increased again following pathological stress in

adult cardiomyocytes. It is shown when Brn-3b mRNA and protein are increased in angiotensin-II (AngII) treated mouse hearts following the hypertrophic changes that display the foetal gene expression including ANP/βMHC (Mele et al., 2019; Budhram-Mahadeo et al*.,* 2021).

In cell culture studies, AngII treatment stimulates the expression of Brn-3b, and its expression correlates with the increased expression of fetal markers, such as ANP/βMHC, and displays sarcomeric remodelling in H9c2 and NRVM cells (Mele et al., 2019). Besides that, GLUT4 is also elevated in AngII-treated heart (WT) and NRVM and H9c2 cell lines, correlating with high Brn-3b expression in these cells/tissues. GLUT4 levels are reduced in AngII-treated Brn-3b KO hearts (Mele et al., 2019). It is indicated that Brn-3b and GLUT-4 are important in driving adaptation by metabolic switching from fatty acid to glucose in response to pathological changes (e.g., stress and metabolic dysfunction). Glucose is required for myocardial adenosine triphosphate (ATP) production to maintain heart contractile function in response to pathological stress (Shao and Tian, 2015). In this study, cyclin D1 was also increased in the mouse heart (WT), as well as in NRVM and H9c2 cell lines. AngII treatment increased the expression of cyclin D1 in these cells/tissues. Mechanistically, cyclin D1 is an important adaptive marker for cardiac hypertrophy (Busk et al., 2002; Mele et al., 2019). Thus, Brn-3b may play an important role in maintaining the cardiac output by controlling adaptive hypertrophic responses in the heart in response to stress.

Furthermore, Brn-3b is also a curial regulator for controlling the injury adaptive response. In the cardiac injury model developed by coronary artery ligation in mouse heart, Brn-3b is highly expressed throughout the injured region and it is co-localised with p53, however, Brn-3b is also found in the non-ischaemic region of the heart, which lacked p53. High expression of Brn-3b and p53 in the injured hearts on day 1 after coronary artery ligation correlated with the increase of apoptotic markers including cleaved caspase-3 and pro-apoptotic proteins such as Bax, Noxa and PUMA, however, antiapoptotic marker which is Bcl-2 and Bcl-XL remain unchanged (Budhram-Mahadeo et al., 2014). The Cardiomyocyte apoptosis mechanism is important to remove the damaged cells in the infarct area in the early phase, however, further apoptosis mechanism will cause

cardiomyocyte loss which is the determinant of morbidity and mortality after myocardial infarction (Kim and Kang, 2010).

Following injury, the response of the immune system is then triggered. Initially, immune cells are recruited to the injured tissue to clear the debris and dead cells and degrade the ECM. Furthermore, programmed resolution of inflammation recruits and activates myofibroblasts for ECM deposition and angiogenesis. Inflammation is crucial for cardiac repair and regeneration. However, the imbalance between the pro and anti-inflammatory programmes that cause prolonged and unresolved inflammation leads to tissue damage, increased infarct size and adverse re-modelling, ultimately causing heart failure (Lai et al., 2018). Brn-3b has been identified in various immune cell populations including PBMCs, T cells, and monocytes (Bhagrava et al., 1993; Ripley et al., 2005; Nurminen et al., 2015). Brn-3b expression is linked to regulating various aspects of cell function, including proliferation, differentiation and apoptosis. Considering its presence in immune cells, Brn-3b might influence inflammatory pathways and potentially have an impact on vascular function, which could be relevant in the progression of vascular diseases (Budhram-Mahadeo et al., 2014; Mele et al., 2019; Bitsi et al., 2016; Budhram-Mahadeo et al., 2021; Yogendran et al., 2023). Therefore, implicating Brn-3b in early responses following injury suggests a potential role in modulating inflammation and adaptation, processes that may contribute to cell survival or reduced cell death (Figure 24) (Budhram-Mahadeo et al., 2014; Mele et al., 2019).

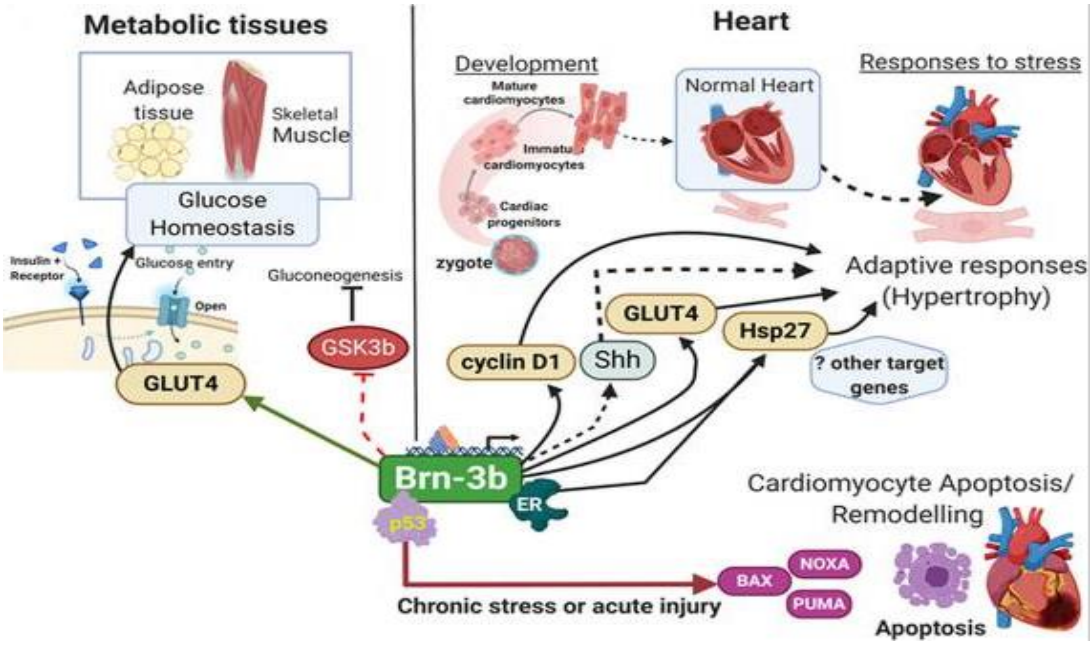

Figure 24: Interaction of Brn-3b and other regulators in metabolic tissue and heart. Brn-3b can control the normal tissue health and response to adaptive changes (e.g. stress or injury) by directly or indirectly co-regulate with the other proteins to promote/inhibit the genes such as metabolic genes (e.g. glucose transporter 4 (GLUT 4), glycogen synthase kinase-3 beta GSK3β), cellular growth genes (e.g. cyclin D1), apoptotic genes (e.g. Bcl-2–associated X (BAX), phorbol-12-myristate-13-acetate-induced protein 1 (NOXA), p53 upregulated modulator of apoptosis (PUMA)) (Budhram-Mahadeo et al., 2021).

1.1.3.2.4 Linking of POU4F2/Brn-3b transcription factor with metabolic dysfunction contributes to CVD

Pathologically, diabetes is a disease that can increase the susceptibility of the blood vessels to CVD by promoting injury or vascular changes (Rask-Madsen & King., 2013). High glucose induces mitochondrial dysfunction and increases ROS production. This intrinsic factor would damage the ECs, recruit monocytes and macrophages and activate T cells to produce cytokines which then promote inflammatory responses (Figure 24). The development of CVD is enhanced due to diabetes mellitus (e.g., hypertension, atherosclerosis, myocardial infarction, stroke, and peripheral vascular disease) (Yuan et al., 2019).

The link between the Brn-3b transcription factor with diabetes mellitus and cardiac dysfunction is previously shown in the review written by (Budhram-Mahadeo et al., 2021). It is illustrated that the loss of Brn-3b contributes to metabolic dysfunction by promoting insulin resistance and hyperglycaemia in

insulin-related tissue, mouse skeletal and adipose tissue. In the cardiac dysfunction issue, Brn-3b KO causes adverse re-modelling after treatment with AngII in male adult heart tissue by promoting contractile dysfunction that contributes to poor cardiac function (Budhram-Mahadeo et al., 2021). The impaired condition in the global Brn-3b KO samples suggests that Brn-3b is important in preventing metabolic dysfunction and adverse remodelling of heart tissue in response to pathological changes (e.g., injury and hemodynamic stress)

In addition, Brn-3b may be an important marker for maintaining the physiology of vascular health, where vascular changes can lead to CVD (Ghebre et al., 2016). The current study by Yogendran et al., (2023) shows that the loss of Brn-3b alters the expression of αSMA and Ki67 proteins in VSMCs isolated from mouse aortas, as well as elastin and MMP2 genes in mouse aorta tissue. The alteration of these genes/proteins can affect the regulation of arterial compliance and vascular tone in vessels, thereby increasing the risk of CVD. However, the mechanisms underlying metabolic dysfunction, adverse remodelling of heart tissue, and vascular changes are not fully understood. As previously mentioned, the Brn-3b transcription factor has been shown to be expressed in immune cells (Bhagrava et al., 1993; Ripley et al., 2005; Nurminen et al., 2015), and immune cells are involved in hyperglycaemia and CVD-related pathological conditions, such as cardiac injury, stress, and vascular changes (Daryabor et al., 2020). The connection between Brn-3b and immune regulation is crucial for understanding its potential role in CVD-related pathological conditions and metabolic dysfunction. This is especially important since inflammatory responses play a critical role in the progression of these diseases (e.g., adverse remodelling of heart tissue) (Li and Wang, 2021). Therefore, an extensive investigation into the link between Brn-3b and immune regulation, which strongly correlates with CVD conditions (e.g., vascular changes, cardiac injury/stress) and metabolic disorders (e.g., diabetes mellitus), is necessary.

1.2 Aims and Hypothesis

In previous studies, glucose and insulin levels were found to increase following glucose bolus administration in Brn-3b global KO mice. GLUT4 expression was reduced, and GSKβ was increased in the adipose tissue and skeletal muscle,

potentially correlating with metabolic dysfunctions such as obesity, insulin resistance, and hyperglycaemia (Bitsi et al., 2016). Brn-3b KO also altered protein and gene expression (αSMA, antigen kiel 67 (Ki-67), MMP2, and elastin), essential for vascular integrity (Yogendran et al., 2023), and reduced adaptive markers (ANP/βMHC, GLUT4, and Cyclin D1), critical for maintaining cardiac output under stress (Mele et al., 2019). Additionally, in a cardiac injury model, Brn-3b co-localized with P53 in infarction areas, suggesting a role in apoptotic clearance *via* BAX, NOXA, and PUMA.

Collectively, these studies suggest that Brn-3b plays a role in regulating metabolic dysfunction, vascular changes, and heart disease (CVD). Since metabolic dysfunction and CVD are inflammation-related diseases involving complex immune pathways, it is hypothesised that Brn-3b may function as a regulator of immune responses and help prevent chronic conditions like T2DM and vascular dysfunction. Evidence of Brn-3b expression in immune cells, including THP-1, Jurkat, and PBMCs (Bhagrava et al., 1993; Ripley et al., 2005; Nurminen et al., 2015), further supports this hypothesis. Preliminary findings also show that Brn-3b KO significantly reduces B cell populations in the spleen and decreases macrophages and dendritic cells in a zymosan-induced peritonitis mouse model (Mele et al., unpublished data). Based on these observations, the following hypothesis is proposed:

Hypothesis: The loss of Brn3b transcription factor may increase pro-inflammatory immune cells and may also contribute to vascular dysfunction

Aims:

1. To investigate how Brn-3b protein expression changes following inflammatory marker treatment in *in vitro* cell lines, THP-1 and T Jurkat cells.
2. To elucidate the potential function of Brn-3b in immune regulation using the global Brn-3b KO mouse model
3. To investigate the potential link between immune response and structural vascular changes protein in the aorta using Brn-3b KO mouse model

2 MATERIALS AND METHODS

2.1 Materials

In this study, all tissue culture reagents were supplied by Gibco and Sigma Aldrich (Poole, Dorset, UK). Tissue culture plastic ware was obtained from Starstedt (Nümbrecht, Germany). Unless otherwise stated, all chemicals and reagents of analytical grade were purchased from Sigma Aldrich (Poole, Dorset, UK) and Merck (Poole, Dorset, UK). Additional laboratory materials were provided by the suppliers shown in Table 16 (Appendix 1).

2.2 Human cell lines study

In this study, both THP-1 and Jurkat cell lines were used to study Brn-3b expression in monocytic and lymphocyte cell lines. THP-1 cells were cultured in RPMI Medium 1640 medium, supplemented with 10% heat-inactivated foetal bovine serum (FBS), 1% penicillin-streptomycin, 2.6 g/L glucose, HEPES, sodium dehydrate and 2-mercaptoethanol (BME). Moreover, Jurkat cells were cultured in RPMI Medium supplemented with 10% heat-inactivated FBS and 1% penicillin-streptomycin until the flask reached 70% confluency. The cells were then used for further experiments. The cell culture procedure was modified from the ATCC guideline protocol and Aldo et al., (2013).

2.2.1 Brn-3b expression in undifferentiated THP1 cells

After the cells reached 70% confluency, $1x10^6$ cells were seeded into each well of 6 well plates. The cell stress due to the centrifuge would affect the inflammatory response data, therefore the cells were pre-incubated overnight in the humidified incubator at 37^o C with 5% CO2. After overnight, the cells were treated with different 0.01, 0.05 and 0.1 uM vitamin D3 for a dose-dependence study. Moreover, the cells were treated with 0.01 uM vitamin D3, 0.1 ug/mL of IFNy and 0.02 ug/ml IL-4 to measure the effects of pro/anti-inflammatory marker on Brn-3b expression of undifferentiated THP-1 cells. After the treatment, the cell was collected into a 15 mL centrifuge tube and centrifuged at 700 x g for 5 minutes.

After the centrifuge, the pellet was collected and proceeded with the cell lysis for western blot assay.

2.2.2 Brn-3b expression in differentiation THP-1 cells

THP-1 cells (≈ $1x10^6$ cells/well) were differentiated into Mo macrophage-like cells by treatment with 150 nM of phorbol 12-myristate 13-acetate (PMA) overnight in 6 well plates. After overnight incubation, the cells were kept in a fresh medium overnight. Afterwards, the cells were further differentiated into M1 and M2 cells using 0.1 ug/mL of IFNy and 0.02 ug/mL of IL-4 for 24 hours. 0.01 uM of vitamin D3 treatment was used as the positive control. In this study, the undifferentiated cells treated with vitamin D3 were used as a reference. After the treatment, the cell was collected into a 15 mL centrifuge tube and centrifuged at 700 x g for 5 minutes. After centrifugation, the pellet was collected and processed for cell lysis to perform the Western blot assay. The protocol of differentiation of THP1 into macrophages was modified from Genin et al., (2015) and Baxter et al., (2020).

2.2.3 Brn-3b expression in quiescent and activated Jurkat cells

In this study, the Brn-3b expression was measured in both quiescent and activated Jurkat Cells. In the quiescent state, $1x10^6$ cells/well were treated with 0.01 uM vitamin D3 and 0.1 ug/mL of IFNy. Moreover, I proceeded with the experiment on activated Jurkat cells. In this study, $1x10^6$ cells/well of Jurkat cells were seeded in 6 well plates and activated the cells by treating with 300 nM of PMA, 30 nM of ionomycin (Iono) and a combination of both PMA and Iono for 2, 6, 18 and 24 hours. After the incubation period, the cell was collected into a 15 mL centrifuge tube and centrifuged at 700 x g for 5 minutes. After the centrifuge, the pellet was collected and proceeded with cell lysis. The toxicity effects of the stimulus treatment on the Jurkat cells were measured using 3-(4,5-dimethylthiazol-2-yl)-2,5-diphenyltetrazolium bromide (MTT) assay. The protocol was modified from Bacher et al., (1996) and Brignall et al., (2017).

2.2.4 Western blot

The cell pellet (THP-1 and Jurkat cells) that were collected were lysed using 100 µL of proteinase K to 5 ml of 1X RIPA buffer. The protein from the cells was then quantified using a BSA assay. Furthermore, 40 µg of the protein and 5 µLof

protein ladder were loaded in 12% gel and the gel electrophoresis was run for 2 hours at 110 V. After 2 hours, the gel was transferred to nitrocellulose membrane overnight at 30 V.

After overnight transfer, the membrane was blocked with 5% blocking milk for 1 hour and then incubated with 1:1000 anti-rabbit Brn-3b primary antibody (Biorbyt) for 2 hours. After 2 hours, the membrane was washed 5 times with phosphate-buffered saline tween (PBST) which was mixed with 0.01% milk buffer. After the washing step, the membrane was incubated with 1: 5000 of secondary anti-rabbit for 1 hour. The membrane was washed 5 times before incubating with ECL substrate for 2 minutes. Furthermore, the membrane was imaged using the Bio-Rad Gel Doc Imager. The membrane was imaged at 3 different exposure times which for 30 seconds, 1 minute and 30 seconds, and finally for 2 minutes and 30 seconds. The optimal exposure times were selected for the data analysis using Licor Bioscience and Image J software. The western blot step was repeated to measure the housekeeping gene (GAPDH).

Furthermore, the signal for both the targeted protein and the HKP was analysed using the formula A to get the HKP normalization factor. Furthermore, the HKP normalization factor was used to get the TP signal normalization data using the formula B. Finally, the fold difference of the target protein was measured using the formula C (Figure 25). Western blot protocol modified from Schnoor et al., (2009) and Kaur & Bachlawat, (2009).

Formula

A. HKP normalisation factor = $\frac{\text{HKP signal of each lane}}{\text{The highest signal of HKP}}$

B. TP normalisation signal = $\frac{\text{TP signal of each lane}}{\text{HKP normalisation factor}}$

C. Fold difference = $\frac{\text{TP normalisation signal of each lane}}{\text{TP normalisation signal of UC}}$

Figure 25: The formula for fold difference of western blot signal quantification. The signal of the western blot band was quantified using Licor bioscience software. The formula for (A) housekeeping protein (HKP) normalisation factor (B) target protein (TP) normalisation factor and (C) Fold difference was shown.

2.2.5 MTT assay

The MTT assay was conducted to measure the effect of the stimulus on the cell viability by assessing the cellular metabolic activity (Gruber and Nickel, 2023). The assay was measured based on the reduction reaction of MTT (yellow tetrazolium dye) to purple formazan crystals by metabolically active cells. The amount of formazan relative to the number of viable cells. The Jurkat cells were seeded for ≈ 100,000 cells/well in 12 wells and treated with 300 nM of PMA, 30 nM of Iono and a combination of both PMA and Iono for 18 hours (overnight). After overnight, 100 µL of 5% MTT (yellow colour) was pipetted into each well in the dark and incubated in the 37° C incubator for 2 hours. After 2 hours of incubation, the media was discarded and dissolved with 250 µL dimethyl sulfoxide (DMSO) for 15 minutes. The dissolved solution was then transferred into 96 well plates to measure the optical density (OD) value using a microplate reader at 570 nm of wavelength.

2.2.6 The study on the global Brn-3b KO mouse model

Brn-3b KO mice were obtained from Xiang's research group (Xiang et al., 1996). Briefly, the Brn3b gene knocked out mouse was produced by targeting vector using neomycin gene cassette (pNeoTK) to replace the mouse Brn3b coding region. Brn3b/ neomycin construct was then inserted into AB-1 embryonic stem cells and injected into C57BL/6J mouse to generate chimeric mice (Brn3b Heterozygous and Brn-3b KO) (Xiang et al., 1996). Brn-3b KO (-/-) and WT (+/+) control mice were generated by crossing Brn3b heterozygous mice (+/-) which gave rise to Mendelian ratio, i.e., 50% +/- mice, 25% +/+ mice and 25% -/- mice. The genotypes of litters were determined by performing a polymerase chain reaction (PCR) on DNA extracted from weaned mouse pup ear tissue biopsies (using proteinase K digestion) using PCR primers designed to amplify Brn3b and neomycin fragments. Brn-3b KO and WT mice were then used for studying the role of Brn-3b in immune response and the consequence of loss of Brn-3b to vascular changes.

2.2.7 Validation of Brn-3b KO mouse model

Before I proceeded with the main experiment in this study, I validated the Brn-3b KO mouse model using the PCR method. I validated this transgenic mouse using

the lyse ear snip sample. Furthermore, I measured the Brn-3b KO in the tissue using two methods, including PCR and immunofluorescent experiment. The tissue that was validated in this study were bone marrow, blood, aorta and spleen.

2.2.7.1 PCR

In this study, Brn-3b KO and WT mice were determined by performing genotyping of DNA that was extracted from the ear tissue of the pup. The ear sample was digested using 100 µl direct PCR lysis reagent (Tail) and 0.2 mg/ml proteinase K and incubated at 55°C overnight. After overnight, proteinase K was inactivated by heating the sample at 85°C for 45 minutes. Furthermore, 2.5 µl of each sample was used to amplify by mixing with 22.5 µL of PCR mix. PCR mix was containing:

1. 0.25 µL (0.1 µM) of Brn3b primers (150bp) (Forward primer: 5' GAGAGAGCGCTCACAATTCC 3' Reverse primer: 5' ATGGTGGTGGTGGCTCTTAC 3') and,
2. 0.25 µL (0.1 µM) of neomycin primers (250bp) (Forward primer: 5' AGACAATCGGCTGCTCTGAT 3' Reverse primer: 5' ATACTTTCTCGGCAGGAGCA 3').

The DNA was amplified using the PCR program:

1. 95°C 15 minutes
2. 94°C 30 seconds
3. 60°C 30 seconds
4. 72°C 30 seconds
5. 72°C 5 minutes
6. 4°C HOLD.

Furthermore, the amplified PCR product was run on 2% agarose gel containing gel red at 100V for 30 minutes in 1X TAE buffer. 100bp DNA Ladder was used as a reference for the expression of Brn3b and neomycin fragment. The expression of Brn-3b KO, WT and HET was visualized using a gel documentation machine (Syngene). A similar method was used to validate the Brn-3b KO in bone marrow, blood, aorta and spleen.

2.2.8 Animal studies

All studies using mouse models were undertaken by following Home Office guidelines (Animals Scientific Procedures Act 1986) and approved by the local Ethics Review Board. Brn3b KO (-/-) and WT (+/+) control mice that were used in animal studies (see chapters 4 to 6) were obtained from approved commercial sources (Harlan UK or Charles River). The mouse was maintained in a 12-hour light/ dark cycle and had ad libitum access to standard chow and water.

2.2.8.1 Mouse tissue sample preparation

The femur, blood, aorta, and spleen were isolated from the mice. The tissues were processed according to the protocol described in the following section.

2.2.8.1.1 Bone marrow

The protocol for cell isolation from bone marrow was adapted from Lui and Quan (2015). All the muscles from bones were removed using a sterile scalpel blade and forceps in the laminar hood. The cells from the bones were flushed using 10 mL PBS into the petri dish. The cells were then re-suspended using a pasture pipette and transferred into a 50 mL tube *via* a 70 µM filter.

The cells were centrifuged at 500 x G for 5 minutes at 6°C. The supernatant was removed, and the pellet was resuspended using 10 ml flow cytometry staining (FACS) buffer for 4 minutes on ice. Afterwards, the cells were centrifuged again at 500 x G for 5 minutes at 6°C, and the supernatant was discarded. One millilitre (mL) of FACS buffer was then added to the pellet and continued for the cell counting using an accustain solution for the flow cytometry experiment. (Note: FACS buffer was prepared using 10 mL of FBS and 800 µL of EDTA mixed in 190 ml of PBS).

Moreover, 2 million cells from the balance of flow cytometry experiment were seeded in the RPMI medium without FBS overnight. After overnight, the supernatant was collected for a V-Plex cytokine assay experiment. The method for producing the bone-marrow condition medium was modified from the study by Li *et al.,* (2005), Golle *et al.,* (2017) & Chang *et al.,* (2018). The bone marrow has been cultured in media without FBS to eliminate the influence of the cytokine present in the FBS to the cytokine analysis.

2.2.8.1.2 Blood

The protocol for blood processing was modified from Skordos et al., (2021). The blood was collected from the mouse heart using a 1 ml syringe and 25G needle. The blood was collected into the EDTA blood collection tube. The blood was kept at room temperature (RT) until used. In this study, the blood was processed for two experiments: flow cytometry and V-Plex cytokine assay. The blood was lysed using 1X RBC lysis buffer for flow cytometry experiment and extracted to get the blood plasma by centrifugation method for V-Plex cytokine assay experiment.

For the flow cytometry experiment, WBC was collected by lysing the whole blood (80 µL) with 5 mL of 1X RBC lysis for 5 minutes at RT. Five millilitres of PBS was then added to stop the lysis reaction. Afterwards, the blood was kept on ice for 5 min, and centrifuged at 500g x 5 min at 6°C. The supernatant was discarded and 1mL of FACS buffer was added to the pellet. This pellet was used for flow cytometry experiments.

For the V-Plex cytokine assay experiment, 100 µL of blood was extracted to plasma by centrifuging at 2000g for 15 min at 6°C. The resulting plasma (approximately 40µL) was collected into a 1.5 mL Eppendorf tube and kept in the -80°C freezer before use. The protocol for plasma extraction was modified from Hernandes *et al.,* (2017).

2.2.8.1.2.1 RBC lysis buffer recipe

The ammonium-chloride-potassium (ACK) lysis buffer was prepared by adding 8.02 g of ammonium chloride, 1 g of potassium bicarbonate and 0.0372 g of disodium EDTA into 800 mL of distilled water in a scotch bottle. The distilled water was added until the volume was 1 L, and the PH was adjusted between 7.2 to 7.4. The solution was stored for up to 6 months at RT. ACK lysis buffer preparations were referred from AAT Bioquest.

2.2.8.1.3 Aorta

The aortic cell isolation protocol was modified from Forester et al., (2005) and Aronoff et al., (2018). The protocol involved the mechanical digestion method by digesting the aorta using curved dissecting scissors and a plunger of the 10 mL syringe until there were no visible pieces and it had a smooth consistency. The aorta was smashed in a petri dish containing 5 mL of PBS. The disassociated

cells were collected into the 15ml Eppendorf tube and centrifuged at 500g x 5min at 6°C. The supernatant was discarded, and the pellet was added with 1 mL of FACS buffer. This pellet was used for flow cytometry experiments.

2.2.8.1.4 Spleen

The protocol for cell isolation from bone marrow was modified from Stagg et al. (2001) and Skordos et al., (2021)). The mouse spleen was placed into a sterile petri dish containing 5 mL of PBS. The spleen was smashed using the plunger of the 10 mL syringe and a pair of straight blunt pointed forceps. The spleen cells were then re-suspended using a pasture pipette, filtered using a 40 µM filter and transferred into a 50 mL tube. The cells were centrifuged at 500 x G for 5 minutes at 6°C. The supernatant was removed, and the pellet was resuspended using a 10 ml FACS buffer for flow cytometry analysis.

2.2.8.2 Flow cytometry assay

The protocol of this experiment was modified from Hristozova et al., (2012) and Gjurich et al., (2015). The differences between live (N) and dead cells (T) were quantified using an automated cell counter. For the flow cytometry study, 50 µL of 0.5 x 10^6 live cells were seeded in round-bottom 96 well plates and kept on ice.

Each sample was seeded in 4 groups (negative control, blue live death (LD) stain, antibody cocktail and fluorescence minus one (FMO). The cells were blocked with Fc Block (CD16/CD32) at 0.001 µg/µL for 5 minutes. Afterwards, the cells were incubated with 50 µL of 0.001 µg/µL of the listed antibodies in Table 6, LD stained, FMO and negative control for 30 minutes in the dark at 4°C. The cells for the LD group were stained with blue LD stain after the cells were heated at 55°C for 15 minutes. LD stains were prepared by adding 1µL of blue live dead stain in 1ml of FACS buffer. The negative control group were just incubated with 50 µL of FACS buffer. (Note: In the basic screening analysis, the antibody incubated was 0.00067 µg/µL). The panel of the antibody is shown in Table 6.

Table 6: The fluorochrome of each antibody used for characterisation of immune cells in this study.

Antibodies	Fluorochrome
CD4	BUV395
CD8	BV786
CkiT/CD117	BV711
Thy-1	PE-Cy7
HSA/CD24	FITC
CD25	PE
CD3	APC-Cy7
TCRβ	APC
CD44	BV421
CD11b	BV711
CD45R/B220	AF488
Thy-1	AF647

After 30 minutes, the cells were centrifuged at 500 x g for 5 minutes at 6° C. The cell pellet was then fixed with 150 µL of 3% PFA and kept in the fridge overnight.

After overnight the cell was centrifuged at 500 x g for 5 minutes at 6° C and the pellet was washed with 150 µL PBS 2 times. Furthermore, the cells were pipetted into the flow tube containing 350µL of PBS. For compensation control, we used compensation beads for each antibody and live cells for the blue live/dead stain. Each antibody was pipetted (3 µL) into 300 µL of PBS that was mixed with one drop of beads. All the samples were kept on ice before the flow cytometry assay using BD LSRII. The events were acquired with a minimum of 10,000 events for each sample.

Flow cytometric data were then analysed using FlowJoX software. The gating strategy is shown in the next section.

2.2.8.2.1 Gating strategy

Flow cytometry gating is crucial for accurately identifying and analysing cell populations based on fluorescence characteristics. The gating strategy used in this study involved several key steps including quality control to ensure proper instrument calibration and compensation. Moreover, I utilized unstained controls and FMO controls. My initial gating was based on forward scatter (FSC) vs side scatter (SSC) by excluding debris and dead cells and gating on the population with appropriate size and granularity characteristics. Furthermore, I excluded dead cells using viability dye to exclude dead cells and discriminated doublets by plotting FSC-Area (FSC-A) versus FSC-Height (FSC-H) and gating on single cells. I identified the population by utilizing specific fluorescence markers to identify cell populations. I set gates for positive and negative populations using single-parameter histograms or dot plots. For some cell populations, I analysed co-expression using two-parameter dot plots. To ensure the right cell population was chosen, I used FMO controls to accurately set gates by identifying background fluorescence, as illustrated in Figure 26. I validated the gated population through repetition using more biological replicate samples. This systematic gating strategy ensured precise and reproducible identification of cell populations, which was essential for the accuracy of the flow cytometric analysis performed in this study. I included the representative plot for each gating strategy in each study section for clear clarification. The general gating strategy was referred from Staats et al., (2019).

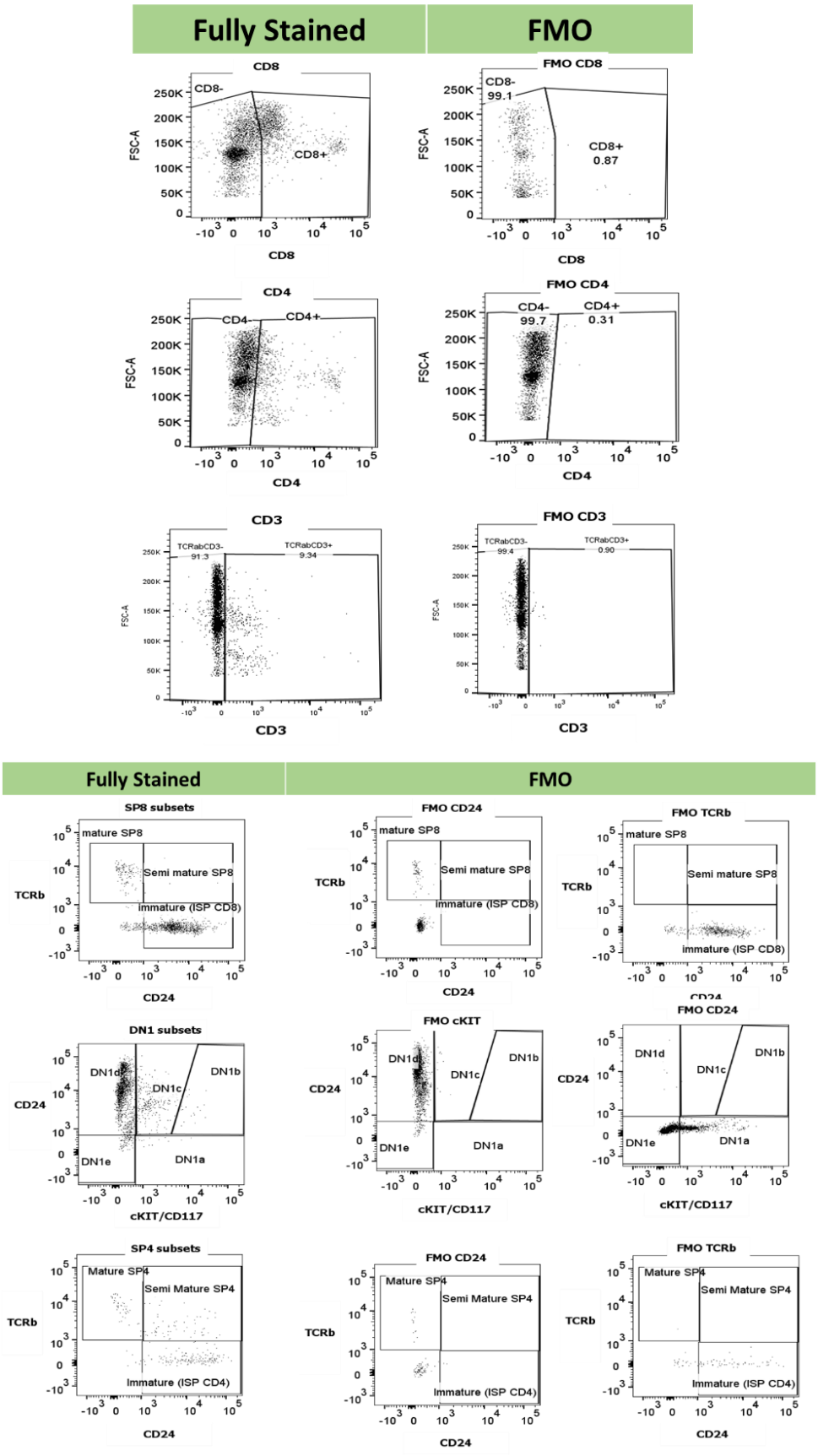

Figure 26: The representative of fluorescence minus one (FMO) control gating strategy in flow cytometry. The tissue was fully stained or without one of a panel of fluorochrome-conjugated antibodies (Table 6) to produce FMO control. This FMO allows to gate on the true positive population.

2.2.8.3 V-plex cytokine assay (MSD cytokine assay)

The protocol for the V-PLEX cytokine assay was based on the MSD cytokine standard method. The earliest step of this protocol involved the preparation of the calibrator standard dilution. The calibrator 1 was prepared by mixing 1 mL of the diluent 41 into the calibrator 1 tube and equilibrated for 30 minutes at RT. The serial dilution step was followed, as illustrated in Figure 27. Furthermore, the sample was prepared by diluting blood plasma in a 1:3 ratio and bone marrow supernatant with whole and 1: 5 ratios. Before proceeding with the assay, the 96-well MSD plate was washed 3 times with 150 µL of 0.05% PBST. Moreover, 50 µL of prepared calibrator standard and samples (bone marrow supernatant and blood plasma) were pipetted into each well. The plate was closed gently and let on the shaker at 750 rpm for 2 hours in RT. The antibodies (Ab) cocktail (IL1β, TNFα and IL-6) was then prepared by adding 60 µL of each ab (50x stock concentration) in 2820 µL of diluent 45. After the incubation time, the samples were washed 3 times with 150 µL of 0.05% PBST. Twenty-five microliters of the detected antibody were then added into each well and incubated for 1 hour 30 minutes on the shaker at 750 rpm for 2 hours in RT. Moreover, 150 µL of the prepared T solution (10 mL of 4x T solution + 10 mL distilled water) was added to each well, and the plate was read using an MSD instrument.

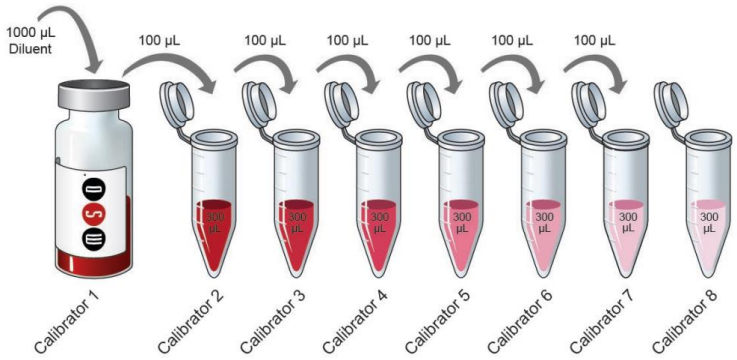

Figure 27: Serial dilution of the calibrator standard in MSD cytokine assay. A 100 µL aliquot of calibrator 1 stock solution was pipetted into a new tube, followed by the transfer of 100 µL into a new tube containing 100 µL of phosphate-buffered saline with Tween 20 (PBST). This serial dilution process was continued until the blank solution (PBST only) was produced.

2.2.8.4 Haemoxylin and eosin (H&E) staining

The morphological structure of the mouse tissue including the aorta and spleen was imaged based on H&E staining. The section was dewaxed and stained using haemoxylin and eosin using the auto-stainer machine. The staining was run for approximately 40 minutes. Afterwards, the slide was gently covered with a coverslip. The Slides were then imaged using a NanoZoomer Digital Pathology (NDP) microscope.

2.2.8.5 Immunofluorescence staining

The immunofluorescent staining was carried out on the paraffin wax section and the method was modified from Zaquot et al., (2020). The section on the slide was dewaxed using the auto-stainer machine. After the dewaxing method, the tissue was immersed in PBS and the antigen retrieval step was performed by heating the sample in a microwave at high heat for 10 minutes in 0.05 M antigen retrieval solution (Sodium Citrate) at pH 6 to 6.8. The tissue was then immersed in the PBS and proceeded with the tissue permeabilization step by immersing the tissue with 0.25% triton-X for 5 minutes. The tissue section was blocked with 3% BCA for 1 hour at RT and humid conditions. After blocking, the tissue was incubated in primary antibody overnight in the dark at 4°C. After overnight, the tissue was washed 5x and incubated in fluorescent secondary antibody for 45 minutes. After incubation, the tissue was then washed 5x using PBS. The nucleus was then either stained individually using 0.01 mg/ml of DAPI, washed for 2x using PBS and mounted with mounting medium or mounted directly with mounting medium containing DAPI. The slides were sealed with nail polish to avoid the fading of fluorescent. The prepared slides were imaged using a Leica DMi8 microscope. The images were analysed using QuPath Software. The concentration of the primary and secondary antibodies is illustrated in Table 7.

Table 7: List of primary antibodies, secondary antibodies and their concentrations used in the immunofluorescent staining experiments.

Antibodies (Ab)	Concentration (mg/mL)
SM22	0.002
Ki67	0.005
αSMA	0.005
Brn-3b	0.005
CD11b	0.005
CD44	0.005
CD45R/B220	0.005
CD3	0.005
Secondary Ab- AF555, Rhodamine Red, AF488, AF647	0.002 (1:1000)

2.2.8.5.1 Image analysis

In this study, the total count of positive stained per area of tissue section (μm^2) or total intensity per area of tissue section (µm2) of the positive stained was quantified using QuPath software. The method was modified from the study by Courtney et al., (2021). The process of quantification of the positive fluorescent staining is illustrated in Figure 28, and the method was modified from the study by Shihan et al., (2021). Analysis of exported data was performed using Microsoft Excel and GraphPad Prism 9.0.2.

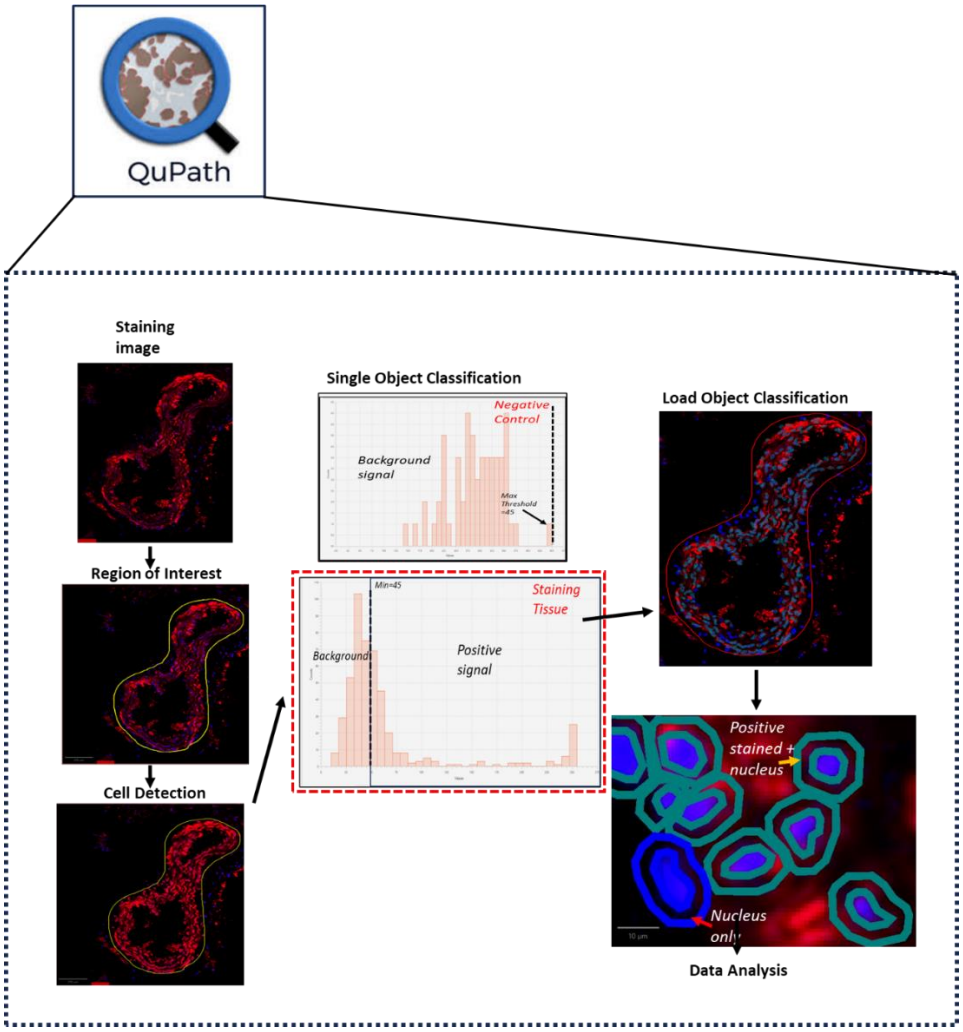

Figure 28: The representative steps in fluorescent image analysis using QuPath software. The positive staining signal of the tissue was quantified in the region of interest (ROI), indicated by the yellow annotation. The true positive signals were measured above the threshold value set by the negative control (negative control threshold = 45).

2.2.8.6 Gene transcription analysis

The gene expression analysis was measured using the RT-qPCR method and the RNA of the sample was extracted using the trizol method. The RNA extraction method was modified from the Invitrogen Life Technologies protocol. Moreover, the cDNA synthesis method was modified from the protocol made by the Section of Cancer Genomics and Ramalho et al., (2004).

2.2.8.6.1 RNA extraction method

The RNA in bone marrow cell pellets were extracted using trizolbased extraction method, as summarised in Figure 29.

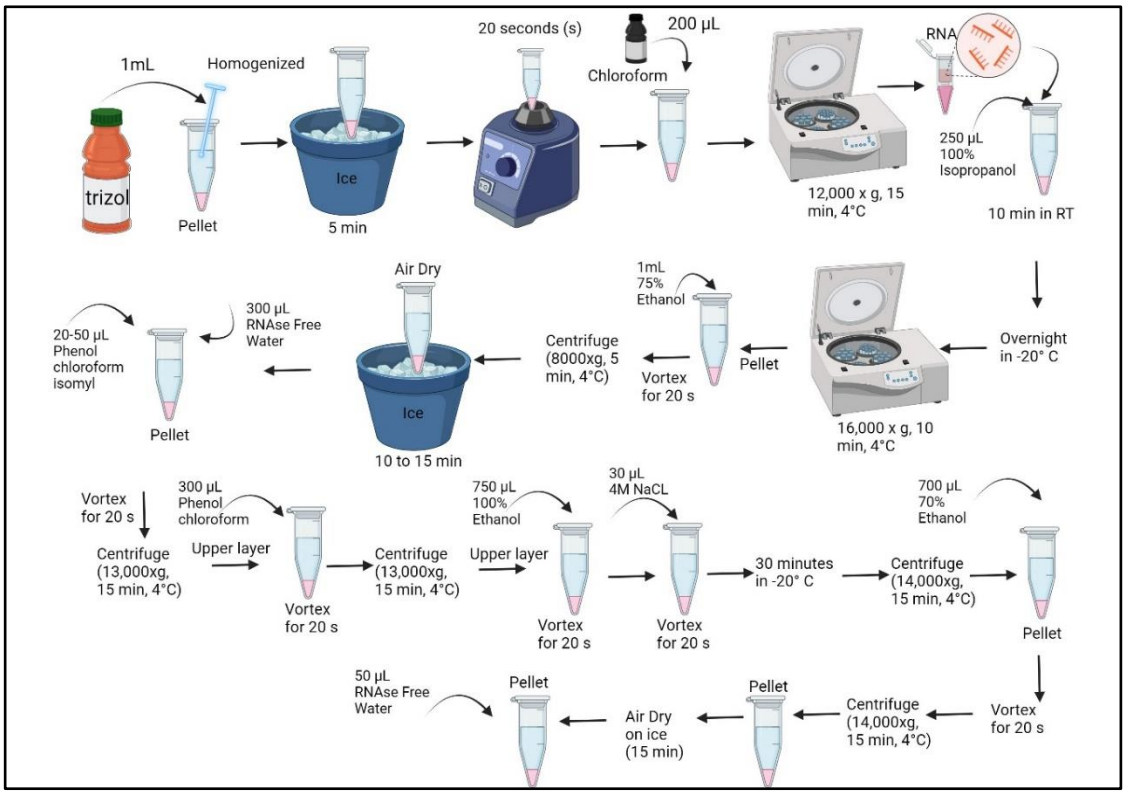

Figure 29: The steps for Trizol-based RNA extraction method. Homogenized samples were incubated with chloroform, followed by phase separation through centrifugation to isolate the aqueous phase containing RNA. RNA was precipitated with isopropyl alcohol, washed with varying concentrations of ethanol, and redissolved in RNase-free water. RNA integrity was assessed by A260/280 ratio and stored at -80°C for future use.

2.3.2.6.1 DNase 1 treatment

The pellet in RNAse-free water (RNA sample) was then added with 6 µL of MgCl2, 2 µL of DNase I and 2 µL of RNase water to discard the contaminated DNA. The sample was incubated at 37°C for 1 hour. Furthermore, 60 µL of phenol: chloroform was added and mixed well by vortexing for 20 seconds. The samples were then centrifuged at 14,000 x g for 10 minutes at 4°C. The supernatant was collected and added with 60 µL of phenol: chloroform, vortexed for 20 seconds and centrifuged again at 14,000 x g for 10 minutes at 4°C. The supernatant was collected into the new tube containing 60 µL of 100% ethanol, added with 30 µL of 4M NaCl and incubated at -80°C freezer for 10 minutes. Furthermore, the sample was centrifuged at 14,000 x g for 10 minutes at 4°C and added 700 µL of 70% ethanol. The sample was centrifuged at 14,000 x g for 15 minutes at 4°C. The pellet was air dried for 10 to 15 minutes and added with 20

to 30 µL of RNAse-free water. RNA was quantified using nanodrop at 260/280 nm and 260/230 nm before being stored in a -80°C freezer.

2.2.8.6.2 cDNA synthesis

In this study, the cDNA was prepared from 500 to 2000 ng of total RNA. 0.5 µL of random primers was added into each tube of prepared sample and vortexed. Each tube was incubated on a 70°C heat block for 5 minutes. While waiting, the cDNA mix was prepared as in Table 8.

Table 8: The cDNA master mix components per PCR tube.

Components	**Volume per sample (µL)**
5x RT buffer	5
dNTP mix	1.3
Super transcript (III) RT polymerase	1
RNase inhibitor	0.6

After the incubation, the samples were placed on ice directly. Furthermore, 7.9 µL of the cDNA were added in each tube and run in the PCR machine at 37°C for 1 hour, 70°C 10 min and held at 4°C. The control included in this study was non-template control (RT without sample) and RT control (no RT with sample). Afterwards, the cDNA (25 µL) was Stored at -80°C before use.

2.2.8.6.3 RT-qPCR

The RT-qPCR protocol was modified from Kuang et al., (2018). The qPCR reaction (20 µL) contained 450 nM (3 µL) of each forward and reverse primer (Table 9: The list of primers (mouse species)) and ten µL Universal SYBR Green Supermix was used. The amount of cDNA used in each qPCR reaction was: 100 ng (2 µL) of bone marrow. The standard thermocycling program consisted of a 95°C denaturation for 30 seconds, followed by 40 cycles of 59-60°C (annealing) and 72°C for 10 minutes (extension). All samples were run in duplicate to triplicate, and the mean Cq values for each sample were calculated. Reactions

with non-template control and RT control were included for each set of primers on each plate.

Table 9: The list of primers (mouse species) used for the qPCR experiments.

Primers	Sequence
TNFα	F-CACAAGATGCTGGGACAGTGA R-TCCTTGATGGTGGTGCATGA
IL-15	F-GTGACTTTCATCCCAGTTGC R-TTCCTTGCAGCCAGATTCTG
CXCR5	F-TGGCCTTCTACAGTAACAGCA R-GCATGAATACCGCCTTAAAGGAC
GAPDH	F-TTCACCACCATGGAGAAGGC R-GGCATGGACTGTGGTCATGA

2.3 Statistical Analysis

Results are presented as average ± Standard Error Mean (SEM). Statistical significance was tested using a t-test and one-way analysis of variance (ANOVA) with Tukey's post hoc test using GraphPad Prism software.

3 A PRELIMINARY STUDY ON THE POTENTIAL ROLE OF BRN-3B PROTEIN IN IMMUNE REGULATION IN HUMAN THP-1 AND JURKAT CELLS

3.1 Introduction

Brn-3b expression in THP-1 cells has been observed to increase following treatment with Vitamin D, a compound recognised for its anti-inflammatory properties (Nurminen et al., 2015; Hashemi et al., 2018; Simakao et al., 2021). The expression of the vitamin D receptor (VDR) and enzymes that metabolise Vitamin D is widespread across various immune cell types, such as monocytes, macrophages, DCs, and activated B and T cells. The active form of Vitamin D, calcitriol (1,25-(OH)2D3, binds to VDR to induce various gene or transcription factors that exert various effects including immunoregulatory effects on innate and adaptive immune response (Figure 30) (Fernandez et al., 2022). Therefore, the evidence of the expression of Brn-3b in the THP-1 monocyte cells after Vitamin D treatment suggests that Brn-3b could be a key protein targeted for immunoregulatory effects. To further explore this notion, I aim to investigate Brn-3b's specific contributions to immune regulation, particularly whether it predominantly influences pro-inflammatory or anti-inflammatory responses.

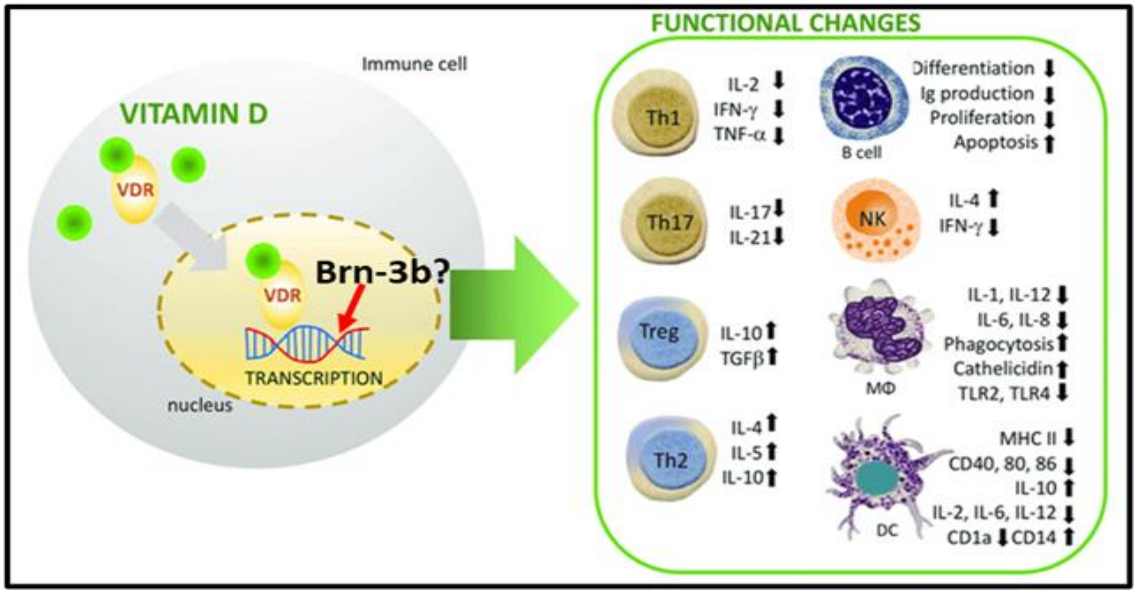

Figure 30: Vitamin D3 activation of cellular immune function *via* vitamin D receptor (VDR) complex. The illustration images depict the transduction pathway activated by vitamin D3 in immune cells, wherein the transcription of various genes leads to changes in the function of immune cells in response to the Vitamin D3-VDR complex (Cyprian et al., 2019).

In this study, I explore the regulation of Brn-3b in immune responses using THP-1 monocytic cells and Jurkat T lymphocyte cells. The THP-1 cell, a human-derived monocyte, is extensively utilized to explore monocyte and macrophage functions, serving as a prominent *in vitro* model for studying inflammatory processes and innate immune responses (Chanput et al., 2014; Pinto et al., 2021). As key players in the innate immune system, monocytes/macrophages act as sentinels, making the study of Brn-3b expression in THP-1 cells pivotal for understanding its impact on innate immunity. Similarly, the Jurkat cell, derived from human lymphocytes and commonly used for the T cells model, enables the examination of critical T cell biology aspects, including signalling and activation processes essential for adaptive immunity (Montano, 2014). By analysing Brn-3b expression in Jurkat cells, the aim is to elucidate the protein's role in the adaptive immune response.

Monocytes and T cells are important for maintaining health but also can contribute to disease progression. Monocytes play a protective role by defending the host from pathogenic intruders; however, an increased survival rate of

infiltrating monocytes/macrophages can promote diseases such as atherosclerosis, liver fibrosis and systemic lupus erythematosus (SLE) (Karlmark et al., 2012). Similarly, T cells mediate cell-based immune responses, helping to maintain host health and prevent diseases. For example, CD4 T cells enhance the anti-tumour response of CD8 T cells. However, disruption of the adaptive immune response can lead to autoimmune conditions, as evidenced by the role of Th17 activity and IL-17 accumulation in serum, synovial fluid and synovial tissue of patients, which promotes chronic joint inflammation and eventually leads to rheumatoid arthritis (RA) (Sun et al., 2023). Thus, studying the Brn-3b function in both immune cell models is relevant to understanding the correlation between Brn-3b expression and the health and disease progression driven by monocytes and T cells.

In this study, I hypothesise that Brn-3b expression in THP-1 cells and Jurkat cells changes upon activation or pro-/anti-inflammatory treatment. The treatment protocols, including concentrations and durations, are detailed in the methodology section. The rationale for using pro- and anti-inflammatory marker treatments is to investigate Brn-3b's function in modulating immune regulation, specifically in promoting or resolving inflammation. By examining how Brn-3b expression changes in response to these treatments, I aim to better understand its involvement in immune regulation. As such, the objectives of this chapter are as follows:

1. To examine the expression of Brn-3b in both undifferentiated and differentiated THP-1 cells upon pro-/anti-inflammatory treatment.
2. To explore the expression of Brn-3b in quiescent and activated Jurkat cells.

3.2 Results

3.2.1 Vitamin D3 (positive control) dose-dependence study

To investigate the effects of vitamin D3 on Brn-3b protein expression in THP-1 cells, the cells were treated with different concentrations of vitamin D3 (0, 0.01. 0.05 and 0.1 µM) for 24 h, as illustrated in Figure 31. The results demonstrated that Brn-3b (S) protein was strongly expressed in the THP-1 cells following vitamin treatment, with Figure 31 (A) illustrating this effect. Specifically, a 0.01 µM concentration of vitamin D3 increased Brn-3b (S) expression by 1.734-fold (p=0.0001) compared to the untreated control (UC), as shown in Figure 31 (B). Given the substantial increase in Brn-3b (S) protein expression at this concentration, 0.01 µM vitamin D3 was selected for further study.

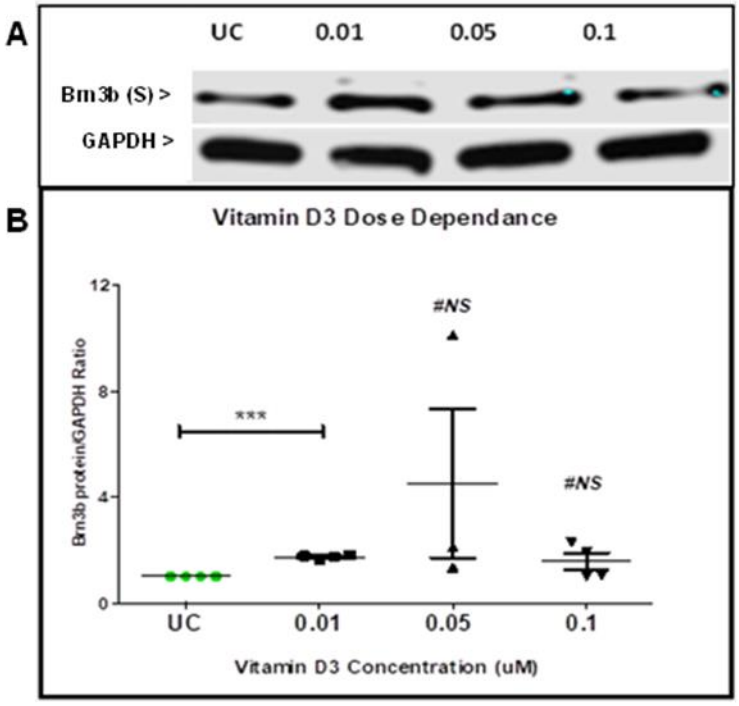

Figure 31: Dose-dependent effects of vitamin D3 (VITD3) on Brn-3b short (S) protein expression in undifferentiated THP-1 cells. Undifferentiated THP-1 cells were treated with 0.01, 0.05 and 0.1 µM of VITD3 for 24 hours (A) Representative western blot image showing Brn3b (S) protein (35 kDa) expression in untreated control (UC) and treated THP1 cells. (B) Graph showing the quantification of Brn3b (S) protein in vitamin D3 treated undifferentiated THP1 compared to UC, normalised to glyceraldehyde 3-phosphate dehydrogenase (GAPDH). Data are presented as mean ± SEM for n = 3-4 (***p < 0.001 and Ns = not significant).

3.2.2 Brn-3b (S) Protein increases expression following vitamin D3 treatments in undifferentiated THP-1 cells.

To determine whether Brn-3b regulates anti-inflammatory or pro-inflammatory in innate immune response, the Brn-3b expression was quantified in undifferentiated and differentiated THP-1 cells. In this study, Brn-3b (S) protein expression was quantified in the undifferentiated THP1 cells after 24 hours of treatment with vitamin D3 (positive control), IL-4 (anti-inflammatory) and IFNγ (pro-inflammatory). The results showed that Brn-3b (S) protein increased in undifferentiated THP-1 cells after treatment with Vitamin D3, IFNγ and IL-4, but the value was not statistically different except for vitamin D3 treatment, as depicted in Figure 32. Vitamin D3 significantly increased Brn-3b expression by 2.005-fold (p=0.0219).

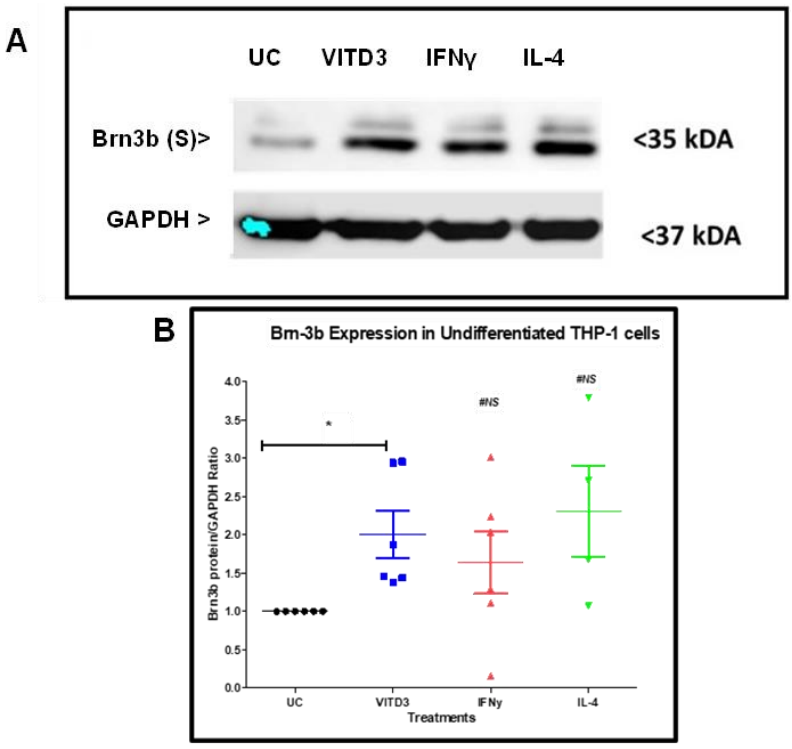

Figure 32: Brn-3b short (S) protein expression in undifferentiated THP-1 cells following cytokine and vitamin D3 (VITD3) treatment. Undifferentiated THP-1 cells were treated with 0.01 µM VITD3, 0.02 ug/ml interleukin 4 (IL-4), and 0.1 ug/mL interferon gamma (IFNγ) for 24 hours (A) Representative western blot image showing Brn3b (s) protein (35 kDa) expression in untreated control (UC) and treated THP1 cells. (B) Graph showing the quantification of Brn3b (S) protein in treated undifferentiated THP1 cells compared to UC, normalised to glyceraldehyde 3-phosphate dehydrogenase (GAPDH). Data are presented as mean ± SEM for n = 4-6 (*p < 0.05 and Ns = not significant).

3.2.3 Brn-3b (S) protein increase in response to vitamin D3 and IL-4 treatment in differentiated THP-1 cells

To further explore whether Brn-3b protein primarily exerts pro-inflammatory or anti-inflammatory effects, its expression levels were assessed in differentiated THP-1 cells. In this study, THP-1 cells underwent differentiation into Mo macrophages through exposure to 150 nM PMA for 24 hours. Subsequently, these cells were directed towards the M1 (pro-inflammatory) phenotype *via* treatment with IFNγ and towards the M2 (anti-inflammatory) phenotype through IL-4 treatment.

The results demonstrated that treatments with vitamin D3 (positive control) and IL-4 markedly elevated Brn-3b (S) expression in differentiated THP-1 cells, by 1.715-fold ($p=0.0114$) and 1.601-fold ($p=0.0205$), respectively, as shown in Figure 33 (B). However, changes in Brn-3b (S) expression due to IFNγ treatment did not reach statistical significance, even though the reduction trend of Brn-3b expression was shown.

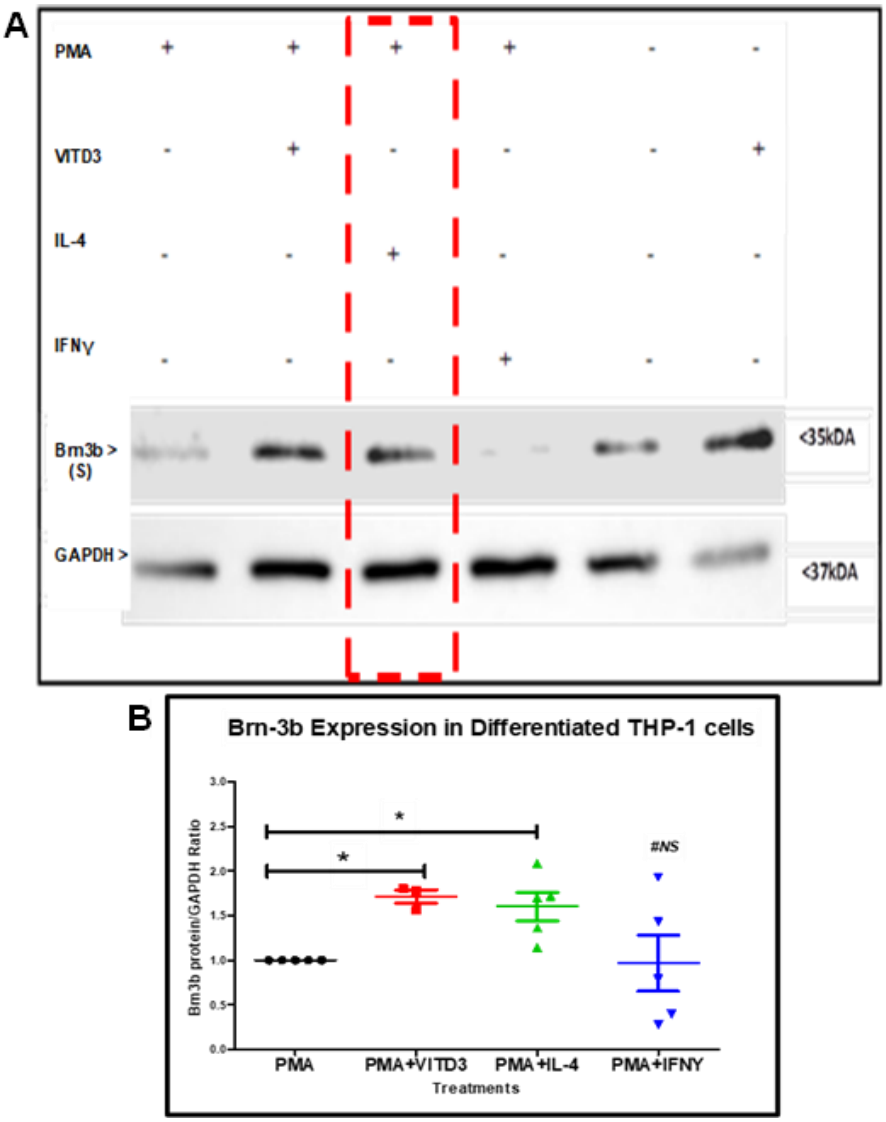

Figure 33: Brn-3b short (S) expression in differentiated THP-1 cells following cytokine and vitamin D3 (VITD3) treatment. THP-1 cells were differentiated with 150 nM phorbol 12-myristate 13-acetate (PMA) for 24 hours, followed by treatment with 0.01 µM VITD3, 0.02 ug/ml interleukin 4 (IL-4), and 0.1 ug/mL interferon gamma (IFNγ) for an additional 24 hours. (A) Representative western blot showing Brn3b (S) protein (35 kDa) levels. (B) Graph showing the quantification of Brn3b (S) protein in treated differentiated THP-1 cells compared to PMA only, normalised to glyceraldehyde 3-phosphate dehydrogenase (GAPDH). The dashed box (red) indicates Brn-3b expression after treatment with PMA + IL-4. Data are presented as mean ± SEM for n = 3-5 (*$p < 0.05$ and Ns = not significant). Abbreviations: +, positive expression; -, negative expression.

3.2.4 Brn-3b expression in quiescent and activated Jurkat cells

Given the significant expression of Brn-3b in both undifferentiated and differentiated THP-1 monocytes, which serve as a crucial model for studying the innate immune response, it becomes imperative to investigate Brn-3b's potential role in the adaptive immune response. To address this, an experimental design was employed involving the activation of Jurkat cells—a model for T lymphocytes using PMA, Iono, or a combination of both (PMA/Iono) for durations of 2, 6, 18, and 24 hours. Additionally, the study included the quantification of Brn-3b expression in quiescent (non-activated) Jurkat cells, providing a baseline for comparison. This approach aims to elucidate the involvement of Brn-3b across different facets of immune functionality, extending the understanding of its role beyond innate responses to encompass potential effects within adaptive immunity.

3.2.4.1 No significant change in Brn-3b (S) expression in quiescent Jurkat cells

The expression of Brn-3b in quiescent Jurkat cells was assessed using western blot analysis following treatment with vitamin D3 and IFNγ for 24 hours. The findings indicated that there was no significant change in Brn-3b (S) expression after treatment with either vitamin D3 or IFNγ when compared to the UC, as shown in Figure 34.

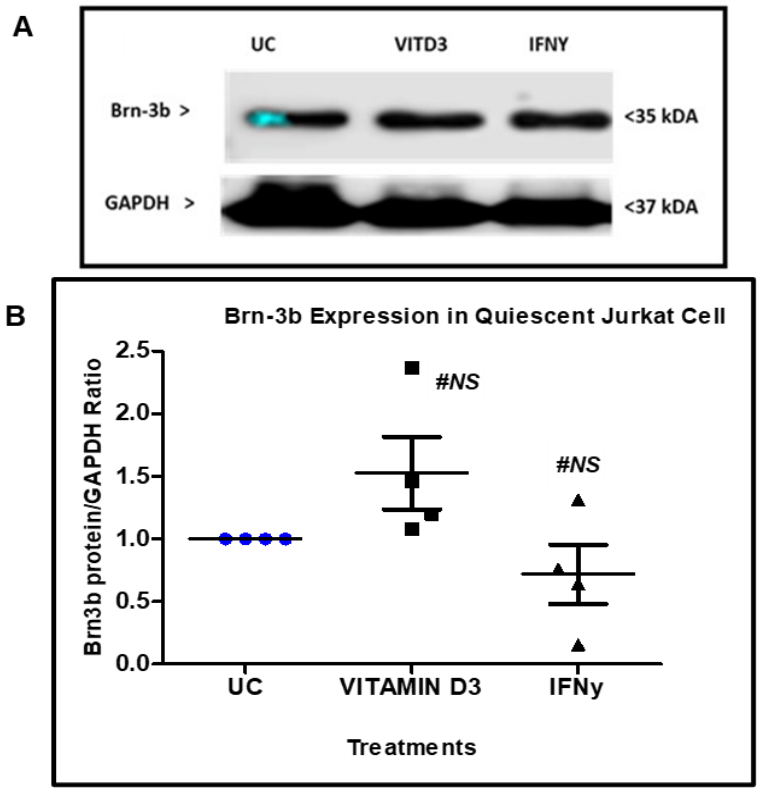

Figure 34: Brn-3b short (S) expression in quiescent Jurkat cells following vitamin D3 (VITD3) and interferon gamma (IFNγ) treatment. Quiescent Jurkat cells were treated with 0.01 µM VITD3 and 0.1 µg/mL IFNγ for 24 hours. (A) Representative western blot showing Brn3b protein (35 kDa) expression in untreated control (UC) and treated quiescent Jurkat cells. (B) Graph showing the quantification of Brn3b protein expression in treated quiescent Jurkat cells compared to UC, normalised to glyceraldehyde 3-phosphate dehydrogenase (GAPDH). Data are presented as mean ± SEM for n=4 (Ns = not significant).

3.2.4.2 The effects of stimulus on Jurkat cells

Before the main experiment, the study assessed whether PMA, Iono and PMA/Iono stimuli had any detrimental effects on Jurkat cells by performing an MTT assay. Jurkat cells were incubated with the stimulus overnight/18 hours. The findings revealed that Iono significantly reduced the cell viability of Jurkat cells in comparison to the UC, whereas treatments with PMA and the combination of PMA/ Iono did not significantly impact cell OD value. Specifically, Iono decreased Jurkat cell proliferation to 82.54% relative to the UC, with a p-value of 0.0075 (as illustrated in Figure 35). Given that treatments with PMA, Iono and a combination of both did not reduce the OD value by more than 30% as compared to UC due to cellular metabolic activity, the stimulus is considered non-toxic. It is referred to

standard ISO 10993-5 guidelines for cytotoxicity assessment (Gruber and Nickel, 2023).

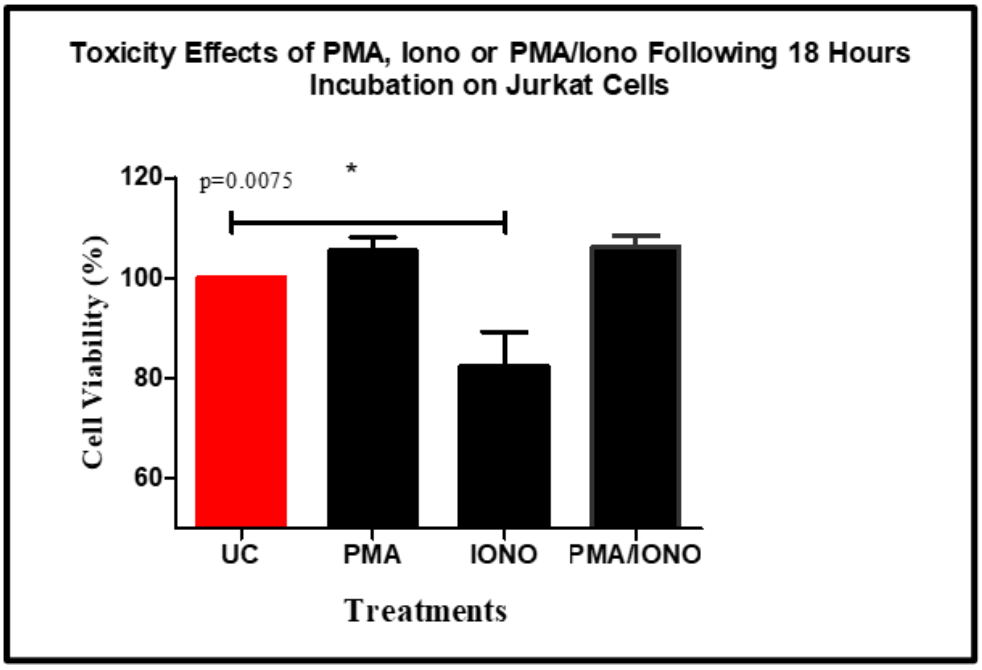

Figure 35: Cytotoxicity effects of phorbol 12-myristate 13-acetate (PMA), ionomycin (Iono) and PMA/Iono on Jurkat Cells. Jurkat cells were treated with 300 nM PMA, 30 nM Iono, or a combination of both for 18 hours (overnight). Graph showing reduced viability of Jurkat cells following treatment with Iono compared to untreated control (UC). Data are presented as mean ± SEM for n = 3 (*p < 0.05).

3.2.4.3 Activated Jurkat cells show no significant alteration in Brn-3b (S) protein expression.

To investigate the potential role of Brn-3b in regulating the adaptive immune system, this study quantified Brn-3b protein levels in Jurkat cells activated by PMA, Iono, and a PMA/ Iono combination after treatment durations of 2, 6, 18, and 24 hours. The results showed that treatments with PMA, Iono, and their combination for 2, 6, 18, and 24 hours did not significantly affect Brn-3b (S) expression in Jurkat cells, as depicted in Figure 36 (B-E).

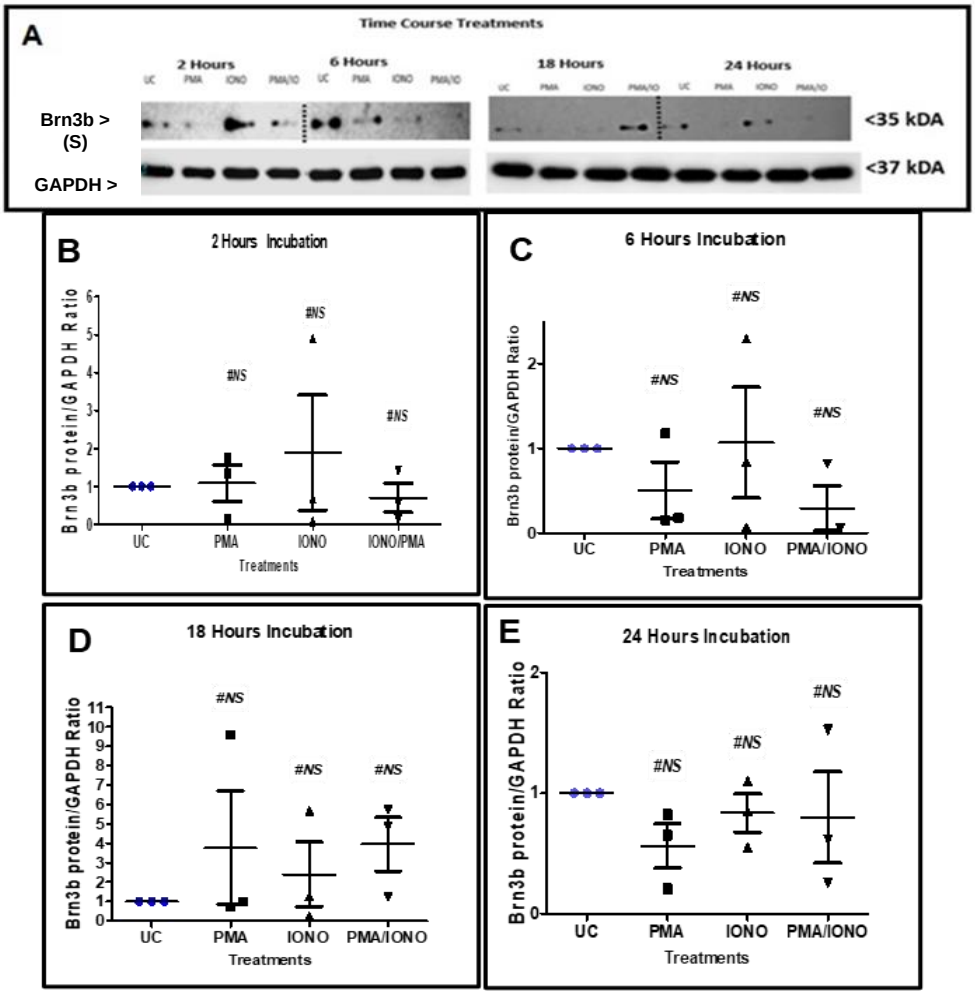

Figure 36: Brn-3b short (S) protein expression in activated Jurkat cells. Jurkat cells were activated using 300 nM phorbol 12-myristate 13-acetate (PMA), 30 nM ionomycin (Iono), or a combination of both for 2, 6, 18, and 24 hours. (A) Representative western blot image showing Brn3b (S) protein (35 kDa) expression in untreated control (UC) and activated Jurkat cells. (B to E) Graph showing the quantification of Brn3b (S) protein in activated Jurkat cells compared to UC, normalised to glyceraldehyde 3-phosphate dehydrogenase (GAPDH). Data are presented as mean ± SEM for n = 3 (Ns = not significant).

3.3 Discussion

This chapter aimed to investigate the function of Brn-3b in immune regulation using *in vitro* models. I utilised THP-1 monocyte and Jurkat T cell lines to study Brn-3b expression under different conditions. Vitamin D3 treatment enhanced Brn-3b expression in THP-1 cells but showed no significant effect in Jurkat cells, suggesting that Brn-3b may play a function in immune regulation in THP-1 cells. These findings provide a basis for future studies, focusing on immune cell profiles in Brn-3b KO mouse tissues, including bone marrow, blood, aorta, and spleen, to explore Brn-3b's function in immune regulation.

3.3.1 Brn-3b expression in THP-1 cell lines

This study investigated Brn-3b expression in undifferentiated and differentiated THP-1 monocyte cell lines under different treatments to explore its function in immune regulation. Previous studies have demonstrated that Brn-3b is expressed in immune cells, including THP-1 cells, and that its expression can be modulated by vitamin D3, a well-established immune modulator (Bhargava et al., 1993; Nurminen et al., 2015). In both undifferentiated and differentiated THP-1 cells, vitamin D3 treatment significantly increased Brn-3b protein expression (Figure 32 and Figure 33). Vitamin D3 is recognised for its ability to regulate genes involved in immune and metabolic functions, suppressing pro-inflammatory responses while promoting anti-inflammatory pathways (Calberg, 2022; Krajewska et al., 2022). These results suggest that Brn-3b may be part of the broader gene network influenced by vitamin D3, which includes both immune and non-immune-related genes, potentially contributing to its effects on immune regulation.

Additionally, IL-4 treatment also enhanced Brn-3b expression in differentiated THP-1 cells (Figure 33). IL-4 is known to promote the differentiation of M2 macrophages, which play key roles in resolving inflammation and maintaining tissue homeostasis (Celik et al., 2020; Gordon, 2003; Genin et al., 2015). This suggests that Brn-3b expression could be linked to the anti-inflammatory phenotype of M2 macrophages, which are characterised by the secretion of IL-4, IL-10, CCL18, and CCL22, and express markers such as CD206 (MRC1) and

CD163 (Gordon, 2003; Genin et al., 2015). In contrast, Brn-3b expression was not significantly altered following IFNγ treatment, which induces M1 macrophages associated with pro-inflammatory responses (Martinez and Gordon, 2014). A slight decrease in Brn-3b expression was observed in differentiated THP-1 cells treated with IFNγ, suggesting that Brn-3b may not be involved in the M1 macrophage-mediated inflammatory response.

These findings indicate that Brn-3b may be regulated by anti-inflammatory stimuli like vitamin D3 and IL-4, suggesting a potential function in immune resolution. Future research could focus on measuring cytokine production in undifferentiated and differentiated THP-1 cells with Brn-3b knockdown or overexpression. Such studies would be essential to understand the downstream effects of Brn-3b in immune regulation and to validate its role in inflammation. While these studies are crucial, it is important to note that *in vitro* models provide only preliminary insights, and further research in physiological settings is necessary to confirm Brn-3b's function.

3.3.2 Brn-3b expression in quiescent and activated human Jurkat cell lines

Since Brn-3b may be expressed by monocytes/macrophages, this section aimed to explore its expression in T cells. Macrophages and T cells are thought to mirror each other, with M1 macrophages resembling Th1 cells and M2 macrophages reflecting Th2 cells (Mantovani et al., 2004).

The findings showed that Brn-3b expression did not significantly change in quiescent Jurkat T cells treated with vitamin D3 or IFNγ (Figure 34). This may be due to the absence of VDR expression in resting T cells (Cantorna and Waddell, 2014) and the complex regulatory role of IFNγ in inflammation (Zhang, 2007). Further analysis in activated Jurkat cells revealed no significant changes in Brn-3b expression following treatments with Iono, PMA, or their combination (Figure 36). PMA and Iono activate T cells through distinct pathways—PMA *via* PKC signalling and Iono through calcium signalling (Brignall et al., 2017; Chatila et al., 1989; Guo et al., 2008; Dagur et al., 2010; Zhu et al., 2010). Despite these known pathways, neither treatment induced significant changes in Brn-3b expression. Even when used together, PMA and Iono can induce robust T cell activation, leading to chromatin remodelling at approximately 2,100 regions, compared to

600 and 350 regions for PMA and Iono alone, respectively (Chatila et al., 1989; Brignall et al., 2017). Yet, this enhanced chromatin remodelling did not translate to changes in Brn-3b expression. These findings suggest that Brn-3b may respond to different stimuli, and future studies using other activators, such as PHA, could provide additional insights into T cell activation and proliferation (Chaudhary et al., 2021).

A limitation of this study is that vitamin D3 treatment was not included in activated Jurkat cells. Previous research by Shifera et al., (2010) showed that vitamin D3 did not prevent the degradation of IκBα in Jurkat T cells, a protein involved in activating the NFκB pathway and promoting inflammation. This suggests that vitamin D3 may not be crucial for correlating with Brn-3b expression in Jurkat cells. However, it would still be useful to include vitamin D3 treatment in future studies to confirm its effects and explore whether its influence differs between T cells and other immune cells, such as monocytes/macrophages.

Overall, Brn-3b appears to have a negligible role in Jurkat T cells. However, given the limited number of experiments, further studies with additional biological replicates are needed to confirm these findings.

3.4 Conclusions

This chapter aimed to investigate the immune-related function of Brn-3b using *in vitro* models. The key findings are:

- Vitamin D3 increased Brn-3b expression in undifferentiated THP-1 cells.
- Both vitamin D3 and IL-4 increased Brn-3b expression in differentiated THP-1 cells.
- Brn-3b expression did not change in quiescent Jurkat T cells after treatment with vitamin D3 or IFNγ.
- Brn-3b expression did not change in activated Jurkat T cells.

These results suggest that Brn-3b may be regulated by vitamin D3 and IL-4 in THP-1 cells, potentially contributing to immune regulation in monocyte/macrophage differentiation. In contrast, Brn-3b appears to have a negligible role in Jurkat T cells under the tested conditions. Future studies should investigate the functional consequences of Brn-3b modulation in immune

responses and explore its role in more complex *in vivo* systems to better understand its potential involvement in immune regulation.

4 IMMUNOPHENOTYPING CHARACTERISATION OF THE IMMUNE CELLS IN THE BONE MARROW OF BRN-3B KNOCK-OUT MOUSE MODEL

4.1 Introduction

In the previous chapter, my preliminary data showed the expression of Brn-3b in THP-1 monocytes and M2-like macrophages, while no changes were observed in Jurkat cells. This suggests a potential involvement of Brn-3b in immune cell regulation in specific immune cell types. To further explore Brn-3b's function in immune cell regulation, I extend the study using the global Brn-3b KO mouse model.

Previous unpublished data (Mele et al.) suggest that Brn-3b deficiency leads to a reduction in B cell populations (CD45+CD19+) and an increase in monocyte populations (Ly6C+) in a zymosan-induced peritonitis model. These observations point to a potential role for Brn-3b in immune regulation. This study aims to further examine Brn-3b’s function by assessing immune status in the bone marrow based on immune cell profiles and protein biomarkers.

4.1.1 Bone marrow

Bone marrow is a key hematopoietic organ for immune cell production and proliferation, as well as a site for immune cell residency (Schirrmacher, 2023). This tissue houses a diverse array of immune cells including monocytes, macrophages, B and T cells, dendritic, neutrophil and NKT cells that are responsible for controlling inflammatory responses (Zhou et al., 2015). The bone

marrow is a crucial site to produce blood cells, making it central to numerous investigations in the fields of haematology and immunology (Hamon *et al.,* 2015). This includes bone marrow tests that assess whether the bone marrow is healthy and producing normal amounts of blood cells.

In this study, I evaluate the immune cell profiles of Brn-3b KO bone marrow, focusing on T cell (early and mature states) and non-T cell (B lymphocytes, monocytes, granulocytes) lineages. This was done using cell surface markers, including CD11b (macrophages/monocytes), CD45R/B220 (B lymphocytes), CD4 and CD8 (T lymphocytes), CD44 (HSCs and activation status), Thy-1 (T cell lineage and activation), cKIT, CD25, CD24/HSA, CD3, and TCRβ. Cytokine expression levels (IL-1β, lL-6, and TNFα) were also assessed in the bone marrow supernatant to further explore immune status.

In this study, I hypothesise that the loss of Brn-3b alters the development and accumulation of immune cell profiles in the bone marrow, leading to a pro-inflammatory status. Accordingly, the objectives of this chapter were delineated as follows:

1. To investigate the changes of immune cell profile including T (early and mature state) and non-T cell (B lymphocytes, monocytes and granulocytes) lineage in Brn-3b KO mouse bone marrow.
2. To explore the changes of protein biomarker profile including IL-1β, lL-6 and TNFα in Brn-3b KO mouse bone Marrow

4.2 Results

4.2.1 Validation of the Brn-3b KO strain

Initial validation of the Brn-3b KO model was conducted using ear samples, followed by PCR analysis on various tissues, including bone marrow, blood, spleen, and aorta, to ensure the effective knockout of the target gene. The presence of a neomycin cassette expression at approximately 250 base pairs (bp) served as the criterion for gene knockout.

The results indicated that genomic DNA from bone marrow, blood, spleen, and aorta displayed a band at approximately 150 bp in WT samples, and a band at approximately 250 bp was observed in Brn-3b KO samples, as illustrated in Figure 37 (A). Genotyping of some of the tissues was re-analysed due to some samples not expressing the expected band, which was attributed to insufficient DNA quantity or the appearance of double bands resulting from sample spillover/cross-contamination between wells (refer to Figure 89 in Appendix 2). The gender details of the mice for each tissue are provided in Appendix 2 (Figure 89).

Furthermore, Brn-3b KO validation at the protein level was conducted within aorta tissue sections through immunofluorescence staining. The representative images showed a slight increase in Brn-3b expression in the WT tissues compared to the negative control, with the signal predominantly observed in the TM. Conversely, Brn-3b expression in the KO tissues appeared to align with that of the negative control, as depicted in Figure 37B(i). Quantitative analysis showed a significant reduction in Brn-3b signal within the region of interest (ROI) of the KO tissues compared to their WT counterparts ($p = 0.0118$), as shown in Figure 37B(ii).

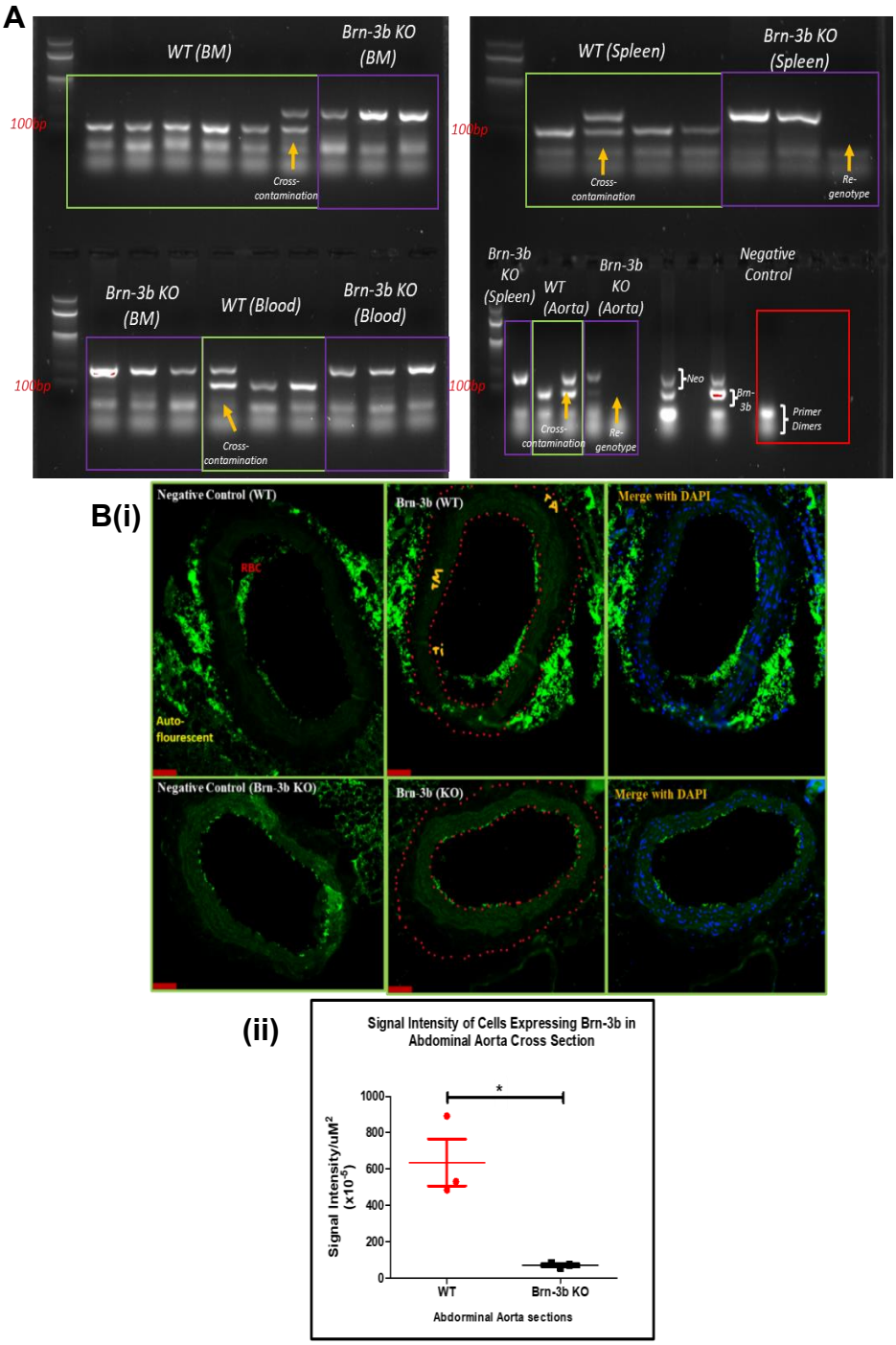

Figure 37: Validation of Brn-3b knock-out (KO) in mouse tissues used in the experiment via PCR and immunofluorescent experiments. The genotypes of the mice were determined using ear-snip samples before the experiment. The knock-out of the Brn-3b gene was measured in the bone marrow (BM), blood, spleen, and aorta using PCR, and protein level in the aorta using immunofluorescence staining. (A) Representative PCR results in BM, blood, spleen, and aorta. (B) Validation at the protein level in the aorta: (i) Representative immunofluorescent staining images; (ii) Quantification of the Brn-3b signal in cross-sections (tunica intima (TI), tunica media (TM) and tunica adventitia (TA)) of wild type (WT) and Brn-3b KO tissues. Data are presented as mean ± SEM for n = 3 (*p < 0.05) (Sex = male/female) (Age = 2-4 months). Region of interest (ROI) is denoted in red (- -) annotation.

4.2.2 No significant difference in total bone marrow cell counts between Brn-3b KO and WT in the femur and tibia

To ascertain the effect of the Brn-3b KO gene on tissue physiology, I compared cell count variations in tissues from both WT and Brn-3b KO mouse models. The analysis revealed that the total number of bone marrow cells within the femur and tibia of both WT and Brn-3b KO mice did not differ significantly, as illustrated in Figure 38.

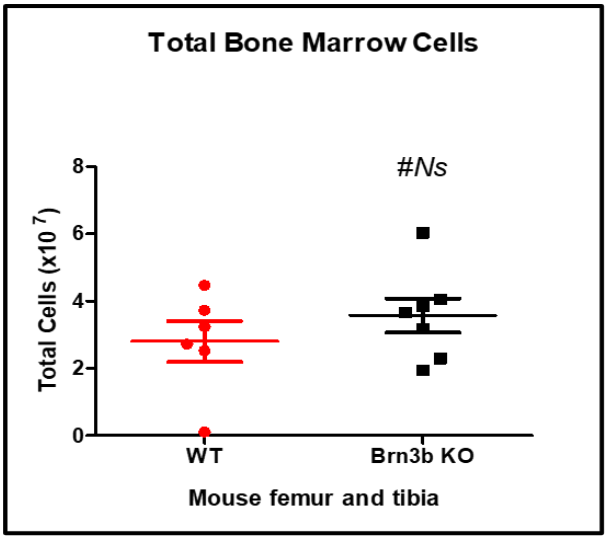

Figure 38: Total bone marrow cell number in femur and tibia of wild type (WT) and Brn-3b knock-out (KO). C57BL/6J mice were euthanised, and the femur and tibia were harvested and flushed using a 25G needle and syringe and passed through a 70 µM cell strainer. Cell numbers were determined using an automated cell counter in Brn-3b KO and WT mouse samples. Data are presented as mean ± SEM for n = 6-7 (Sex = male) (Age = 2–4 months) (Ns = not significant).

4.2.3 Basic screening of T cell lineage and activation status in mouse bone marrow

To delineate the immune cell profile within the bone marrow cells, live and single cells on scatter parameters were initially sub-gated based on single immune cell surface markers, a process depicted in Figure 39 (A). Following this, cells were categorized into major components for a fundamental screening, which included DN for the early stage and DP and SP cells for the mature stage of T cell development, as shown in Figure 39 (B). Further sub-gating was conducted within

each major component cell group to assess T cell lineages in DN and T cell activation status in DP and SP cells. Unstained samples were used as a control in the gating strategy to exclude background signals.

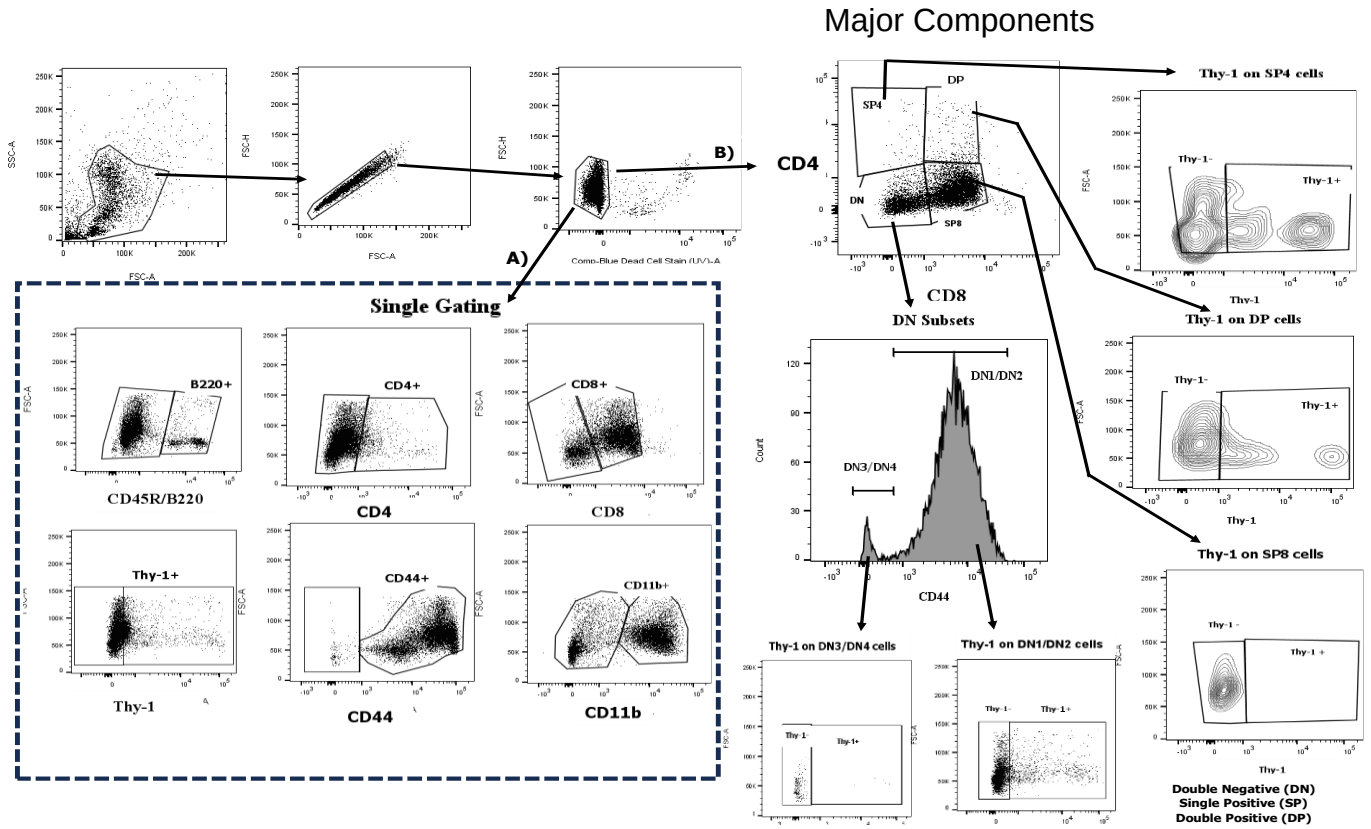

Figure 39: Gating strategy for identifying single markers and basic screening of T cell lineage populations in the bone marrow. Cells were isolated from digested mouse tibia and femur, and live cells were identified by excluding debris and doublets using forward scatter (FSC) and side scatter (SSC) parameters. (A) A single marker was first screened to identify the main populations expressing marker: CD45R/B220+, CD4+, CD8+, CD11B+, Thy-1, and CD44+. (B) Identification of major compartments: double negative (DN), single positive 4 (SP4), SP8 and double positive (DP) against CD4 and CD8 expression. DN cells were further divided into DN1/DN2 and DN3/DN4 populations based on their differing expression of CD44. Non-T and T cell lineages within the DN population and activated T cells were analysed in the DP, SP4, and SP8 populations based on Thy-1 expression.

4.2.3.1 No significant changes of cells expressing single surface markers in Brn-3b KO mouse bone marrow

To study the effect of the loss of Brn-3b on immune regulation, the basic immune cell profile for macrophages, T cells, and B cells in the bone marrow was quantified. The immune cells were stained using CD11b (macrophages), CD4 (T cells), CD8 (T cells), B220/CD45 (B regulatory cells), CD44 (T cell development/MSC), and CD90/Thy-1 (T cell surface marker) using a flow cytometry assay.

The results demonstrated that only the proportion of CD44 markers was statistically significant in the Brn-3b KO bone marrow sample population, with a p-value of 0.0213. However, when considering the total number of CD44+ cells within the entire tissue, no significant change was observed. For other cell surface markers examined, including B220, CD4, CD8, CD11b, and Thy-1, neither the percentages within the sample populations nor the total cell counts in the entire bone marrow tissue of Brn-3b KO mice showed significant differences, as demonstrated in Figure 40.

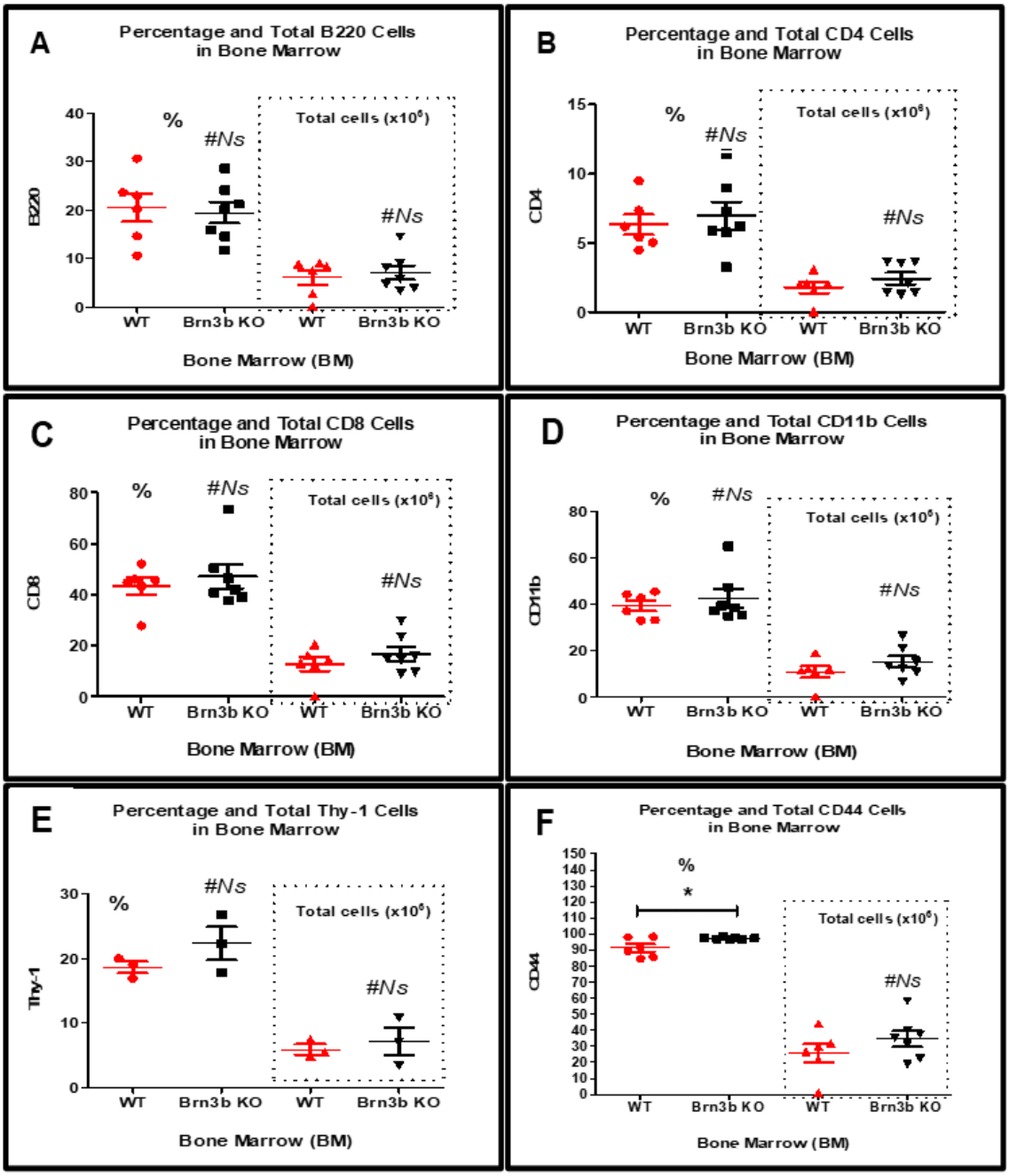

Figure 40: Single surface marker expression in the bone marrow of wild type (WT) and Brn-3b knock-out (KO) mice. C57BL6/J mice were euthanised, and the femur and tibia were harvested and flushed using a 25G needle and syringe and passed through a 70 µM cell strainer. Half a million bone marrow cells were stained for polychromatic flow cytometry analyses. Depicted are (A) CD45R/B220+ (B), CD4+ (C) CD8+, (D) CD11B+, (E) Thy-1+ and (F) CD44+ in WT and Brn-3b KO mouse bone marrow. Data are presented as mean ± SEM for n = 3-7 (Sex = male) (Age = 2–4 months) (*p < 0.05 and Ns = not significant). Note: The Thy-1 marker was stained for n=3 only (left-hand panel = % and right-hand panel = total cells).

4.2.3.2 No significant changes in immune cell profile within major CD4 and CD8 expression compartments of Brn-3b KO mouse bone marrow

Although the results for single markers did not reach statistical significance, the potential impact of Brn-3b loss on immune cell subsets should not be overlooked. To explore this further, I specifically investigated immune cell profiles associated with markers showing a near-positive trend in expression, namely CD44 and Thy-1.

The analysis of Brn-3b KO on major T cell subsets, including early development (DN) and maturation checkpoints (DP, SP4, and SP8), is depicted in Figure 41. The data revealed that Brn-3b deficiency did not significantly change DN cell counts, as evidenced by the close clustering of data points. Similarly, no significant differences were observed in the SP4 cell populations between WT and Brn-3b KO bone marrow samples. While some variability in SP8 cell counts was noted in Brn-3b KO bone marrow, the overlapping error bars suggest these differences were not statistically significant. The DP cell counts followed similar trends, with no significant alterations between WT and Brn-3b KO bone marrow samples.

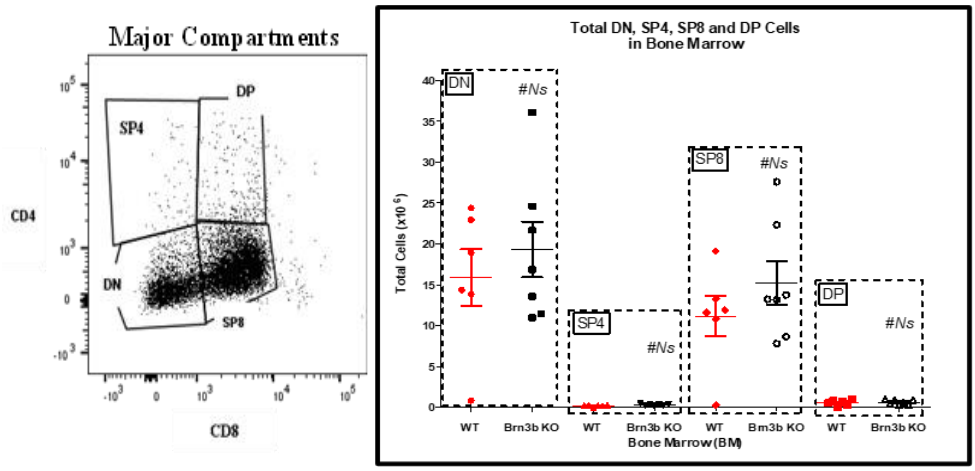

Figure 41: The basic screening of double negative (DN), single positive 4 (SP4), SP8 and double positive (DP) cells in the bone marrow of wild type (WT) and Brn-3b knock-out (KO) mice. C57BL6/J mice were euthanised, and the femur and tibia were harvested and flushed using a 25G needle and syringe and passed through a 70 µM cell strainer. Half a million bone marrow cells were stained for polychromatic flow cytometry analyses. Depicted are CD4-CD8- (DN), CD4+CD8- (SP4), CD4-CD8+ (SP8) and CD4+CD8+ (DP) in WT and Brn-3b KO mouse bone marrow. Data are presented as mean ± SEM for n = 6-7 (Sex = male) (Age = 2–4 months) (Ns = not significant).

4.2.3.2.1 T cell commitment in DN Subsets

In this section, I focus on assessing the profile of CD44-immune-related cells. I specifically examined the DN cell subsets, applying additional gating on DN cells with CD44 markers. The findings revealed that the absence of Brn-3b did not significantly impact the total cells of the DN1/DN2 subsets in bone marrow tissue. Although some variability was observed in the cell counts of the DN3/DN4 subsets, the presence of overlapping error bars suggested that these differences were not statistically significant, as illustrated in Figure 42 (A).

I further investigated the developmental potential of cells within the DN subsets towards non-T and T cell lineages by gating for Thy-1 marker expression. The findings indicated that the loss of Brn-3b did not significantly influence the total number of DN1/DN2 cells expressing either Thy-1 negative or Thy-1 positive, as depicted in Figure 42 (B). Conversely, within the DN3/DN4 cell subsets, the loss of Brn-3b markedly decreased the total of Thy-1- cells, yet it did not significantly alter the count of Thy-1+ cells, as depicted in Figure 42 (C).

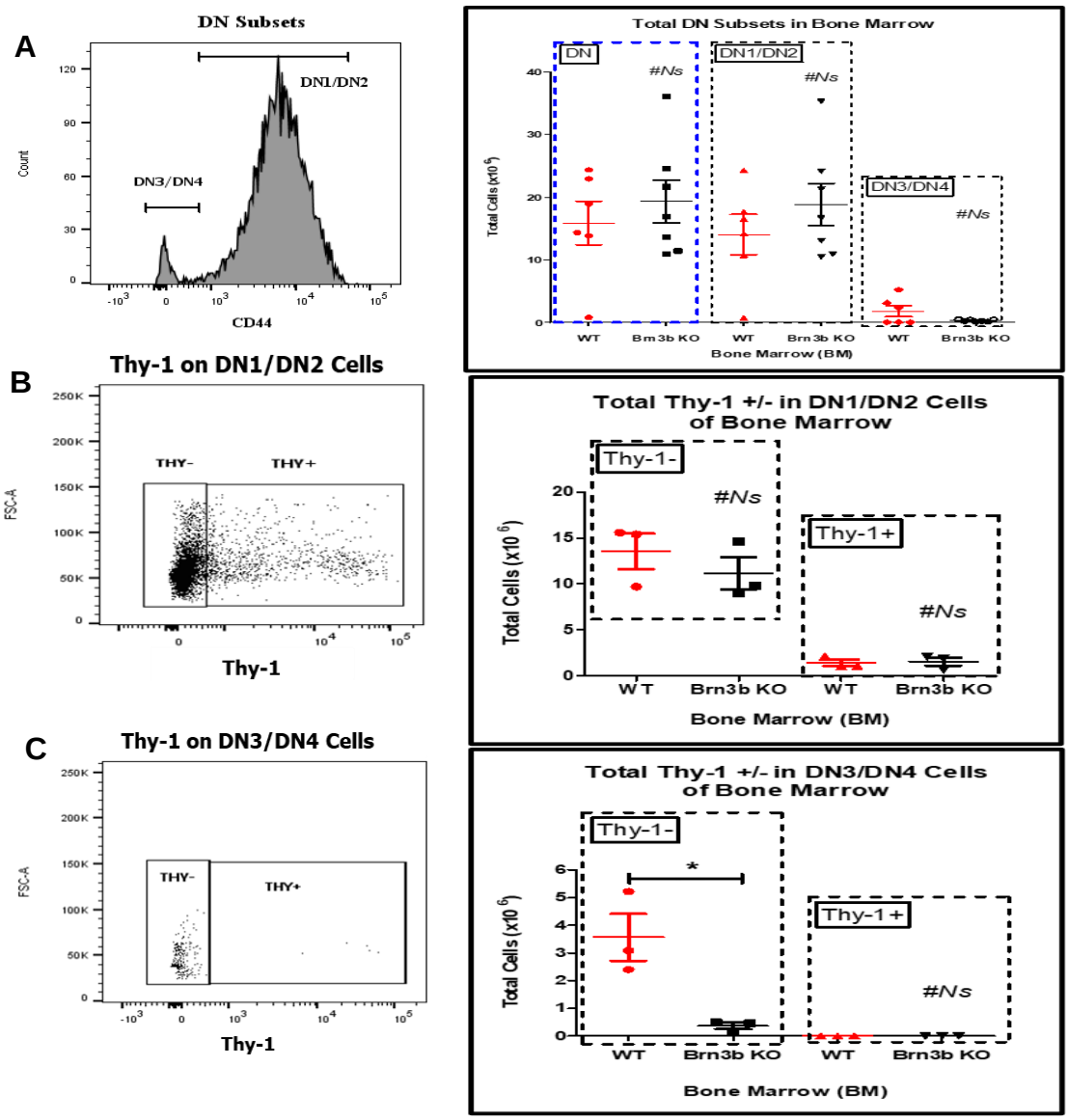

Figure 42: Basic screening of T cell lineage on double negative (DN) subsets in the bone marrow of wild type (WT) and Brn-3b knock-out (KO) mice. C57BL6/J mice were euthanised, and the femur and tibia were harvested and flushed using a 25G needle and syringe and passed through a 70 µM cell strainer. Half a million bone marrow cells were stained for polychromatic flow cytometry analyses. Depicted are (A) DN subsets, and T cell lineage (Thy-1+) in (B) DN1/DN2 and (C) DN3/DN4 in WT and Brn-3b KO mouse bone marrow. Data are presented as mean ± SEM for n = 3-7 (Sex = male) (Age = 2–4 months) (* $p < 0.05$ and Ns = Not significant). Note: The Thy-1 marker was stained for n=3 only.

4.2.3.2.2 Accumulation of activated DP and SP cells

Following the investigation of non-T and T cell lineage at an early checkpoint of T cell commitment, I extend the research to assess Thy-1 expression on mature DP and SP cells in Brn-3b KO Bone Marrow. The findings indicated that the loss of Brn-3b did not significantly alter the expression of Thy-1, either positively or negatively on mature cells, as depicted in Figure 43. Notably, I observed some variability in Thy-1+ expression among DP and SP4 cells within the Brn-3b KO bone marrow; however, these differences were not statistically significant when compared to the WT samples, as illustrated in Figure 43 (A) and (C).

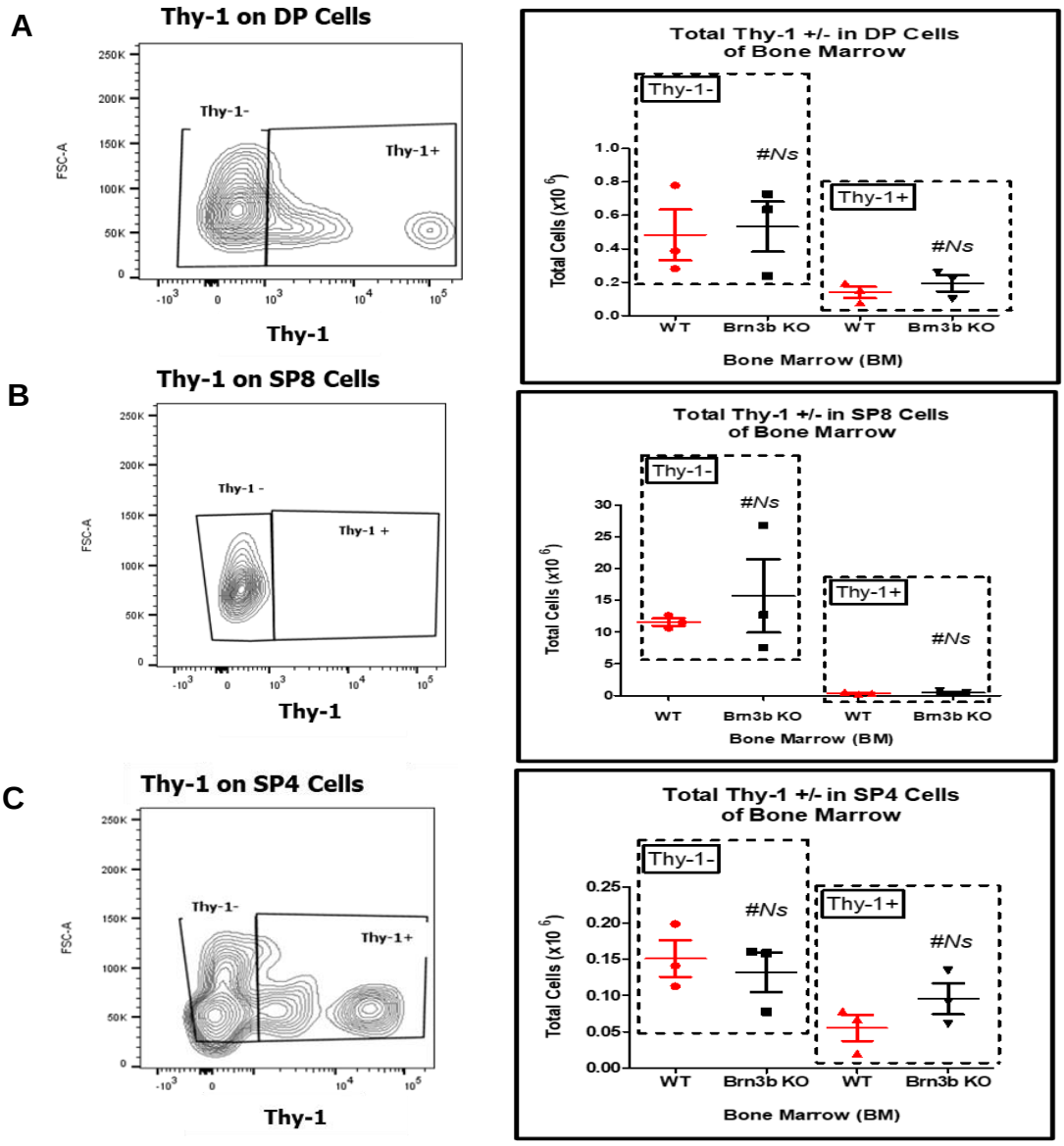

Figure 43: Basic screening of activated double positive (DP), single positive 8 (SP8) and SP4 cells in the bone marrow of wild type (WT) and Brn-3b knock-out (KO) mice. C57BL6/J mice were euthanised, and the femur and tibia were harvested and flushed using a 25G needle and syringe and passed through a 70 µM cell strainer. Half a million bone marrow cells were stained for polychromatic flow cytometry analyses. Depicted are activated (Thy-1+) of (A) DP, (B) SP8 and (C) SP4 in WT and Brn-3b KO mouse bone marrow. Data are presented as mean ± SEM for n = 3 (Sex = male) (Age = 2–4 months) (Ns = Not significant).

4.2.4 Deep characterisation of T cell lineage and activation status in mouse bone marrow

After initial screening showed significant changes in Thy-1- expression in DN3/DN4 cells and variable, yet non-significant, Thy-1+ expression in DP and SP4 cells of Brn-3b KO bone marrow, I proceeded with a more detailed examination of these immune profiles. A comprehensive phenotypic characterisation of early (DN) and mature (DP and SP) T cells in the bone marrow of Brn-3b KO mice and their WT counterparts was conducted using nine cell surface markers, as shown in Figure 44. The gating strategy included unstained samples and FMO as a control to exclude any background fluorescence or non-specific binding.

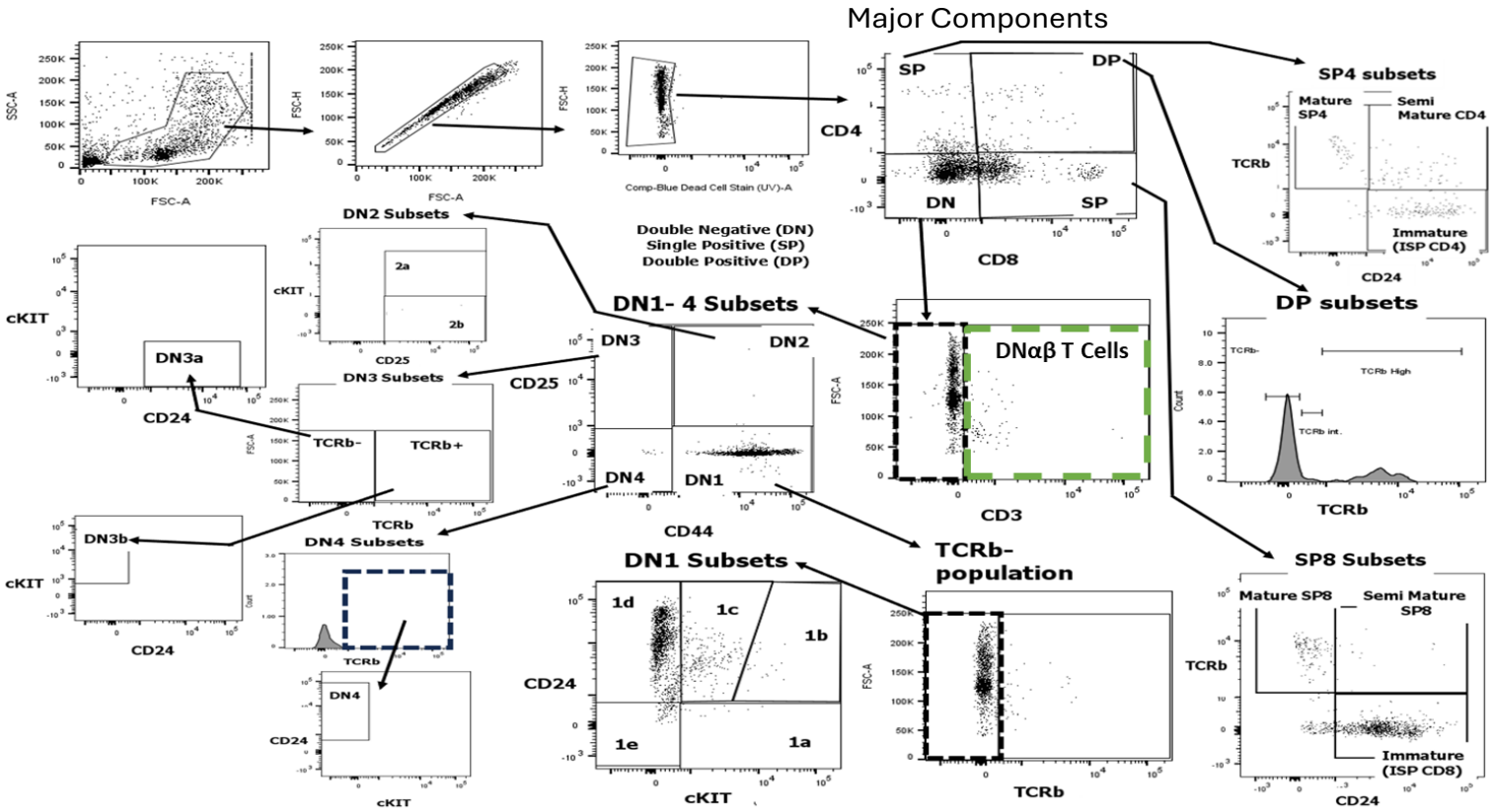

Figure 44: Deep characterisation of the T cell lineage populations in the bone marrow of wild type (WT) and Brn-3b knock-out (KO) mice. Cells were isolated from digested mouse tibia and femur, and live cells were identified by excluding debris and doublets using forward scatter (FSC) and side scatter (SSC) parameters. Major compartments were identified as double negative (DN), single positive 4 (SP4), SP8 and double positive (DP) against CD4 and CD8 expression. DN cells were further divided into DN1-4 subsets based on their differing expression of CD3, CD44, CD25, TCRβ, cKIT and CD24/HSA. All SP and DP subsets were identified based on their differing expression profile of TCRβ and CD24/HSA.

4.2.4.1 No significant changes in additional surface markers in Brn-3b KO bone marrow

In deep characterisation of T cell lineage, the additional markers were included in the flowcytometric antibody cocktails which were CD3, TCRβ, CD25, cKIT/CD117 and CD24/HSA, as shown in Figure 44. Regardless of sex, the total bone marrow cells expressing these markers exhibited minimal variability, with a small error bar, indicating that combining data from both sexes was appropriate for the analysis.

Before the comprehensive investigation of the immune cell profile, I compared the changes of the single surface marker between Brn-3b KO and normal Bone Marrow. The finding showed no significant changes of additional markers in Brn-3b KO mouse bone marrow as compared to the WT, as illustrated in Figure 45.

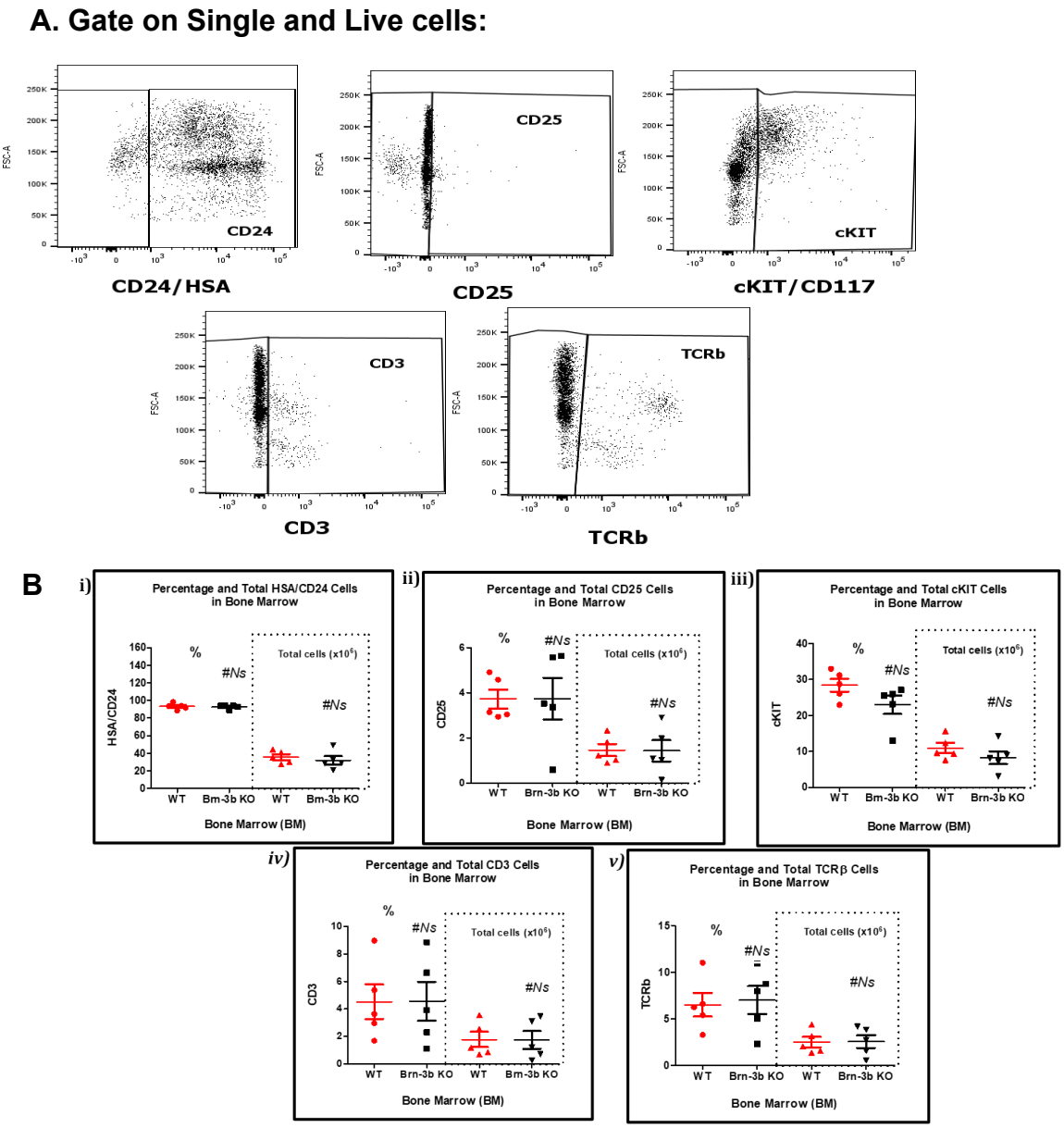

Figure 45: Surface expression of additional markers for identification of T cell lineage in the bone marrow of wild type (WT) and Brn-3b knock-out (KO) mice. C57BL6/J mice were euthanised, and the femur and tibia were harvested and flushed using a 25G needle and syringe and passed through a 70 µM cell strainer. Half a million bone marrow cells were stained for polychromatic flow cytometry analyses. Depicted are (A) dot plot images and (B) the scatter plot graph of (i) CD3+ (ii) CD24+ (iii) CD25 (iv) Ckit and (v) TCRβ in WT and Brn-3b KO mouse bone marrow. Data are presented as mean ± SEM for n = 5 (Sex = male/female) (Age = 2–4 months) (Ns = not significant) (left-hand panel = % and right-hand panel = total cells).

4.2.4.2 Loss of Brn-3b does not change DN subset cells in mouse bone marrow

Furthermore, I conducted a deeper characterization of the DN components using essential markers CD3, CD44, and CD25 to identify the immature DN subsets, including DN1 to DN4, as shown in Figure 46. The scattered plot showed that the expression of DN1 was highly expressed, DN2 and DN4 populations were relatively low, and no expression showed for DN3 in Bone Marrow. The findings revealed that the loss of Brn-3b did not significantly alter the total DN1 to DN4 cell subsets compared to the WT.

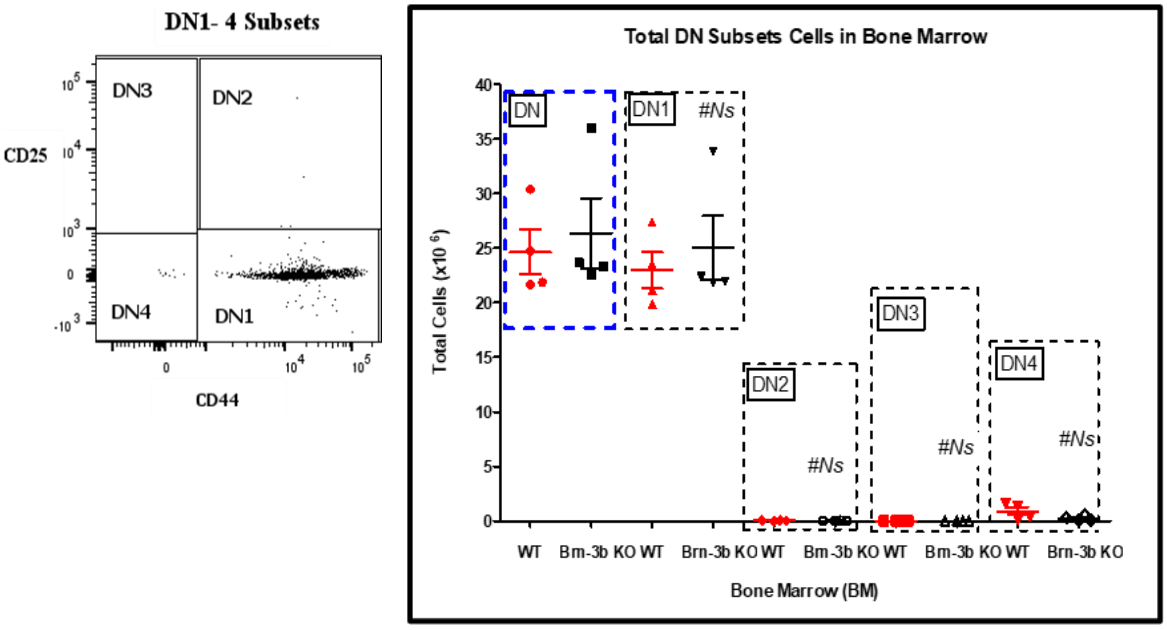

Figure 46: The number of double negative (DN) subsets in the bone marrow of wild type (WT) and Brn-3b knock-out (KO) mice. C57BL6/J mice were euthanized, and the femur and tibia were harvested and flushed using a 25G needle and syringe and passed through a 70 µM cell strainer. Half a million bone marrow cells were stained for polychromatic flow cytometry analyses. Depicted are CD44+CD25-(DN1), CD44+CD25+(DN2), CD44-CD25+(DN3), and CD44-CD25-(DN4) in WT and Brn-3b KO mouse bone marrow. Data are presented as mean ± SEM for n = 4 (Sex = male/female) (Age = 2–4 months) (Ns = not significant).

4.2.4.3 No significant changes of DN1 subsets and DNαβ T cells (early stage) and DP, SP4, and SP8 cells (mature stage) in Brn-3b KO bone marrow

Following the deep characterization of the DN subset, only DN1 was expressed, while DN2 to DN4 were either low or absent in the bone marrow. Consequently, DN2 to DN4 subsets were excluded from further investigation. Table 10 summarises the detailed immunophenotype of DN1 subsets and DNαβ T cells during the early T cell development stage, as well as DP and SP cells during the mature stage.

The findings showed that the loss of Brn-3b did not significantly alter the expression of DN1 subsets (DN1a to e) and DNαβ T cells in the bone marrow. In addition, the loss of Brn-3b also did not significantly change the expression of DP, SP4 and SP8 at different maturation stages (immature, semi-mature and mature) in mouse bone marrow as compared to their WT control.

Table 10: Deep characterisation of cells in the early and mature stages of T cell development in the bone marrow of wild type (WT) and Brn-3b knock-out (KO) mice. C57BL6/J mice were euthanised, and the femur and tibia were harvested and flushed using a 25G needle and syringe and passed through a 70 µM cell strainer. Half a million bone marrow cells were stained for polychromatic flow cytometry analyses. Depicted are double negative 1 (DN1) subsets and DNαβ T cells (early stage), and double positive (DP), single positive 4 (SP4), and SP8 cells at different maturation stages (mature stage) in WT and Brn-3b KO mouse bone marrow. Data are presented as mean ± SEM for n = 4 (Sex = male/female) (Age = 2–4 months) (Ns = not significant).

Early Stage	**Total Cells in Bone Marrow ± SEM (x 10^6)**		
	WT	**Brn-3b KO**	**P value**
DN1	22.96 ± 1.65	24.99 ± 2.95	Ns
• DN1a	0.121 ± 0.03	0.06473 ± 0.02	Ns
• DN1b	0.22 ± 0.03	0.1951 ± 0.04	Ns
• DN1c	2.02 ± 0.25	1.889 ± 0.34	Ns
• DN1d	19.25 ± 1.74	21.05 ± 2.75	Ns
• DN1e	0.744 ± 0.18	0.9498 ± 0.29	Ns
DNαβ T	0.7742 ± 0.30	1.086 ± 0.46	Ns
Mature Stage			
DP	1.031 ± 0.17	0.6833 ± 0.12	Ns
• Low TCRβ	0.834 ± 0.14	0.5215 ± 0.04370	Ns
• Intermediate TCRβ	0.047 ± 0.02	0.024 ± 0.01	Ns
• High TCRβ	0.1434± 0.07	0.132 ± 0.07	Ns
SP4	1.104 ± 0.44	0.676 ± 0.07	Ns
• Immature	0.737± 0.22	0.466 ± 0.03	Ns
• Semi Mature	0.177 ± 0.14	0.036 ± 0.01	Ns
• Mature	0.225 ± 0.08	0.184 ± 0.04	Ns
SP8	10.32 ± 2.1	9.330 ± 1.92	Ns
• Immature	8.838 ± 2.07	8.142 ± 1.82	Ns
• Semi Mature	0.120 ± 0.04	0.094 ± 0.02	Ns
• Mature	0.749± 0.18	0.564 ± 0.12	Ns

4.2.4.3.1 Loss of Brn-3b significantly alters DN1a with a lack of Thy-1 expression

As the loss of Brn-3b may not affect the T cell lineage (DN, DP and SP cells) in the bone marrow, I extended the analysis by conducting a detailed characterization of DN1 subsets using the Thy-1 marker to distinguish between T and non-T cell lineages. Additionally, Thy-1 expression was measured on mature cells (DP and SP) to assess the potential effect of Brn-3b KO on the activation status of these mature cells in the bone marrow.

Table 11 presents the expression of T cells (Thy-1+) and non-T cells (Thy-1-) within DN1 subsets (DN1a to e), as well as activated cells (Thy-1+) in mature populations (DP, SP4, and SP8 cells). The findings showed that the loss of Brn-3b did not significantly alter Thy-1+ expression in DN1 subsets or mature cells (DP, SP4, and SP8 cells). However, the loss of Brn-3b significantly affected the total DN1a cells lacking Thy-1 expression in the bone marrow ($p = 0.0241$). It is important to note that the presence of DN1a cells in the bone marrow was relatively low, which limited the statistical robustness of this analysis.

Table 11: Deep characterisation of T cell lineage and activation of T cells based on Thy-1 expression of wild type (WT) and Brn-3b knock-out (KO) mice. C57BL6/J mice were euthanised, and the femur and tibia were harvested and flushed using a 25G needle and syringe and passed through a 70 µM cell strainer. Half a million bone marrow cells were stained for polychromatic flow cytometry analyses. Depicted are Thy-1-/+ expression on double negative 1 (DN1) subsets (early stage), and double positive (DP), single positive 4 (SP4) and SP8 cells (mature stage) in WT and Brn-3b KO mouse bone marrow. Data are presented as mean ± SEM for n = 4 (Sex = male/female) (Age = 2–4 months) (* $p < 0.05$ and Ns = Not significant). Abbreviation: ND, not determined.

Early Stage	**Total Cells in Bone Marrow ± SEM (x 10^6)**					
	Thy-1-			**Thy-1+**		
	WT	**Brn-3b KO**	**P value**	**WT**	**Brn-3b KO**	**P value**
DN1						
• DN1a	0.078 ± 0.01	0.031 ± 0.01	**0.0241**	0.024 ± 0.01	0.027 ± 0.01	Ns
• DN1b	0.171 ± 0.02	0.149 ± 0.03	Ns	0.047 ± 0.02	0.044 ± 0.02	Ns
• DN1c	1.726 ± 0.27	1.614 ± 0.30	Ns	0.243 ± 0.03	0.227 ± 0.03	Ns
• DN1d	16.75 ± 1.11	"18.07 ± 2.17	Ns	1.268 ± 0.32	1.292 ± 0.39	Ns
• DN1e	0.396 ± 0.09	0.568 ± 0.18	Ns	0.252 ± 0.06	"0.287 ± 0.09	Ns
Mature Stage						
DP						
• Low TCRβ	0.564 ± 0.12	0.285 ± 0.02	Ns	0.315 ± 0.05	0.237 ± 0.03	Ns
• Intermediate TCRβ	0.021 ± 0.02	ND	Ns	0.031 ± 0.01	"0.014 ± 0.01	Ns
• High TCRβ	0.008 ± 0.004	0.011 ± 0.01	Ns	0.145 ± 0.07	0.121 ± 0.06	Ns
SP4			Ns			Ns
• Immature	0.513 ± 0.25	0.319 ± 0.07	Ns	0.1554 ± 0.03	0.147 ± 0.05	Ns
• Semi Mature	ND	ND		0.149 ± 0.11	0.036 ± 0.01	Ns
• Mature	ND	ND		0.138 ± 0.04	0.182 ± 0.04	Ns
SP8			Ns			Ns
• Immature	9.090 ± 2.79	7.631 ± 1.73	Ns	0.61 ± 0.12	0.515 ± 0.1	Ns
• Semi Mature	0.013 ± 0.01	0.005 ± 0.003	Ns	0.121 ± 0.04	0.09 ± 0.02	Ns
• Mature	ND	ND		0.813 ± 0.18	0.578 ± 0.11	Ns

4.2.5 Immunophenotyping of non-T cell lineage in Brn-3b KO mouse bone marrow

In the previous section, I observed that the loss of Brn-3b did not significantly affect the accumulation or development of the CD44-related T cell lineage in the whole tibia and femur. To further investigate Brn-3b's function in immune cell regulation, I extended the analysis to explore its potential influence on CD44-related non-T cell lineage. The gating strategy for identifying subsets of non-T cell lineages, including monocytes, B lymphocytes, and granulocytes, is outlined.

4.2.5.1 Gating strategy using scatter parameter and CD24 marker

The sequential gating method for identifying monocytes, B cells, and granulocytes is illustrated in Figure 47. These non-T cell lineages were distinguished based on scattered parameters (FSC and SSC) following the exclusion of T cell lineage (CD3+ and Thy-1+) in the bone marrow. Monocytes, B cells, and granulocytes were identified based on CD24 expression at different SSC sizes. Specifically, CD24+ expression at low SSC was categorized as B cells (rough B cell), CD24+ and CD24– expression at intermediate SSC as monocytes, and CD24+ expression at high SSC as granulocytes (Raife et al., 1994; Alghetany and Patel, 2002; Sheng et al., 2017; Tarfi et al., 2018; Cherian et al., 2018; Sadofsky et al., 2019; Altevogt et al., 2021; Panagiotou et al., 2022).

The activation or differentiation state of these cell populations was further discerned based on the expression of the CD44 marker. The gating strategy employed unstained samples and FMO as a control to exclude any background fluorescence or non-specific binding.

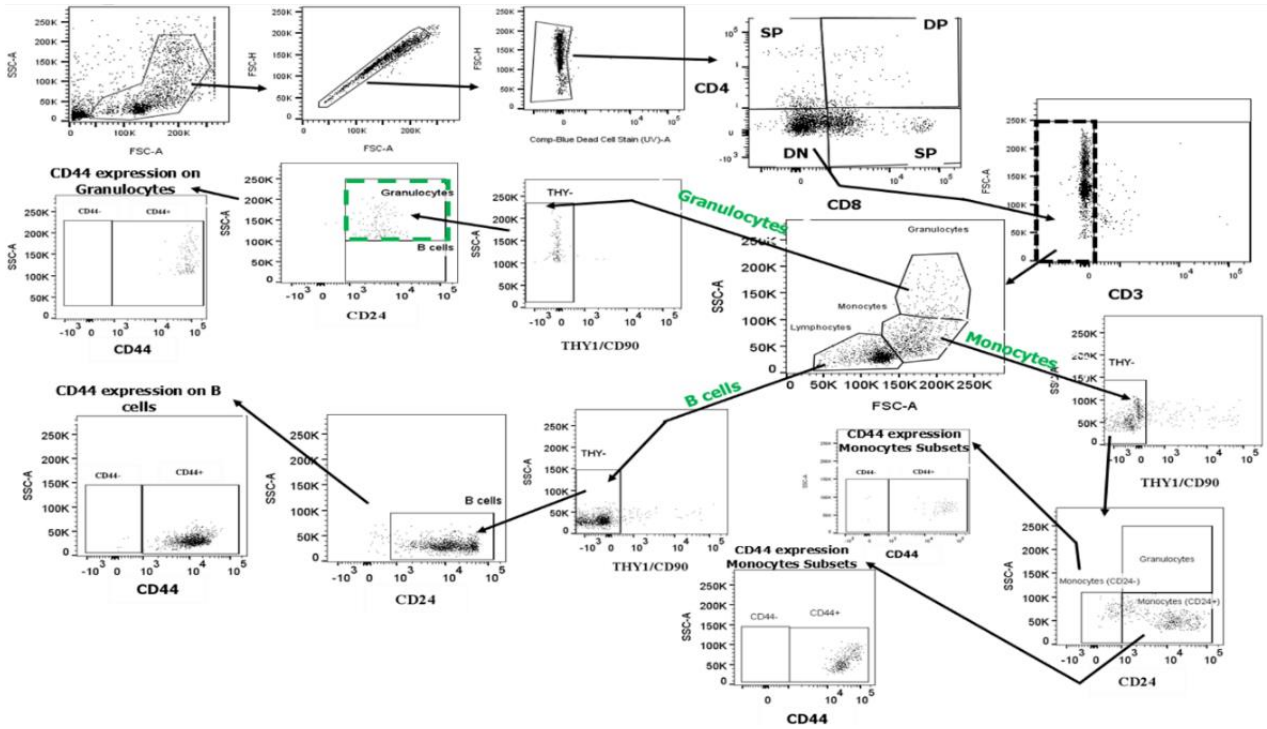

Figure 47: Identification of the B cells, monocytes and granulocytes in the bone marrow of wild type (WT) and Brn-3b knock-out (KO) mice. Cells were isolated from digested mouse tibia and femur, and live cells were identified by excluding debris and doublets using forward scatter (FSC) and side scatter (SSC) parameters. T cell lineages (double positive (DP), single positive 4 (SP4), SP8 and CD3+ cells) were discarded. Double negative (DN) with CD3- cells were further discriminated into lymphocytes, monocytes and granulocytes based on the FSC and SSC. The T cell lineage in each gate of scattered parameters was further gated out using the Thy-1 marker. B cells, granulocytes, and monocytes in each FSC and SSC gate were identified based on CD24 expression. CD24 expression at low SSC was characterised as B cells, CD24 positive at high SSC as granulocytes and CD24 (+/-) in monocytes gate for monocytes. Furthermore, the activated and non-activated B cells, granulocytes and monocytes were identified based on their differing expression of CD44.

4.2.5.2 Rough selection of lymphocytes, monocytes and granulocytes in bone marrow

The analysis of B lymphocytes, monocytes, and granulocytes in the whole bone marrow is depicted in the scatter plot image and graph in

Figure 48. In the dot plot image, lymphocyte cell populations were selected based on FSC low and SSC low, monocytes on FSC int/high and SSC int, and granulocytes on FSC int/high and SSC high. Lymphocyte populations (excluding T cells) were found to be highly expressed in the bone marrow, followed by monocytes and granulocytes. The findings showed that loss of Brn-3b did not significantly change the total number of lymphocytes, monocytes, and granulocytes in the bone marrow as compared to their WT control. The next section provides a more in-depth analysis utilizing marker expression within each gate of scatter parameters.

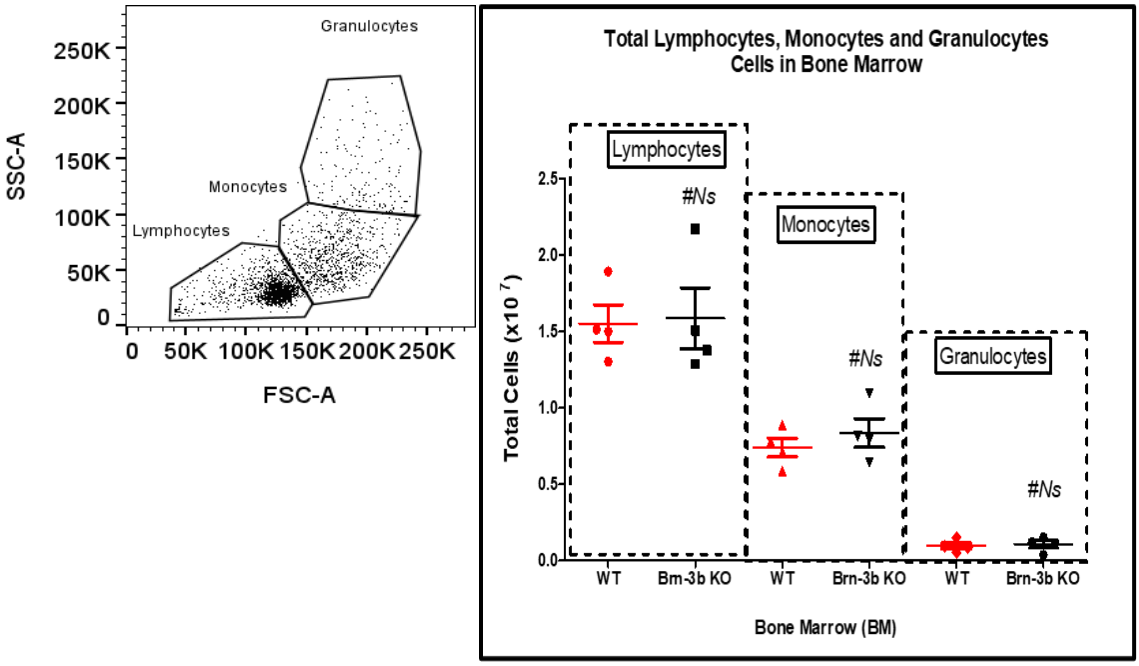

Figure 48: The number of lymphocytes, monocytes and granulocytes in the bone marrow of wild type (WT) and Brn-3b knock-out (KO) mice. C57BL6/J mice were euthanised, and the femur and tibia were harvested and flushed using a 25G needle and syringe and passed through a 70 µM cell strainer. Half a million bone marrow cells were stained for polychromatic flow cytometry analyses. Depicted are the total numbers of lymphocytes, monocytes, and granulocytes in WT and Brn-3b KO mouse bone marrow. Data are presented as mean ± SEM for n = 4 (Sex = male/female) (Age = 2–4 months) (Ns = Not significant).

4.2.5.2.1 No significant difference of B cells (CD24+ SSC^{low}) and their activation status in Brn-3b KO bone marrow

Furthermore, I quantified B cells within the lymphocyte gate using the expression of CD24 at low SSC and further identified their activation status based on CD44 expression on CD24+ B cells, as illustrated in the scatter plot in Figure 49. The scatter plot shows that CD24+ B cells are predominantly located within the lymphocyte gate, with a majority expressing CD44. However, the loss of Brn-3b did not significantly alter the number of CD24+ cells within the lymphocyte gate in the bone marrow compared to the WT counterpart. Additionally, no significant differences in activation status (CD44+/CD44-) were observed for B cells from Brn-3b KO and WT samples.

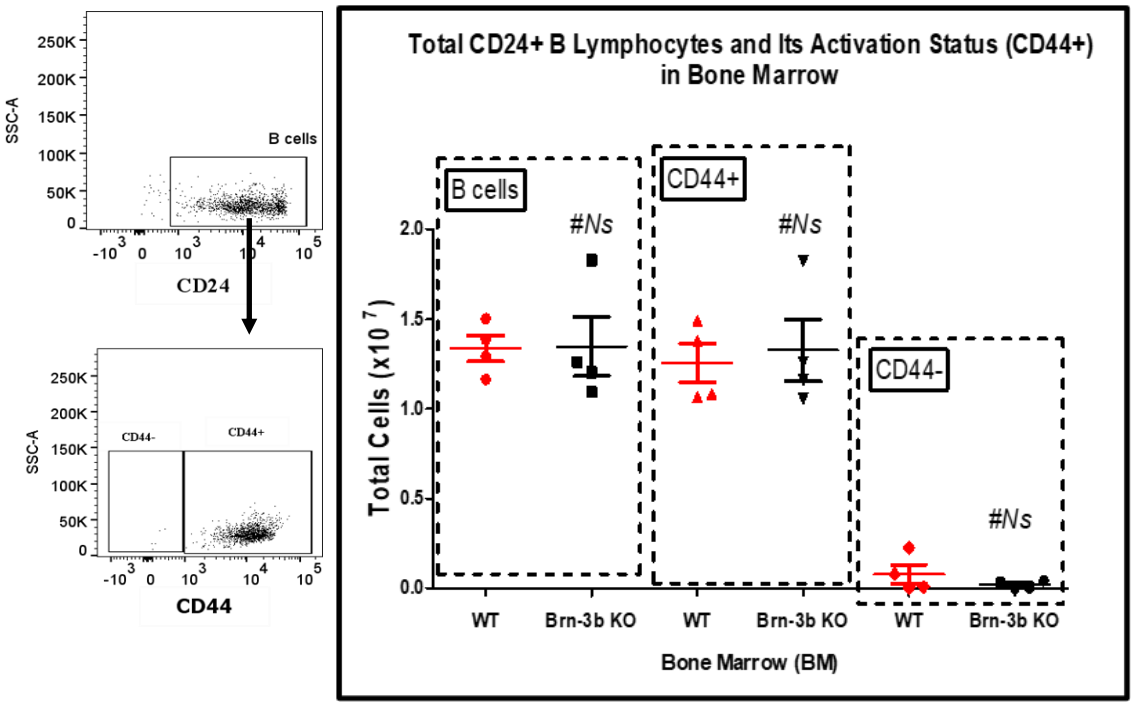

Figure 49: The number of B cells and their activation status in the bone marrow of wild type (WT) and Brn-3b knock-out (KO) mice. C57BL6/J mice were euthanised, and the femur and tibia were harvested and flushed using a 25G needle and syringe and passed through a 70 µM cell strainer. Half a million bone marrow cells were stained for polychromatic flow cytometry analyses. Depicted are the total numbers of B cells (CD24+ SSC^{low}) within the lymphocyte gate and their activation status (CD44+) in WT and Brn-3b KO mouse bone marrow. Data are presented as mean ± SEM for n = 4 (Sex = male/female) (Age = 2–4 months) (Ns = Not significant).

4.2.5.2.2 No significant difference of monocyte cells (CD24- and +) and their differentiation status in Brn-3b KO bone marrow

In this investigation, I analysed the expression of CD24-positive and CD24-negative markers within the monocyte scatter parameter, as delineated in Figure 50. The scatter plot shows a high number of monocyte-derived cells expressing CD24 at intermediate SSC in the bone marrow, compared to those without CD24 expression. Furthermore, the loss of Brn-3b did not significantly alter the expression of CD24+/- monocytes in the bone marrow compared to the WT control. The expression of CD44+/- (differentiation status) on monocytes also did not significantly differ between Brn-3b KO and WT bone marrow tissue.

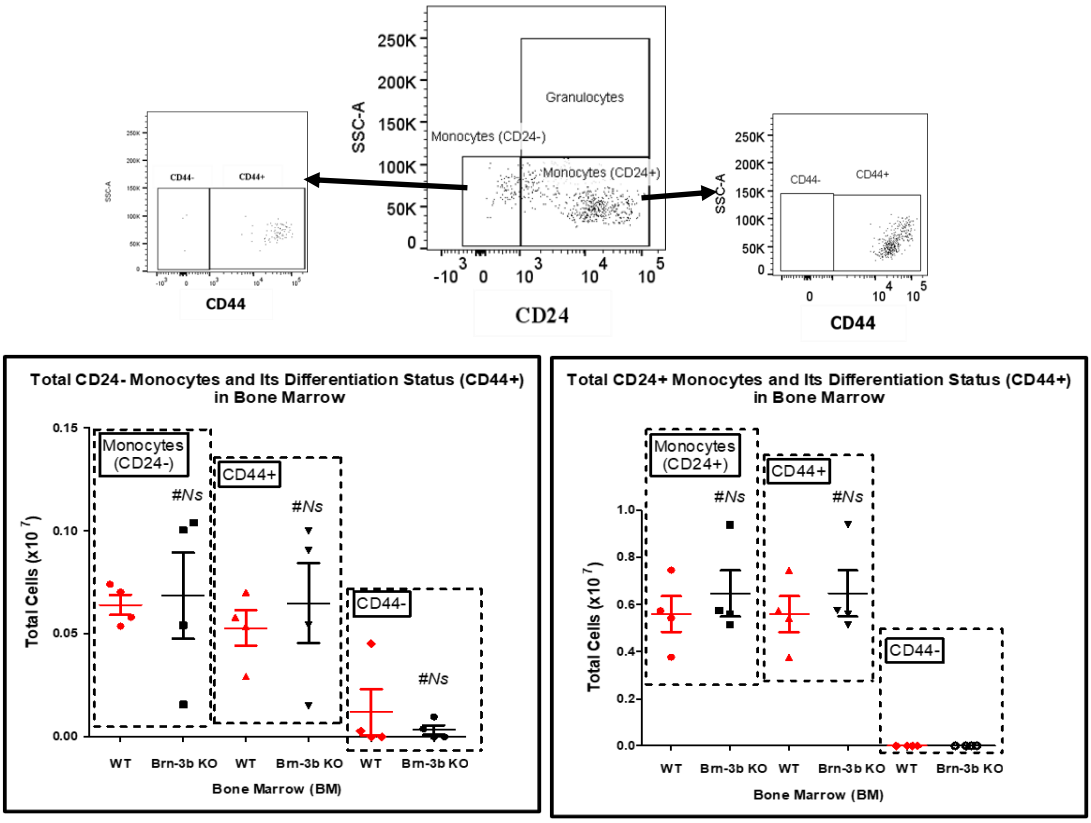

Figure 50: The number of monocytes cells and their differentiation status in the bone marrow of wild type (WT) and Brn-3b knock-out (KO) mice. C57BL6/J mice were euthanised, and the femur and tibia were harvested and flushed using a 25G needle and syringe and passed through a 70 µM cell strainer. Half a million bone marrow cells were stained for polychromatic flow cytometry analyses. Depicted are the total numbers of monocytes (CD24+/-) within the monocyte gate and its differentiation status (CD44+) in WT and Brn-3b KO mouse bone marrow. Data are presented as mean ± SEM for n = 4 (Sex = male/female) (Age = 2–4 months) (Ns = Not significant).

4.2.5.2.3 No significant difference of granulocytes with (CD24+ SSC^{high}) and their activation status in Brn-3b KO bone marrow

The investigation of CD24 expression on granulocytes was extended to address the research question regarding the potential impact of Brn-3b loss on the accumulation/development of CD24+ granulocytes and their activation phenotype (CD44+) within the bone marrow. The scatter plot in Figure 51 shows a high expression of CD24+ within the granulocyte gate, with most cells exhibiting a CD24+CD44+ phenotype in the bone marrow. However, the loss of Brn-3b did not significantly alter the total number of CD24+ granulocytes or CD24+CD44+ phenotype cells in the bone marrow.

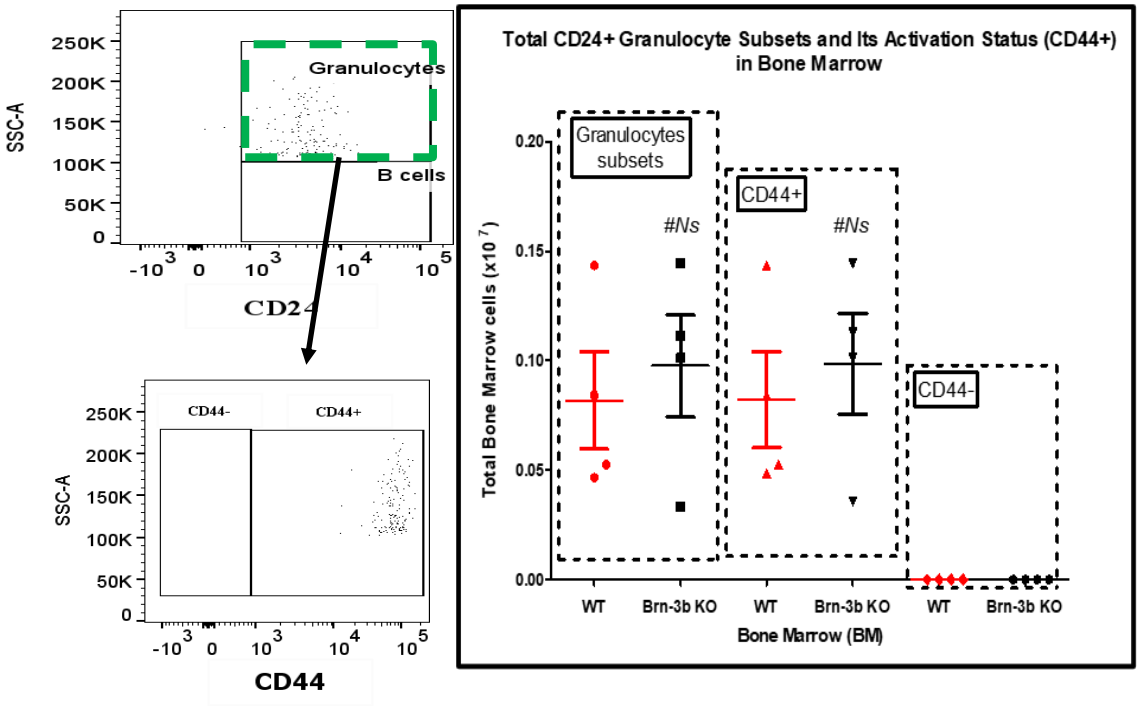

Figure 51: The number of granulocytes and their activation status in the bone marrow of wild type (WT) and Brn-3b knock-out (KO) mice. C57BL6/J mice were euthanised, and the femur and tibia were harvested and flushed using a 25G needle and syringe and passed through a 70 µM cell strainer. Half a million bone marrow cells were stained for polychromatic flow cytometry analyses. Depicted are the total numbers of granulocyte cells (CD24+ SSC^{high}) within the granulocyte gate and its activation status (CD44+) in WT and Brn-3b KO mouse bone marrow. Data are presented as mean ± SEM for n = 4 (Sex = male/female) (Age = 2–4 months) (Ns = Not significant).

4.2.5.3 Back gating strategy using CD45R/B220 and CD11b

In the previous section, monocytes, B lymphocytes, and granulocytes, characterized based on scatter parameters and the CD24 marker, showed no significant changes between Brn-3b KO and normal bone marrow tissue. Furthermore, I characterized non-T cell lineages based on the expression of B220 (B cells) (Rodig et al., 2005) and CD11b (granulocytes and monocytes) markers (Rhein et al., (2010), Yu et al., (2016) & Wang et al., (2017) and proceeded with a back-gating strategy to confirm the immune cell profile in the bone marrow. The gating strategy employed unstained samples as a control to exclude any background fluorescence, as illustrated in Figure 52.

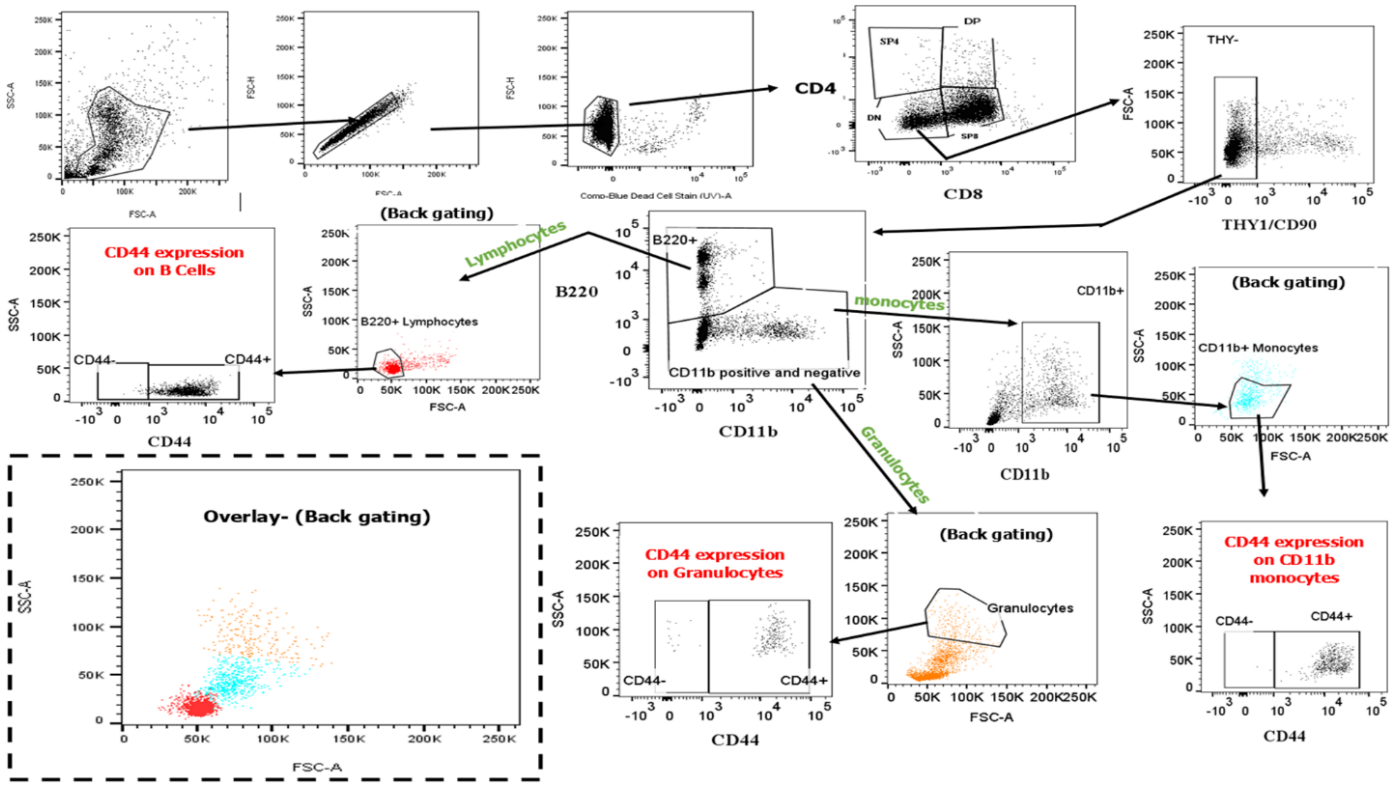

Figure 52: Identification of the B cells, monocytes and granulocytes in the bone marrow of wild type (WT) and Brn-3b knock-out (KO) mice. Cells were isolated from digested mouse tibia and femur, and live cells were identified by excluding debris and doublets using forward scatter (FSC) and side scatter (SSC) parameters. T cell lineages (double positive (DP), single positive 4 (SP4), and SP8) were discarded, and the T cell lineage in the double negative (DN) gate was further excluded using the Thy-1 marker. The B cell lymphocytes, granulocytes, and monocytes were discriminated using B220 and CD11b markers. The B220+ cells were backgated at low FSC and SSC to confirm the B cell population, CD11b+ cells at intermediate FSC and SSC to confirm monocytes, and CD11b+/- cells at intermediate FSC and high SSC to confirm granulocytes. Furthermore, activated and non-activated B cells, granulocytes, and monocytes were identified based on their differing expression profiles of the CD44 marker. Abbreviation: Int, intermediate.

4.2.5.3.1 No significant difference of B220+ lymphocytes and their activation status in Brn-3b KO bone marrow

Further analysis employing a back-gating strategy using the B220 marker is illustrated in Figure 53. The graph demonstrates that the loss of Brn-3b did not significantly alter the expression of B220+ cells at low SSC compared to the WT counterpart. Subsequent analysis of B cell activation status also showed that the loss of Brn-3b did not significantly affect the accumulation or development of non-activated (CD44-) and activated (CD44+) B cells.

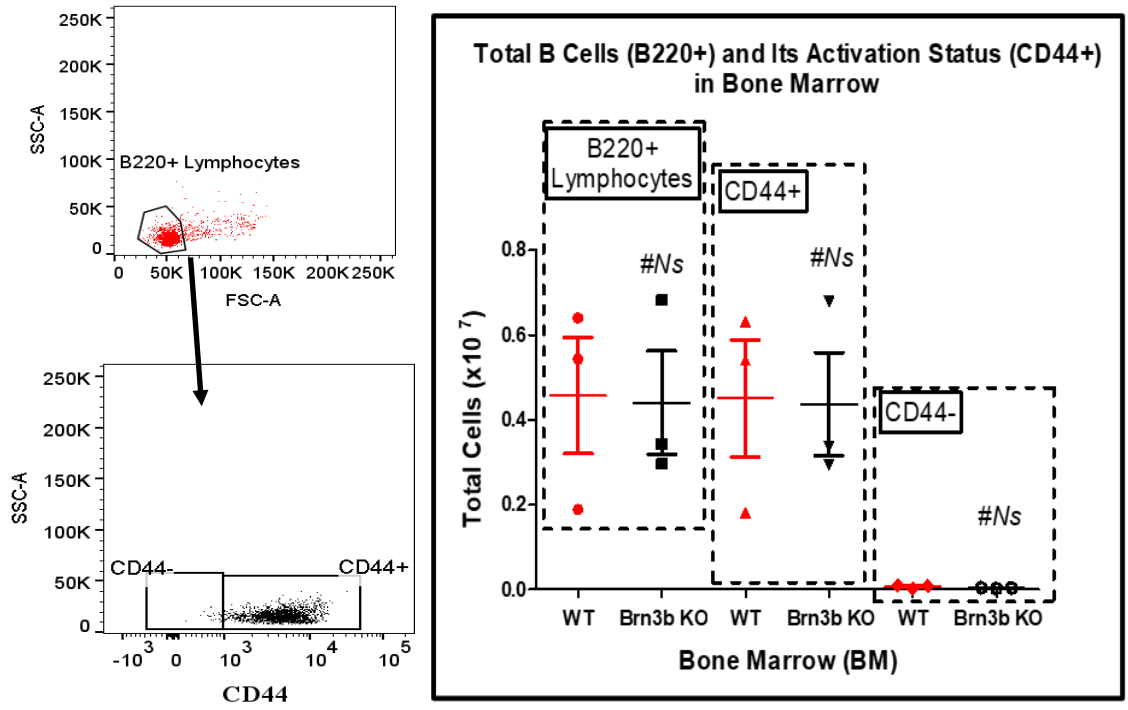

Figure 53: The number of B cells and their activation status in the bone marrow of wild type (WT) and Brn-3b knock-out (KO) mice. C57BL6/J mice were euthanised, and the femur and tibia were harvested and flushed using a 25G needle and syringe and passed through a 70 µM cell strainer. Half a million bone marrow cells were stained for polychromatic flow cytometry analyses. Depicted are the total numbers of B cells (B220+) and their activation status (CD44+) expression on B220 cells in WT and Brn-3b KO mouse bone marrow. Data are presented as mean ± SEM for n = 3 (Sex = male) (Age = 2–4 months) (Ns = Not significant).

4.2.5.3.2 No significant difference of CD11b+ monocytes and their differentiated status in Brn-3b KO bone marrow

Furthermore, this section illustrates the impact of Brn-3b KO on the total monocyte population (CD11b+ at intermediate SSC and FSC) in the bone marrow, as depicted in Figure 54. The findings indicated that the loss of Brn-3b did not significantly affect the expression of CD11b+ monocytes in the bone marrow compared to the WT counterpart. Further analysis of the differentiation status of CD11b+ monocytes revealed that most cells expressed CD44+ (differentiated), and the loss of Brn-3b did not significantly alter this.

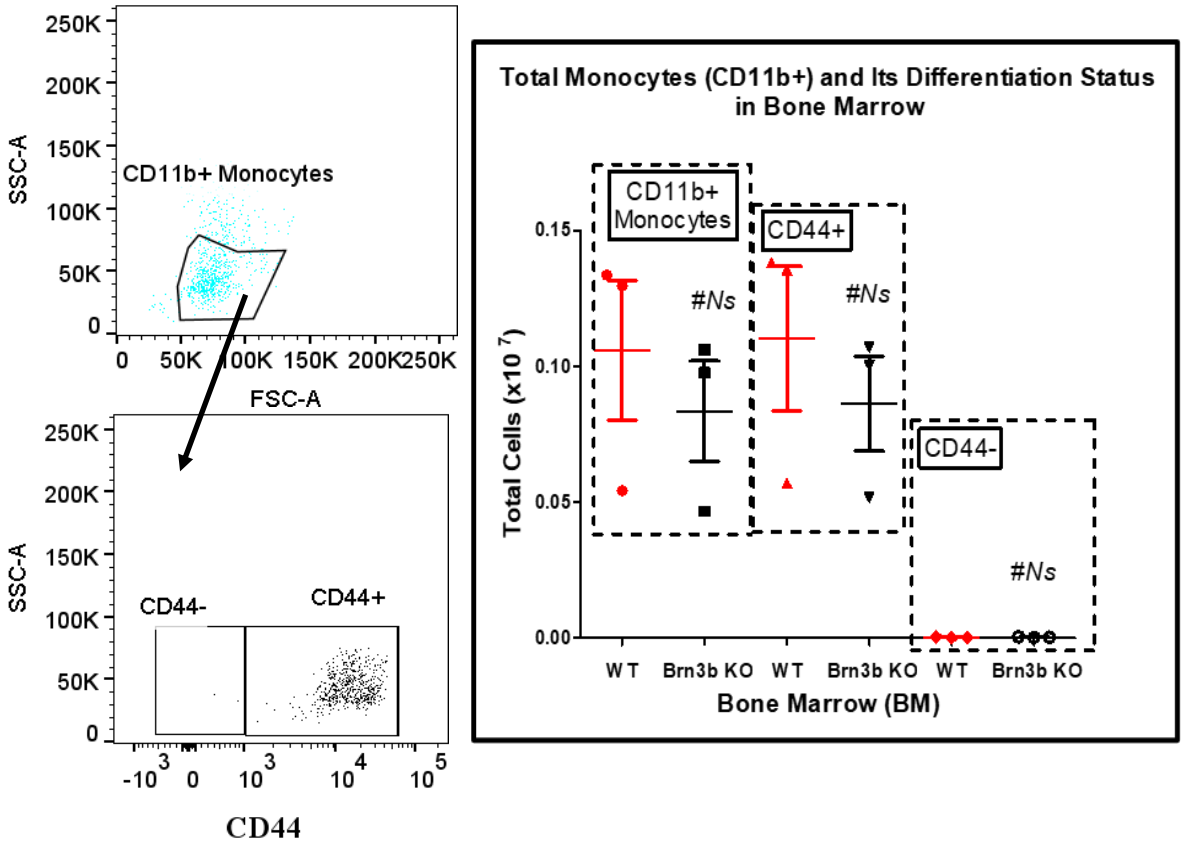

Figure 54: The number of monocytes and their differentiation status in the bone marrow of wild type (WT) and Brn-3b knock-out (KO) mice. C57BL6/J mice were euthanised, and the femur and tibia were harvested and flushed using a 25G needle and syringe and passed through a 70 µM cell strainer. Half a million bone marrow cells were stained for polychromatic flow cytometry analyses. Depicted are the total numbers of monocytes (CD11b+) and their differentiation status (CD44+) in WT and Brn-3b KO mouse bone marrow. Data are presented as mean ± SEM for n = 3 (Sex = male) (Age = 2–4 months) (Ns = Not significant).

4.2.5.3.3 No significant difference of Granulocytes (CD11b+/-) and their activation status in Brn-3b KO bone marrow

Further analyses were conducted to assess the effect of the loss of Brn-3b on the granulocyte population (CD11b+/- at high SSC and intermediate FSC) in the bone marrow, as illustrated in the scatter plot of Figure 55. The findings indicated that the loss of Brn-3b did not significantly change the total number of CD11b+/- granulocytes in the bone marrow. Additionally, the loss of Brn-3b did not significantly affect the activation status of CD11b+/- granulocytes, as the CD44 marker expression mirrored that of their WT control.

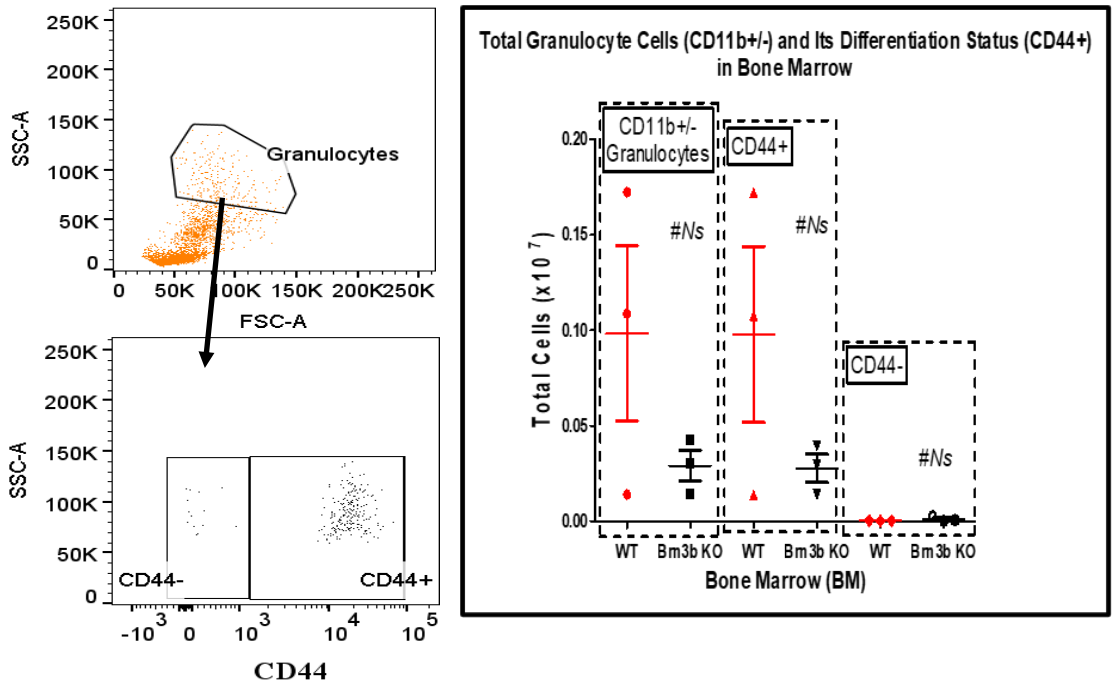

Figure 55: The number of granulocytes and their activation status in the bone marrow of wild type (WT) and Brn-3b knock-out (KO) mice. C57BL6/J mice were euthanised, and the femur and tibia were harvested and flushed using a 25G needle and syringe and passed through a 70 µM cell strainer. Half a million bone marrow cells were stained for polychromatic flow cytometry analyses. Depicted are the total numbers of granulocytes (CD11b+/-) and their activation status (CD44+) in WT and Brn-3b KO mouse bone marrow. Data are presented as mean ± SEM for n = 3 (Sex = male) (Age = 2–4 months) (Ns = Not significant).

4.2.6 Loss of Brn-3b does not significantly change the TNFα, IL-1β and IL-6 concentration in bone marrow supernatant

In the preceding section, I investigated the potential link between Brn-3b and the immunoregulatory function, focusing on the immune cell profile present in the bone marrow. To further validate Brn-3b's function in immune regulation, I expanded the analysis by measuring cytokine concentrations (TNFα, IL-1β, and IL-6) secreted in the conditional medium of bone marrow using the Vplex mouse cytokine assay.

The results revealed that the loss of Brn-3b did not significantly alter TNFα, IL-1β, and IL-6 concentration in the bone marrow supernatant, as illustrated in Figure 56.

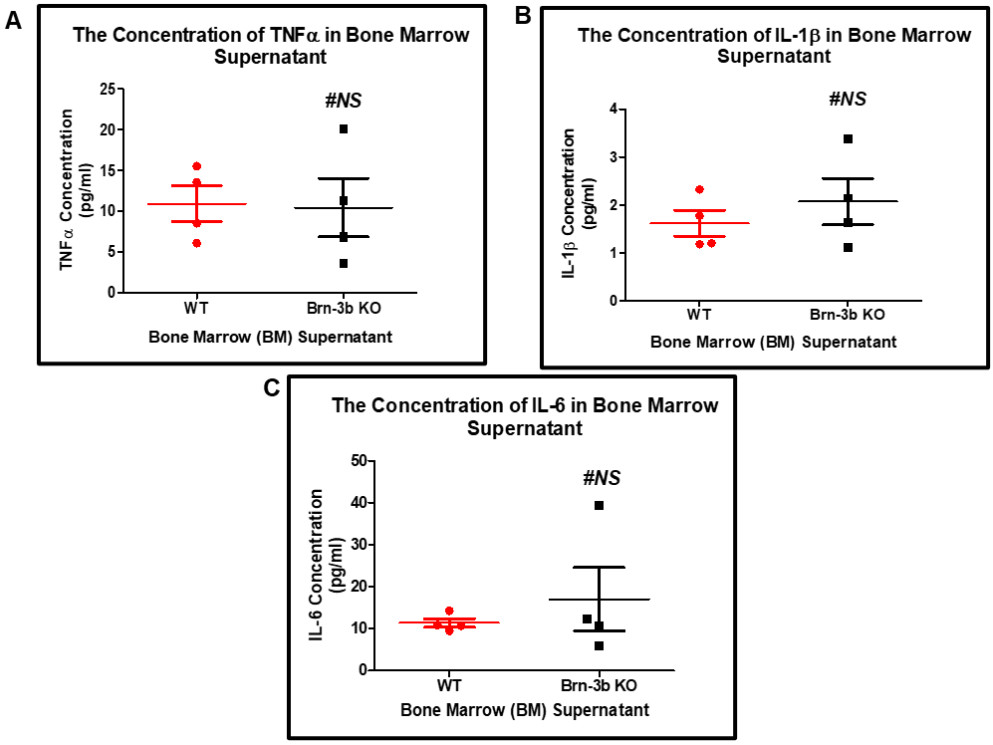

Figure 56: The expression of tumour necrosis factor alpha (TNFα), interleukin 6 (IL-6) and interleukin 1 beta (IL-1β) protein in the bone marrow of wild type (WT) and Brn-3b knock-out (KO) mice. C57BL6/J mice were euthanised, and the femur and tibia were harvested and flushed using a 25G needle and syringe and passed through a 70 µM cell strainer. Two million cells were seeded in 2mL of RPMI without foetal bovine serum (FBS) for 24 Hours. The supernatant was collected, and the concentration of cytokines was measured using an MSD Vplex custom kit. Depicted are the concentration of (A) TNFα (B) IL-1β and (C) IL-6 in WT and Brn-3b KO mouse bone marrow. Data are presented as mean ± SEM for n = 4 (Sex = male/female) (Age = 2–4 months) (Ns = Not significant).

4.2.6.1 Correlation of immune cell population and cytokine profiling

Despite the findings showing no significant differences in the immune cell population and cytokine profile in Brn-3b KO bone marrow compared to WT controls, my curiosity persisted regarding potential correlations between specific immune cell subsets and cytokine release. To explore this, I conducted a Pearson X-Y correlation analysis, which revealed intriguing insights.

The results demonstrated a very strong negative correlation between DP T cells and IL-1β secretion (r = -0.9619, p = 0.0381) in Brn-3b KO bone marrow, a correlation that was negligible in the WT control. Moreover, other immune cells did not show significant correlations with IL-1β secretion in the bone marrow. Similarly, no significant correlations were observed between the secretion of IL-6 or TNFα and any immune cell subsets in the bone marrow, as summarised in Table 12.

Table 12: Correlation between immune cell profile and cytokine secretion in mouse bone marrow of wild type (WT) and Brn-3b knock-out (KO) mice. C57BL6/J mice were euthanised, and the femur and tibia were harvested, flushed, and passed through a 70 µM cell strainer. Cells were stained for flow cytometry and seeded in RPMI without FBS for cytokine measurement. Depicted are Pearson r values between immune cell populations (B cells, monocytes, granulocytes, double negative (DN), double positive (DP), single positive 4 (SP4) and SP8 cells) and cytokine secretion (interleukin 6 (IL-6), interleukin 1 beta (IL-1β), tumour necrosis factor alpha (TNF-α)) in WT and Brn-3b KO bone marrow. Data are for n = 4 (Sex = male/female) (Age = 2–4 months) (* p <0.05 and Ns = Not significant).

	IL-1β		IL-6		TNFα	
	WT	Brn-3b KO	WT	Brn-3b KO	WT	Brn-3b KO
Lymphocytes (B cells)	-0.4966	-0.5063	-0.4153	-0.4715	0.3907	-0.08135
Monocytes	-0.734	0.02927	-0.9273	-0.03813	0.9619	0.1574
Granulocytes	-0.8404	0.8455	-0.6181	0.7541	0.0843	0.6276
DN	-0.75	-0.3675	-0.7191	-0.3504	0.6245	0.01251
DP	0.1284	**-0.9619**	0.5053	-0.8528	-0.7409	-0.5188
SP4	-0.4016	-0.5627	-0.04069	-0.4053	-0.5162	0.09038
SP8	-0.6829	-0.5137	-0.5335	-0.4057	0.3579	0.05837

4.2.6.2 Exploring the interplay between Brn-3b and immune-related key genes

In the preceding section, I assessed the potential function of Brn-3b in immune regulatory status by examining the impact of Brn-3b KO on the accumulation and development of immune cell phenotypes, and secretion of cytokine in the Bone Marrow. However, the findings did not yield promising results. Therefore, I expanded the analysis to include gene expression data related to the development of immune cells and cytokine profiles.

As shown in Figure 57, I investigated the expression of TNFα, IL-15, and CXCR5 genes in the bone marrow samples. The results revealed that the loss of Br-3b did not significantly change the expression of TNFα and IL-15 gene in the bone marrow as compared to WT. Similarly, CXCR5 gene expression followed consistent patterns between WT and Brn-3b KO bone marrow samples, with most data points showing slight variation. However, the changes in CXCR5 gene expression in both samples could not be statistically validated due to inadequate sample size for statistical analysis.

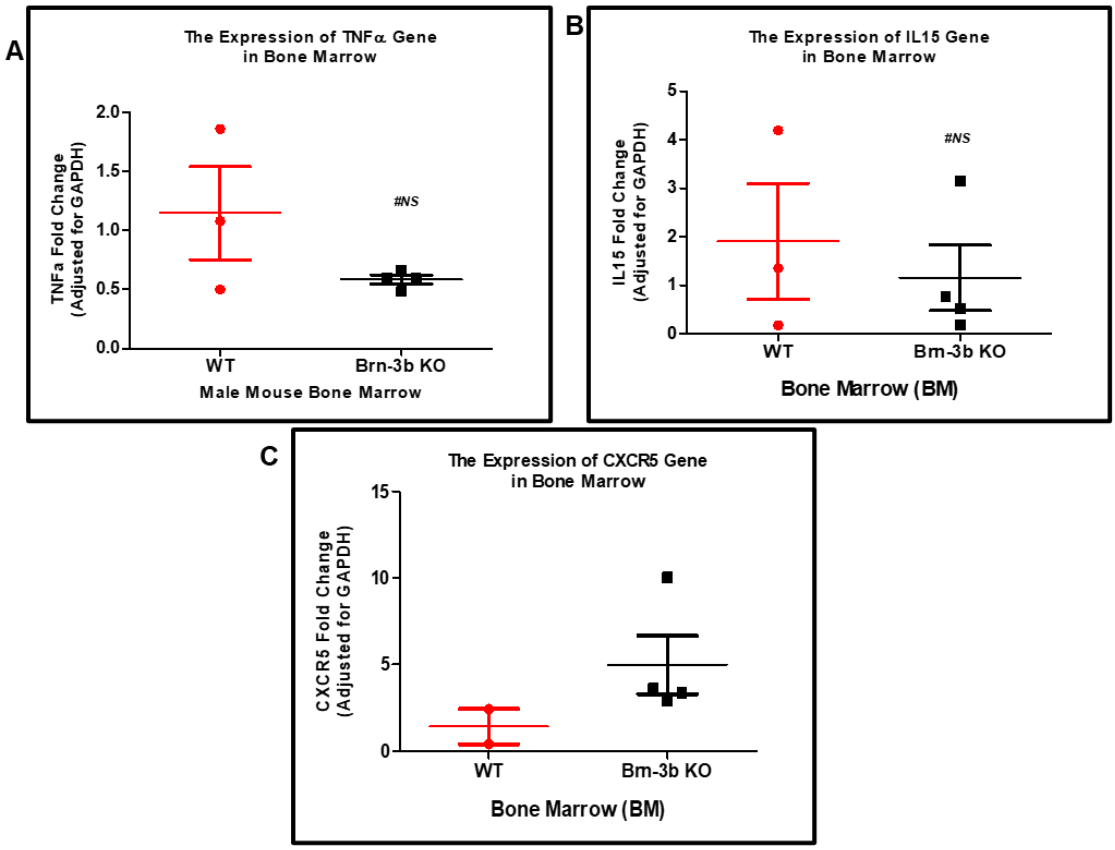

Figure 57: The expression of tumour necrosis factor alpha (TNFα), interleukin 15 (IL-15) and C-X-C chemokine receptor type 5 (CXCR5) gene in bone marrow of wild type (WT) and Brn-3b knock-out (KO) mice. C57BL6/J mice were euthanised, and the femur and tibia were harvested and flushed using a 25G needle and syringe and passed through a 70 µM cell strainer. Cells were lysed in lysis buffer and RNA was extracted for qPCR. Depicted are the expression of (A) TNFα (B) IL-15 and (C) CXCR5 in WT and Brn-3b KO mouse bone marrow. For those cycle threshold (CT) values where the target was undetermined after 40 cycles, a CT value of 35 was used for calculation. Data are presented as mean ± SEM for n = 2-4 (Sex = male) (Age = 2–4 months) (Ns = Not significant).

4.3 Discussion

This chapter aimed to investigate the function of Brn-3b in immune regulation using a global Brn-3b KO mouse model. Specifically, I examined the effect of Brn-3b deficiency on the expression of immune cell profiles, including T cell and non-T cell lineages, as well as inflammatory markers such as IL-1β, IL-6, and TNF-α in the bone marrow. These immune cells and cytokines markers are critical regulators of inflammatory responses (Zhang and An, 2007), and their expression levels provide valuable insights into how Brn-3b may modulate immune regulation, particularly in inflammatory contexts.

4.3.1 The effect of the loss of Brn-3b on T immune cell profile in the bone marrow

This chapter showed that the loss of Brn-3b potentially affects the expression of the CD44 marker in the bone marrow, as illustrated in Figure 40. To explore this further, I investigated the effect of Brn-3b KO on CD44-related immune cell profiles in the bone marrow.

CD44 is a structurally diverse cell surface receptor expressed on most cells (Larkin et al., 2006). First identified on lymphocytes, this cell adhesion protein is involved in cell-cell interactions, cell motility, cell migration, cell differentiation, cell signalling, and gene transcription (Mishra et al., 2019). In the context of the immune cell profile, CD44 is broadly expressed on the membranes of B cells, granulocytes, monocytes, erythrocytes, thymocytes, and mature T cells (Mak and Saunders, 2006). On lymphocytes such as T cells, CD44 plays a crucial role in T cell development and activation/ polarisation. The loss of CD44 results in a poor capacity of CD44–/– T lineage cells to compete with WT cells at multiple levels, implicating CD44 as essential for normal T cell function (Graham et al., 2007).

This study investigated the effect of Brn-3b deficiency on T cell lineage populations at early and mature T-stage development. The findings showed that the loss of Brn-3b did not significantly affect the DN and DN1 subsets (early stages of T cell development) in the bone marrow (Figure 42, Figure 46 and Table 10). Further investigation on DN1 subsets using the Thy-1 marker also showed no significant differences of this cell subset (DN1a to e) between Brn-3b KO bone marrow and WT control. However, a notable alteration was observed in DN1a

cells lacking Thy-1, with their expression being significantly affected in Brn-3b KO bone marrow compared to WT controls.

Thy-1 is a critical marker of T lineage progenitor activity, necessary for efficient T cell development. T cell progenitors lacking Thy-1, CD127, or high levels of CD117 do not efficiently generate T lineage progeny (Saran et al., 2012). Thy-1 is also a pan-T cell marker, abundantly expressed on mature T cells, serving as an important criterion for T cell identity (Haeryfar and Hoskin, 2004; Furlong et al., 2018). The significant alteration in DN1a cells lacking Thy-1 expression suggests that, while the loss of Brn-3b does not broadly affect the accumulation/development of total early T cell lineage (DN1 subsets), it may influence the accumulation/development of non-T cell lineages. This is particularly relevant because DN1 subset (DN1a to e) cells exhibit heterogeneity and have the potential to produce both T and non-T cell lineages (Porritt et al., 2004; Oh et al., 2023).

However, these observations are speculative and warrant further investigation to determine whether Brn-3b deficiency shifts the balance of non-T cell lineage expression. Additionally, the low cell numbers of DN1a cells lacking Thy-1 limit the robustness of the statistical analysis. Future studies with larger sample sizes and increased event acquisition during flow cytometry are needed to validate these findings and improve the statistical reliability of the data.

For mature T cells, the finding showed the expression of DP, SP4 and SP8 cells in the Brn-3b KO mouse bone marrow did not significantly change as compared to WT control. Further analysis of the Thy-1 expression on these mature T cell populations also showed no significant difference between Brn-3b KO and WT control. On mature T cells, Thy-1 functions differently whereas their signal promotes the T cell activation and differentiation. Thy-1 provides the TCR-like signal that is sufficient for T cells including CD4 T cells to proliferate and differentiate into the effector T cells (Furlong et al., 2018). Therefore, the loss of Brn-3b might not affect the accumulation/development of activated mature T cells in bone marrow.

Building on these findings, the next section will focus on the effect of Brn-3b loss on non-T cell lineage expression in the bone marrow.

4.3.2 The effect of the loss of Brn-3b on non-T cell lineage in the bone marrow

Non-T cell lineages, including B cells, monocytes, and granulocytes, are involved in inflammatory diseases and cancers. In this study, I investigated these populations that are known derived from the bone marrow (Fang et al., 2018), and employed two distinct gating strategies for analysis, including CD24 sequential gating and B220 or CD11b back-gating.

The CD24 marker in non-T cell lineages has clinical relevance, with CD24 blockade showing promise in preclinical studies and monoclonal antibodies targeting CD24 demonstrating safety in clinical trials, establishing it as a potential target for cancer immunotherapy (Panagiotou et al., 2022). Similarly, CD11b and B220 markers are pivotal in immune-targeted therapies, particularly within the tumour microenvironment, where they influence the efficacy of immune checkpoint blockade therapies (Cheng et al., 2023). Investigating Brn-3b's function in the expression of these markers could provide insights into its potential influence on immune modulation.

The findings showed that the loss of Brn-3b did not significantly alter the expression of B cells, monocytes, or granulocytes in the bone marrow, despite using two distinct gating strategies (Figure 49 to Figure 55). This result does not align with my initial assumption, which was based on findings that showed a significant reduction of DN1a cells with the lack of Thy-1 (a non-T cell lineage progenitor) in Brn-3b KO bone marrow (Table 10). I had anticipated that Brn-3b deficiency would affect these non-T cell lineages as well. However, this assumption was not supported by the data.

Additionally, the findings did not align with previous reports by Mele et al. (unpublished data), which demonstrated that the loss of Brn-3b significantly affected monocyte (Ly6C+) numbers in zymosan-induced peritonitis and B cell populations (CD45+CD19) in the spleen. The discrepancies may arise from differences in marker selection, the pathological context and the tissue utilised. In this study, distinct markers were used to assess these populations in baseline mice, while Mele et al., (unpublish data) study used different markers to measure B cells and assessed monocyte expression under inflammatory conditions. These findings suggest that Brn-3b may have a more pronounced effect under inflammatory conditions. Future studies should further investigate Brn-3b

deficiency in both baseline and induced pathological states to better understand its role in non-T cell lineages. Additionally, employing other markers may help confirm the effects of Brn-3b deficiency on the non-T cell lineage profile in bone marrow tissue.

Furthermore, I explored CD44 expression on non-T cell lineages, as it plays a crucial role in immune cell activation and function. On B lymphocytes, CD44 expression is vital for B cell activation, with inhibition of this protein marker suppressing B cell activation (Yi et al., 2023). Similarly, CD44 functions in neutrophil cell polarisation and recruitment (Iqbal et al., 2022). On monocytes, the CD44 marker serves as an indicator of monocyte differentiation, particularly as monocytes polarise into macrophages (Zhang et al., 2014).

This finding showed that the loss of Brn-3b did not significantly alter CD44 expression in B cells, monocytes, or granulocytes compared to WT controls (Figure 49 to Figure 55). This suggests that Brn-3b deficiency may not affect CD44 expression under baseline conditions and possibly could influence CD44 expression in response to inflammatory signals, which was not assessed in this study. The lack of significant findings may also be attributed to the limited number of biological replicates. Increasing the number of replicates would strengthen the statistical analysis and provide more robust conclusions.

In summary, the expression profiles of T (DN, DP, and SP cells) and non-T cell lineages (B cells, monocytes, and granulocytes) in the bone marrow of Brn-3b KO mice were mirrored to WT controls. These findings suggest that Brn-3b may not significantly impact immune regulation in the bone marrow, based on these specific immune cell profiles. Further investigation is required to assess the immune regulation status in Brn-3b KO bone marrow tissue, potentially by measuring other indicators, such as soluble proteins (cytokines).

4.3.3 The effect of the loss of Brn-3b to protein biomarker (cytokine) profile and its correlation with immune cell profile

Identifying immune-inflammatory indicators is crucial for predicting the severity of disease disorders and disease diagnosis, particularly in the context of emerging infectious diseases. These indicators not only provide insights into the progression and severity of the disease but also guide medical therapy, allowing for more targeted and effective treatments (Ghofrani *et al.,* 2023). Cytokines play

a critical role in cell-cell communication within the immune system and have emerged as important therapeutic targets (Cui et al., 2024). The cytokines assessed in this study, including IL-1, IL-6, and TNFα, are typically classified as pro-inflammatory cytokines, which mediate inflammatory responses (Calson et al., 1999; Umare et al., 2014; Walsh et al., 2023). This study evaluated the concentration of these cytokines in the bone marrow supernatant of Brn-3b KO mice to explore the potential function of Brn-3b in immune regulation.

The results showed that the loss of Brn-3b did not significantly affect the expression levels of IL-1β, IL-6, or TNFα in the bone marrow supernatant when compared to WT controls (Figure 56). These cytokines are produced by various cells, including monocytes, macrophages, B and T lymphocytes, DCs, and neutrophils (Kany et al., 2019; Walsh et al., 2023). Given this, further analysis was conducted to explore the correlation between cytokine release and the expression of T and non-T cell lineages in the Brn-3b KO bone marrow compared to the WT. A significant negative correlation was observed between IL-1β and DP cells in the Brn-3b KO bone marrow, but no significant correlation was observed between the other cytokines and immune cell profiles (Table 12).

These findings suggest that the loss of Brn-3b does not significantly affect the overall immune cell profile and cytokine release in the bone marrow. The observed negative correlation between IL-1β and DP cells indicates that Brn-3b may regulate specific subsets of immune cells and cytokines, rather than affecting the broader immune cell profile or cytokine levels in the bone marrow as a whole. This highlights the need for further analysis of isolated DP cells from Brn-3b KO bone marrow to measure IL-1β expression at both the transcriptional and protein levels in these cells, as well as to investigate molecular pathways such as NFκB or MAPK. These studies could provide valuable insights into Brn-3b's role in regulating immune responses through DP cells and IL-1β expression.

However, it is worth noting that the mouse model used in this study is a global Brn-3b KO model, which represents a complete loss of Brn-3b across the entire organism, rather than a cell-specific knockout (Gurumurthy et al., 2021). While this approach allows for observation of the overall effects of Brn-3b deficiency, it does not pinpoint which specific cell types (such as immune cells) are responsible for the observed effects. To gain more detailed mechanistic insights, future

studies using a cell-specific Brn-3b knockout model, such as the cre-lox system, would help clarify which immune cell subsets are involved.

Additionally, to validate Brn-3b's role in immune regulation, it is essential to extend the analysis to other tissues that are highly correlated with the bone marrow, such as blood circulation. Normal haematopoiesis in the bone marrow results in a balanced production of blood cells, which are released into circulation. In pathological conditions, however, the number of blood cells can be significantly altered (Boes and Durham, 2017). Therefore, future studies should explore the impact of Brn-3b deficiency on the accumulation of T and non-T cell populations in the blood.

4.4 Conclusions

The objective of this chapter was to investigate the immune-related role of Brn-3b by analysing the immune cell phenotype development/infiltration and soluble protein in the bone marrow tissue of the Brn-3b KO mouse model. Some of the key findings include:

- The loss of Brn-3b did not significantly alter the total of CD44, Thy-1, B220, CD4, CD8, and CD11b cell in the whole tibia and femur.
- Development/infiltration of T cell lineage in Brn-3b KO bone marrow mirrored those of the WT control.
- Development/infiltration of non-T cells including B-lymphocytes, monocytes and granulocytes in Brn-3b KO bone marrow mirrored those of the WT control.
- Brn-3b deficiency did not significantly influence the secretion of pro-inflammatory cytokines including TNFα, IL-1β, and IL-6 in bone marrow supernatant.

5 EVALUATION OF LEVELS OF INFLAMMATORY-BASED MARKERS IN THE BLOOD OF BRN-3B KNOCK-OUT MOUSE MODEL

5.1 Introduction

All cells, including RBCs, WBCs, and platelets found in the blood, originate from the bone marrow. Blood consists of 55 to 60% plasma, approximately 1% WBCs, and about 40% RBCs (Dean, 2005; Wang et al., 2021). The components in the blood have been extensively explored clinically to diagnose various health conditions. Blood analysis is a cornerstone of medical diagnostics due to its ability to provide critical information about a patient's immune status, metabolic health, and the presence of diseases such as infections, inflammatory conditions, and malignancies (Seo and Lee, 2022). Recently, several efforts have been made to simplify methods for tracking inflammatory status, primarily focusing on the evaluation of blood biomarkers. These methods include peripheral blood cell-derived inflammatory scores, which are based on equations involving blood cell counts, particularly white cell subtypes and platelets, along with other clinical parameters (Banna et al., 2022). Clinically, the presence of immune biomarkers in peripheral blood aids in guiding treatment decisions for patients (Hiam et al., 2021).

5.1.1 Assessment of inflammatory prognosis based on cellular and protein biomarker

Blood sampling is a relatively simple and minimally invasive method compared to accessing other tissues/organs, such as the brain in multiple sclerosis or the joints in RA, which present significant challenges for assessment. However, immune cells from the organ become primed/trained and execute their functions

by recirculating between central and peripheral lymphoid organs and migrating to and from sites of injury *via* the blood (Chaussabel et al., 2010). Consequently, alterations in the cellular and protein components in the blood can correlate with the conditions of primary and secondary organs and reflect the pathological state of the immune system (Boes and Durham, 2017). Therefore, primary diagnosis of the inflammatory status usually could be assessed by collecting blood samples from the patient.

In the blood, various cell lineages have been found and characterised for further diagnosis. Therefore, the development or progression of inflammatory conditions is often measured by the accumulation of cellular biomarkers, including bone marrow progenitors, immature neutrophils, monocytes, semi-mature DCs, and lymphocytes in the blood. Theoretically, immature immune cells, such as stem cell progenitors are found in the blood as they circulate into the blood from the bone marrow before migrating to various immune organs, including the spleen, thymus, and lymph nodes, for further development or residence (Boes and Durham, 2017). Furthermore, these immune cells undergo activation and perform their functions by recirculating to the targeted tissue *via* the blood. The complex patterns of recirculation depend on the state of cell activation, the adhesion molecules expressed by immune and ECs, and the presence of soluble chemotactic molecules such as chemokines and cytokines that selectively attract populations of blood cells (Chaussabel et al., 2010).

As the expression of soluble protein mediators such as IL-6, IL-1β, TNFα, IL-2, IL-4, IL-8, and IL-10 in the blood is also crucial for the attraction and regulation of blood cells, these markers are essential for evaluating inflammatory status (Hiam et al., 2021). In correlation with immune cells, cytokines such as interferons (IF) and IL are produced by accumulated immune cells like macrophages, B and T lymphocytes, mast cells, and ECs to systematically perform their roles (Menzel et al., 2021). These immune cells usually were found in the WBCs layer and the soluble mediator were founded in the plasma (Wang et al., 2021). The imbalances of the immune cells in the WBC layer and soluble mediators in the plasma would reflect the inflammatory status of the blood (Dean, (2005) & Pettengill *et al.,* (2014).

Building on findings from the previous chapter, which demonstrated that Brn-3b deficiency did not significantly affect immune cell profiles in the bone marrow, this

chapter investigates whether the loss of Brn-3b alters inflammatory markers in the blood. This evaluation includes both cellular and protein biomarkers, offering additional insights into Brn-3b's potential role in immune regulation.

In this study, I hypothesise that the loss of Brn-3b would affect the development and accumulation of immune cell profiles in the blood that would cause inflammation. Accordingly, the objectives of this chapter were delineated as follows:

1. To explore the alterations of immune cell profile including T (early and mature state) and non-T cell (B lymphocytes and monocytes) lineage within the blood of Brn-3b KO mice.

2. To explore the changes in protein biomarker including IL-1β, IL-6 and TNFα in the Brn-3b KO mouse blood

5.2 Results

5.2.1 No significant alteration of the total WBC in Brn-3b ko mouse blood

As observed in the previous chapter, the loss of Brn-3b did not significantly alter the expression of T and non-T cell lineages in the bone marrow. To further investigate this, I analysed blood, a tissue closely related to the bone marrow, focusing on changes in the WBC components.

As shown in Figure 58, the loss of Brn-3b did not significantly change the total number of WBC in the 80 µL of blood compared to WT counterparts. On average, there were 382,200 ± 0.7940 cells per 80 µL (or 4,777.5 cells/µL) of WBCs in normal mouse blood, compared to 309,000 ± 0.5026 cells per 80 µL (or 3,862.2 cells/µL) in Brn-3b KO mouse blood.

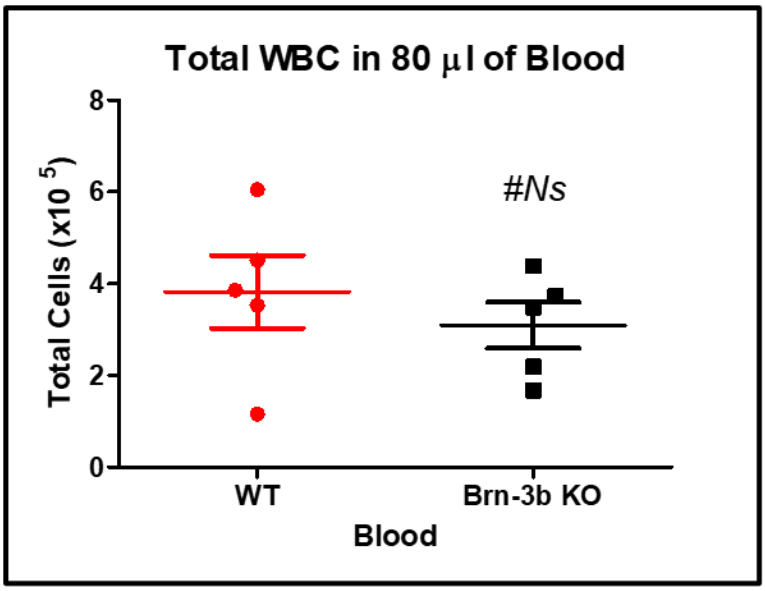

Figure 58: Total WBC number in 80 µL of blood of wild type (WT) and Brn-3b knock-out (KO) mice. C57BL6/J mice were euthanised, and blood was collected using a 25G needle and syringe, then kept in ethylenediaminetetraacetic acid (EDTA) blood collection tubes at room temperature (RT). The blood was lysed using red blood cell (RBC) lysis buffer, and the white blood cells (WBCs) were counted using an automated cell counter. Data are presented as mean ± SEM for n = 5 (Sex = male/female) (Age = 2–4 months) (Ns = not significant).

5.2.2 Gating strategy for single immune cell surface markers in mouse WBC

Following the comparison of the number of rough WBCs present in both normal and Brn-3b KO blood, I extended the investigation to focus on specific leukocytes, including T and non-T cell lineage present in the blood of both groups. These leukocytes were identified based on their surface marker expression, as depicted in Figure 59.

The gating strategy was employed to identify single markers on live and single cells. The cells were discriminated using scatter parameters, following the exclusion of debris, doublets, and dead cells, as illustrated in Figure 59. The gating strategy for the stained samples was validated against FMO and unstained controls to minimize background fluorescence signals.

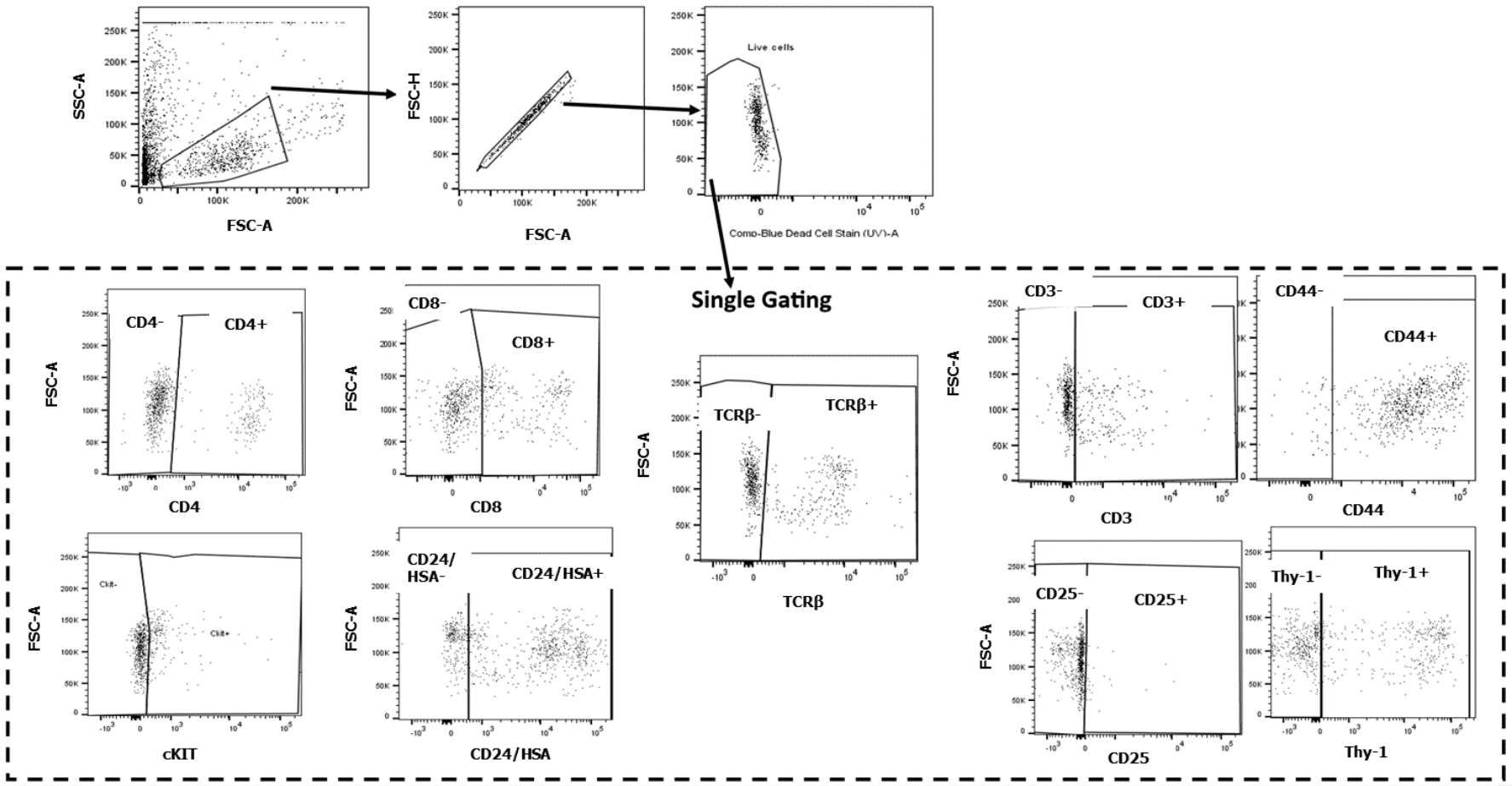

Figure 59: Gating strategy for identifying single markers in blood of wild type (WT) and Brn-3b knock-out (KO) mice. Blood was collected using a 25G needle and syringe, and lysed using red blood cell (RBC) lysis buffer and live cells were identified by excluding debris and doublets using forward scatter (FSC) and side scatter (SSC) parameters. Ten thousand cells from 80 µL of blood were stained for polychromatic flow cytometry analyses. Depicted are single markers (black box) for CD4+, CD8+, Ckit+, CD24+, TCRβ+, CD3+, CD25+, Thy-1+, and CD44+.

5.2.2.1 No significant different of single markers expression in Brn-3b KO mouse blood

In this section, the expression of single surface markers was analysed. WBCs were stained with surface markers, including CD4, CD8, CD3, CD44, Thy-1, CD24, cKIT, CD25, and TCRβ. A representative image of these marker expressions is shown in Figure 59.

The results revealed that the loss of Brn-3b did not significantly alter the expression of these markers in 80 µL of mouse blood compared to the WT control, as depicted in Figure 60.

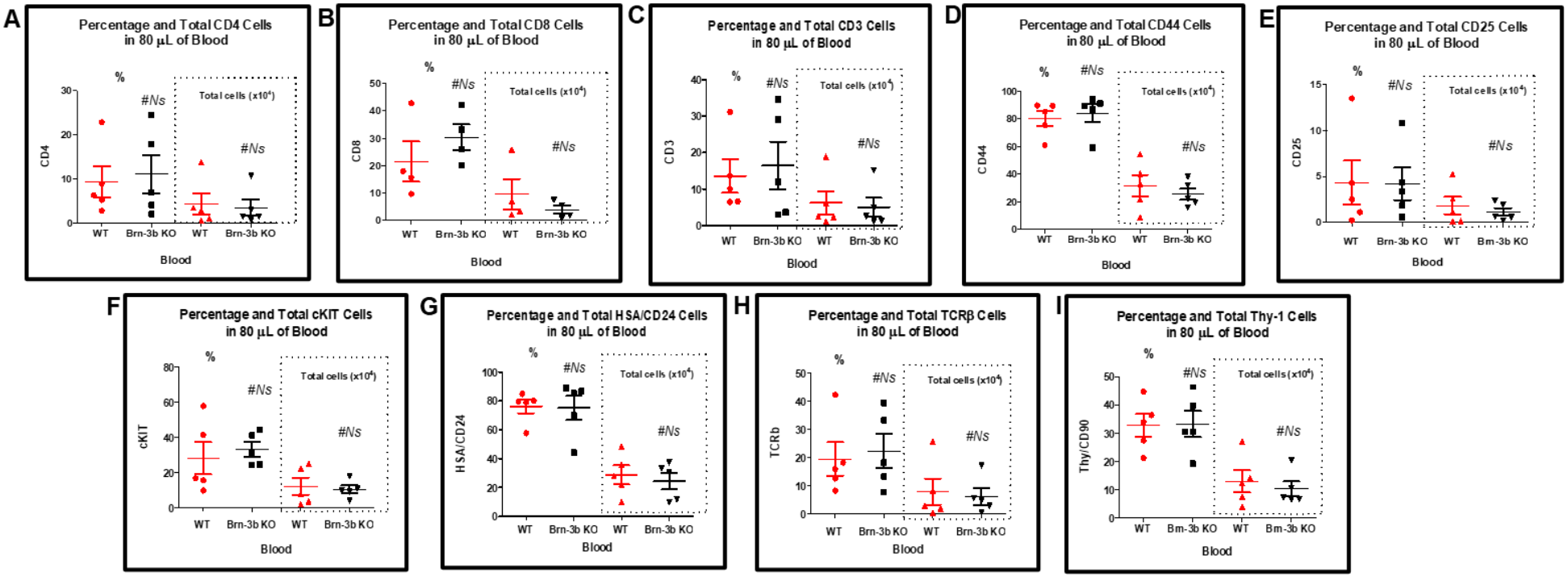

Figure 60: Single surface markers expression in blood of wild type (WT) and Brn-3b knock-out (KO) mice. C57BL6/J mice were euthanised, and blood was collected using a 25G needle and syringe, then kept in ethylenediaminetetraacetic acid (EDTA) blood collection tubes at room temperature (RT). A total of 80 µL of blood was lysed using red blood cell (RBC) lysis buffer, and 10,000 white blood cells (WBCs) were stained for polychromatic flow cytometry analyses. Depicted are (A) CD4+ (B) CD8+ (C) CD3+ (D) CD44+ (E) CD25 (F) cKIT (G) CD24 (H) TCRβ and (I) Thy-1 in WT and Brn-3b KO mouse blood. Data are presented as mean ± SEM for n = 4-5 (Sex = male/female) (Age = 2–4 months) (Ns = not significant) (left-hand panel = % and right-hand panel = total cells).

5.2.3 Gating strategy of comprehensive phenotyping of T cell lineage

Following the quantification of single marker expression, I further analysed the comprehensive phenotype of the T cell lineage. The T cell lineage in the blood was examined using the gating strategy illustrated in Figure 61. This comprehensive phenotypic characterization of the immune cell profile encompassed both early and maturation stages of T cell development, utilising nine cell surface markers.

At the early stage of T cell development, the DN cells were identified by excluding CD4, CD8, and CD3 markers. The DN subsets were further characterised by manipulating the expression of CD44, CD25, TCRβ, cKIT, and CD24. For the maturation stages of T cell development, the immune cell profiles were identified by analysing the positive expression of CD4 and CD8 with TCRβ and CD24 expression. Unstained samples and FMO controls were employed in the gating strategy to exclude background fluorescence and non-specific binding.

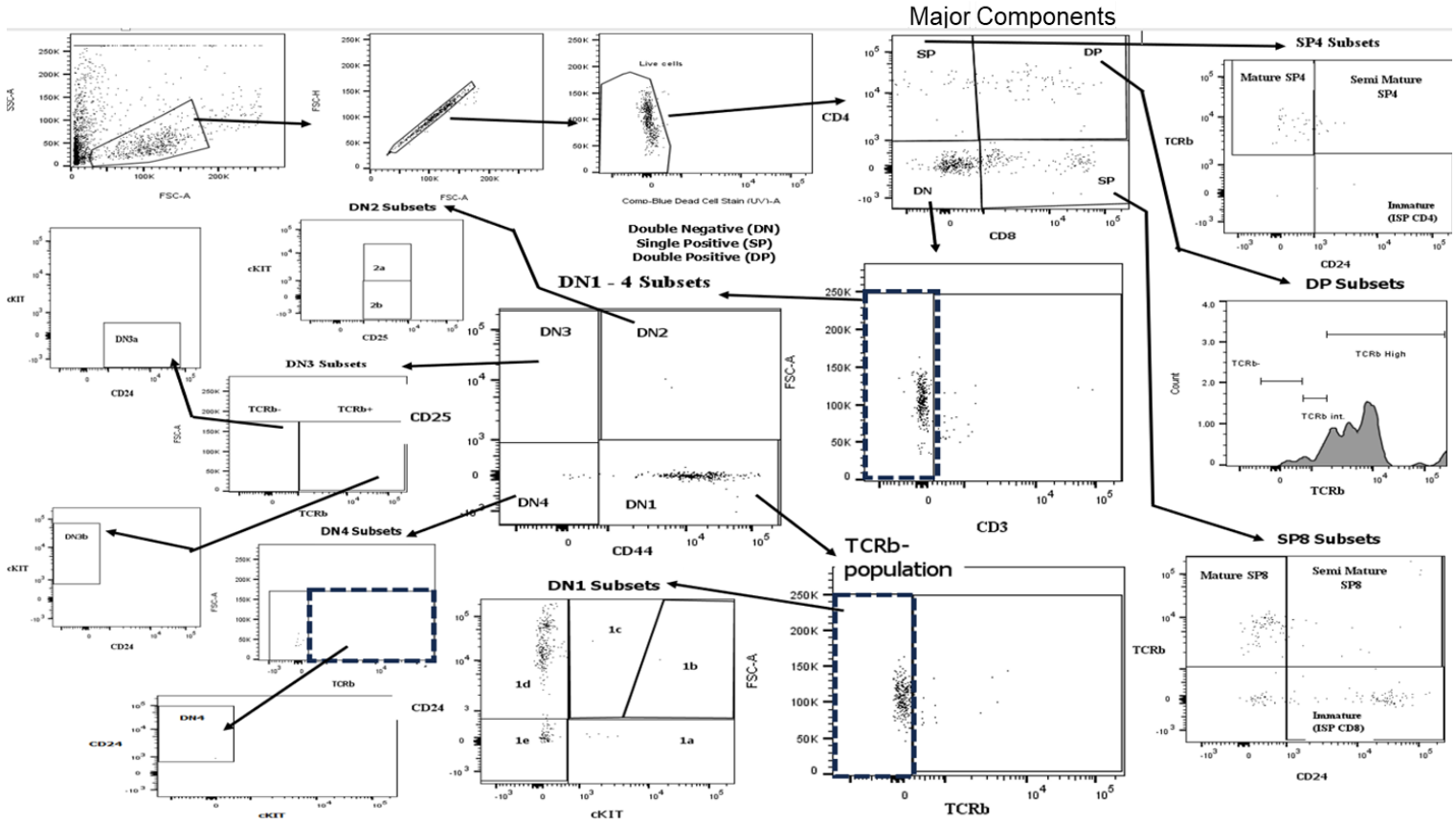

Figure 61: Deep characterisation of the T cell lineage populations in the blood of wild type (WT) and Brn-3b knock-out (KO) mice. Blood was collected using a 25G needle and syringe and lysed using red blood cell (RBC) lysis buffer, and ten thousand cells from 80 µL of blood were stained for polychromatic flow cytometry analyses. Live cells were identified by excluding debris and doublets using forward scatter (FSC) and side scatter (SSC) parameters. Major compartments were identified as double negative (DN), single positive 4 (SP4), SP8 and double positive (DP) against CD4 and CD8 expression. DN cells were further divided into DN1-4 subsets based on their differing expression of CD3, CD44, CD25, TCRβ, cKIT and CD24/HSA. All SP and DP subsets were identified based on their differing expression profile of TCRβ and CD24/HSA.

5.2.3.1 Loss of Brn-3b does not change the immune cell profile within major CD4 and CD8 components of mouse blood

In this section, I examined the expression of DN cells (early stage) and DP and SP cells (mature stage) in the blood of Brn-3b KO mice compared to WT control. As shown in dot plot images (Figure 62), DN cells were highly accumulated in the blood as compared to DP, SP4, and SP8. The finding showed that the loss of Brn-3b did not significantly change the total of DN cells and DP, SP4, and SP8 in the 80 µL of mouse blood compared to the WT control.

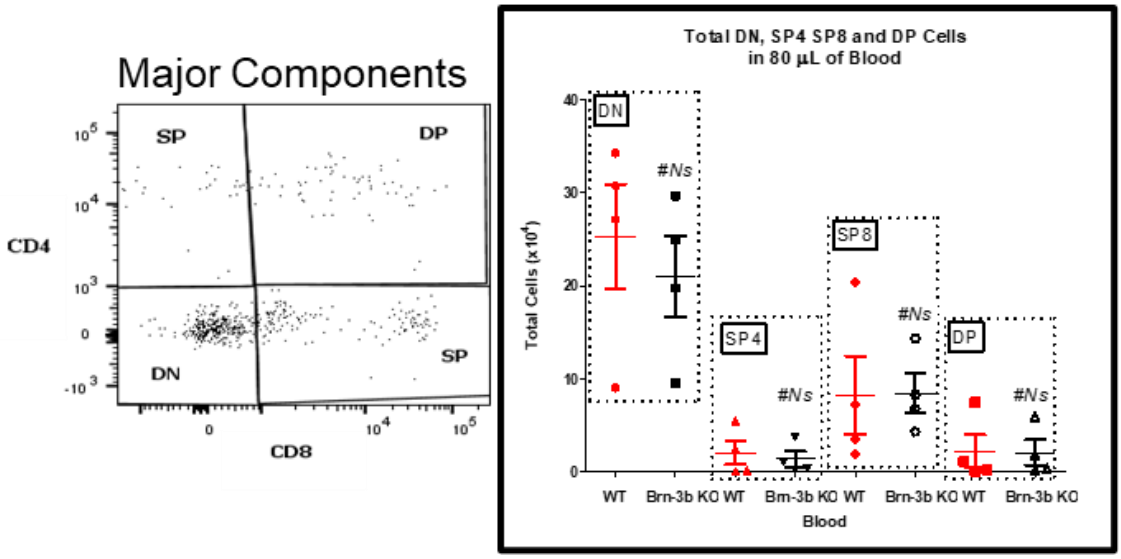

Figure 62: The number of double negative (DN), single positive 4 (SP4), SP8 and double positive (DP) cells in blood of wild type (WT) and Brn-3b knock-out (KO) mice. C57BL6/J mice were euthanised, and blood was collected using a 25G needle and syringe, then kept in ethylenediaminetetraacetic acid (EDTA) blood collection tubes at room temperature (RT). A total of 80 µL of blood was lysed using red blood cell (RBC) lysis buffer, and 10,000 white blood cells (WBCs) were stained for polychromatic flow cytometry analyses. Depicted are CD4-CD8- (DN), CD4+CD8- (SP4), CD4-CD8+ (SP8) and CD4+CD8+ (DP) in WT and Brn-3b KO mouse blood. Data are presented as mean ± SEM for n = 4 (Sex = male/female) (Age = 2–4 months) (Ns = not significant).

5.2.3.2 Loss of Brn-3b did not significantly alter the DN subset in the blood

Furthermore, I extended the investigation by conducting an in-depth analysis of DN cells (the early stage of T cell development). This analysis identified immature DN cell subsets, including DN1 to DN4, by gating on CD3-negative cells and manipulating the CD44 and CD25 markers, as demonstrated in Figure 61. As shown in the dot plot image in Figure 63, DN1 subsets were highly expressed in the blood, while DN2, DN3, and DN4 subsets showed very low or absent expression. The analysis revealed that the loss of Brn-3b did not significantly alter the expression of DN1 to DN4 in 80 µL of mouse blood compared to WT controls.

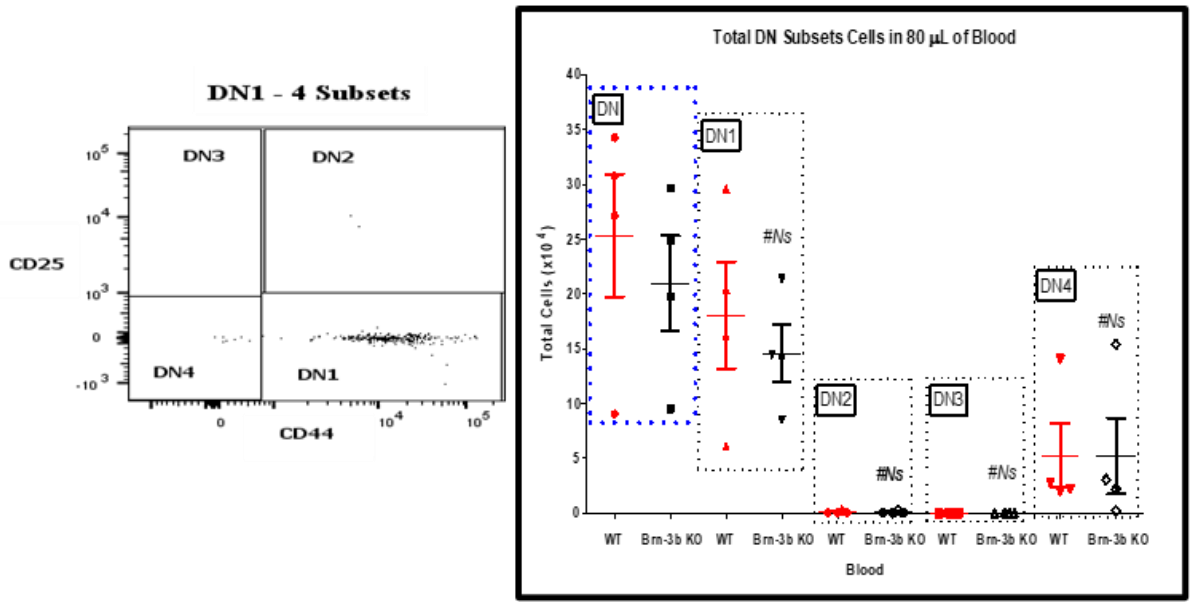

Figure 63: The numbers of double negative (DN) subsets in blood of wild type (WT) and Brn-3b knock-out (KO) mice. C57BL6/J mice were euthanised, and blood was collected using a 25G needle and syringe, then kept in ethylenediaminetetraacetic acid (EDTA) blood collection tubes at room temperature (RT). A total of 80 µL of blood was lysed using red blood cell (RBC) lysis buffer, and 10,000 white blood cells (WBCs) were stained for polychromatic flow cytometry analyses. Depicted are CD44+CD25-(DN1), CD44+CD25+(DN2), CD44-CD25+(DN3), and CD44-CD25-(DN4) in WT and Brn-3b KO mouse blood. Data are presented as mean ± SEM for n = 4 (Sex = male/female) (Age = 2–4 months) (Ns = not significant).

5.2.3.3 No significant changes of DN1 subsets and DNαβ T cells (early stage) and DP, SP4, and SP8 cells (mature stage) in Brn-3b KO blood

Since only DN1 was expressed while DN2 to DN4 were either low or absent in mouse blood, further analysis was conducted on DN1 cells, with DN2 to DN4 subsets excluded. Table 13 summarises the detailed immunophenotype of DN1 subsets and DNαβ T cells during the early T cell development stage, as well as DP and SP cells during the mature stage.

The findings revealed that the loss of Brn-3b did not significantly alter the expression of DN1 subsets (DN1a to e) and DNαβ T cells in the blood. Additionally, the loss of Brn-3b did not significantly change the expression of DP, SP4, and SP8 cells at different maturation stages (immature, semi-mature, and mature) in 80 µL of mouse blood compared to WT controls.

Table 13: Deep characterisation of cells in the early and mature stage of T cell development in blood of wild type (WT) and Brn-3b knock-out (KO) mice. C57BL6/J mice were euthanised, and blood was collected using a 25G needle and syringe, then kept in ethylenediaminetetraacetic acid (EDTA) blood collection tubes at room temperature (RT). A total of 80 µL of blood was lysed using red blood cell (RBC) lysis buffer, and 10,000 white blood cells (WBCs) were stained for polychromatic flow cytometry analyses. Depicted are double negative 1 (DN1) subsets and DNαβ T cells (early stage), and double positive (DP), single positive 4 (SP4) and SP8 cells at different maturation stages (mature stage) in WT and Brn-3b KO mouse blood. Data are presented as mean ± SEM for n = 4 (Sex = male/female) (Age = 2–4 months) (Ns = not significant).

Early Stage	**Total Cells in 80 µL of Blood ± SEM (x 10^4)**		
	WT	**Brn-3b KO**	**P value**
DN1	18.07 ± 4.89	14.56 ± 2.64	Ns
• DN1a	0.083 ± 0.05	0.071 ± 0.02	Ns
• DN1b	ND	ND	
• DN1c	0.08 ± 0.04	0.093 ± 0.02	Ns
• DN1d	12.72 ± 3.75	10.85 ± 2.33	Ns
• DN1e	3.070 ± 0.74	2.430 ± 0.33	Ns
DNαβ T	1.505 ± 1.06	1.092 ± 0.69	Ns
Mature Stage			
DP	2.188 ± 1.76	2.058 ± 1.34	Ns
• Low TCRβ	0.41 ± 0.33	0.387 ± 0.22	Ns
• Intermediate TCRβ	0.605 ± 0.55	0.476 ± 0.4	Ns
• High TCRβ	1.138 ± 0.86	1.133 ± 0.72	Ns
SP4	2.010 ± 1.27	1.356 ± 0.82	Ns
• Immature	0.112 ± 0.07	0.102 ± 0.06	Ns
• Semi Mature	0.664 ± 0.49	0.552 ± 0.41	Ns
• Mature	1.287 ± 0.73	0.763 ± 0.42	Ns
SP8	8.262 ± 4.21	8.438 ± 2.13	Ns
• Immature	5.302 ± 3.09	5.874 ± 1.68	Ns
• Semi Mature	1.197 ± 0.75	0.778 ± 0.43	Ns
• Mature	1.26 ± 0.34	1.101 ± 0.44	Ns

5.2.3.3.1 Loss of Brn-3b significantly alters DN1a with Thy-1 expression

Since the loss of Brn-3b may not significantly affect the presence of T cell lineage (DN, DP, and SP cells) in the mouse blood, I further analysed the DN1 subsets in detail using the Thy-1 marker to distinguish between T and non-T cell lineages. Additionally, Thy-1 expression was measured on mature cells (DP and SP) to assess the potential effect of Brn-3b deficiency on the activation status of mature cells in the mouse blood.

The findings showed that the loss of Brn-3b significantly altered the total DN1a expressing Thy-1 ($p = 0.0465$), while it did not significantly affect other DN1 subsets or mature cells (DP, SP4, and SP8) with Thy-1 expression (Table 14). It is important to note that the presence of DN1a cells in the mouse blood was relatively low, which limited the statistical robustness of this analysis.

Table 14: Deep characterisation of T cell lineage and T cell activation status based on Thy-1 expression of wild type (WT) and Brn-3b knock-out (KO) mice. C57BL6/J mice were euthanised, and blood was collected using a 25G needle and syringe, then kept in ethylenediaminetetraacetic acid (EDTA) blood collection tubes at room temperature (RT). A total of 80 µL of blood was lysed using red blood cell (RBC) lysis buffer, and 10,000 white blood cells (WBCs) were stained for polychromatic flow cytometry analyses. Depicted are Thy-1-/+ expression on double negative 1 (DN1) subsets (early stage), and double positive (DP), single positive 4 (SP4) and SP8 cells (mature stage) in WT and Brn-3b KO mouse blood. Data are presented as mean ± SEM for n = 4 (Sex = male/female) (Age = 2–4 months) (* $p < 0.05$ and Ns = Not significant).

Early Stage	**Total Cells in 80 µL of Blood ± SEM (x 10^4)**					
	THY-			**THY+**		
	WT	**Brn-3b KO**	**P value**	**WT**	**Brn-3b KO**	**P value**
DN1						
• DN1a	0.081 ± 0.05	0.036 ± 0.02	Ns	ND	0.035 ± 0.01	**0.0465**
• DN1b	ND	ND		ND	ND	
• DN1c	0.075± 0.04	0.059 ± 0.02	Ns	ND	0.028 ± 0.02	Ns
• DN1d	10.48 ± 3.25	8.556 ± 1.93	Ns	1.029 ± 0.14	1.491 ± 0.73	Ns
• DN1e	1.637 ± 0.47	1.508 ± 0.24	Ns	1.398 ± 0.34	0.887 ± 0.10	Ns
Mature Stage						
DP						
• Low TCRβ	0.038 ± 0.03	ND	Ns	0.348 ± 0.31	0.346 ± 0.24	Ns
• Intermediate TCRβ	ND	ND		0.605 ± 0.55	0.471 ± 0.4	Ns
• High TCRβ	ND	ND		1.049 ± 0.84	1.118 ± 0.72	Ns
SP4						
• Immature	ND	0.014 ± 0.01	Ns	0.1 ± 0.07	0.088 ± 0.06	Ns
• Semi Mature	ND	ND		0.633 ± 0.50	0.547 ± 0.41	Ns
• Mature	ND	ND		1.166 ± 0.71	0.763 ± 0.42	Ns
SP8						Ns
• Immature	3.89 ± 2.68	4.168 ± 1.56	Ns	1.160 ± 0.49	1.655 ± 0.26	Ns
• Semi Mature	0.035 ± 0.04	0.093 ± 0.07	Ns	0.7008 ± 0.5	0.616 ± 0.49	Ns
• Mature	ND	ND		1.543 ± 0.53	1.170 ± 0.2	Ns

5.2.4 Immunophenotyping of non-T cell lineage in 80µL blood of Brn-3b KO mouse model

In this study, I expanded the investigation to evaluate the effect of Brn-3b deficiency on the number of non-T cell lineages, including B lymphocytes and monocytes, present in the blood. Immune cell phenotypes were identified using the gating strategy illustrated in Figure 64. Based on FSC and SSC parameters, lymphocytes and monocytes were predominantly detected, with granulocytes being absent.

Following the exclusion of T cell lineages (CD4+, CD8+, CD3+) from the WBC component, lymphocytes and monocytes were further gated based on their scatter properties (FSC and SSC). Monocytes and B cells were distinguished using CD24 expression at different SSC sizes, where CD24+ B cells were expressed at low SSC, while CD24+ and CD24- monocytes were expressed at intermediate SSC (Raife et al., 1994; Alghetany and Patel, 2002; Sheng et al., 2017; Tarfi et al., 2018; Cherian et al., 2018; Sadofsky et al., 2019; Altevogt et al., 2021; Panagiotou et al., 2022).

The activation or differentiation states of these populations were further analysed based on CD44 expression. The gating strategy employed unstained samples and FMO as a control to exclude any background fluorescence or non-specific binding.

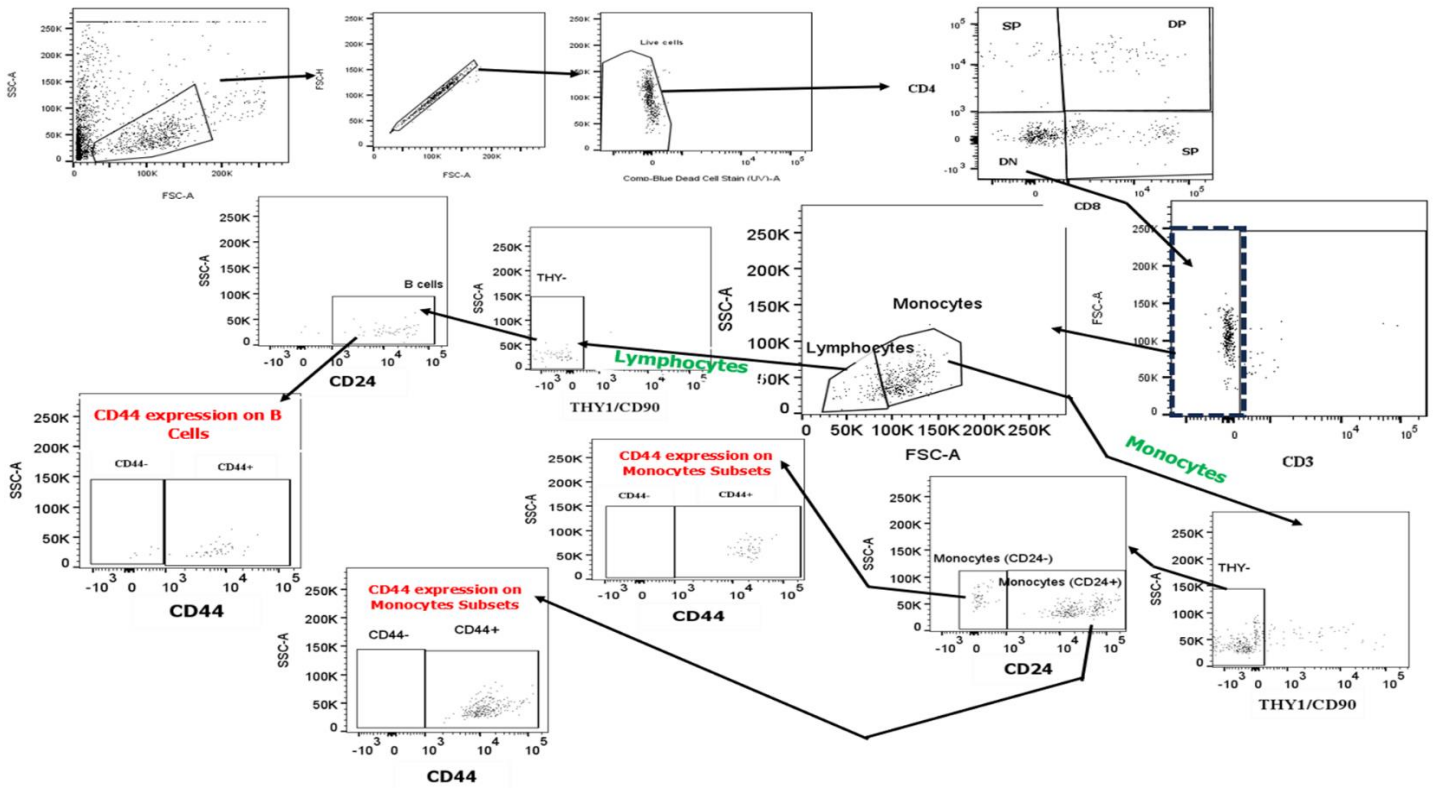

Figure 64: Identification of the B cells, monocytes and granulocytes in 80µL of blood of wild type (WT) and Brn-3b knock-out (KO) mice. Blood was collected using a 25G needle and syringe and lysed using red blood cell (RBC) lysis buffer, and ten thousand cells from 80 µL of blood were stained for polychromatic flow cytometry analyses. Live cells were identified by excluding debris and doublets using forward scatter (FSC) and side scatter (SSC) parameters. T cell lineages (double positive (DP), single positive 4 (SP4), SP8 and CD3+ cells) were discarded. Double negative (DN) with CD3- cells were further discriminated into lymphocytes and monocytes based on the FSC and SSC. The T cell lineage in each gate of scattered parameters was further gated out using the Thy-1 marker. B cells, granulocytes, and monocytes in each FSC and SSC gate were identified based on CD24 expression. CD24 expression at low SSC was characterised as B cells and CD24 (+/-) in monocytes gate for monocytes. Furthermore, the activated and non-activated B cells and monocytes were identified based on their differing expression of CD44.

5.2.4.1 Rough selection of lymphocytes and monocytes in Brn-3b KO mouse model

In the blood, the rough populations of monocytes and lymphocytes (based on FSC and SSC parameters) were identified, as illustrated in Figure 64. Monocytes were more abundant than lymphocytes, as depicted in the dot plot image of Figure 65. In normal mouse blood, the total monocytes were 166,000 ± 4.431 cells per 80 µL (2,075/µL), while lymphocytes (excluding T cells) totalled 71,570 ± 2.364 cells per 80 µL (894.63/µL).

The finding showed that the loss of Brn-3b did not significantly alter the expression of monocytes or lymphocytes in 80 µL of mouse blood compared to the WT control.

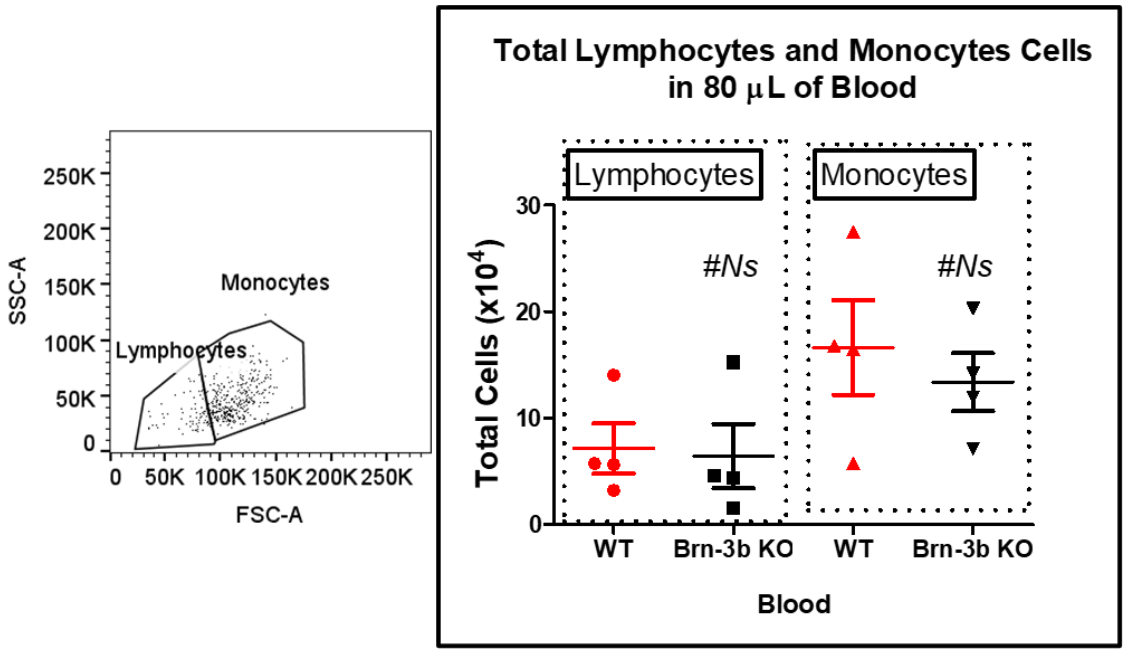

Figure 65: The number of lymphocytes and monocytes in blood of wild type (WT) and Brn-3b knock-out (KO) mice. C57BL6/J mice were euthanised, and blood was collected using a 25G needle and syringe, then kept in ethylenediaminetetraacetic acid (EDTA) blood collection tubes at room temperature (RT). A total of 80 µL of blood was lysed using red blood cell (RBC) lysis buffer, and 10,000 white blood cells (WBCs) were stained for polychromatic flow cytometry analyses. Depicted are the total numbers of lymphocytes, monocytes, and granulocytes in WT and Brn-3b KO mouse blood. Data are presented as mean ± SEM for n = 4 (Sex = male/female) (Age = 2–4 months) (Ns = Not significant).

5.2.4.1.1 Total B cells with CD24+ (SSC^{low}) and non-and activated B cells

In this section, the dot plot image showed high expression of B cells (CD24+ SSC^{low}), and most of these cells were expressing CD44+, as illustrated in the dot plot image of Figure 66. The analysis showed that the loss of Brn-3b did not significantly change the number of B cells (CD24+ SSC^{low}) in 80 µL of mouse blood compared WT control. Additionally, no significant differences in activation status (CD44+/CD44-) were observed for B cells from Brn-3b KO and WT samples.

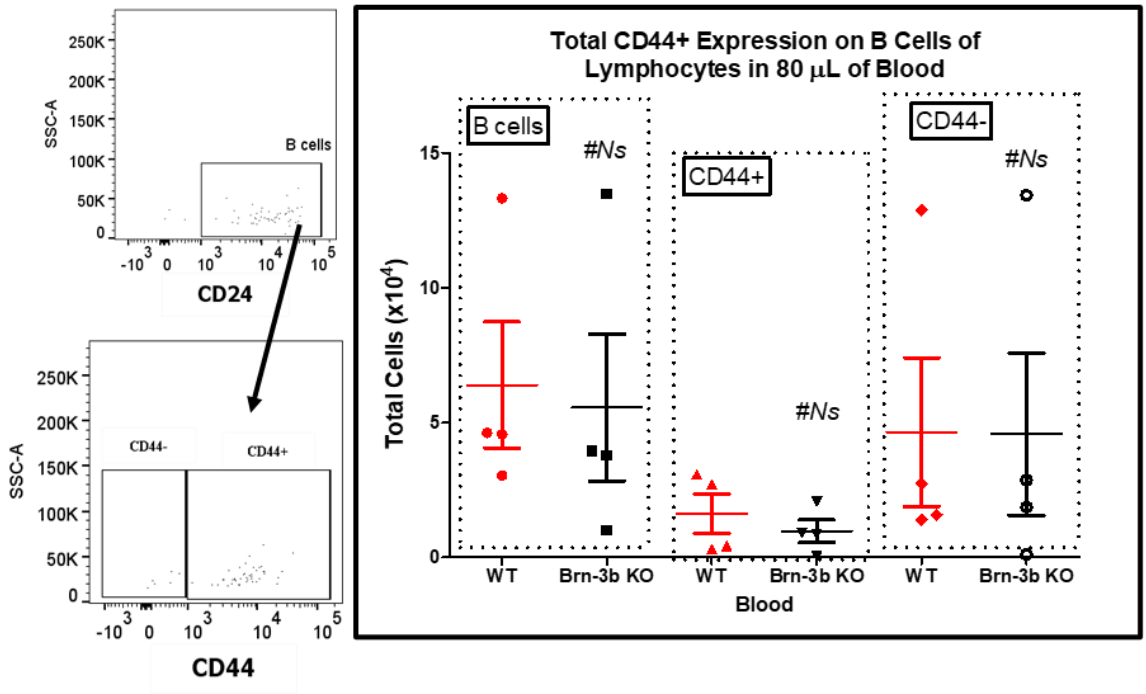

Figure 66: The number of B cells and their activation status in blood of wild type (WT) and Brn-3b knock-out (KO) mice. C57BL6/J mice were euthanised, and blood was collected using a 25G needle and syringe, then kept in ethylenediaminetetraacetic acid (EDTA) blood collection tubes at room temperature (RT). A total of 80 µL of blood was lysed using red blood cell (RBC) lysis buffer, and 10,000 white blood cells (WBCs) were stained for polychromatic flow cytometry analyses. Depicted are the total numbers of B cells (CD24+ SSC^{low}) within the lymphocyte gate and their activation status (CD44+) in WT and Brn-3b KO mouse blood. Data are presented as mean ± SEM for n = 4 (Sex = male/female) (Age = 2–4 months) (Ns = Not significant).

5.2.4.1.2 Total Monocytes cells with CD24+/- and their Differentiation status

Moreover, the CD24-based marker monocytes were quantified in the rough monocyte gate. The discrimination using the CD24 marker produced two populations of monocyte-derived cells which were CD24- monocytes and CD24+ monocytes, and both of these types of monocytes were mostly expressed CD44 surface markers, as illustrated in the dot plot image in Figure 67.

The analysis showed that the loss of Brn-3b did not significantly change the expression of monocytes (CD24+/-) in 80 µL of mouse blood compared WT control. Additionally, no significant differences in differentiation status (CD44+/CD44-) were observed for monocyte cells from Brn-3b KO and WT blood.

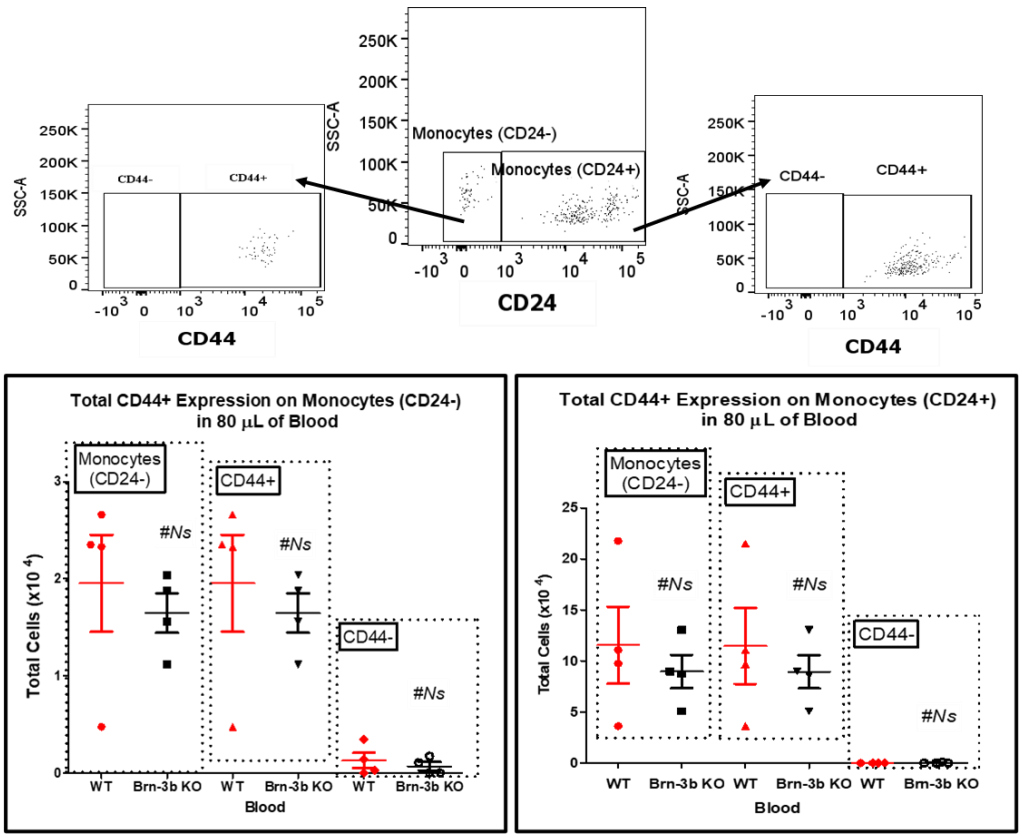

Figure 67: The number of monocytes cells and their differentiation status in blood of wild type (WT) and Brn-3b knock-out (KO) mice. C57BL6/J mice were euthanised, and blood was collected using a 25G needle and syringe, then kept in ethylenediaminetetraacetic acid (EDTA) blood collection tubes at room temperature (RT). A total of 80 µL of blood was lysed using red blood cell (RBC) lysis buffer, and 10,000 white blood cells (WBCs) were stained for polychromatic flow cytometry analyses. Depicted are the total numbers of monocytes (CD24+/-) within the monocyte gate and

its differentiation status (CD44+) in WT and Brn-3b KO mouse blood. Data are presented as mean ± SEM for n = 4 (Sex = male/female) (Age = 2–4 months) (Ns = Not significant).

5.2.5 Loss of Brn-3b significantly reduced IL-1β protein expression in blood plasma

In the blood plasma, the expression of IL-1β, TNFα, and IL-6 was investigated. The concentration of IL-1β in 100 µL of blood was just above the minimum baseline level, in comparison to IL-6 and TNFα (Figure 68 A).

The results showed that the loss of Brn-3b significantly reduced the expression of IL-1β in the blood plasma, compared to the WT control ($p = 0.0040$). However, no significant changes were observed in the expression of IL-6 and TNFα in 100 µL of blood compared to the WT control.

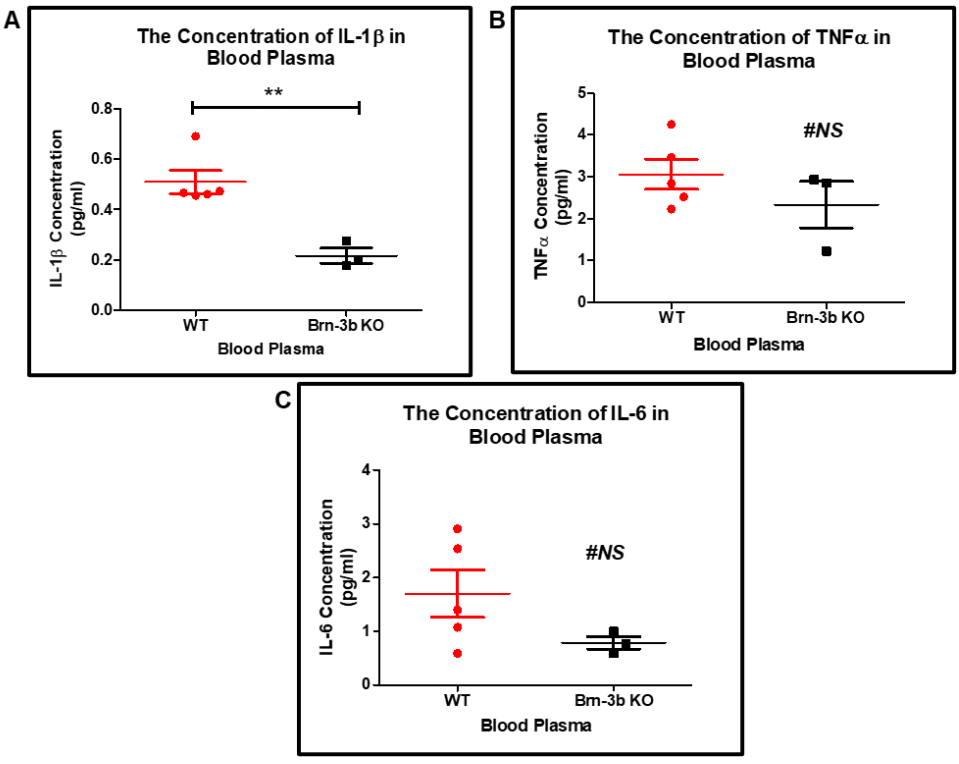

Figure 68: The expression of tumour necrosis factor alpha (TNFα), interleukin 1 beta (IL-1β) and interleukin 6 (IL-6) protein in blood plasma of wild type (WT) and Brn-3b knock-out (KO) mice. C57BL6/J mice were euthanised, and the blood was collected using a 25G needle and syringe and kept in the ethylenediaminetetraacetic acid (EDTA) blood collection tube at room temperature (RT). The blood plasma was collected by centrifuge of 100 µL of blood at 2000 X g for 15 minutes at 6°C. The concentration of cytokines was measured using an MSD Vplex custom kit. Depicted are the concentration of (A) TNFα (B) IL-1β and (C) IL-6 in WT and Brn-3b KO mouse blood plasma. Data are presented as mean ± SEM for n = 3-5 (Sex = male/female) (Age = 2–4 months) (** $p < 0.01$ and Ns = Not significant).

5.2.5.1 Correlation of immune cells profile and IL-1β, IL-6 and TNFα protein secretion in normal and Brn-3b KO blood

In this study, the results showed that the loss of Brn-3b significantly altered the expression of IL-1β protein in the blood compared to the WT, but did not significantly affect the expression of TNFα, IL-6, or the immune cell profile (Figure 62 to Figure 68). To explore whether Brn-3b deficiency influences specific immune cells that secrete cytokines, I conducted a Spearman X-Y correlation analysis to assess the relationship between the immune cell profile and cytokine production in the blood (Table 15).

Table 15: Correlation between immune cell profile and cytokine secretion in mouse blood of wild type (WT) and Brn-3b knock-out (KO) mice. C57BL6/J mice were euthanized, and the blood was collected using a 25G needle and syringe and kept in the ethylenediaminetetraacetic acid (EDTA) blood collection tube at room temperature (RT). White blood cells (WBCs) were stained for flow cytometry and blood plasma was collected for cytokine measurement. Depicted are Spearman r values between immune cell populations (B cells, monocytes, double negative (DN), double positive (DP), single positive 4 (SP4), SP8 cells) and cytokine secretion (interleukin 1 beta (IL-1β), interleukin 6 (IL-6), tumour necrosis factor alpha (TNF-α)) in WT and Brn-3b KO mouse blood. Data are for n = 3-5 (Sex = male/female) (Age = 2–4 months) (Ns = Not significant).

	IL-1β		IL-6		TNFα	
	WT	Brn-3b KO	WT	Brn-3b KO	WT	Brn-3b KO
Lymphocytes (B cells)	0.2	0.5	0.6	-0.5	0.2	0.5
Monocytes	-0.6	-0.5	-0.2	ND	-0.6	-0.5
DN	0	0.5	-0.4	-0.5	0	0.5
DP	ND	-0.5	0.2	0.5	ND	-0.5
SP4	ND	-0.5	0.2	0.5	ND	-0.5
SP8	-0.8	-0.5	0.4	ND	-0.8	-0.5

5.3 Discussion

This chapter aimed to further investigate the function of Brn-3b in immune regulation by analysing the impact of Brn-3b deficiency on immune cell profiles and cytokine expression in mouse blood. Using the same parameters as in the bone marrow study, I examined the expression of T and non-T cell lineages as well as the inflammatory cytokines IL-1β, IL-6, and TNF-α in the WBC component of Brn-3b KO and WT mice. Measuring immune markers in the blood provides an accessible indicator of immune status and reflects conditions in immune organs such as bone marrow (Carter, 2018). Changes in blood immune markers that reflect alterations in immune organs may provide valuable insights into the broader effects of Brn-3b deficiency.

5.3.1 Assessing the Brn-3b KO mouse immune status in the blood based on T cell and non-T cell lineage expression

This study screened the physiological immune status of mice by evaluating WBC counts. The findings showed that the loss of Brn-3b did not significantly alter WBC counts in the blood compared to WT controls (Figure 58). This approach aligns with routine clinical practices, where WBC counts are often used as general indicators of immune function. WBC-based inflammatory indices are also prognostic markers for inflammatory diseases, including cardiovascular disease, diabetes, cancer, and infections (Dean, 2005; Fest et al., 2018; Seo & Lee, 2022). Based on these observations, the loss of Brn-3b does not appear to significantly impact immune status under baseline conditions.

To provide a more detailed assessment, I extended the investigation to evaluate immune marker expression using flow cytometry. The loss of Brn-3b significantly altered the expression of DN1a cells with Thy-1 in the blood (Table 13). While DN1a cells with Thy-1+ have a higher potential to give rise to T cell lineages (Saran et al., 2012), this change did not significantly affect the production of downstream T cell subsets, including DP, SP4, and SP8. However, the low abundance of DN1a cells in the blood may limit the robustness of these findings, emphasising the need for future studies with larger sample sizes and increased event acquisition during flow cytometry to enhance statistical reliability.

Similarly, the expression of non-T cell lineage profiles (lymphocytes and monocytes) was not significantly affected by Brn-3b loss compared to WT

controls (Figure 65 to Figure 67). However, this analysis was based solely on CD24-sequential gating. Incorporating more specific markers for lymphocytes and monocytes in future studies will be critical for confirming these observations.

Alterations in immune cell profiles, including T and non-T cell lineages, are known to play roles in the pathogenesis of various diseases. For example, T cell lymphoblastic lymphoma and leukaemia arise from immature T progenitors (Kroeze et al., 2020), while changes in DP T cells have been associated with diseases like HIV, COVID-19, multiple sclerosis (MS), RA, and cancers (Hagen et al., 2023). Additionally, alterations in CD4 and CD8 T cells are linked to atherosclerosis, where they recognize lipid- and endothelial-derived antigens and secrete proinflammatory cytokines, contributing to disease progression (Schwartz et al., 2020). Non-T cell lineages, such as monocytes and macrophages, are implicated in autoimmune diseases like SLE and RA, and changes in B lymphocytes often serve as pathological markers for these conditions (Ma et al., 2019).

As the findings did not show a strong significant alteration in immune cell profiles in Brn-3b KO mice at baseline, further investigation of Brn-3b function in disease-induced mouse models could provide valuable insights into how Brn-3b regulates immune cell profiles relevant to these diseases. Modulating Brn-3b expression in specific immune cells, especially those highly expressed in disease-induced models, using techniques like cre-lox, could help elucidate its potential role in the development and progression of these diseases.

Having assessed the cellular immune profiles, the next section explores the effect of Brn-3b deficiency on the expression of key inflammatory cytokines, including IL-1β, TNFα, and IL-6, in the blood plasma.

5.3.2 The loss of Brn-3b significantly reduced IL-1β in the blood plasma

This study compared the expression of IL-1β, TNFα, and IL-6, soluble plasma cytokines, in the blood plasma of normal and Brn-3b KO mice. The findings revealed that the loss of Brn-3b significantly altered the expression of IL-1β in the blood plasma, as compared to WT control, but did not significantly affect IL-6 or TNFα (Figure 68).

These cytokines were included as pro-inflammatory factors secreted by immune cells (Tylutka et al., 2024). Monocytes and macrophages are the primary sources of IL-1β, although it is also expressed by neutrophils, DCs, and B cells (Pullugulla et al., 2018; Kany et al., 2019). IL-1β plays a crucial role in immune activation, particularly by enhancing the expansion or priming of CD4 and CD8 T cells (Ben-Sasson et al., 2013; Van Den Eechkout et al., 2021). However, IL-1β expression is absent in non-activated or resting T cells and unstimulated myeloid cells (Pullugulla et al., 2018). Therefore, the significant reduction of IL-1β in the blood plasma of Brn-3b KO mice may be attributed to an immature or resting state of T cells and myeloid cells.

IL-1β is a key mediator of inflammation, primarily responsible for recruiting immune cells to sites of infection or injury (Lopez-Castejon and Brough, 2011). The observed reduction in IL-1β in Brn-3b KO mice might suggest a weaker inflammatory response, but its exact biological significance under baseline conditions remains uncertain. Further studies are needed to explore whether this reduction persists or changes under activated conditions.

Future studies could expose Brn-3b KO mice to inflammatory stimuli, such as LPS, to assess whether their ability to produce IL-1β is impaired under activated conditions. *In vitro* experiments using isolated monocytes, macrophages, or dendritic cells from Brn-3b KO mice could provide further insights into the role of Brn-3b in regulating IL-1β production. Additionally, transcriptomic or proteomic analyses of immune cells could help identify upstream regulators and downstream targets of IL-1β influenced by Brn-3b loss. This could clarify the pathways controlled by Brn-3b in immune cells. Finally, it would be valuable to investigate whether the reduction of IL-1β in Brn-3b KO mice affects systemic or local inflammatory responses and whether this has implications for disease susceptibility or progression.

It is important to note that the IL-1β levels observed were close to the detection limit of the assay, which may limit their biological significance under baseline conditions. More sensitive assays or inflammatory stimuli could offer more accurate insights into the function of Brn-3b in IL-1β regulation.

In conclusion, this chapter demonstrates that the loss of Brn-3b does not significantly impact overall immune cell profiles or cytokine expression under

baseline conditions, although a notable reduction in IL-1β levels was observed. This suggests a potential alteration in immune regulation in the Brn-3b KO mice. However, as the immune system is dynamic and responsive to various stimuli, further studies, particularly those assessing immune responses under inflammatory conditions, are needed to better understand how Brn-3b influences inflammation.

The next chapter will focus on immune cell infiltration in the aorta, aiming to investigate how Brn-3b deficiency might contribute to vascular changes, particularly within the framework of immune regulation.

5.4 Conclusions

The objective of this chapter was to investigate the immune-related role of Brn-3b by analysing the immune cell phenotype development/infiltration and plasma cytokine protein in the blood of the Brn-3b KO mouse model. Some of the key findings include:

- The loss of Brn-3b did not significant alterations the expression of CD3, CD4, CD8, TCRβ, CD24, CD25, CD44, Thy-1 cell markers in 80 µL of mouse blood.
- Development/infiltration of cells of T cell lineage in Brn-3b KO mouse blood mirrored those of the WT control.
- Development/infiltration of non-T cell lineage in Brn-3b KO blood mirrored those of the WT control.
- IL-1β significantly reduced in Brn-3b KO blood plasma as compared to WT control, but not TNFα and IL-6
- No significant correlation between the T and non-T cell lineage cell population and cytokine plasma measured (IL-1β, TNFα and IL-6) in the Brn-3b KO blood.

6 INVESTIGATIONS OF A POSSIBLE LINK BETWEEN THE IMMUNE RESPONSE AND CHANGES OF STRUCTURAL VASCULAR PROTEIN IN BRN-3B KO MOUSE AORTA

6.1 Introduction

The activation of the immune system, including T cell activation and systemic inflammation, contributes to CVD. Immune-related diseases such as viral infections (e.g., Cytomegalovirus (CMV) and SARS-CoV-2), autoimmune diseases (e.g., SLE) and RA), ageing and diabetes mellitus increase the incidence of CVD by causing gradual progression of vascular damage and declining cardiovascular function (Reali et al., 2021; Girard and Vandiedonck, 2022).

Vascular damage can be classified into macrovascular damage (e.g., affecting the aorta, coronary, and renal arteries) and microvascular damage (e.g., affecting smaller arteries) (Li et al., 2023). Vascular damage in organs, such as the aorta in the heart, plays a pivotal role in the progression of cardiovascular disease (CVD) (Berbudi et al., 2020; Lopez et al., 2023). For example, in T2DM, hyperglycaemia and insulin resistance activate the immune system, causing vascular damage and promoting the progression of CVD. This process is summarized in Figure 69.

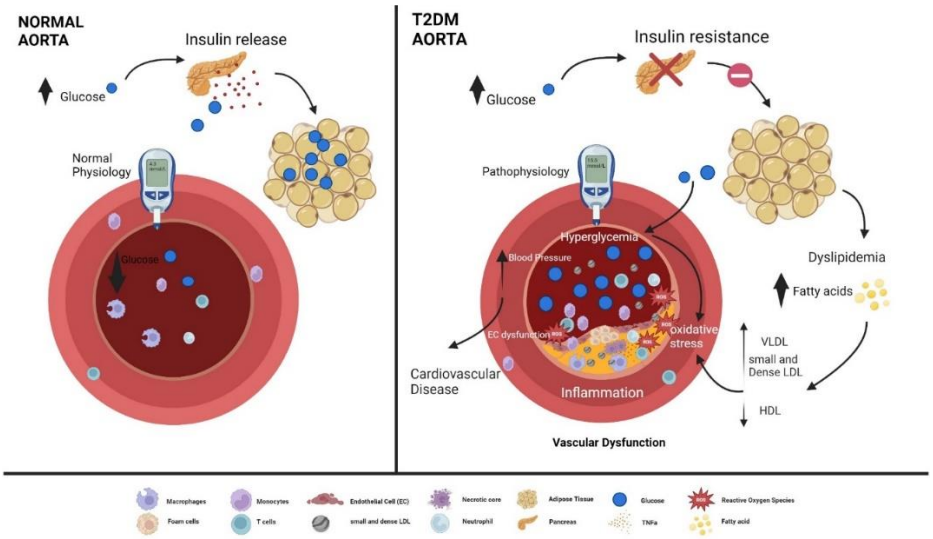

Figure 69: The overview of the link between type 2 diabetes mellitus (T2DM), inflammation activation and cardiovascular disease (CVD). Hyperglycemia and dyslipidemia, resulting from insulin resistance (IR), induce oxidative stress, which damages endothelial cells (ECs). This damage facilitates the entry of low-density lipoprotein (LDL) into the tunica intima (TI) where they are oxidised to form oxidised low-density lipoprotein (oxLDL). The presence of oxLDL attracts monocytes that differentiate into foam cells, which release signals to recruit additional immune cells, including CD8+ T cells, thereby promoting inflammation and the formation of a necrotic core. Foam cells and inflammation also stimulate vascular smooth muscle cells (VSMCs) to migrate and produce extracellular matrix (ECM), leading to the formation of a fibrous cap around atherosclerotic plaques. These pathological changes result in stiffened blood vessels, luminal narrowing, and increased blood pressure, collectively heightening the risk of CVD (Tabas and Lichtman, 2017; Schafer and Zernecke, 2020; Lacolley et al., 2020). (*BioRende*r).

6.1.1.1 The master regulator behind the pathological of diabetes mellitus, inflammation and cardiovascular disease

Transcription factors, including ATF3, FOXP3, AP1, and NFκB, play crucial roles in regulating the progression of diseases such as diabetes, inflammation, and CVD (Figure 70) (Zhou et al., 2018; Prasad et al., 2019; Ku and Cheng, 2020; Wu et al., 2022). Targeting these transcription factors has been explored in therapeutic approaches. For instance, aspirin, sodium salicylate, and dexamethasone have been shown to suppress NFκB activation, reducing inflammation in cancer (Yu et al., 2020). Moreover, NFκB is targeted by drugs like insulin and salsalate for the treatment of diabetes and vascular complications (Pollack et al., 2016). Exploring transcription factors as therapeutic targets holds significant promise for advancing clinical treatments for these diseases.

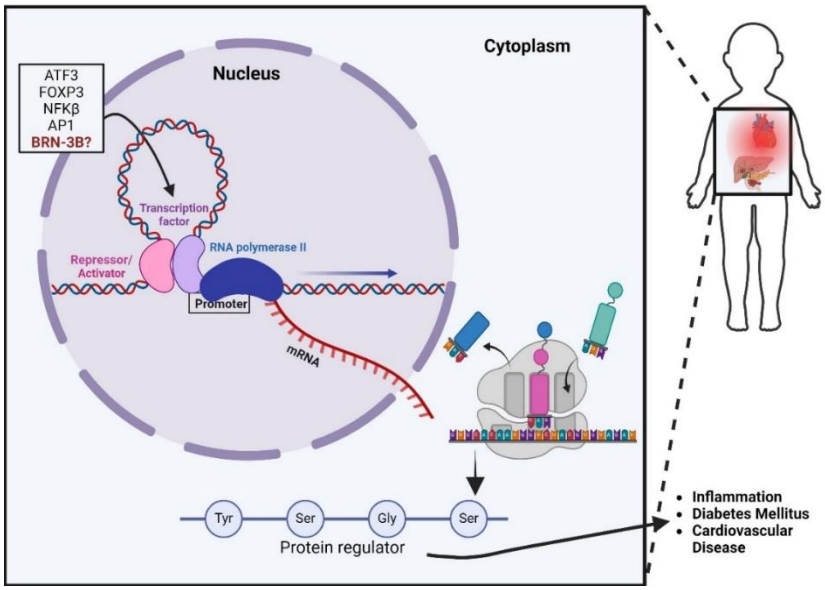

Figure 70: The modulation disease progression *via* transcription factor. Specific transcription factors regulate the expression of functional proteins, which drive or exacerbate the development of diabetes mellitus, inflammation, and cardiovascular disease (*BioRender*).

The Brn-3b transcription factor also has been associated with potential roles in disease mechanisms, including vascular changes (Yogendran et al., 2023). This study seeks to investigate the relationship between Brn-3b deficiency and vascular changes observed in the aorta of Brn-3b KO mice with a focus on possible links to immune regulation. Prior findings by Yogendran et al. (2023) identified downregulation of immune-related genes, such as IL-1β, CXCR2, and CCL12, in Brn-3b KO aortic tissue, suggesting that Brn-3b might influence immune responses in the aorta. However, further research is needed to clarify the extent and implications of these observations.

Here, I examine the expression of immune markers (CD3, CD11b, B220), mesenchymal markers (CD44), and vascular wall markers (αSMA, SM22, Ki67) in the aortic tissue of Brn-3b KO mice.

I hypothesise that the loss of Brn-3b affects the immune cell expression and structural vascular proteins in the mouse aorta. Accordingly, the objectives of this chapter were delineated as follows:

1. To explore alterations in structural vascular protein (αSMA, SM22), proliferative marker (Ki67), immune cell infiltration (CD3, CD11b, B220) and immune/ Mesenchymal marker CD44 in the thoracic and abdominal aorta of Brn-3b KO mice.

6.2 Results

6.2.1 The effect of Brn-3b KO on the histology of mouse aorta

In this study chapter, I explored the effects of the loss of Brn-3b on immune cell infiltration in the mouse aorta. I screened immune cell infiltration within the aortic wall, focusing specifically on the aorta and excluding the heart, as illustrated in Figure 71 (A).

The observational analysis finding illustrated that there were no obvious differences between the Brn-3b KO and normal mouse aorta's structure as depicted in Figure 71 (B). The morphological characteristics, including the aortic lumen, TA, TM, and TI, in the Brn-3b KO mouse aorta closely resembled those in the normal WT control. Additionally, both Brn-3b KO and WT aortas displayed a free lumen.

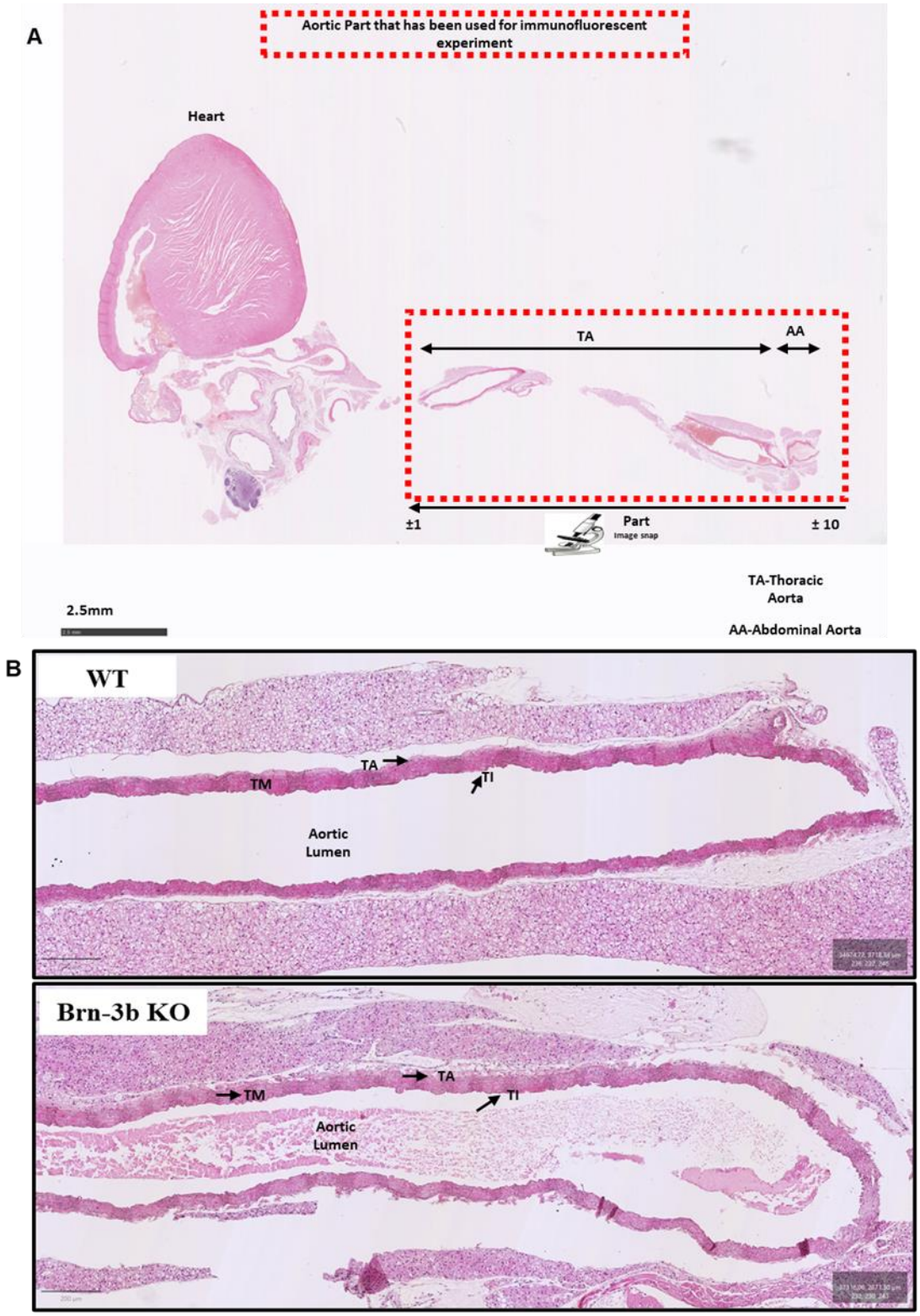

Figure 71: Representative histology staining of aortic segments of wild type (WT) and Brn-3b knock-out (KO) mice. C57BL/6J mice were euthanised, and aortas were isolated, processed, and embedded in paraffin wax. The aortas were sectioned longitudinally at a thickness of 5 µm. The tissue sections were stained with haematoxylin and eosin (H&E) and imaged using a Nanozoomer microscope at 20× magnification. Depicted are (A) the aortic regions studied and (B) the histological structure of the tunica adventitia (TA), tunica media (TM), and tunica intima (TI) in WT and Brn-3b KO mouse aorta. Data are presented for n = 2-4 (Sex = male) (Age = 2–4 months).

6.2.2 The effect of Brn-3b KO on total cell counts in the mouse aorta

In the preceding section, I investigated the morphology of the mouse aorta in Brn-3b KO mice compared to WT control. To assess a different parameter, I investigated the total number of cells freshly isolated from both groups of mouse aorta using the mechanical digestion method. The finding showed that the loss of Brn-3b did not significantly alter the total cell count in the mouse aorta as compared to the WT control, as illustrated in Figure 72.

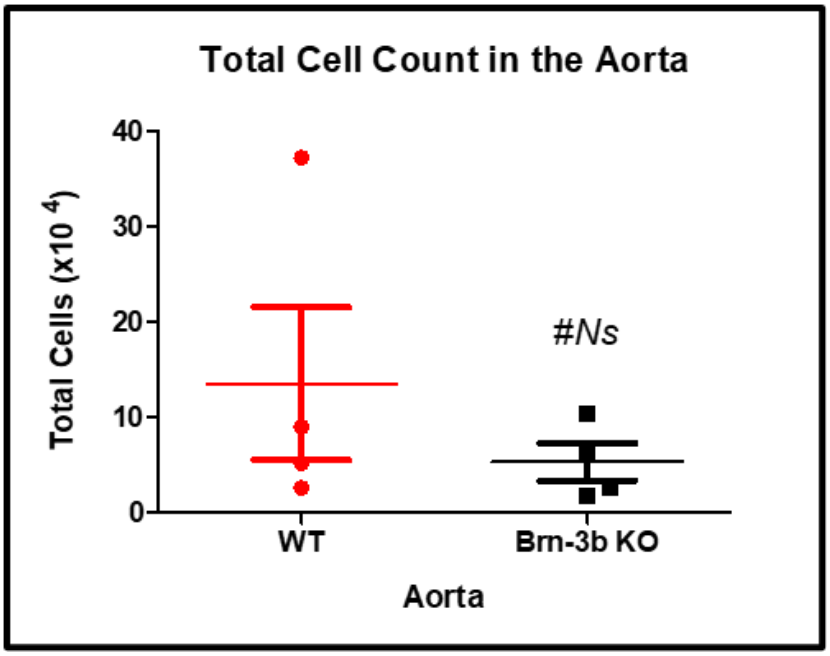

Figure 72: Total cell count in the aorta of wild type (WT) and Brn-3b knock-out (KO) mice. C57BL/6J mice were euthanised, and aortas were isolated, mechanically digested, and filtered through a 40 µm filter. The dissociated cells were counted using an automated cell counter. The figure shows the total cell count in WT and Brn-3b KO mouse aorta. Data are presented as mean ± SEM for n = 3-5 (Sex = male/female) (Age = 2–4 months) (Ns = Not significant).

6.2.2.1 Flow cytometric screening of single immune cell marker in normal and Brn-3b KO aorta

In the previous section of this chapter, I investigated the effect of Brn-3b deficiency on the histological vascular structure and total cell counts in the aorta. In this section, I focused on another parameter: the expression of immune markers in the aorta. The gating strategy for measuring the expression of single immune cell markers is shown in Figure 73 (A). Positive cellular markers were

selected following the exclusion of debris, doublets, and dead cells. Further discrimination was achieved using FMO and unstained controls to discard auto-fluorescent cells. The finding showed that only CD44 was highly expressed, while other protein markers (CD3, CD4, CD8, CD11b and B220) were present at very low levels or nearly undetectable in the aorta (Figure 73 (A and B)). Due to the limited sample size, I did not perform statistical comparisons with Brn-3b KO mouse aorta, as the data were insufficient to determine significant differences.

A

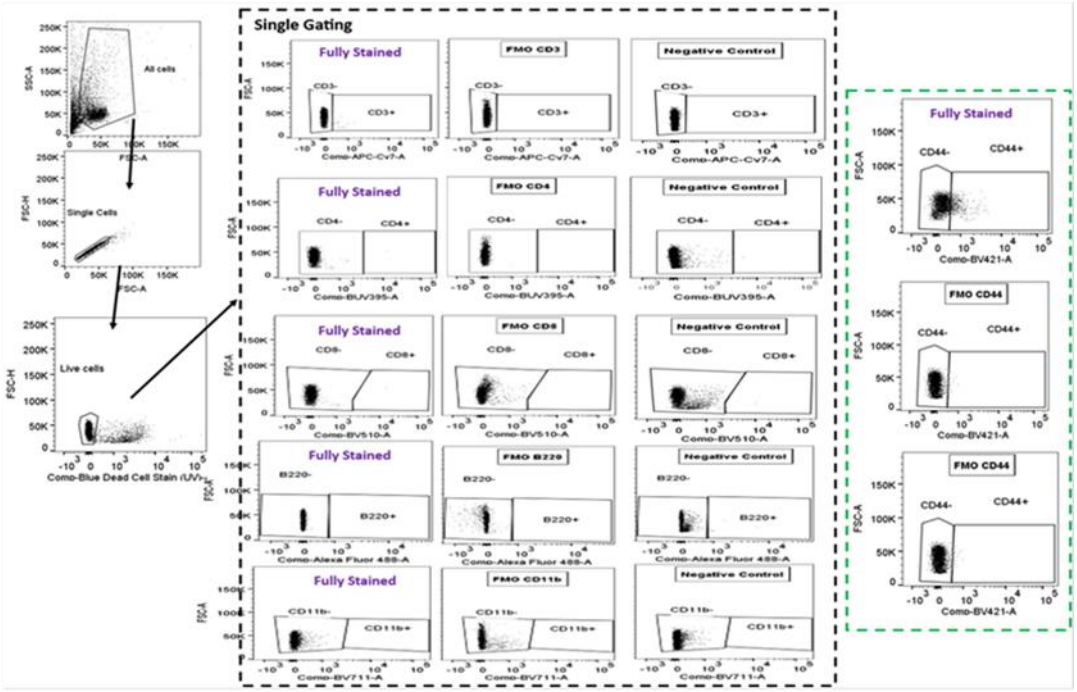

B

Protein Markers	WT	Brn-3b KO
	Average Total Cells ± SEM per Aorta	Average Total Cells ± SEM per Aorta
CD3	21.96 ± 14.10 (x 10)	ND
CD4	0.532 ± 0.12 (x 10)	ND
CD8	ND	ND
CD11b	1.439 ± 0.13 (x 10)	2.624 ± 2.17 (x 10)
B220	ND	ND
CD44	**6.270 ± 1.80 (x 10^3)**	11.61 ± 6.77 (x 10^3)

Figure 73: Screening of immune marker expression in the aorta of wild type (WT) and Brn-3b knock-out (KO) mice. C57BL/6J mice were euthanised, and aortas were isolated, mechanically digested, and filtered through a 40 µm filter. 8,000 cells were stained for polychromatic flow cytometry analyses. Depicted are (A) the gating strategy of single markers and (B) the expression of CD3, CD4, CD8, B220, CD11b, and CD44 in WT and Brn-3b KO mouse aorta. Data are presented as mean ± SEM for n = 2 (Sex = male/female) (Age = 2–4 months) (Ns = Not significant).

6.2.3 The immunofluorescent staining on mouse aorta

Although morphological images in the previous section showed no apparent changes between Brn-3b KO and WT aortas, structural changes may not be visible with brightfield microscopy. In this study, I explored potential alterations in the aorta by measuring the expression of vascular markers (αSMA, SM22), and proliferative marker (Ki67). Additionally, I assessed their potential link with immune regulation by measuring the expression of immune markers (CD3, B220, CD11b, and CD44). Immunofluorescent staining was performed on both longitudinal and transverse aortic sections, as illustrated in Figure 74, to provide additional insight into the aorta's structure and pathology.

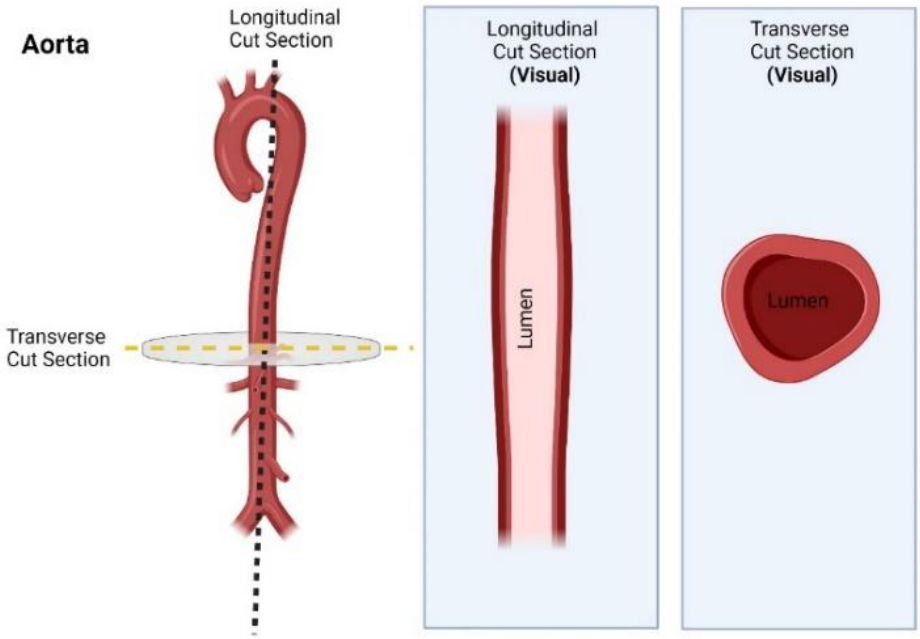

Figure 74: Longitudinal and transverse cut section of the aortic histological plane for experimental analysis. Illustration depicting the longitudinal and transverse cut sections of the aorta. The diagram highlights the different orientations of the aortic tissue for histological analysis (*BioRende*r).

6.2.3.1 Experimental on the longitudinal cut section of the descending aorta

On longitudinal cut sections of the aorta, I measured the expression of vascular markers including αSMA and SM22, and the infiltration of immune markers B220, CD11b, and immune/ Mesenchymal marker CD44. An example of how the positive signal of these markers is expressed in the longitudinal cut sections of the aorta is illustrated in Appendix 3. The images were enlarged to improve visibility, as the original signals on the longitudinal sections of the aortic wall were difficult to visualise due to the thinness of the wall. For clarity, I chose to illustrate how these markers' positive signals appear on the tissue.

For vascular marker expression, the qualitative results showed the reduction pattern of αSMA signal and a slight increase of SM22 signal in Brn-3b KO aorta as compared to WT control, as depicted in Figure 75 (A to D). The graphs confirmed the reduction trend for αSMA markers, but the SM22 data points overlapped with those of the WT control. Statistical analysis across three independent experiments did not reveal significant differences (Figure 75 (E to F)).

For immune marker expression, the loss of Brn-3b slightly caused a reduction trend in B220 and an increasing trend in CD44, while the CD11b data points seemed not much different from the normal control. The statistical analysis indicated that the differences in these markers were not significantly different compared to the WT counterpart (Figure 75 (G to I)).

Co-staining results indicated no alteration in the trend of SM22+B220+ and SM22+CD11b+ expression in the Brn-3b KO aorta, but there was an increased expression of SM22+CD44+ compared to the WT control (Figure 75 (J to L)).

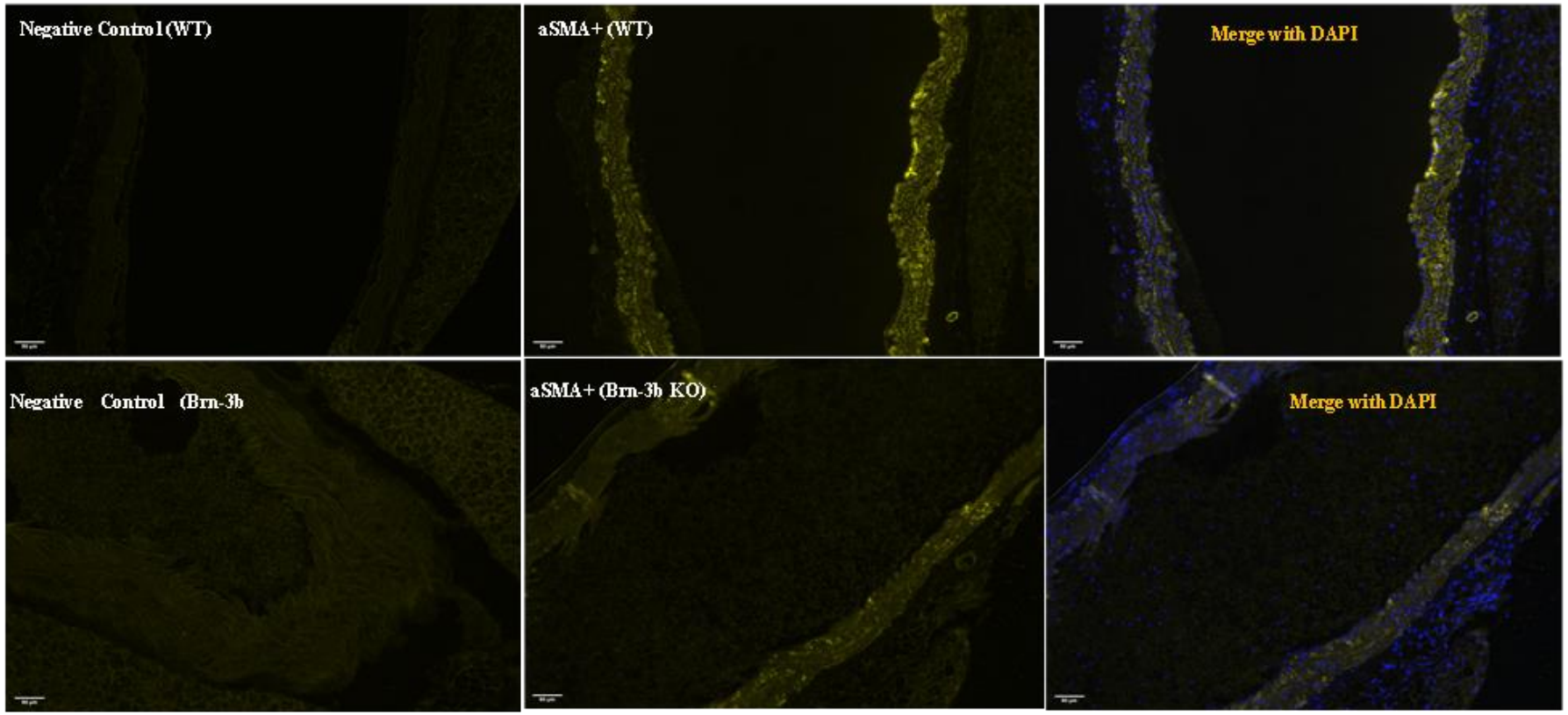
A
Negative Control (WT)
aSMA+ (WT)
Merge with DAPI
Negative Control (Brn-3b
aSMA+ (Brn-3b KO)
Merge with DAPI

B

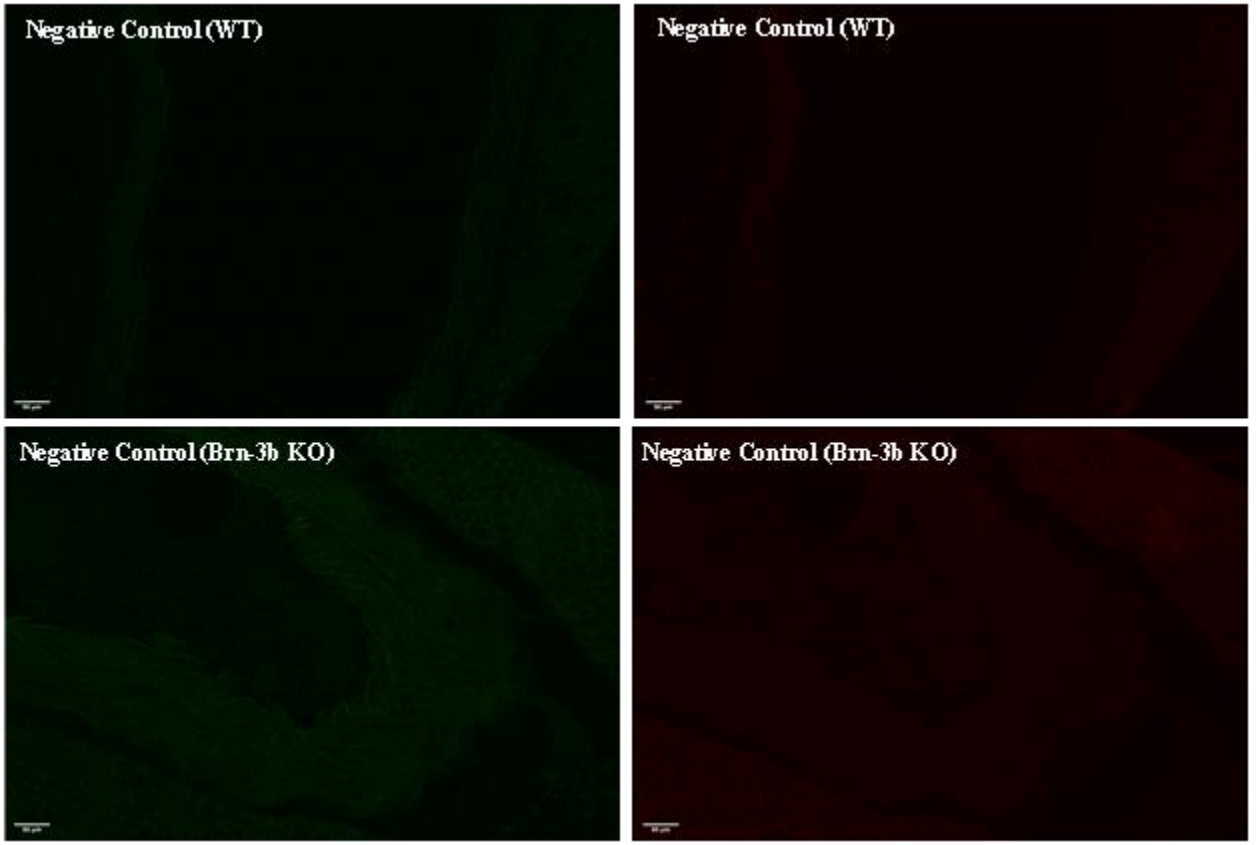
Negative Control (WT)
Negative Control (WT)
Negative Control (Brn-3b KO)
Negative Control (Brn-3b KO)

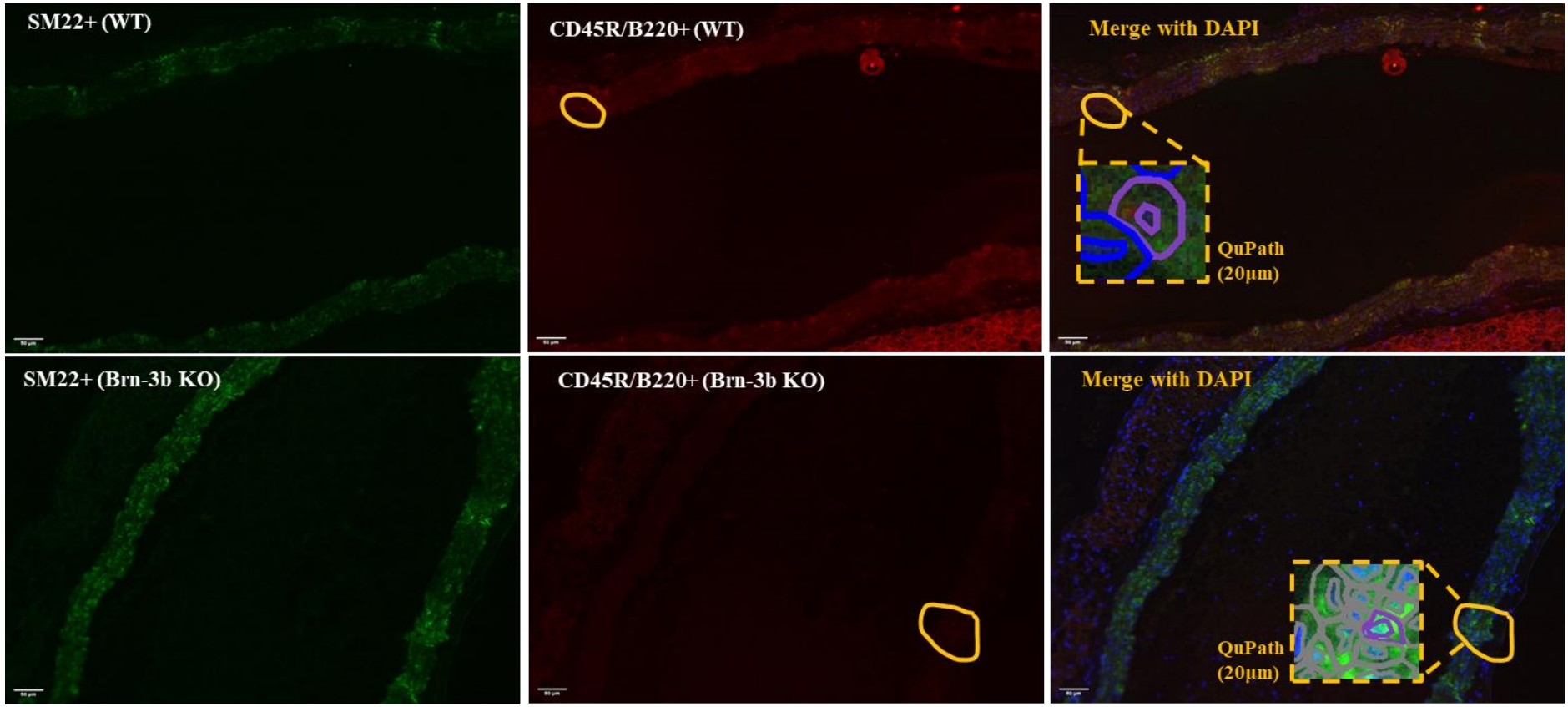
SM22+ (WT)
CD45R/B220+ (WT)
Merge with DAPI
QuPath
(20µm)
SM22+ (Brn-3b KO)
CD45R/B220+ (Brn-3b KO)
Merge with DAPI
QuPath
(20µm)

C

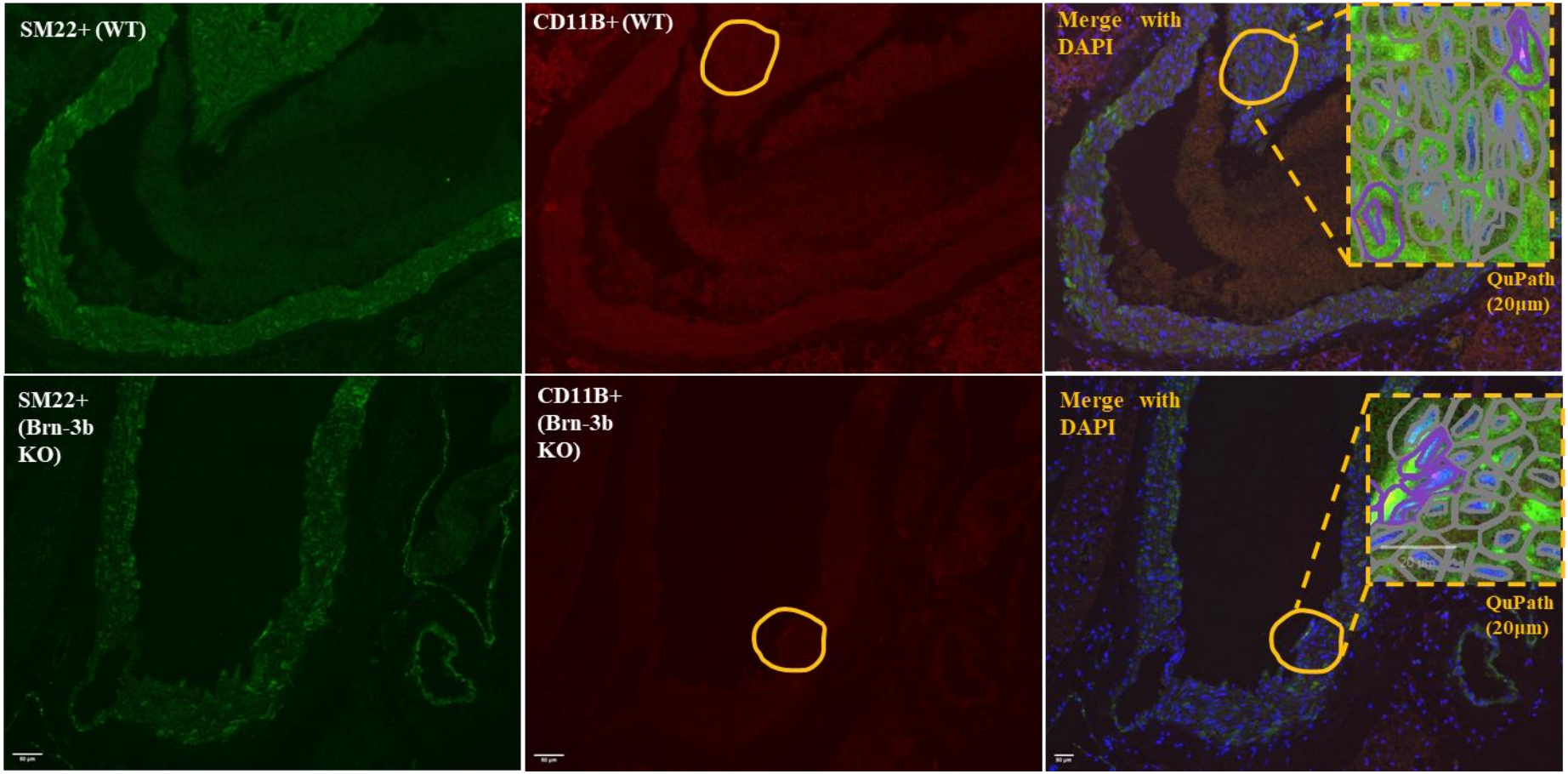
SM22+ (WT)
CD11B+ (WT)
Merge with DAPI
QuPath (20µm)
SM22+ (Brn-3b KO)
CD11B+ (Brn-3b KO)
Merge with DAPI
QuPath (20µm)

D

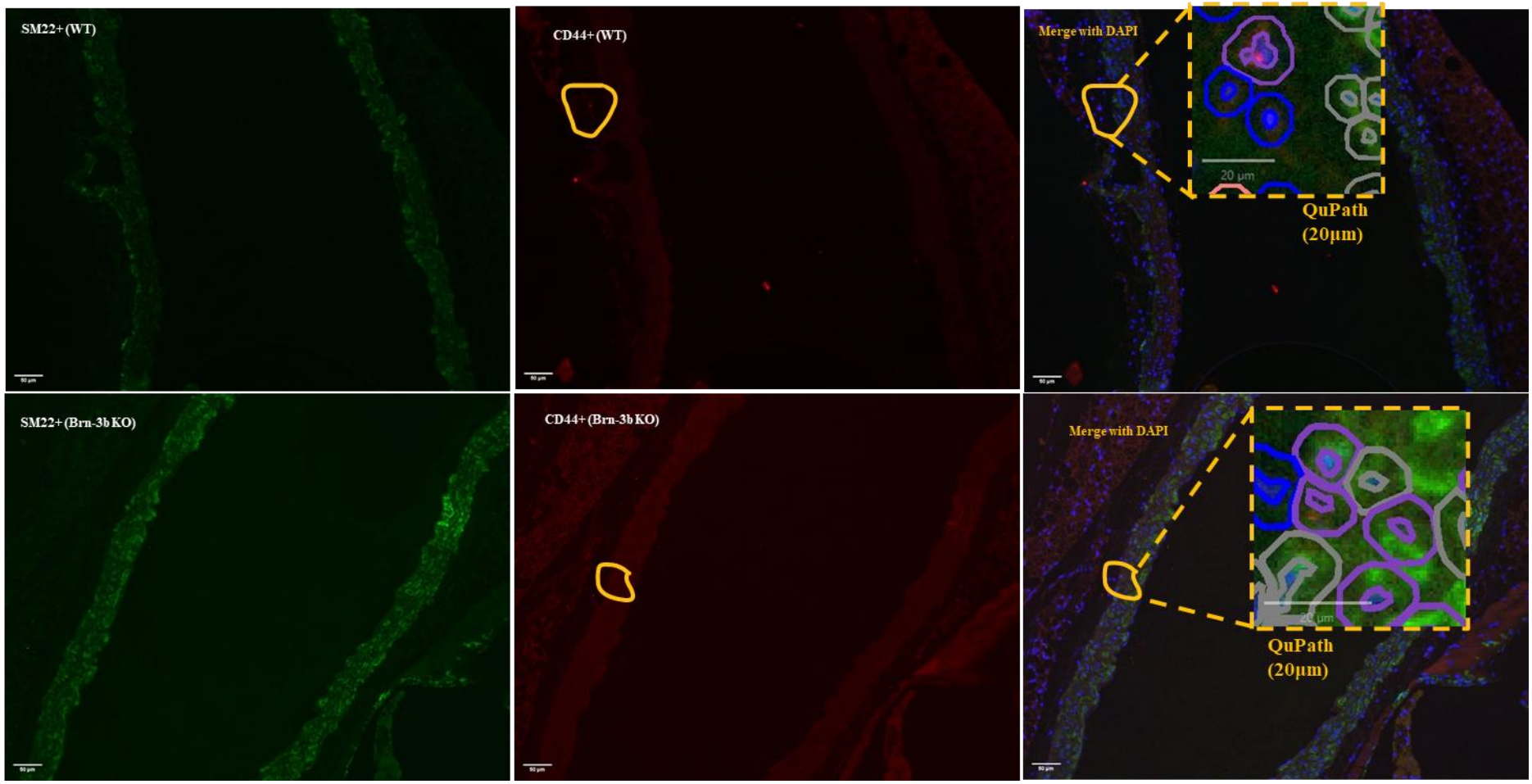
SM22+(WT)
CD44+(WT)
Merge with DAPI
20 µm
QuPath
(20µm)
SM22+(Brn-3b KO)
CD44+(Brn-3b KO)
Merge with DAPI
QuPath
(20µm)

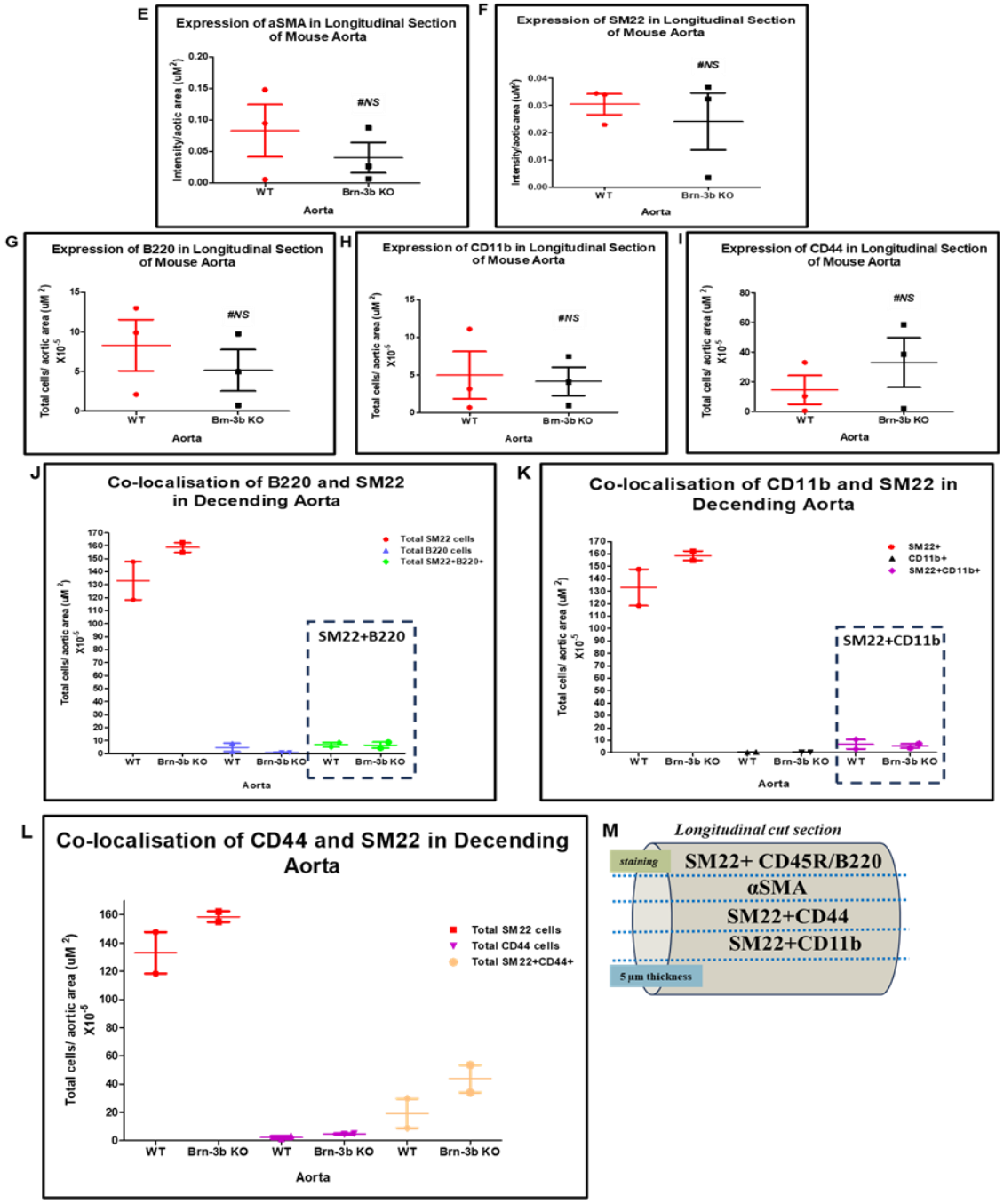

Figure 75: The representative images and quantification of immunofluorescent stained images of the aorta of wild type (WT) and Brn-3b knock-out (KO) mice. C57BL/6J mice were euthanised, and aortas were isolated, processed, and embedded in paraffin wax. The aortas were sectioned longitudinally at a thickness of 5 µm. The tissue sections were stained and imaged using a Leica DMi8/Olympus microscope at 10x and 20x magnification. Depicted are (A) alpha smooth muscle actin (αSMA), (B) smooth Muscle Protein 22 (SM22) and CD45R/B220, (C) SM22 and CD11b, (D) SM22 and CD44, (E-I) statistical results of single marker staining, (J-L) co-staining, and (M) staining design for each section of WT and Brn-3b KO aorta. The analysis was performed using QuPath 0.4.3 software. Data are presented as mean ± SEM for n = 4 (tissue sections = 1-4 per mouse) (Sex = male) (Age = 2–4 months) (Ns = Not significant). Note: The yellow paint (--) was drawn to localise the example expression of the markers.

6.2.3.2 Experimental on the transverse cut section of mouse aorta

Longitudinal sections offer insights into the continuity and distribution of changes along the length of the aorta. To further validate the findings, I measured the morphological structure and the expression of vasculature and immune marker proteins on the transverse plane, as illustrated in Figure 74. This approach provides detailed information on the histological architecture and localised abnormalities.

6.2.3.2.1 Thoracic aorta

Based on visualization on the transverse plane, the loss of Brn-3b did not alter the general morphology of the aorta compared to the WT counterpart, as illustrated in Figure 76 (A). The free lumen can be observed for both Brn-3b KO and their WT control.

The finding showed that the loss of Brn-3b did not significantly alter the average approximate thickness (r) of TI, TM and TA for thoracic aorta compared to WT control (Figure 76 (B to C).

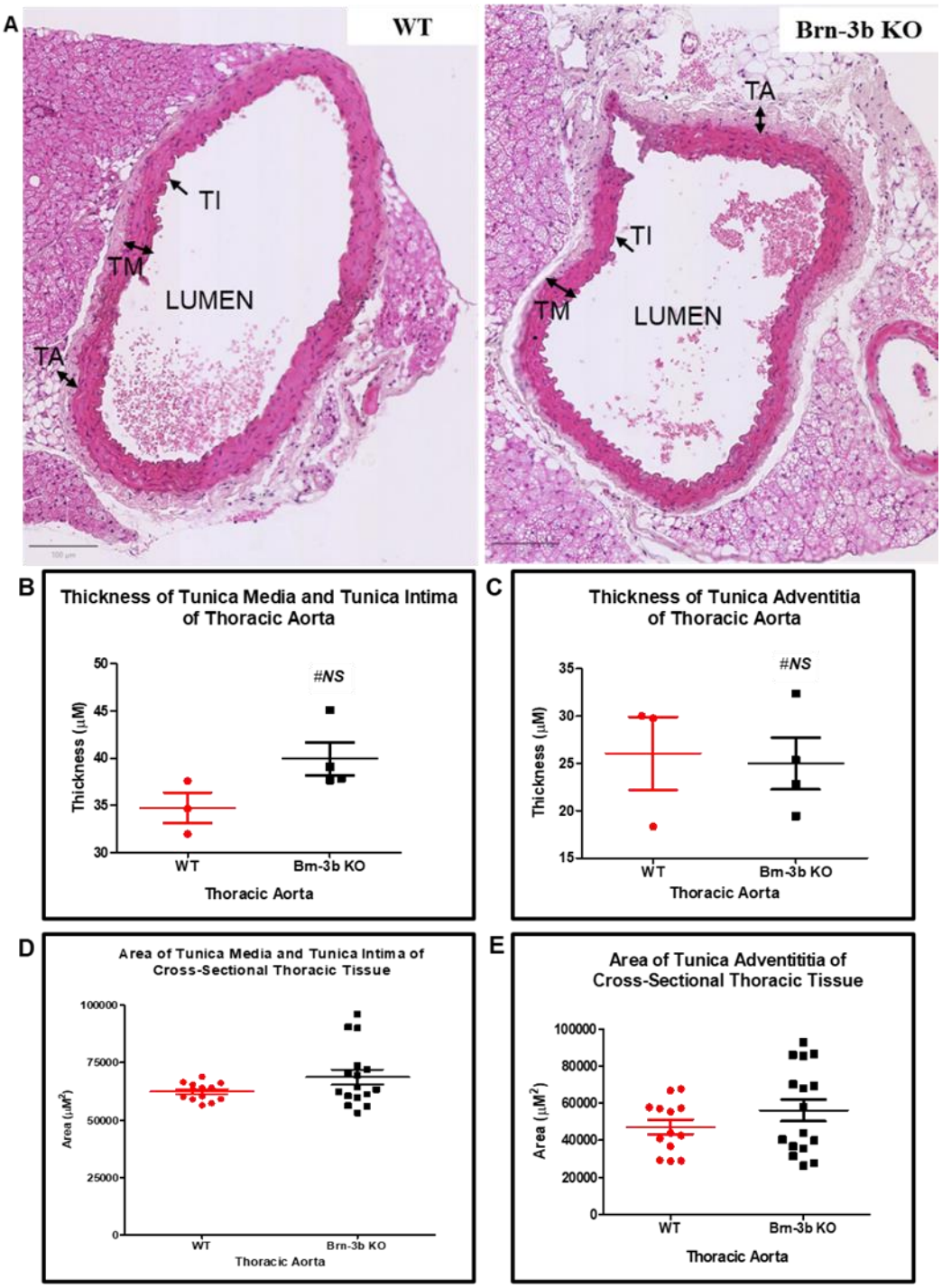

Figure 76: The thickness of thoracic aorta wall of wild type (WT) and Brn-3b knock-out (KO) mice. C57BL/6J mice were euthanised, and aortas were isolated, processed, and embedded in paraffin wax. The aortas were sectioned transversely at a thickness of 5 µm. The tissue sections were stained with haematoxylin and eosin (H&E) and imaged using a Nanozoomer microscope at 20× magnification. Depicted are (A) a representative image of the thoracic aorta, (B-C) the average thickness (r) of tunica media (TM), tunica intima (TI), and tunica adventitia (TA), and (D-E) the area of TI, TM, and TA for each tissue section in WT and Brn-3b KO mouse aorta. ROI for both TM, TI, and TA are illustrated in Appendix 4. Data are presented as mean ± SEM for n = 3-4 (tissue sections = 2-4 per mouse) (Sex = male) (Age = 2–4 months) (Ns = Not significant). Note: The formula for thickness is provided in Appendix 4.

6.2.3.2.1.1 The expression of aSMA- structural vascular protein

Furthermore, the analysis focused on the expression of αSMA (vascular marker) in the thoracic cross-section tissue, as illustrated in Figure 77. Representative images indicated an increase in αSMA expression in the Brn-3b KO thoracic aorta compared to the WT controls, with the marker localized in the TI and TM layers. Quantitative analysis revealed a trend toward increased αSMA signal in the Brn-3b KO aorta relative to the WT control. However, statistical analysis did not show significant differences between the two groups.

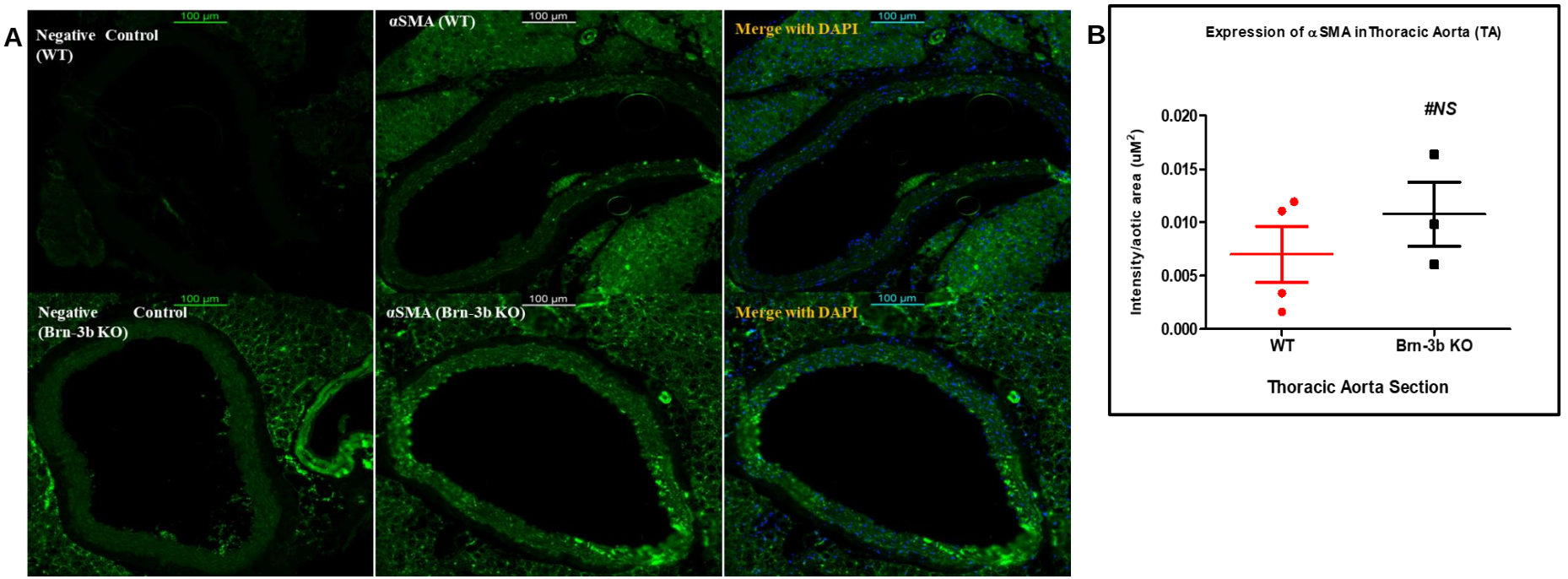

Figure 77: The representative images and quantification of αSMA immunofluorescent staining on the thoracic aorta of wild type (WT) and Brn-3b knock-out (KO) mice. C57BL/6J mice were euthanised, and aortas were isolated, processed, and embedded in paraffin wax. The aortas were sectioned transversely at a thickness of 5 µm. The tissue sections were stained and imaged using a Leica DMi8/Olympus microscope at 10x and 20x magnification. Depicted are (A) the representative image and (B) the quantification analysis of alpha smooth muscle actin (αSMA) protein in WT and Brn-3b KO mouse aorta. The analysis was performed using QuPath 0.4.3 software. Data are presented as mean ± SEM for n = 3 (tissue sections = 2-4 per mouse) (Sex = male) (Age = 2–4 months) (Ns = Not significant)

6.2.3.2.1.2 The expression of SM22- structural vascular protein

Moreover, I investigated the expression of the SM22 marker in the thoracic cross-sections. The representative staining images in Figure 78 illustrated a reduction of SM22 marker expression in Brn-3b KO aorta as compared to WT controls, in which the marker was localised in the TI and TM regions. The quantitative analysis showed a decreasing trend of SM22 signal in Brn-3b KO aorta compared to WT counterparts, but the difference was not statistically significant.

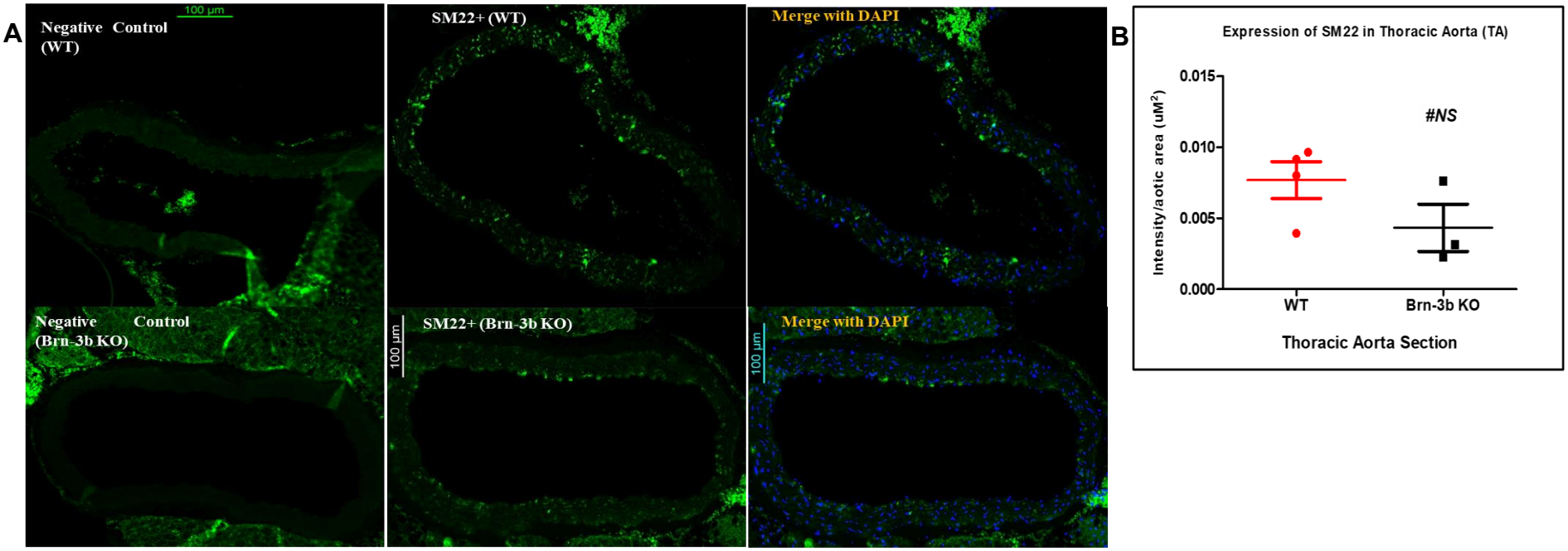

Figure 78: The representative images and quantification of SM22 immunofluorescent staining on the thoracic aorta of wild type (WT) and Brn-3b knock-out (KO) mice. C57BL/6J mice were euthanised, and aortas were isolated, processed, and embedded in paraffin wax. The aortas were sectioned transversely at a thickness of 5 µm. The tissue sections were stained and imaged using a Leica DMi8/Olympus microscope at 10x and 20x magnification. Depicted are (A) the representative image and (B) the quantification analysis of smooth Muscle Protein 22 (SM22) protein in WT and Brn-3b KO mouse aorta. The analysis was performed using QuPath 0.4.3 software. Data are presented as mean ± SEM for n = 3 (tissue sections = 2-4 per mouse) (Sex = male) (Age = 2–4 months) (Ns = Not significant).

6.2.3.2.1.3 The expression of immune surface antigen markers

Furthermore, the analysis focused on the expression of immune and mesenchymal markers in the thoracic aorta. Herein, I measured the effect of Brn-3b deficiency on the infiltration of immune cell markers CD3, B220, CD11b, and immune/ Mesenchymal-like CD44 marker across the thoracic aorta section.

The results showed that the loss of Brn-3b did not significantly alter the expression of CD3, B220, CD11b, or CD44 markers compared to WT controls. These markers were localized in the TI, TM, and TA regions in both Brn-3b KO and WT mouse thoracic tissue (Figure 79).

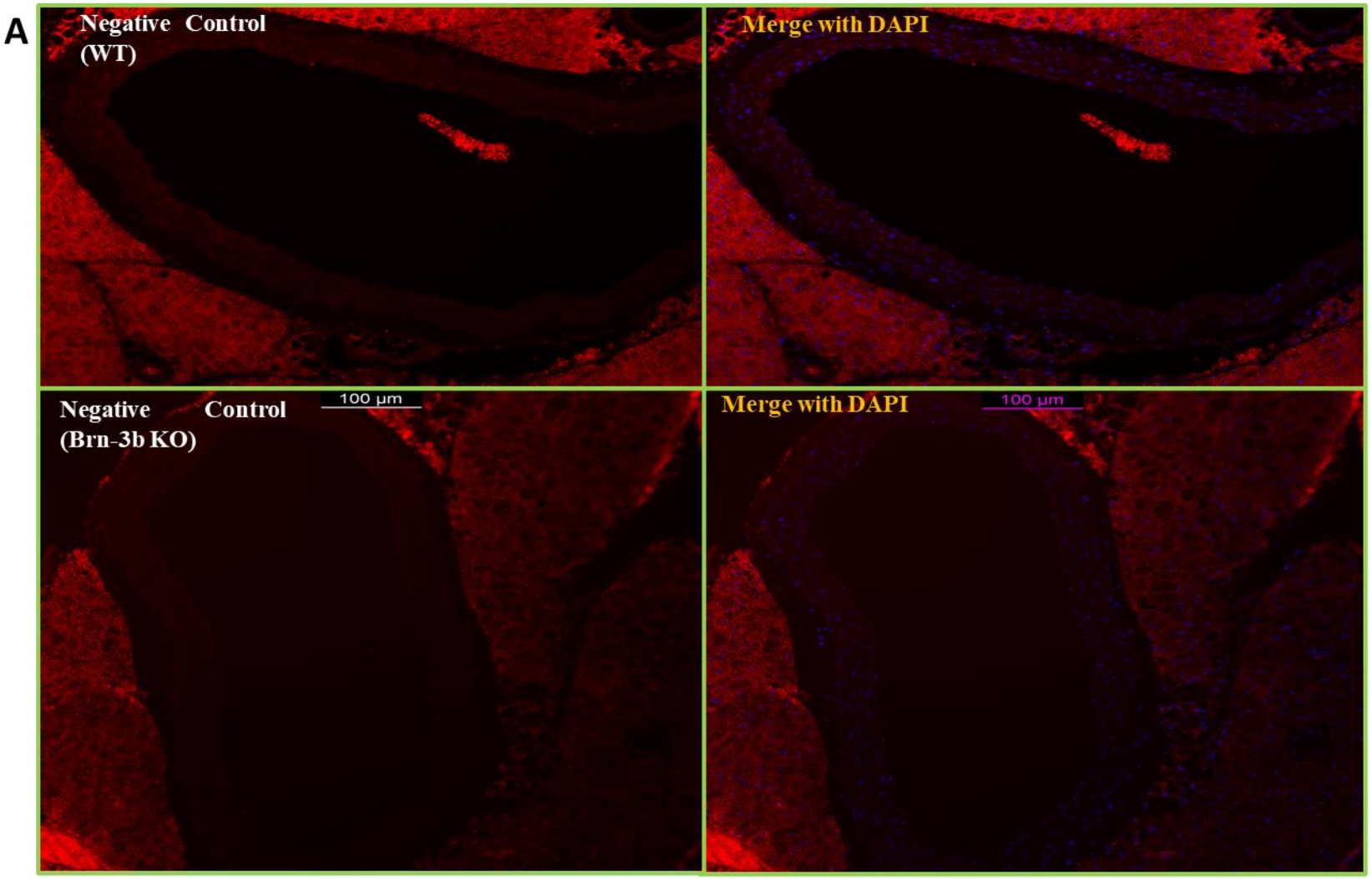
A
Negative Control (WT)
Merge with DAPI
Negative Control (Brn-3b KO)
100 µm
Merge with DAPI
100 µm

i)

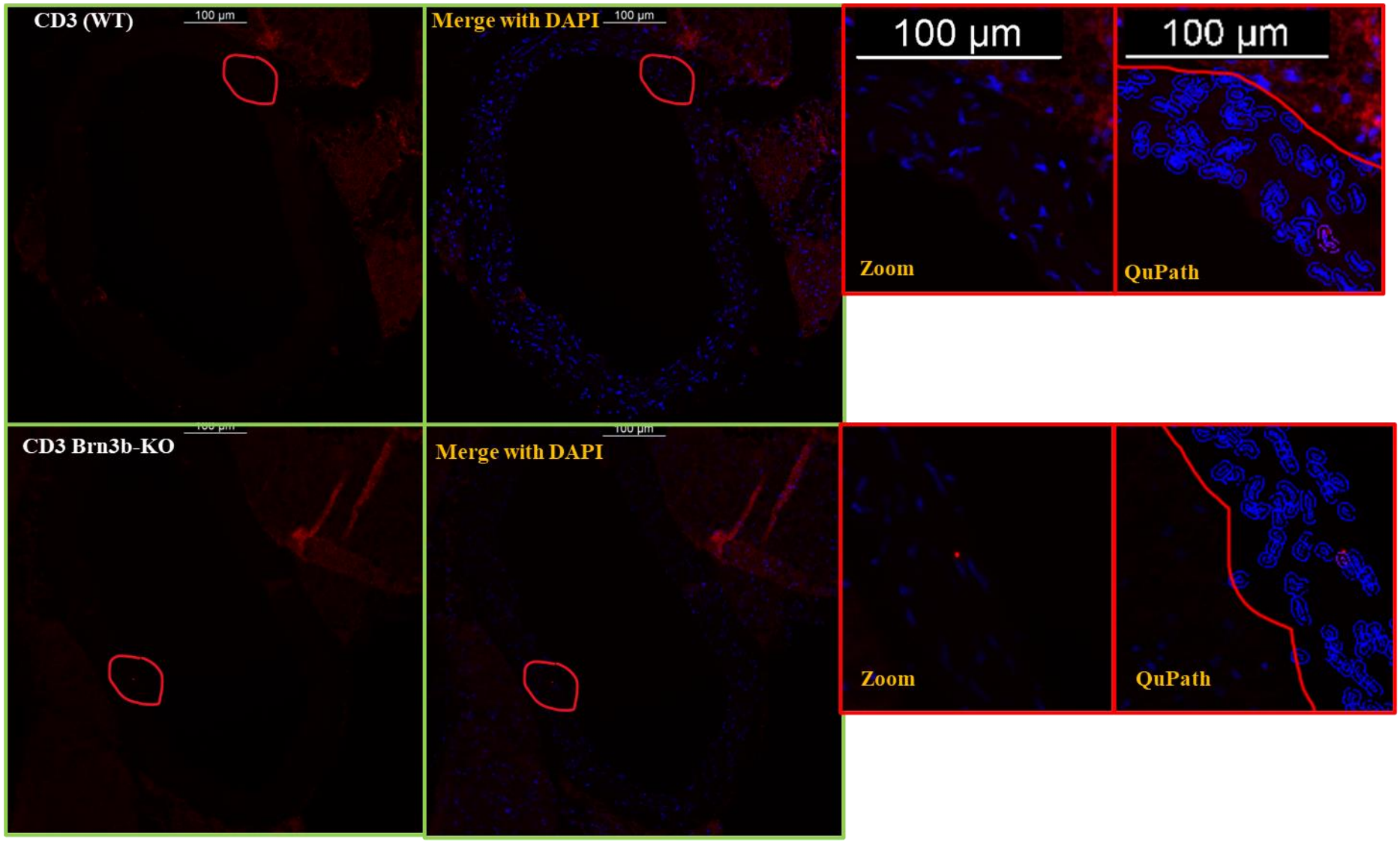
CD3 (WT)
100 µm
Merge with DAPI
100 µm
100 µm
Zoom
100 µm
QuPath
CD3 Brn3b-KO
Merge with DAPI
Zoom
QuPath

ii)

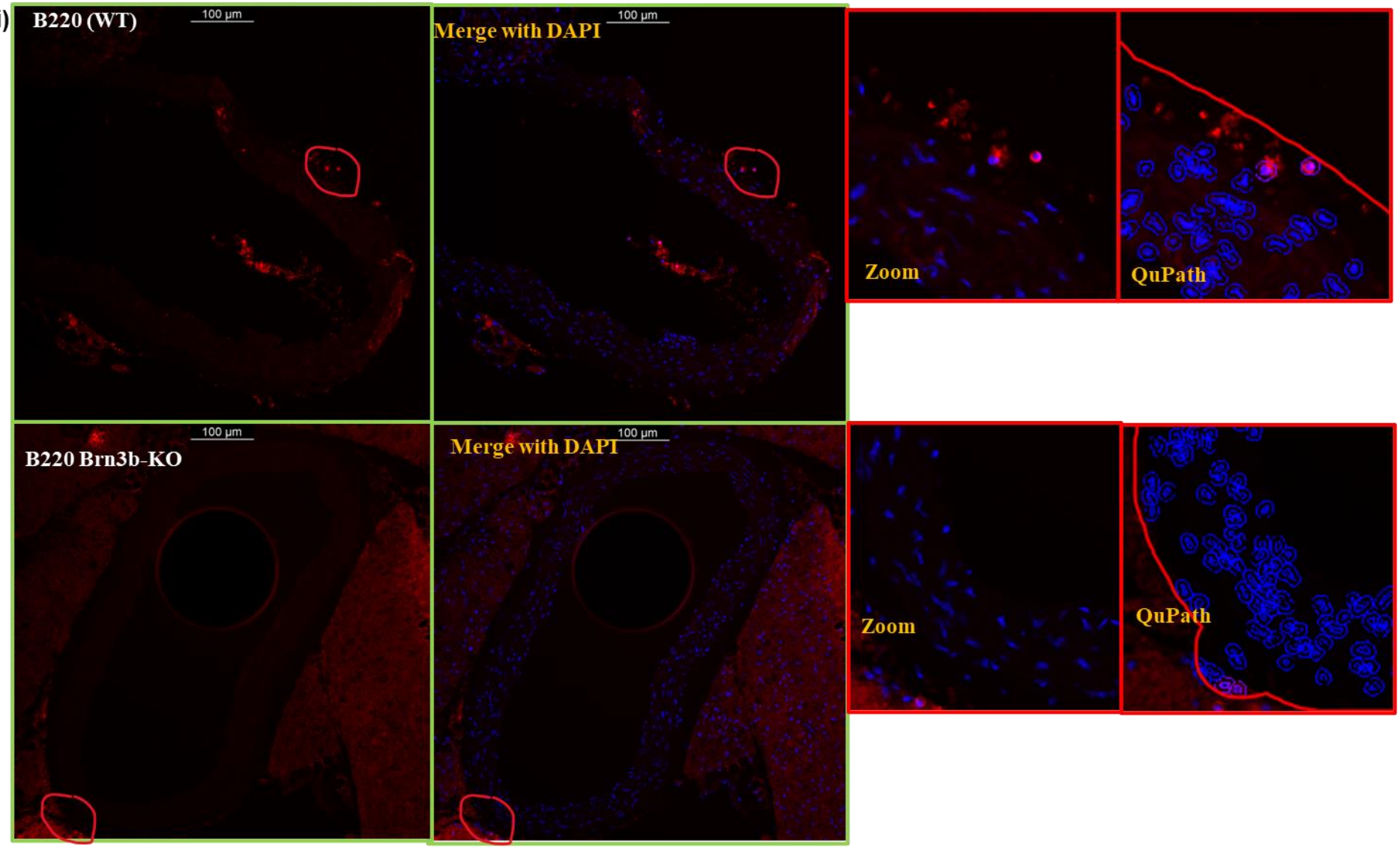
B220 (WT)
100 µm
Merge with DAPI
100 µm
Zoom
QuPath
B220 Brn3b-KO
100 µm
Merge with DAPI
100 µm
Zoom
QuPath

iii)

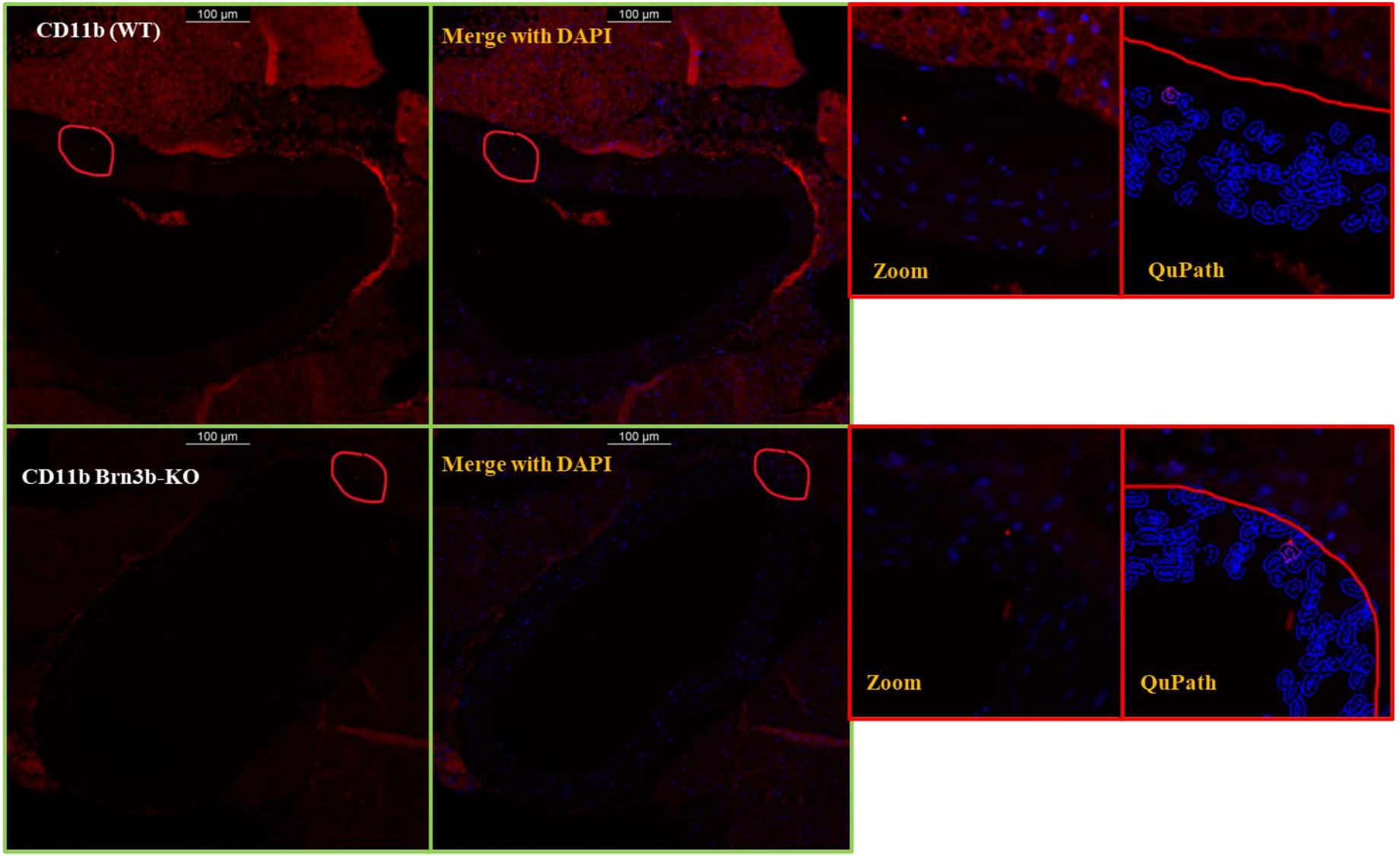
CD11b (WT)
100 µm
Merge with DAPI
100 µm
Zoom
QuPath
CD11b Brn3b-KO
100 µm
Merge with DAPI
100 µm
Zoom
QuPath

iv)

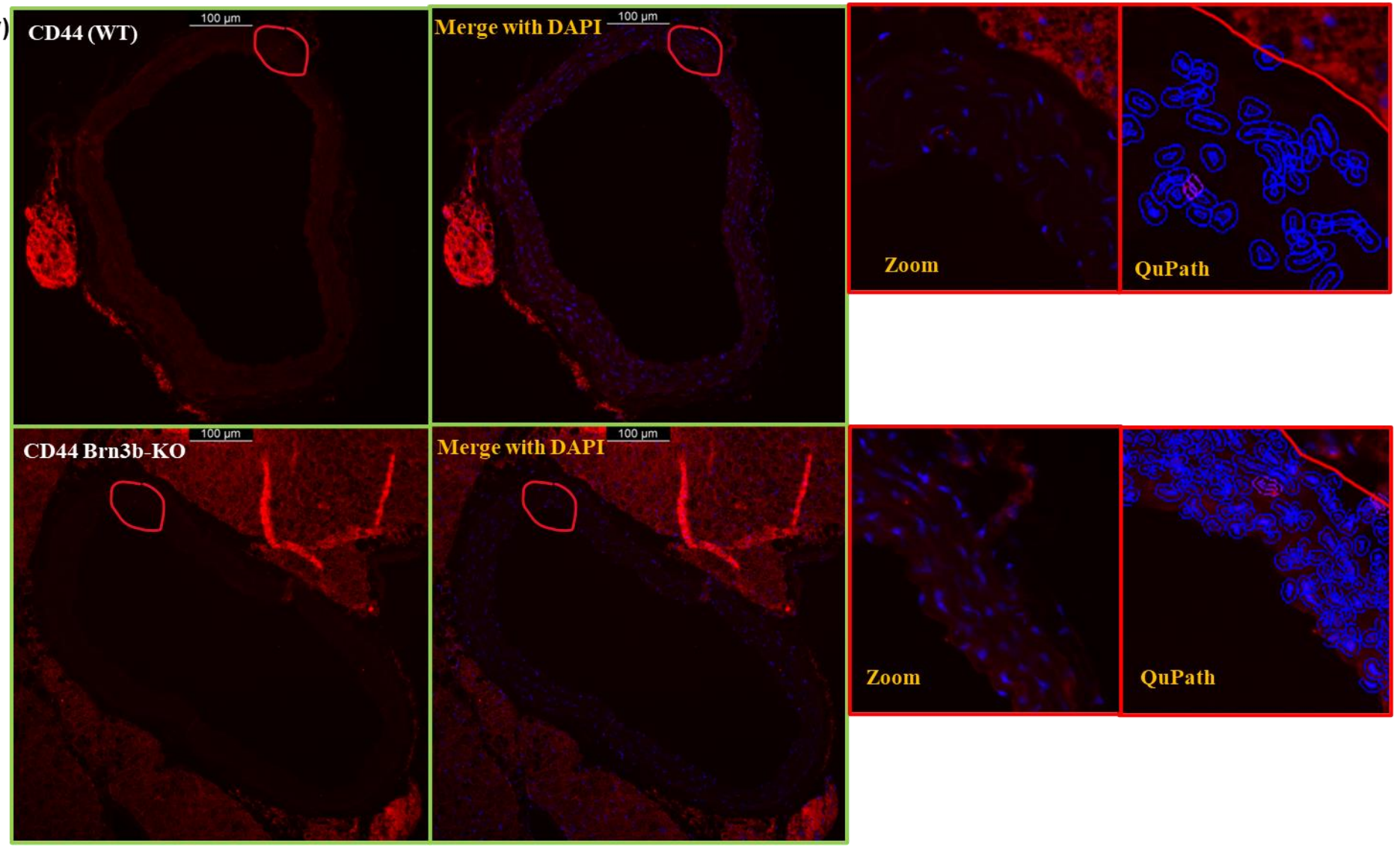
CD44 (WT)
100 µm
Merge with DAPI
100 µm
Zoom
QuPath
CD44 Brn3b-KO
100 µm
Merge with DAPI
100 µm
Zoom
QuPath

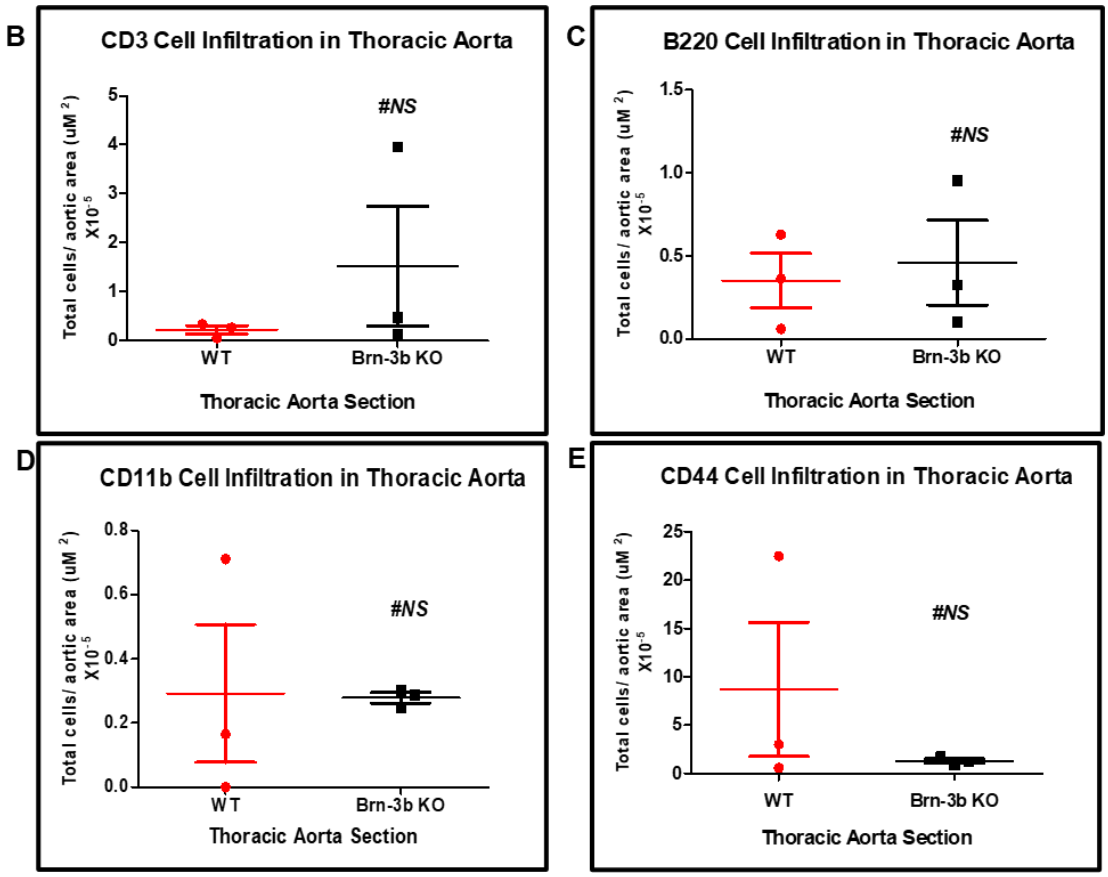

Figure 79: The representative images and quantification of immune/mesenchymal markers immunofluorescent staining on the thoracic aorta of wild type (WT) and Brn-3b knock-out (KO) mice. C57BL/6J mice were euthanised, and aortas were isolated, processed, and embedded in paraffin wax. The aortas were sectioned transversely at a thickness of 5 µm. The tissue sections were stained and imaged using a Leica DMi8/Olympus microscope at 10x and 20x magnification. Depicted are (A) the representative image and (B-E) the quantification analysis of CD3, B220, CD11b and CD44 protein in WT and Brn-3b KO mouse aorta. The analysis was performed using QuPath 0.4.3 software. Data are presented as mean ± SEM for n = 3-4 (tissue sections = 2-4 per mouse) (Sex = male) (Age = 2–4 months) (Ns = Not significant). Note: The red paint (---) was drawn to localise the example expression of the markers.

6.2.3.2.2 Abdominal aorta

In the prior section, the investigation was conducted on the descending aorta (longitudinal cut) and thoracic aorta (transverse cut). Herein, I opted to further investigate the effect of Brn-3b deficiency on the structural integrity and immune cell infiltration in the abdominal aorta.

The morphological structure of the abdominal aorta is shown in the H&E image of Figure 80. This image indicates the free lumen of Brn-3b KO mouse abdominal aortas, which mirror their WT control. However, some disorganisation of the nuclei arrangement and elastic lamella structure was observed in the Brn-3b KO abdominal aorta compared to the normal control.

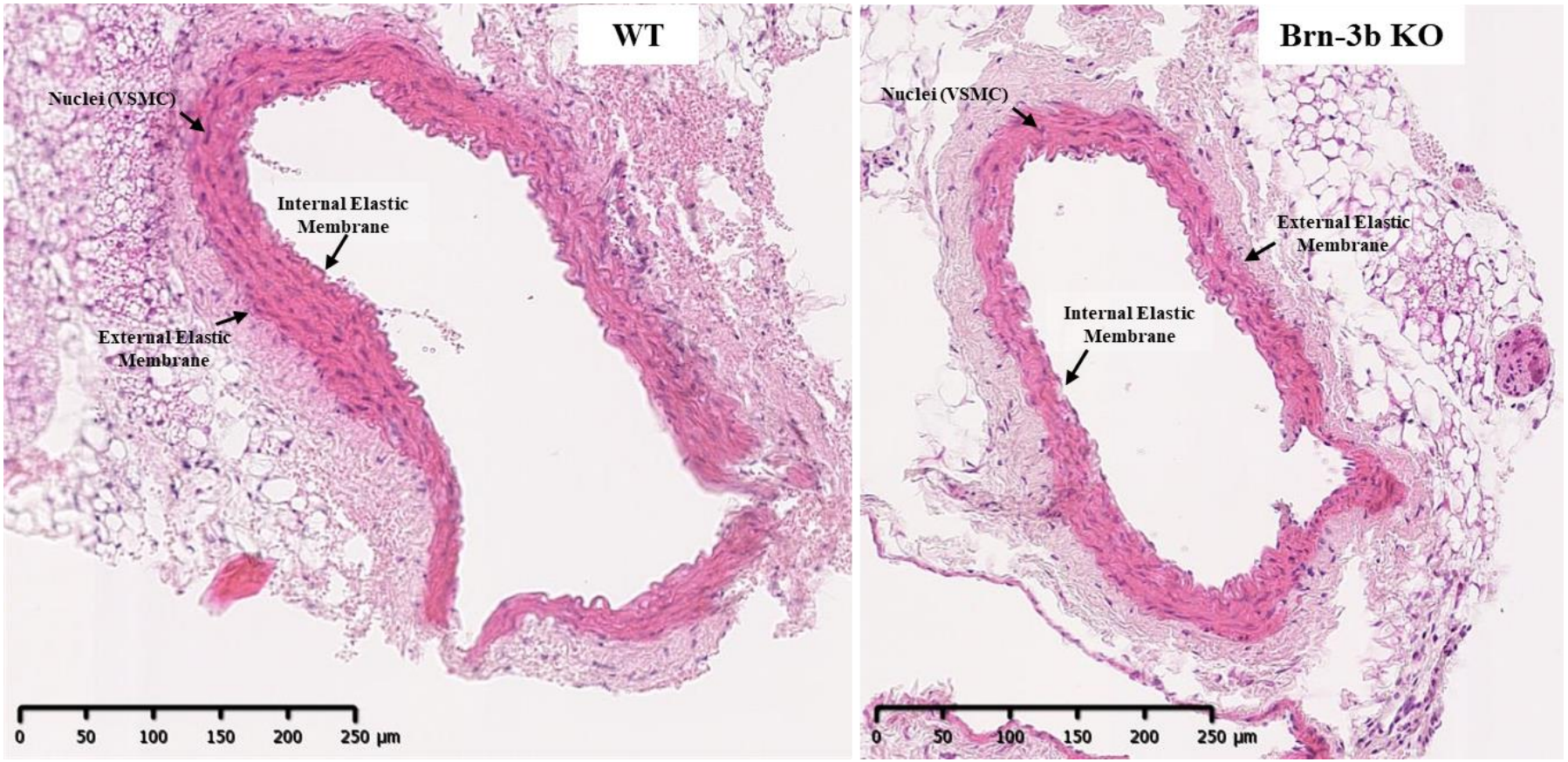

Figure 80: Representative histology staining of abdominal aorta of wild type (WT) and Brn-3b knock-out (KO) mice. C57BL/6J mice were euthanised, and aortas were isolated, processed, and embedded in paraffin wax. The aortas were sectioned transversely at a thickness of 5 µm. The tissue sections were stained with haematoxylin and eosin (H&E) and imaged using a Nanozoomer microscope at 20× magnification. Depicted are (A) the histological structure of the abdominal aorta in WT and Brn-3b KO mouse aorta. Data are presented for n = 3 (Sex = male) (Age = 2–4 months).

6.2.3.2.2.1 The expression of αSMA- structural vascular protein

Furthermore, I investigated the expression of vascular markers, αSMA in abdominal aorta cross-sections. Observational analysis revealed reduced αSMA expression in Brn-3b KO abdominal aortas compared to WT, as shown in Figure 81. In both groups, αSMA was localized in the TI and TM regions.

Quantitative analysis indicated a reduction trend in αSMA expression in Brn-3b KO tissue; however, the difference was not statistically significant.

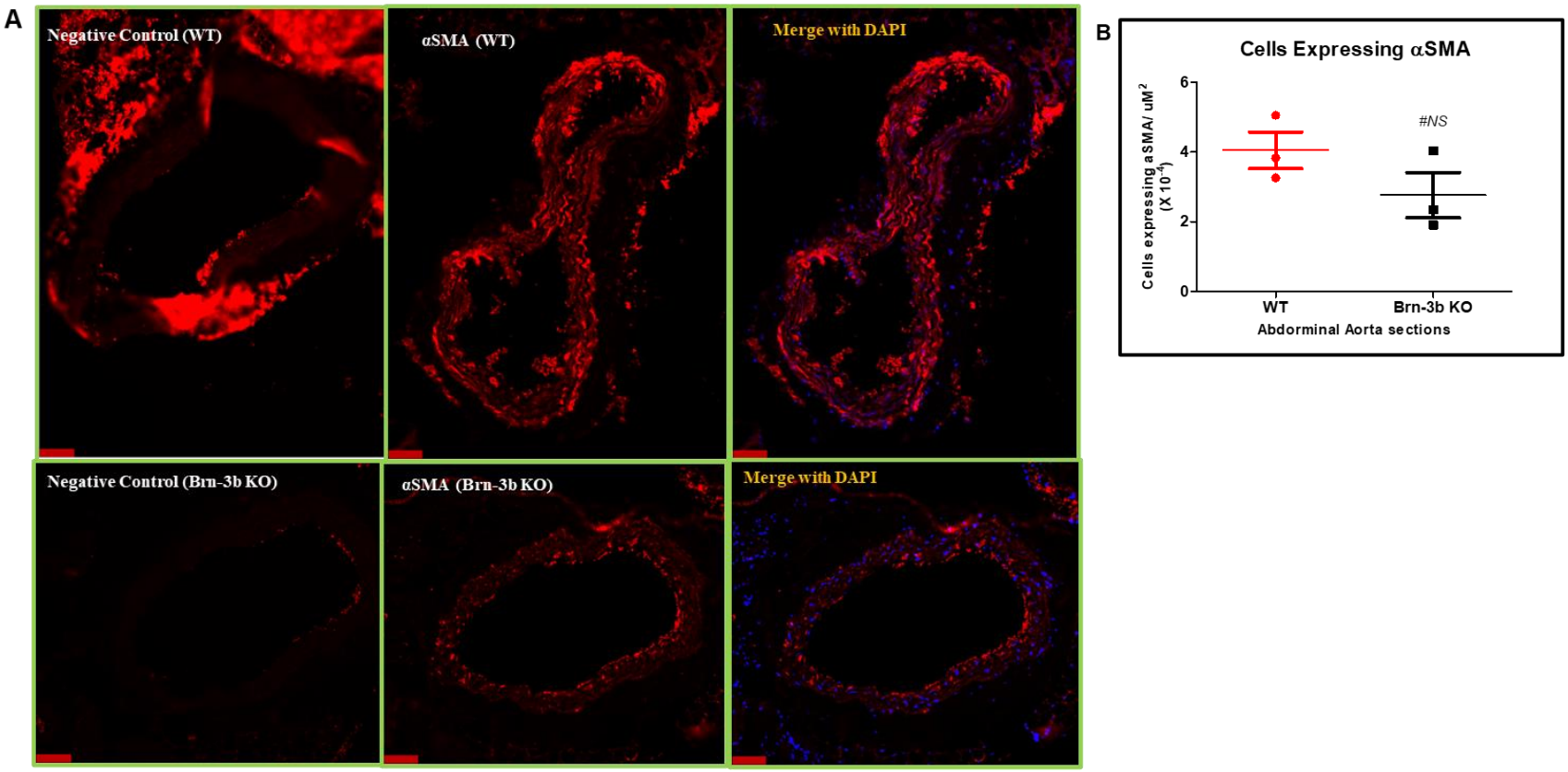

Figure 81: Representative images and quantification of αSMA immunofluorescent staining on the thoracic aorta of wild type (WT) and Brn-3b knock-out (KO) mice. C57BL/6J mice were euthanised, and aortas were isolated, processed, and embedded in paraffin wax. The aortas were sectioned transversely at a thickness of 5 µm. The tissue sections were stained and imaged using a Leica DMi8/Olympus microscope at 10x and 20x magnification. Depicted are (A) the representative image and (B) the quantification analysis of alpha smooth muscle actin (αSMA) protein in WT and Brn-3b KO mouse aorta. The analysis was performed using QuPath 0.4.3 software. Data are presented as mean ± SEM for n = 3 (tissue sections = 2-4 per mouse) (Sex = male) (Age = 2–4 months) (Ns = Not significant).

6.2.3.2.2.2 The expression of single immune markers in abdominal aorta

Furthermore, I investigated the effect of Brn-3b deficiency on the infiltration of immune markers CD3, B220, CD11b, and immune/ Mesenchymal like CD44 in the abdominal aorta. These markers were localized in the TI, TM, and TA regions in both Brn-3b KO and WT tissues, as shown in Figure 82 (A).

The quantitative analysis presented in Figure 82(B to E(i)), indicated no significant differences in the expression of CD3, B220, or CD44 between Brn-3b KO and WT cross-sections. However, a reduction trend in CD11b expression was observed in Brn-3b KO tissues compared to WT, although statistical analysis was limited by the small sample size (n = 2) for the WT control.

Additionally, shape analysis revealed that the cells expressing these markers exhibited a predominantly spherical morphology (circularity index ≈ 0.85), with no obvious differences observed between Brn-3b KO and normal tissue sections (Figure 82(B to E(ii)).

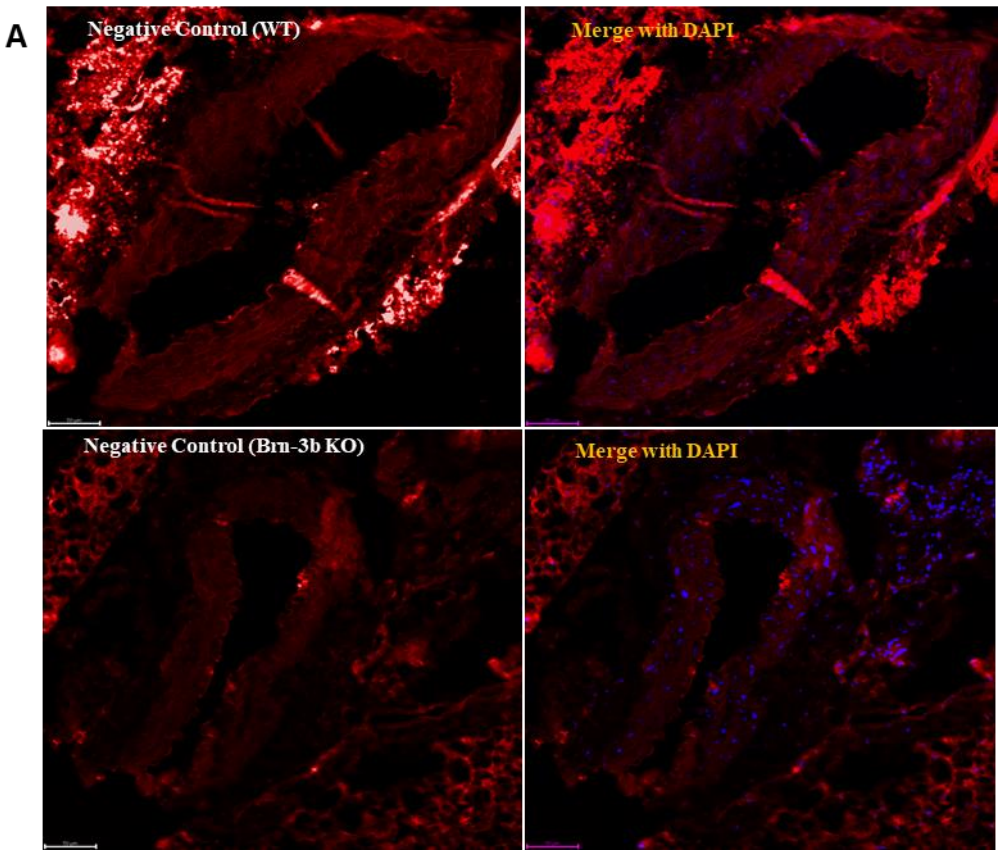

i)

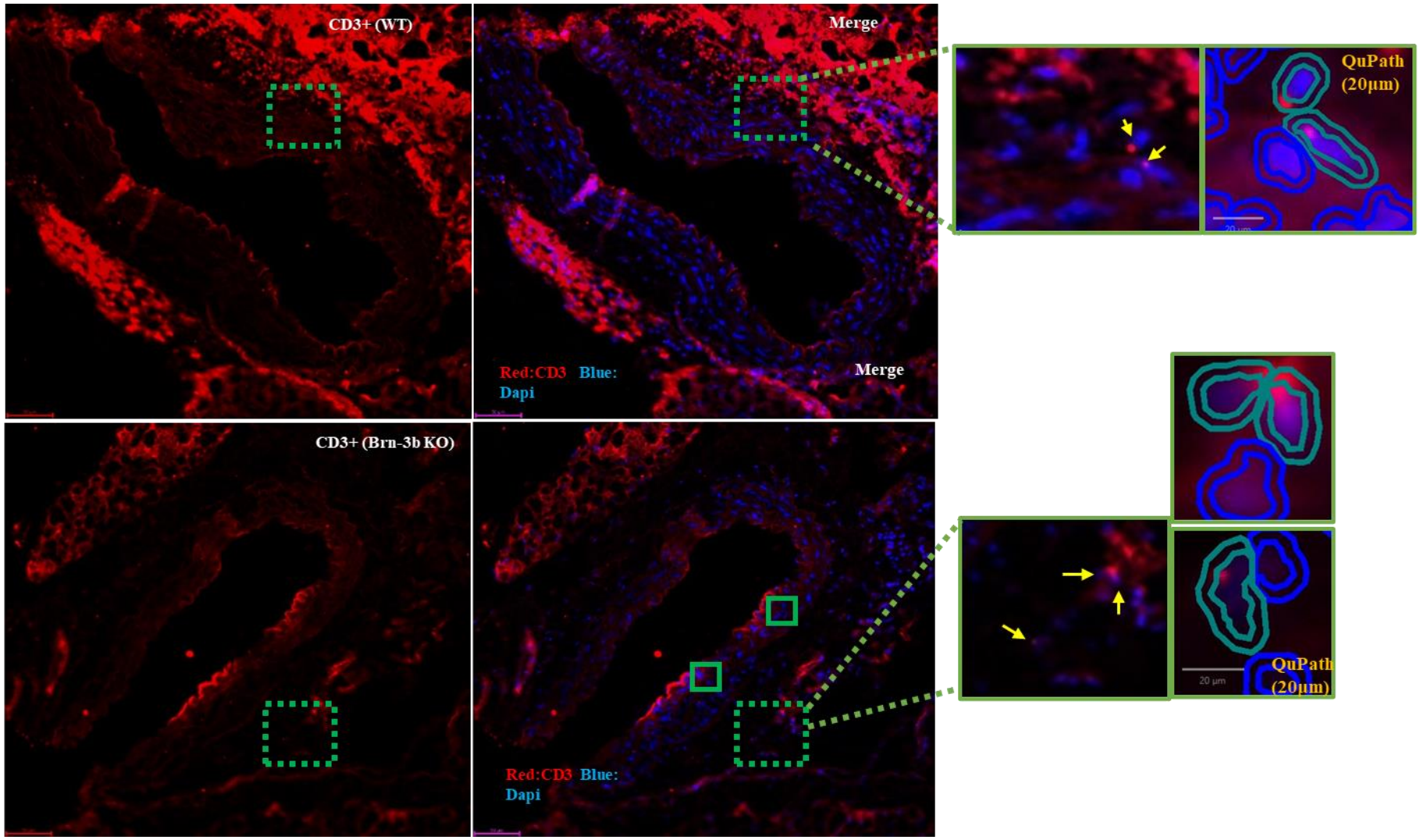
CD3+ (WT)
Merge
Red:CD3 Blue:
Dapi
Merge
QuPath
(20µm)
CD3+ (Brn-3b KO)
Red:CD3 Blue:
Dapi
20 µm
QuPath
(20µm)

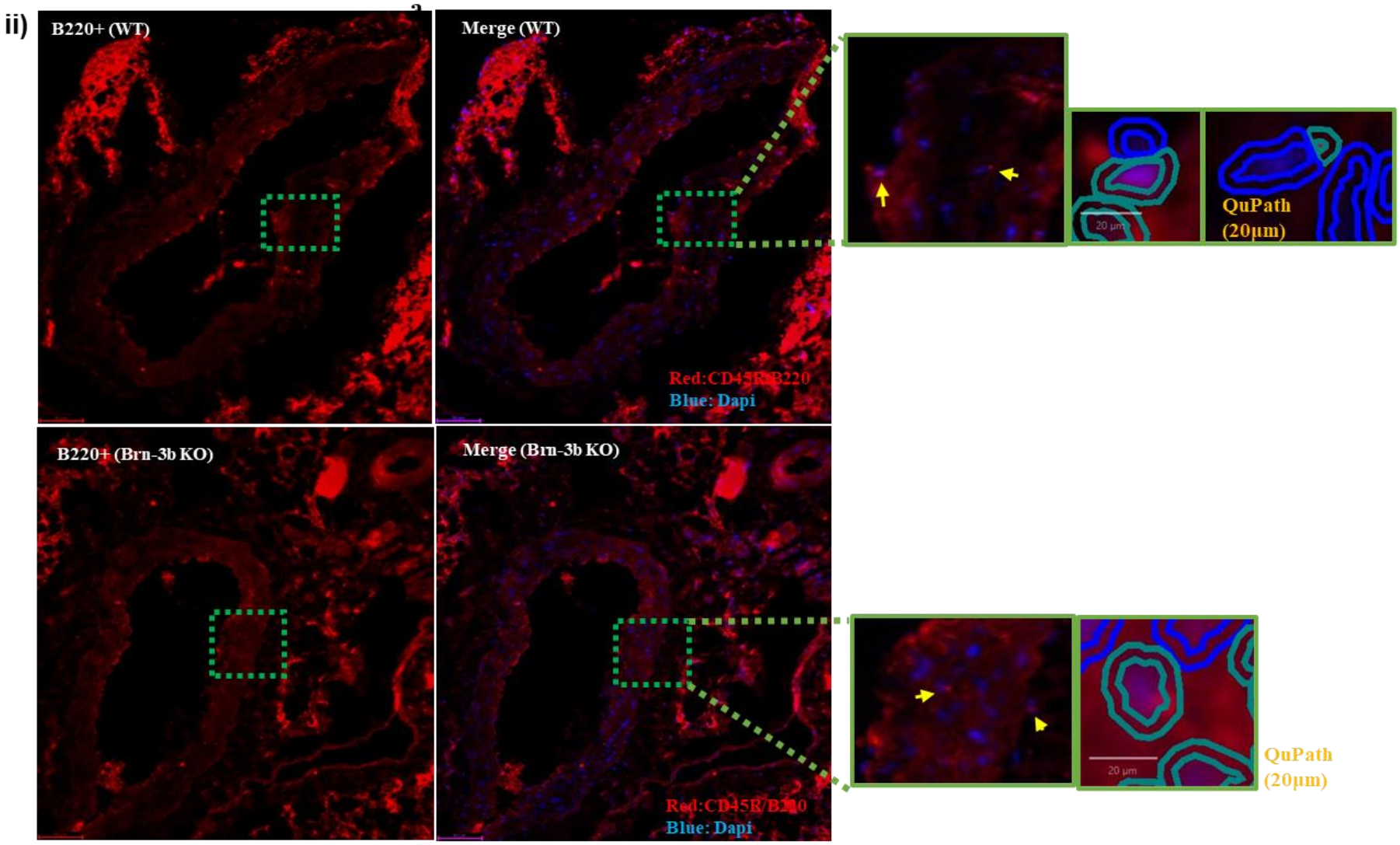
ii)
B220+ (WT)
Merge (WT)
Red:CD45R/B220
Blue: Dapi
20 µm
QuPath
(20µm)
B220+ (Brn-3b KO)
Merge (Brn-3b KO)
Red:CD45R/B220
Blue: Dapi
20 µm
QuPath
(20µm)

iii)

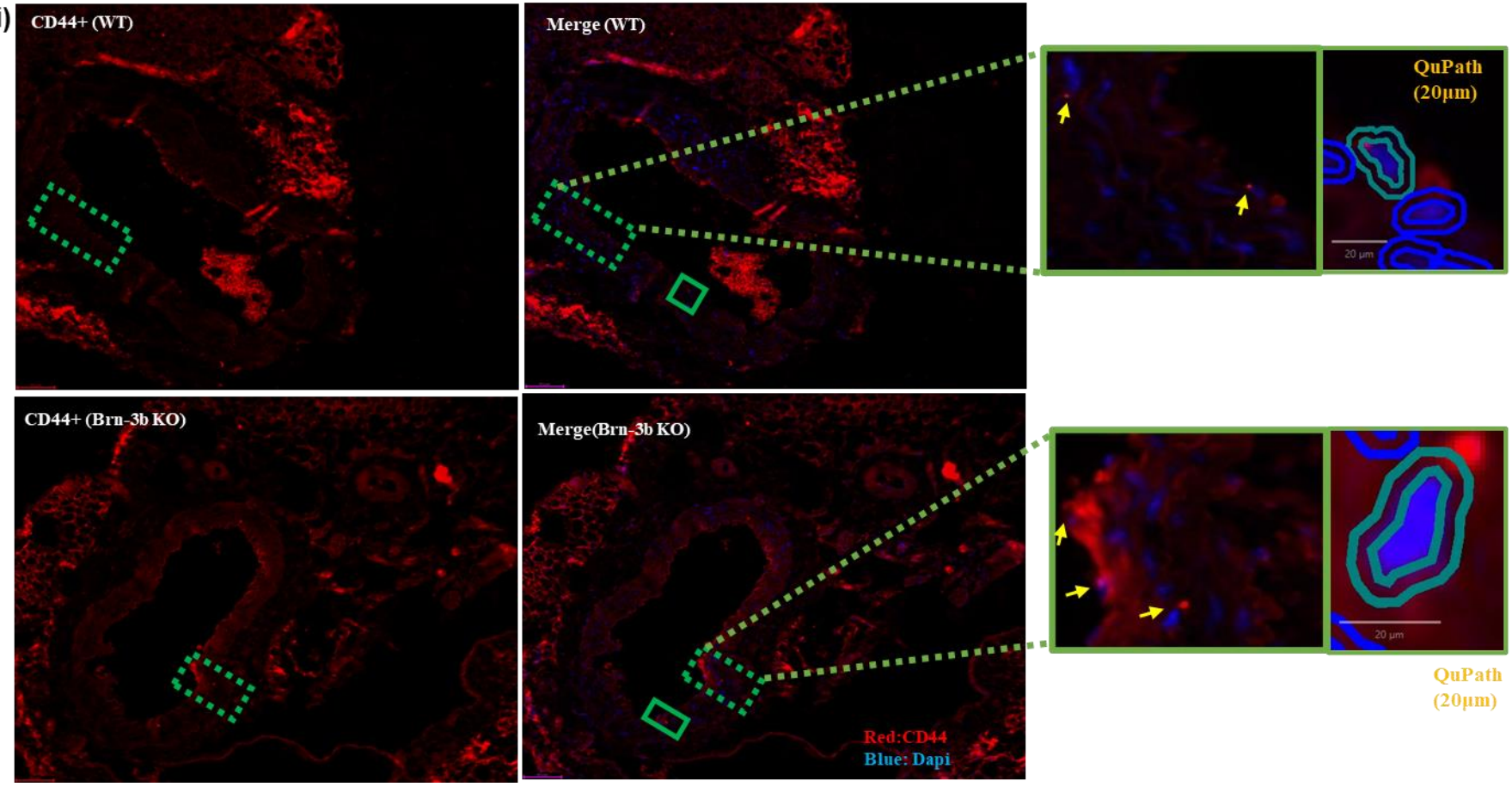
CD44+ (WT)
Merge (WT)
QuPath
(20µm)
20 µm
CD44+ (Brn-3b KO)
Merge(Brn-3b KO)
Red:CD44
Blue: Dapi
20 µm
QuPath
(20µm)

iv)

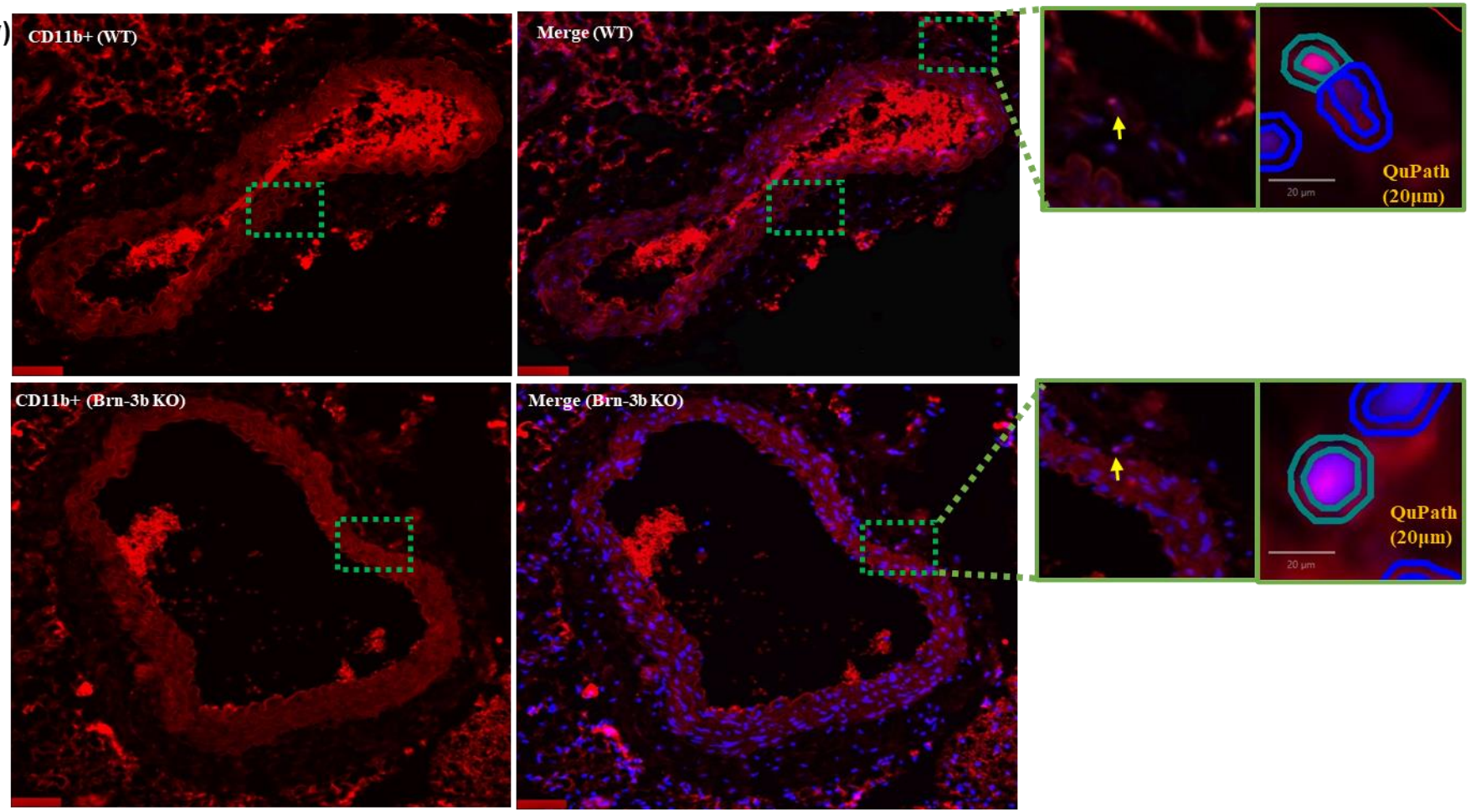
CD11b+ (WT)
Merge (WT)
QuPath (20µm)
CD11b+ (Brn-3b KO)
Merge (Brn-3b KO)
QuPath (20µm)

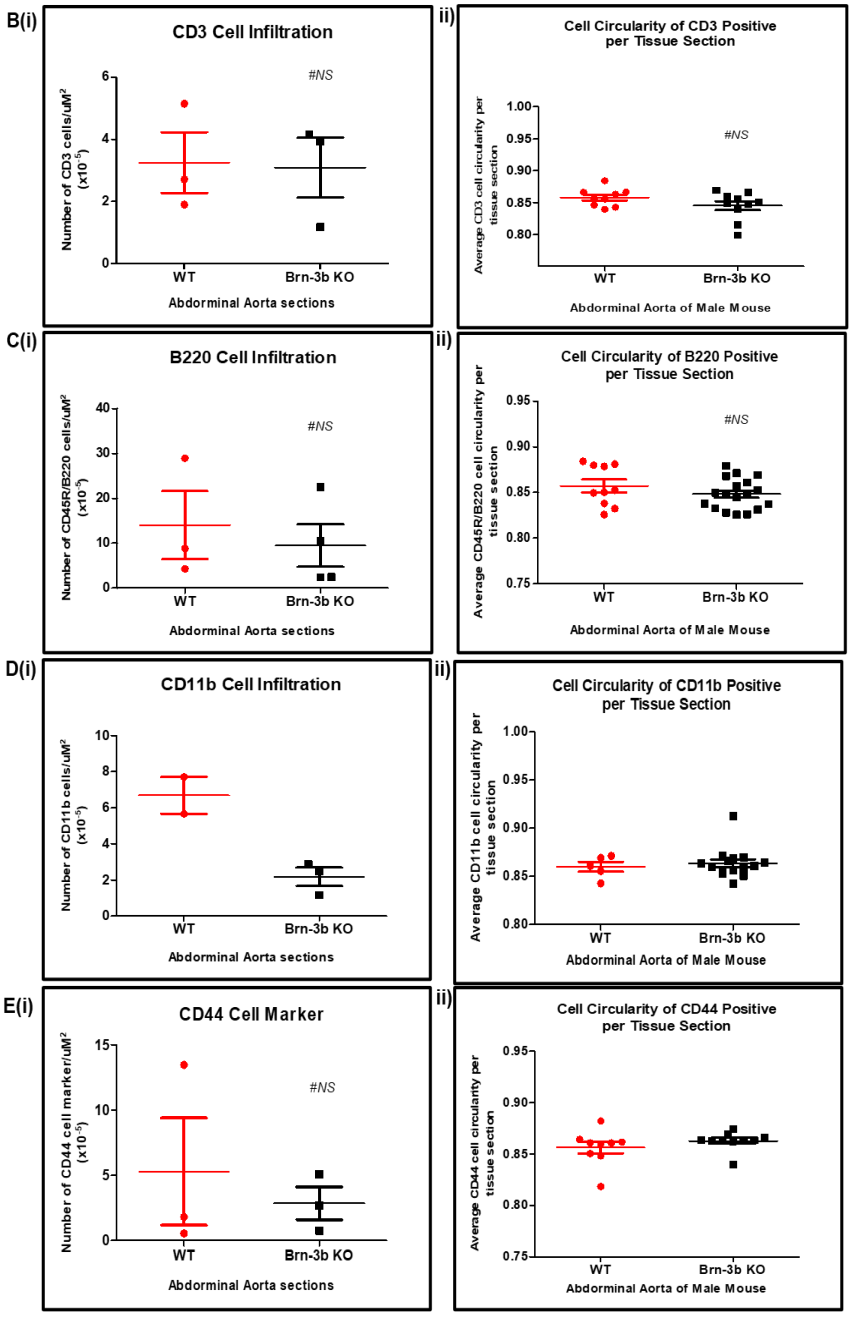

Figure 82: Representative and quantification of immune/mesenchymal markers immunofluorescent staining on the abdominal aorta of wild type (WT) and Brn-3b knock-out (KO) mice. C57BL/6J mice were euthanised, and aortas were isolated, processed, and embedded in paraffin wax. The aortas were sectioned transversely at a thickness of 5 µm. The tissue sections were stained and imaged using a Leica DMi8/Olympus microscope at 10x and 20x magnification. Depicted are (A) the representative image and (B-E (i)) the quantification analysis of CD3, B220, CD11b and CD44 protein and (B-E (ii)) the cell circularity index of these markers in WT and Brn-3b KO mouse aorta. The analysis was performed using QuPath 0.4.3 software. Data are presented as mean ± SEM for n = 2-4 (tissue sections = 2-4 per mouse) (Sex = male) (Age = 2–4 months) (Ns = Not significant). Note: The green box (--) was drawn to localise the example expression of the markers.

6.2.3.2.2.3 Correlation between αSMA and SM22 and their co-localisation with B220 marker in Brn-3b KO abdominal aorta

To specifically investigate the effect of Brn-3b deficiency on vascular changes and to determine whether these changes are potentially linked to immune regulation in the abdominal aorta, I further investigated by conducting co-immunostaining (triple multiplex staining) experiments using SM22, αSMA, and the B220 marker.

The representative image in Figure 83 (A) demonstrated that the expression of both αSMA and SM22 was reduced in the Brn-3b KO abdominal aorta compared to the WT control. Quantitative analysis revealed a reduction trend in both αSMA and SM22 (single signals) in Brn-3b KO tissue (Figure 83 (B)).

Co-staining results showed that both αSMA and SM22 expression were in a reduction trend in Brn-3b KO abdominal aorta compared to WT controls (Figure 83 (C)). Furthermore, the quantitative analysis of B220 immune cell infiltration around αSMA+SM22 is presented in Figure 83 (D). The findings indicated a reduction trend in B220 expression near αSMA+SM22 in Brn-3b KO tissues compared to WT controls. However, statistical analysis of the data in this section was limited due to the small sample size (n = 2) for the WT control.

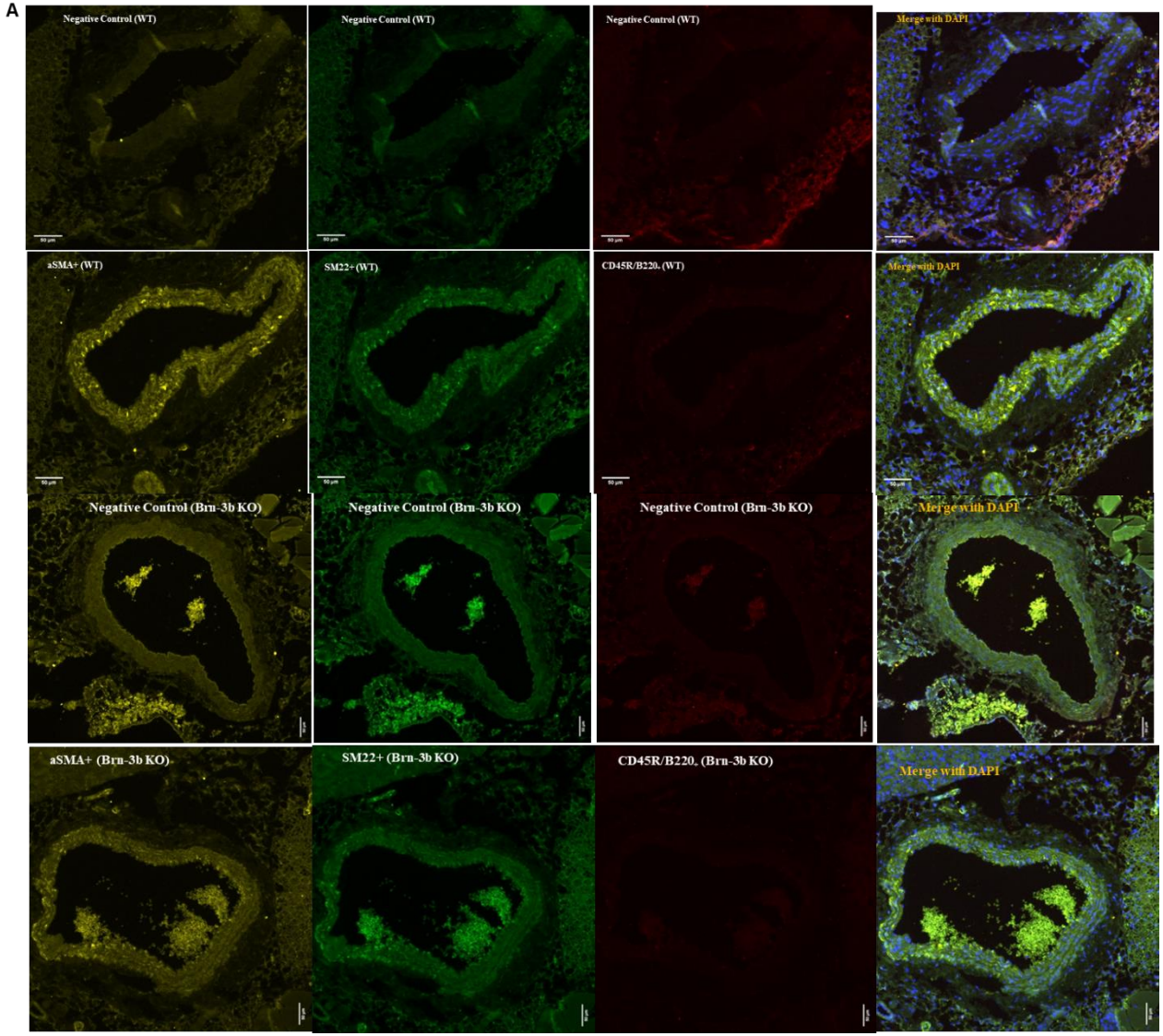
A
Negative Control (WT)
Negative Control (WT)
Negative Control (WT)
Merge with DAPI
aSMA+ (WT)
SM22+ (WT)
CD45R/B220+ (WT)
Merge with DAPI
Negative Control (Brn-3b KO)
Negative Control (Brn-3b KO)
Negative Control (Brn-3b KO)
Merge with DAPI
aSMA+ (Brn-3b KO)
SM22+ (Brn-3b KO)
CD45R/B220+ (Brn-3b KO)
Merge with DAPI

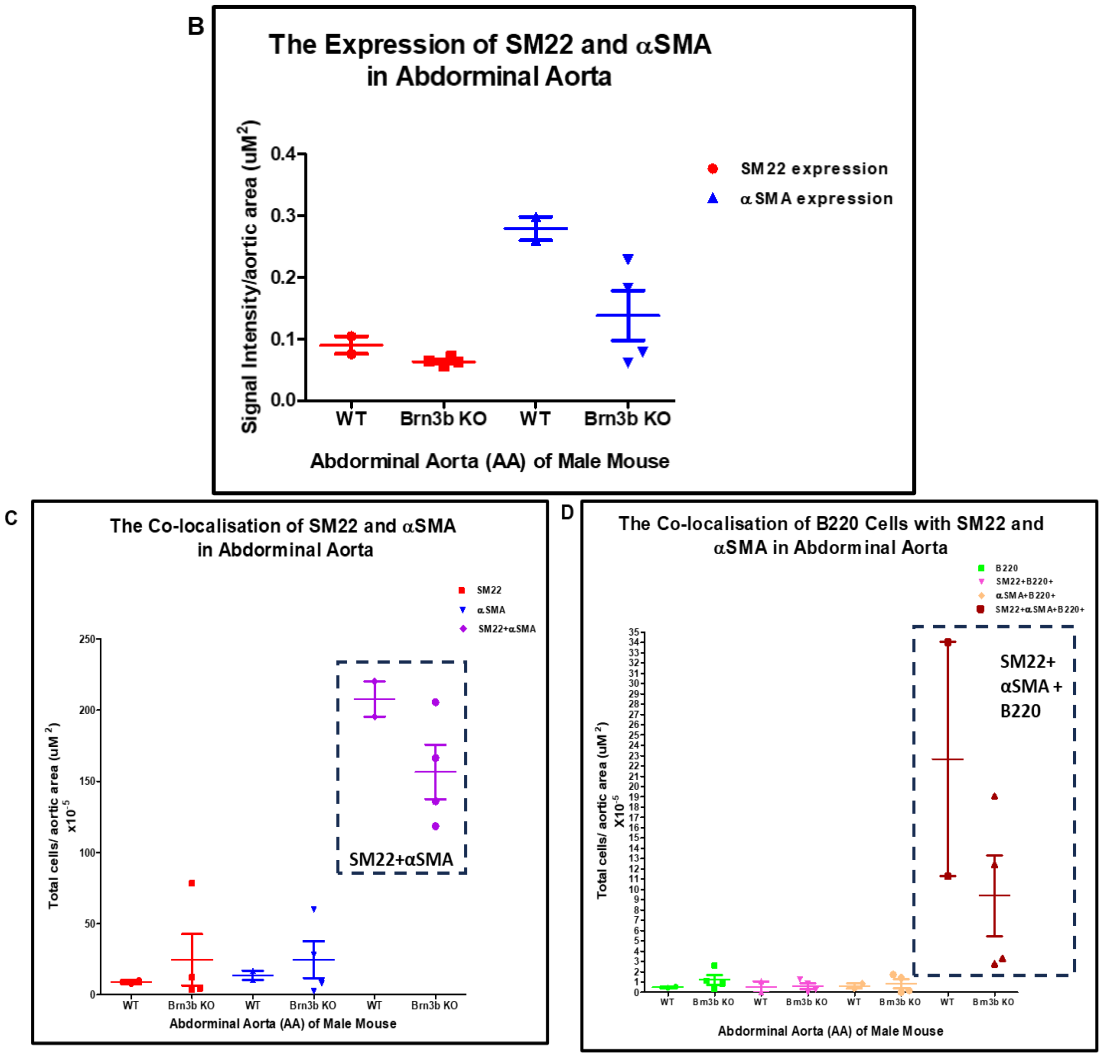

Figure 83: Representative and quantitative immunofluorescent staining (alpha smooth muscle actin (αSMA), smooth Muscle Protein 22 (SM22) and B220) on the abdominal aorta of wild type (WT) and Brn-3b knock-out (KO) mice. C57BL/6J mice were euthanised, and aortas were isolated, processed, and embedded in paraffin wax. The aortas were sectioned longitudinally at a thickness of 5 µm. The tissue sections were stained and imaged using a Leica DMi8/Olympus microscope at 10x and 20x magnification. Depicted are (A) the representative images of co-staining (αSMA, SM22, and B220), (B) the signal intensity of αSMA and SM22, (C) the co-expression of αSMA and SM22, and (D) B220 expression near αSMA and SM22 in WT and Brn-3b KO mouse aorta. The analysis was performed using QuPath 0.4.3 software. Data are presented as mean ± SEM for n = 2 (tissue sections = 2-4 per mouse) (Sex = male) (Age = 2–4 months).

6.2.3.2.2.4 Correlation between αSMA and Ki67 and their co-localisation with B220 marker in Brn-3b KO abdominal aorta

To further explore the relationship between Brn-3b deficiency and vascular integrity, I investigated the expression of an additional marker, Ki67, a critical marker for vascular structural integrity and cell proliferation (Li et al., 2024). In this section, I performed co-immunostaining (triple multiplex staining) of Ki67, αSMA, and the B220 immune marker.

The qualitative findings showed a reduction in αSMA expression, while the Ki67 marker exhibited an increasing trend in Brn-3b KO abdominal aorta compared to WT control (Figure 84 (A)). The quantitative data presented in Figure 84 (B), indicated a reduction trend in αSMA expression and a slight increase in Ki67 expression (single signals).

Co-staining results showed that the expression of both αSMA and Ki67 did not demonstrate an obvious trend in Brn-3b KO mice compared to WT controls (Figure 84 (C)). Furthermore, the expression of the B220 marker infiltrating near αSMA+Ki67 did not show any noticeable differences in Brn-3b KO abdominal aorta cross-sections compared to WT controls (Figure 84 (D)). However, statistical analysis of the data in this section was limited due to the small sample size (n = 2) for the WT control.

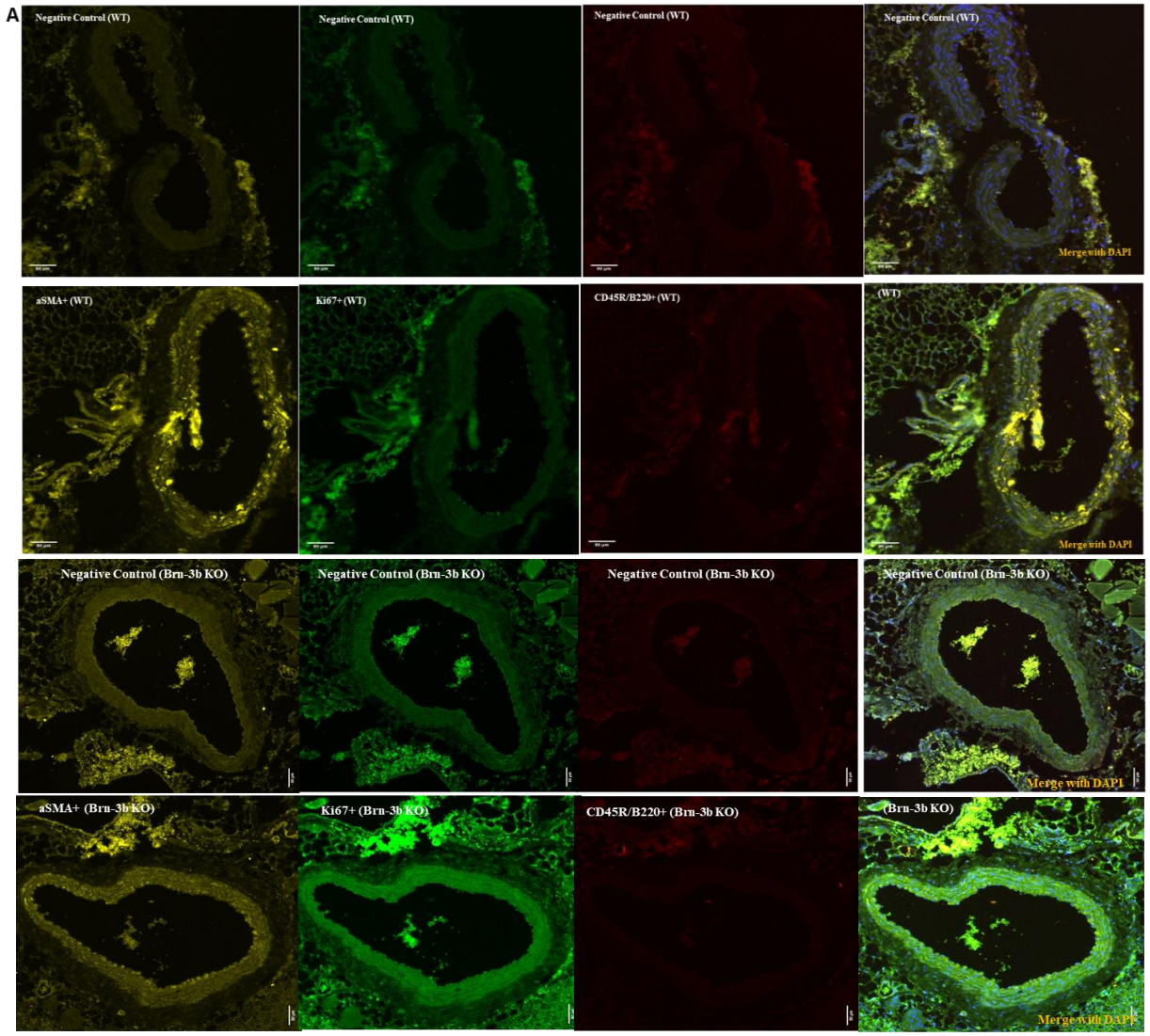
A
Negative Control (WT)
Negative Control (WT)
Negative Control (WT)
Negative Control (WT)
Merge with DAPI
aSMA+ (WT)
Ki67+ (WT)
CD45R/B220+ (WT)
(WT)
Merge with DAPI
Negative Control (Brn-3b KO)
Negative Control (Brn-3b KO)
Negative Control (Brn-3b KO)
Negative Control (Brn-3b KO)
Merge with DAPI
aSMA+ (Brn-3b KO)
Ki67+ (Brn-3b KO)
CD45R/B220+ (Brn-3b KO)
(Brn-3b KO)
Merge with DAPI

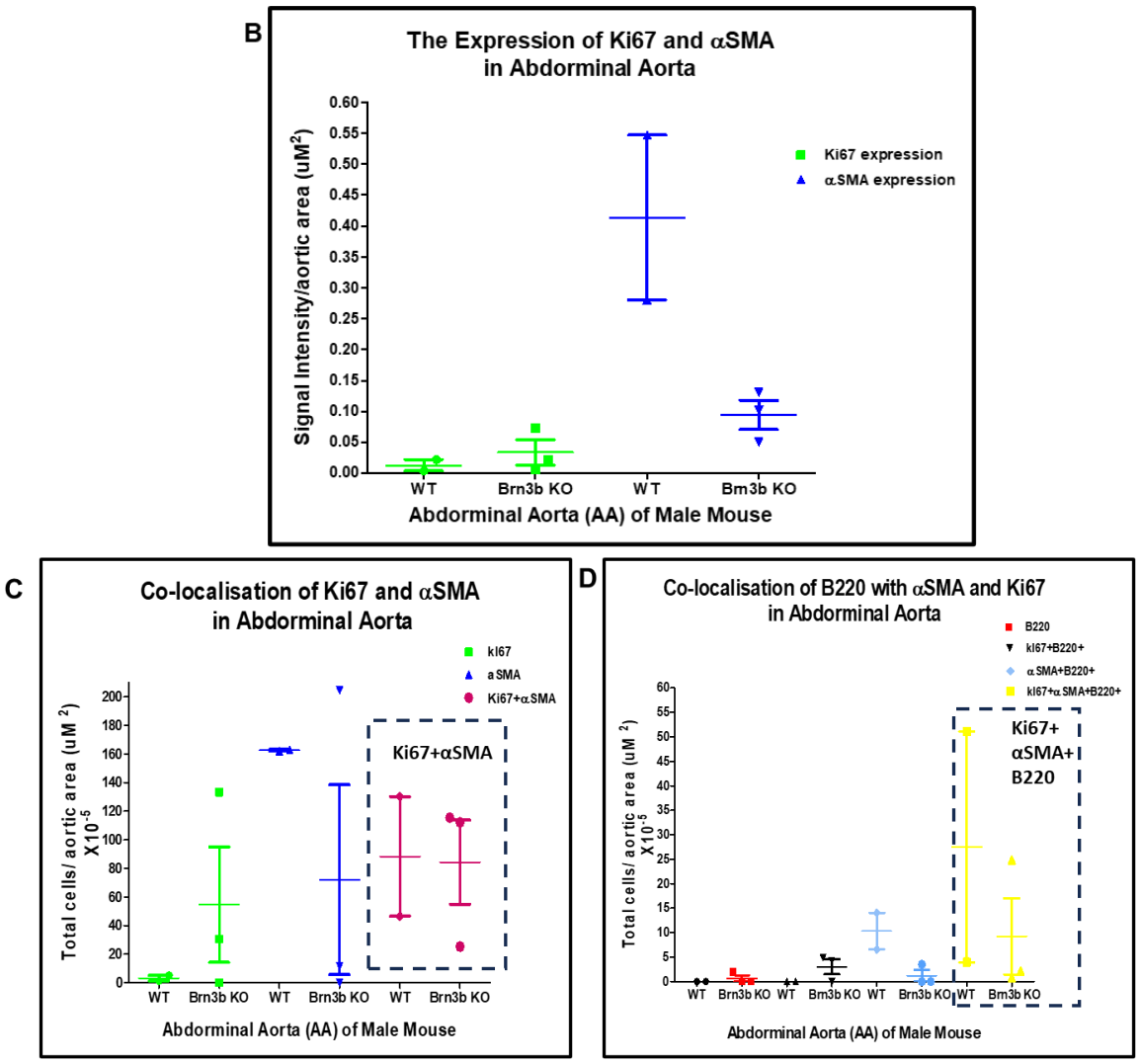

Figure 84: Representative and quantitative immunofluorescent staining (antigen kiel 67 (Ki67), alpha smooth muscle actin (αSMA) and B220) in the abdominal aorta of wild type (WT) and Brn-3b knock-out (KO) mice. C57BL/6J mice were euthanised, and aortas were isolated, processed, and embedded in paraffin wax. The aortas were sectioned longitudinally at a thickness of 5 µm. The tissue sections were stained and imaged using a Leica DMi8/Olympus microscope at 10x and 20x magnification. Depicted are (A) the representative images of co-staining (Ki67, αSMA, and B220), (B) the signal intensity of αSMA and Ki67, (C) the co-expression signal of αSMA and Ki67, and (D) the co-localization of B220 near αSMA and Ki67 in WT and Brn-3b KO mouse aorta. The analysis was performed using QuPath 0.4.3 software. Data are presented as mean ± SEM for n = 2-3 (tissue sections = 1-2 per mouse) (Sex = male) (Age = 2–4 months).

6.2.4 Investigation of the possible changes of immune cell infiltration in Brn-3b KO mouse spleen

In the final section of this chapter, I presented additional data exploring the potential infiltration of immune cells into the spleen. Spleens were dissected from Brn-3b KO and WT mice and processed for various experiments, including histology analysis, histological analysis, flow cytometry, and immunofluorescence.

6.2.4.1 The histology structure of spleen

The histological structure of the spleen was examined using qualitative analysis. As shown in Figure 85, the sub-cellular components, including WP and RP, appeared organised in both Brn-3b KO and WT mouse spleens. A clear distinction between the RP, WP and MZ was evident in the spleens of both experimental groups of mice. Moreover, the capsule of the Brn-3b KO spleen also showed no obvious difference compared to their WT control.

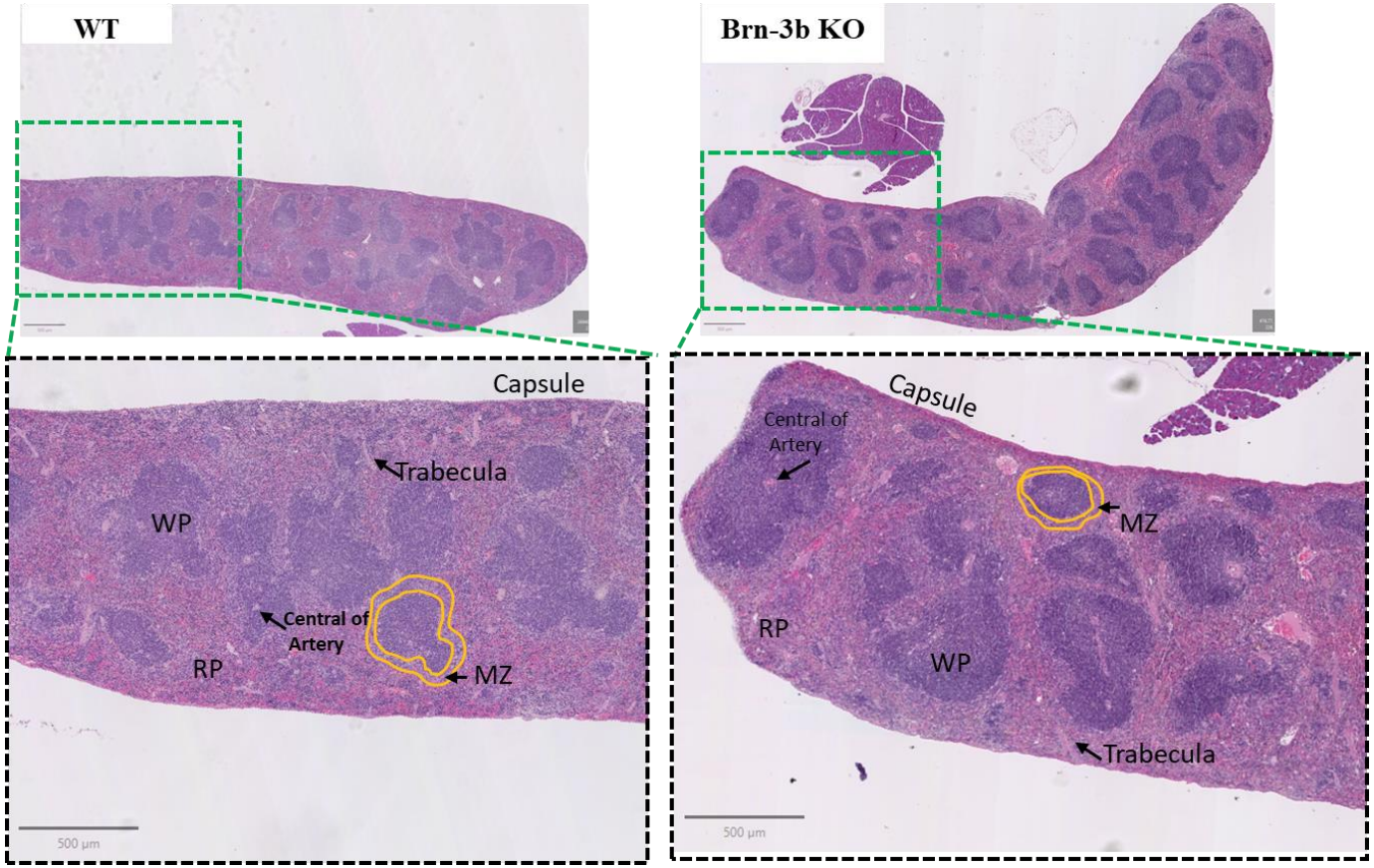

Figure 85: Histology structure of the spleen of wild type (WT) and Brn-3b knock-out (KO) mice. C57BL/6J mice were euthanised, and spleens were isolated, processed, and embedded in paraffin wax. The spleens were sectioned longitudinally at a thickness of 5 µm. The tissue sections were stained with haematoxylin and eosin (H&E) and imaged using a Nanozoomer microscope at 20× magnification. Depicted are the morphological structures of the spleen in WT and Brn-3b KO mice. Data are presented for n = 1 (Sex = male) (Age = 2–4 months).

6.2.4.2 The loss of Brn-3b did not affect the weight of the whole spleen and the total number of cells in the 0.05g spleen.

Additionally, I compared other parameters of the spleen that could serve as indicators of physiological changes, including spleen weight and total cell count. As shown in Figure 86, there were no significant differences in either spleen weight or total cell count in 0.05g of spleen between Brn-3b KO mice and their WT controls.

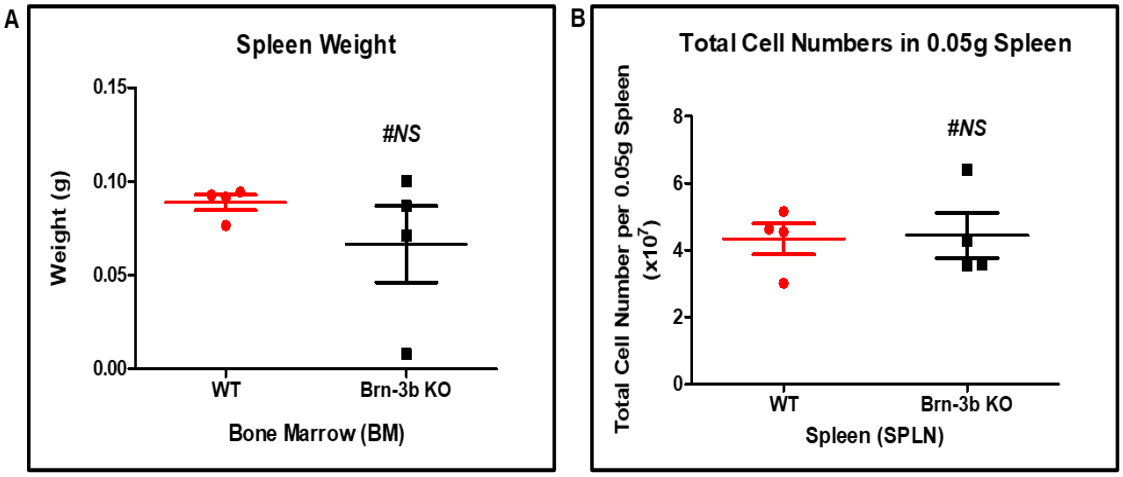

Figure 86: Weight and total cell count of the spleen of wild type (WT) and Brn-3b knock-out (KO) mice. C57BL/6J mice were euthanised, and spleens were isolated, weighed, digested, and passed through a 40 µm cell strainer. Cell numbers were determined using an automated counter. Depicted are (A) spleen weight and (B) total cell count in 0.05g of spleen from WT and Brn-3b KO mice. Data are presented as mean ± SEM for n = 4 (Sex = male/female) (Age = 2–4 months) (Ns = Not significant).

6.2.4.2.1 The flow cytometric screening of infiltration of immune cells in normal and Brn-3b KO spleen

In the previous section of this chapter, the histological structure, weight, and total cell count parameters were studied to measure the effect of Brn-3b deficiency on spleen immune status. Here, I focus on the parameter that specifically measures immune cells based on the expression of immune markers, including CD3, CD8, CD4, CD11b, B220, CD44, and Thy-1, in the spleen. These markers were gated on live and singlet cells, following the exclusion of doublets and dead cells. Auto-fluorescent cells were gated out using FMO controls and unstained controls.

The results indicated that the loss of Brn-3b did not significantly affect the expression of CD3, CD8, CD4, and CD44 in the spleen compared to WT controls, as shown in Figure 87. Additionally, the expression trends of CD11b, B220, and Thy-1 in the Brn-3b KO spleen did not show noticeable differences compared to their WT controls.

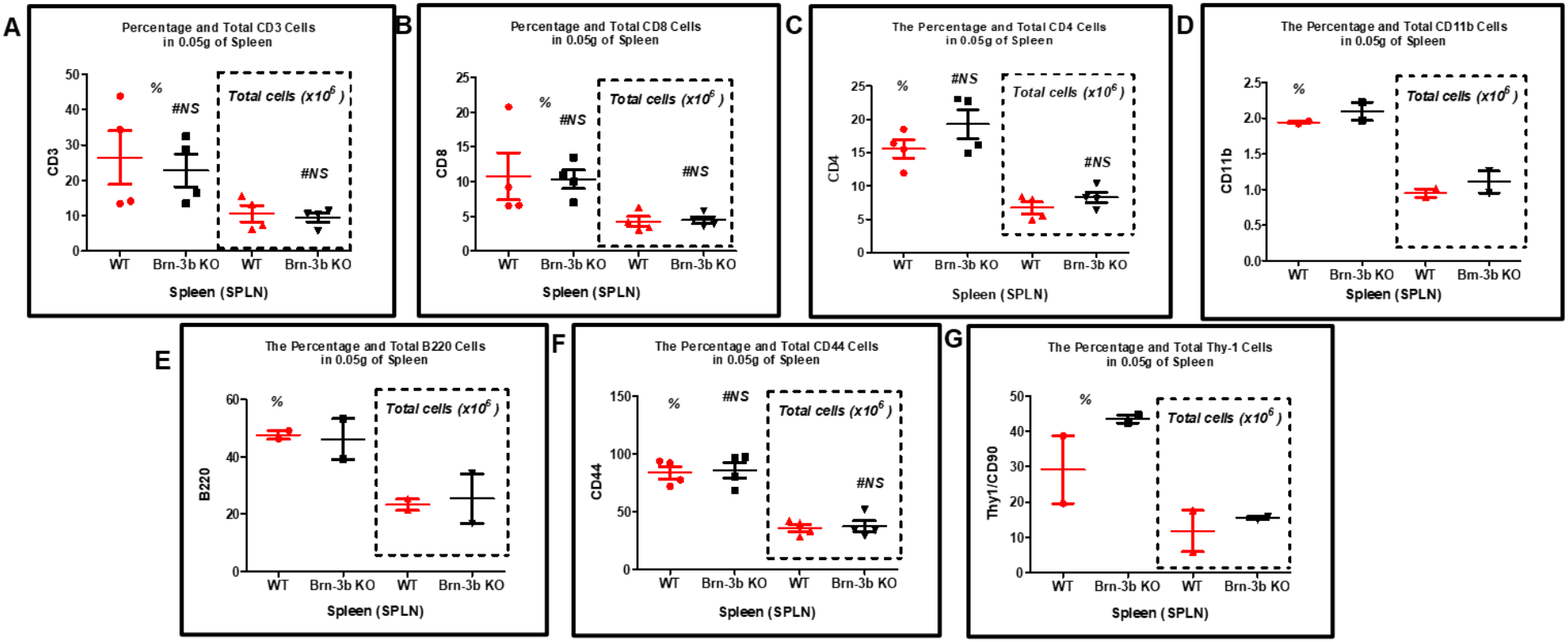

Figure 87: Single surface marker expression in the spleen of wild type (WT) and Brn-3b knock-out (KO) mice. C57BL/6J mice were euthanised, and spleens were isolated, weighed, digested, and passed through a 40 µm cell strainer. Half a million spleen cells were stained for polychromatic flow cytometry analyses. Depicted are (A) CD3, (B) CD8, (C) CD4, (D) CD11b (E) B220 (F) cKIT and (G) Thy-1 expression in WT and Brn-3b KO mouse spleen. Data are presented as mean ± SEM for n = 2-4 (Sex = male/female) (Age = 2–4 months) (*p < 0.05 and Ns = not significant) (left-hand panel = % and right-hand panel = total cells).

6.2.4.2.2 The immunofluorescence image of immune cell infiltration in normal and Brn-3b KO spleen.

Furthermore, I investigated the localisation of the B220, CD11b, CD44, and CD3 markers in the spleen. Based on the observable analysis, B220 was expressed around the BCZ, as indicated by the yellow arrow in Figure 88A(i). CD11b was localized around the MZ and was also present in both the RP and WP areas. CD3 appeared to be expressed primarily in the WP area, while CD44 was mainly expressed in the RP. The regions of RP, WP, and MZ are indicated in Figure 85.

The qualitative finding analysis showed that the loss of Brn-3b might slightly alter the expression of B220 and CD44 markers in the spleen; however, the expression of CD11b and CD3 were mirrored to those in the WT control.

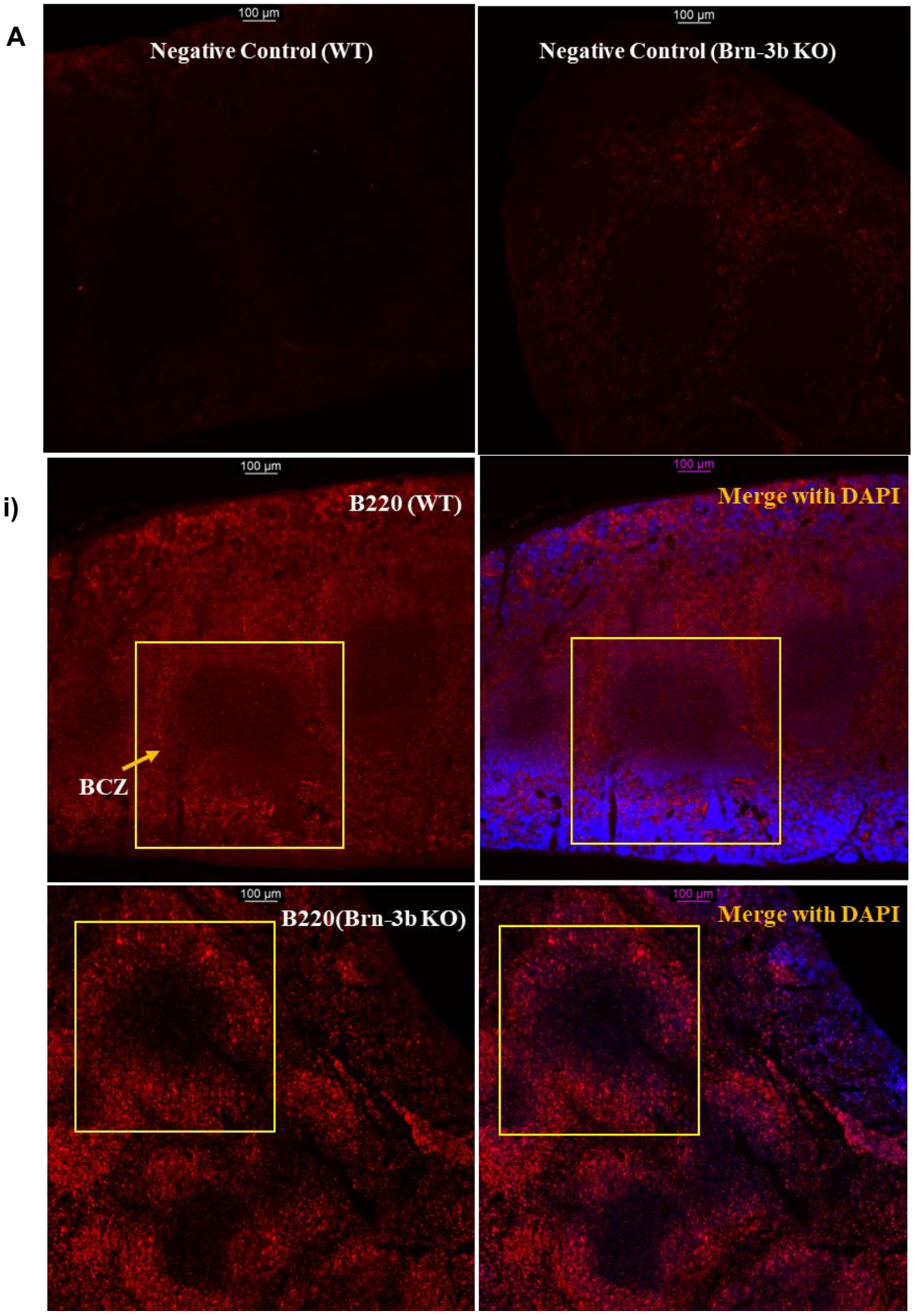
A
100 µm
Negative Control (WT)
100 µm
Negative Control (Brn-3b KO)
i)
100 µm
B220 (WT)
BCZ
100 µm
Merge with DAPI
100 µm
B220(Brn-3b KO)
100 µm
Merge with DAPI

ii)

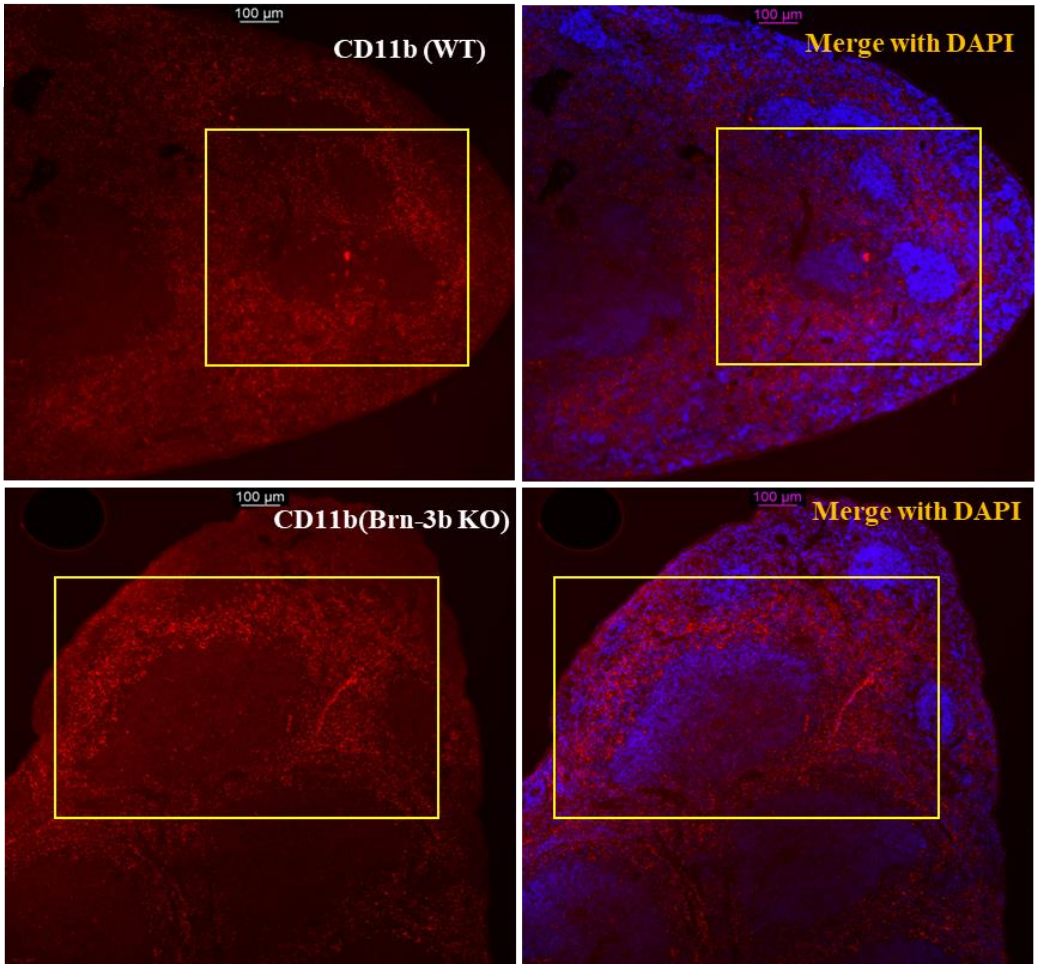
100 µm
CD11b (WT)
100 µm
Merge with DAPI
100 µm
CD11b(Brn-3b KO)
100 µm
Merge with DAPI

iii)

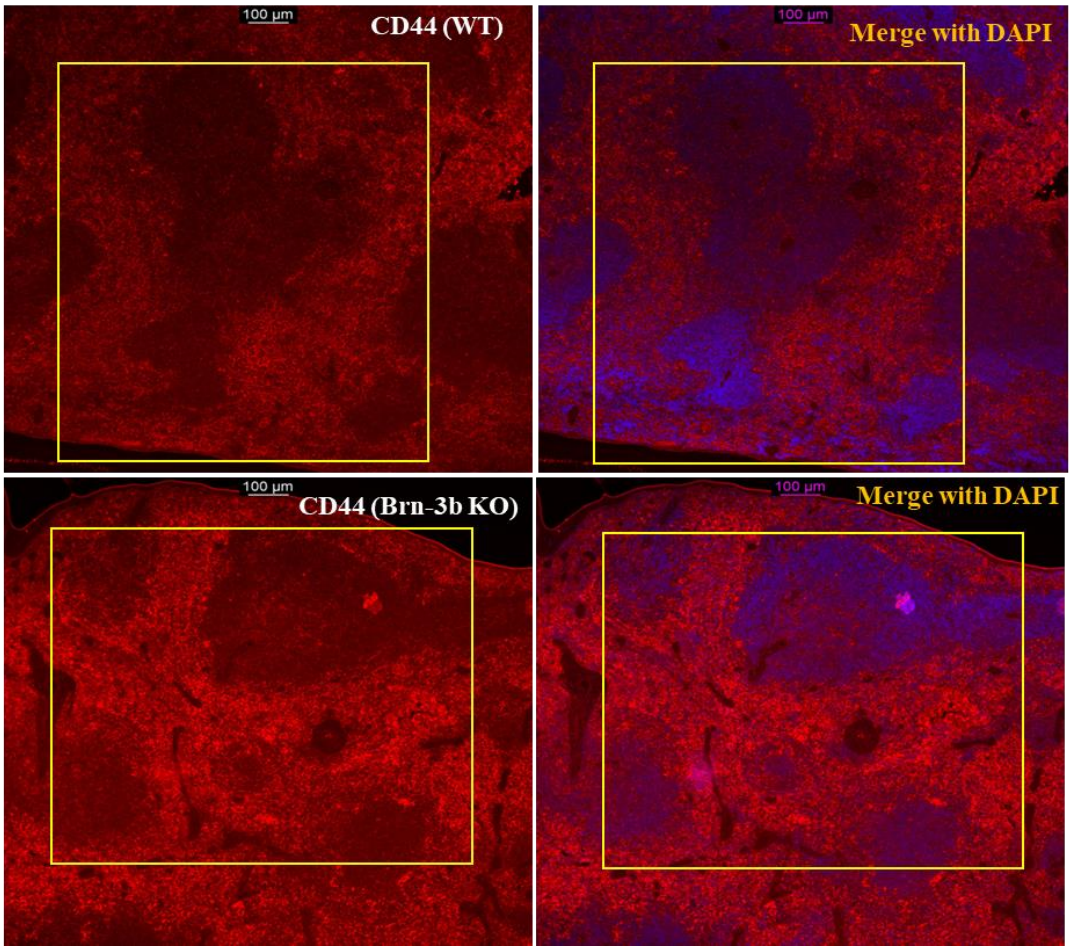
100 µm
CD44 (WT)
100 µm
Merge with DAPI
100 µm
CD44 (Brn-3b KO)
100 µm
Merge with DAPI

B

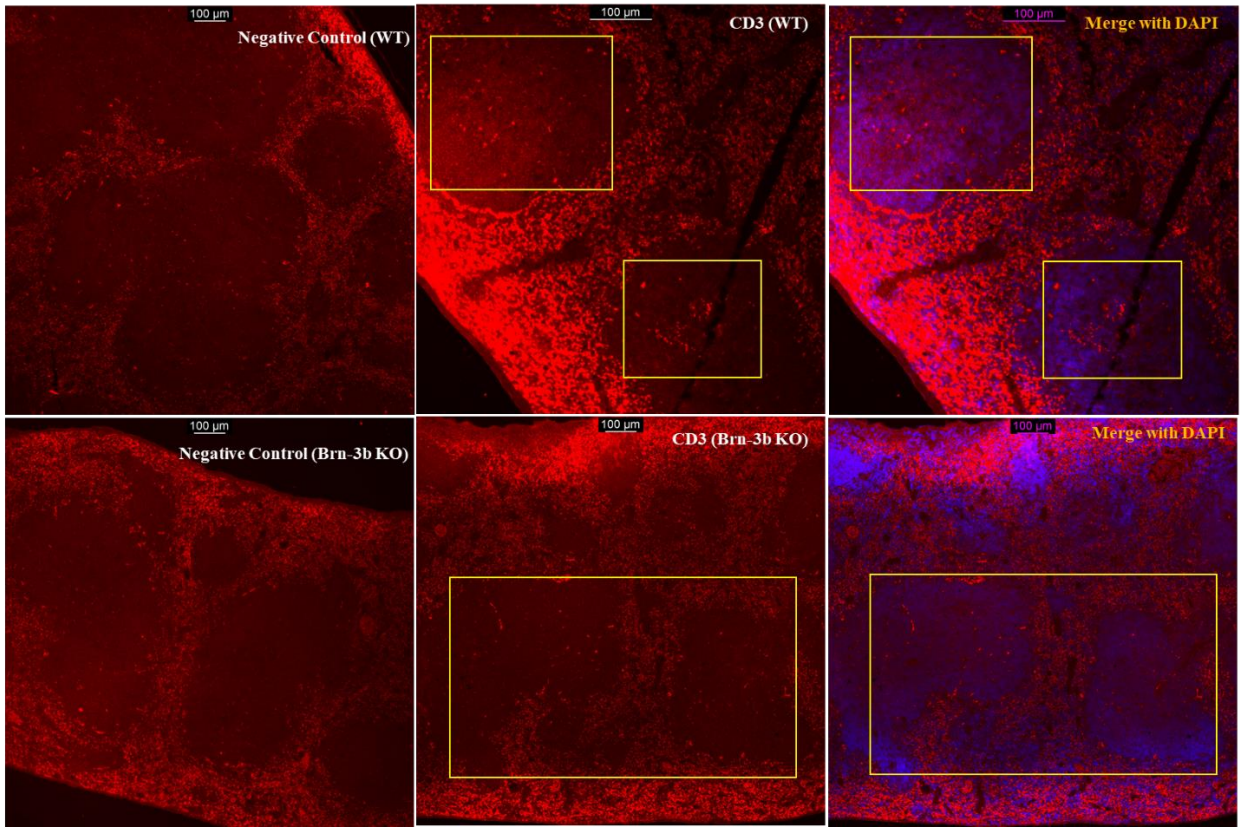

Figure 88: Representative immune markers immunofluorescent staining on the spleen of wild type (WT) and Brn-3b knock-out (KO) mice. C57BL/6J mice were euthanised, and spleens were isolated, processed, and embedded in paraffin wax. The spleens were sectioned longitudinally at a thickness of 5 µm. The tissue sections were stained and imaged using a Leica DMi8/Olympus microscope at 10x magnification. Depicted are (A) the representative images of (i) CD45R/B220, (ii) CD11b, (iii) CD44, and (B) CD3 in WT and Brn-3b KO mouse spleen. Data are presented as for n = 3 (tissue sections = 2-4 per mouse) (Sex = male/female) (Age = 2–4 months). Note: The yellow box (---) highlights the localized expression of the markers.

6.3 Discussion

This chapter investigates the potential relationship between vascular dysfunction and immune regulatory factors in the Brn-3b KO mouse aorta. Even though the previous chapters showed that Brn-3b deficiency did not significantly impact the immune cell profile (T and non-T cell lineage) in the bone marrow (Chapter 4) or blood (Chapter 5) and suggested that Brn-3b may not substantially affect the immune profile in these tissues.

However, the central hypothesis (the loss of Brn-3b may increase pro-inflammatory immune cells and may also contribute to vascular dysfunction) requires further validation. To address this, I examined the effect of Brn-3b loss on immune cell infiltration in the aortic wall and its potential correlation with changes in vascular structure. I proposed that disrupted immune cell trafficking within the aorta could contribute to vascular changes, similar to what is observed in conditions like thoracic aortic disease, where immune cell infiltration induces hyperplastic changes (Harky et al., 2021). This investigation aims to enhance my understanding of how Brn-3b deficiency may influence immune responses and vascular integrity.

6.3.1 Aortic morphological structure in Brn-3b KO mouse aorta

In this study, I examined the structural conditions in the Brn-3b KO aorta, focusing on the descending, thoracic, and abdominal aortas. The analysis was conducted using both longitudinal and transverse planes. The longitudinal plane provided information on vascular lumen and potential changes along the vessel (Bathala et al., 2013; Currie et al., 2017), while the transverse plane offered insights into the blood vessel wall, plaques, patency, and carotid bifurcation levels (Bathala et al., 2013).

The findings showed some disorganisation of the nuclear arrangement and elastic lamella structure in the Brn-3b KO abdominal aorta compared to WT (Figure 80). However, both the longitudinal and transverse sections of the descending, thoracic, and abdominal aortas showed a free lumen without apparent pathological changes (Figure 71, Figure 76 and Figure 80).

Clinically, vascular dysfunction typically manifests as abnormal morphological structures, including false lumen formation due to aortic dissection, aneurysms, fatty streaks, or bulges in the wall. These structures are often associated with immune cell trafficking to the pathological site (Li et al., 2018; Yuan et al., 2022; Tiwari et al., 2022). Since no significant morphological changes were observed in this study, it suggests that Brn-3b deficiency might not lead to major lumen structural changes but could affect the organisation of cellular components in the abdominal aorta.

However, this study was just based on H&E staining, which is commonly used in pathology to assess tissue structure and cellular architecture (Himmel et al., 2018). Further validation using vascular structure-specific markers or additional techniques, such as Masson's Trichrome, is necessary for a more comprehensive analysis.

Furthermore, the finding on aortic wall thickness (TI, TM, and TA) in the thoracic aorta of Brn-3b KO mice did not show significant alterations (Figure 76). This contrasts with a previous study by Yogendran et al. (2023), which reported increased TA thickness in the Brn-3b KO aorta. The discrepancy may be due to differences in the planes used for measurement, as our study used cross-sectional, while their study used longitudinal sections. Additionally, methodological differences could also contribute to this variation. Yogendran et al. (2023) utilised approximately 50 equidistant measurements across the aortic wall, while I calculated the TA area by dividing the perimeter (the average of the inner and outer contour lengths), a method adapted from Galaska et al. (2023).

Clinically, vascular dysfunction involves both structural and functional abnormalities (Rehan et al., 2023). Further analysis is suggested to evaluate functional changes in the Brn-3b KO aorta by assessing key functional markers essential for vascular integrity.

6.3.2 Aortic functional analysis in Brn-3b KO mouse aorta

While structural vascular changes were minimal in Brn-3b KO mice, the functional effect on the aorta remains unknown. To address this, I analysed the expression of vascular markers αSMA, SM22, and Ki67 across the descending, thoracic, and abdominal aortas.

The results showed a decreasing trend in αSMA and SM22 expression in the abdominal aorta of Brn-3b KO mice, with no major alteration in Ki67 expression (Figure 81 to Figure 84), and no significant trends observed in the descending or thoracic aortas (Figure 75, Figure 77 and Figure 78). This aligns with findings by Yogendran et al. (2023), who reported reduced αSMA expression in Brn-3b KO aortic VSMC primary cultures. Furthermore, the co-staining analysis revealed a similar reduction trend in αSMA+SM22 expression within the TI and TM of the abdominal aorta compared to WT controls (Figure 83).

It is important to note that SM22 expression in adults is restricted to smooth muscle (SM) tissues. During early developmental stages, SM22α can also be found in skeletal and cardiac muscle (Li et al., 1996; Fagginger et al., (1999), Feil et al., (2004), Rattan et al., (2015) and Zhang et al., (2021)). SM22 protein is important for maintaining the differentiated phenotype and contractile function of VSMC (Rattan et al., (2015). Pathological conditions, including atherosclerosis and neointima formation, are associated with the downregulation of SM22 expression (Zhang et al., 2021). Moreover, αSMA is a contractile phenotype protein typically found in SMCs. A lack of αSMA expression in aortic tissues indicates the extent of SMC degeneration or a phenotypic switch between contractile and synthetic SMCs (Yuan and Wu, 2018; Balint et al., 2023).

Therefore, the observed decreasing trend in both αSMA and SM22 expression suggests that Brn-3b deficiency may impact the functional integrity of the abdominal aorta by altering SMC stability and contractility. Further studies with more biological replicates are necessary to confirm these findings. Expanding the analysis to include other vascular markers such as MYH11+ CD68 and galectin-3 (LGALS3) (Sorokin et al., 2020), would provide a more comprehensive assessment of vascular integrity. Additionally, investigating isolated aortic cells from the abdominal aorta, expressing αSMA and SM22 *in vitro*, and manipulating Brn-3b protein levels *via* knockdown or overexpression, could help clarify the relationship between Brn-3b and these markers.

6.3.3 The possible link of vascular changes with immune cell infiltration in Brn-3b KO mouse aorta

This section aims to address the main hypothesis of this chapter. The overall findings of immune cell infiltration revealed a decreasing trend in CD11b cells in the Brn-3b KO abdominal aorta (Figure 82 (D)), but no significant changes in the descending or thoracic aortas compared to WT controls. Additionally, expression of CD3, B220, and CD44 was not significantly altered in the Brn-3b KO aorta (in the descending, thoracic, and abdominal regions). Co-staining experiments further showed a reduced trend of B220 expression near SM22+αSMA+ cells in the Brn-3b KO abdominal aorta compared to WT controls (Figure 83).

These findings contradict those of Yogendran et al., (2023), who reported high lymphocyte infiltration in Brn-3b KO perivascular adipose tissue (PVAT). However, in this study, I did not assess immune cell infiltration in PVAT due to the technical challenges posed by the high autofluorescence in this tissue. To further investigate this, it would be beneficial to explore the effect of Brn-3b deficiency in PVAT by incorporating additional methods in the immunofluorescence imaging steps, such as Z-depth reduction and autofluorescence quenching, for accurate quantification of immune cells in the highly auto-fluorescent PVAT region (Willow et al., 2022).

Additionally, vascular dysfunction, such as atherosclerotic plaque formation, typically results from high vascular permeability that facilitates the infiltration of LDL, as well as the rapid and extensive trafficking of macrophages and lymphocytes within the aortic wall (Zernecke et al., 2020; Botts et al., 2021; Mussbacher et al., 2022). Since the results showed a reduced trend in CD11b (single-stained) and B220 expression near SM22+αSMA+ cells (co-staining) in the Brn-3b KO abdominal aorta, which contradicts our initial expectation, this suggests the need for further investigation. It is recommended to use specific markers to identify the cells involved, such as CD86 (M1 macrophages) and CD206 (M2 macrophages) (Sun et al., 2020) and explore cytokine release by these cells at both the transcription and protein levels.

6.4 Conclusions

The objective of this chapter was to investigate the potential link between vascular dysfunction trends and immune cell infiltration in the Brn-3b KO mouse

aorta wall. This objective was pursued through a comparative analysis of morphology structure, expression of structural vascular proteins, and immune cell marker infiltration in Brn-3b KO aortas compared to WT controls. Key findings include:

- The loss of Brn-3b did not reveal extensive changes in morphology structure that could indicate immune cell trafficking compared to WT controls.
- There was a decreasing trend of SM22 and αSMA expression in the abdominal aorta of Brn-3b KO mice compared to WT controls.
- There was a decreasing trend of CD11b in Brn-3b KO mouse abdominal aorta compared to WT controls.
- There was a reduction trend in B220 expression around SM22+ αSMA cells of the Brn-3b KO abdominal aorta compared to WT controls.

7 MAIN CONCLUSION AND FUTURE DIRECTIONS

7.1 Summary of thesis findings

The data presented in this thesis highlight that Brn-3b might not be a key player in the functional immune system in bone marrow, blood (WBC) and aorta wall. Although Brn-3b expression was significantly increased in non-differentiated and differentiated THP-1 cells following vitamin D3 treatment (Figure 31 to Figure 33), this finding is based on an *in vitro* model and requires validation in a more complex *in vivo* system, which has not yet been thoroughly explored.

Investigations using the Brn-3b KO mouse model revealed that the immune cell profiles, including T and non-T cell lineages (B lymphocytes, monocytes, and granulocytes), in the bone marrow (Chapter 4) and blood (Chapter 5) were comparable to those in WT mice. In terms of soluble protein, IL-1β levels were significantly reduced in Brn-3b KO blood compared to WT (Figure 68), not in bone marrow. The other markers, TNFα and IL-6 expression were not significantly altered in either the bone marrow or blood of Brn-3b KO mice. Additional analysis of the spleen revealed no noticeable changes in immune marker expression (CD3, CD4, CD8, B220, CD44, Thy-1, and CD11b) compared to WT controls (Figure 87). These findings suggest that Brn-3b may not regulate pro-inflammatory activity in the bone marrow, blood, or spleen.

This study then explored the potential link between immune responses and vascular changes in the Brn-3b KO mouse aorta, addressing the main hypothesis outlined in Chapter 1. The results showed that the loss of Brn-3b reduced the expression trends of vascular markers, SM22 and αSMA (both single and co-staining), in the TI and TM of the abdominal aorta (Figure 83). Regarding immune markers, CD11b expression showed a decreasing trend in the abdominal aorta, while CD3, B220, and CD44 expression remained unchanged in the aortic wall (descending, thoracic, and abdominal regions) compared to WT controls. A

reduced expression trend for B220 was observed near SM22+αSMA in the Brn-3b KO abdominal aorta (Figure 83).

These findings suggest that the loss of Brn-3b does not increase immune cell infiltration (based on the markers investigated) in the aortic wall. Instead, the observed trends in vascular changes in Brn-3b KO mice may be attributed to alterations in structural protein expression, likely occurring independently of immune regulatory factors.

7.2 Limitations and future directions

The experiments conducted in this thesis were performed on cell lines and mice, making the findings primarily pre-clinical. To efficiently translate these findings into clinical outcomes, further studies in humans are necessary.

For the *in vitro* study using THP-1 cells, future research could focus on measuring cytokine production in both undifferentiated and differentiated THP-1 cells with Brn-3b knockdown or overexpression. These studies would be crucial for understanding the downstream effects of Brn-3b in immune regulation and validating its role in inflammation.

Furthermore, in this study, I used the global Brn-3b KO mouse model, the global Brn-3b KO model, which represents a complete loss of Brn-3b across the entire organism, rather than a cell-specific knockout. Further studies using a cell-specific Brn-3b knockout model, such as the cre-lox system, would help to clarify the effect of Brn-3b deficiency on the immune cell subsets involved.

Additionally, due to limited resources, the Brn-3b KO mouse cohort included both male and female mice in the flow cytometry experiments, specifically in the deep immunophenotyping of immune cell profiles (2 males and 2 females). However, the data points for total cells and immune cell profiles seem similar/not much different between genders. Future experiments should be conducted with a focus on gender-specific analysis to validate these findings.

In the immunofluorescence experiments, slight fluorescent signals were present in the negative control of the aorta. This limitation was mitigated by setting the ROI around the aortic wall, excluding the lumen and fat, and subtracting the autofluorescence signal in the wall of the negative control tissue to obtain the real threshold of positive expression signals. For H&E staining, variability in stain

intensity was observed between tissue sections, despite using the same auto-stainer machine for the experiment. This variability can affect the accuracy of qualitative assessments.

Furthermore, in some experiments, particularly in Chapter 6, the limited number of samples prevented robust statistical analysis, and findings were elaborated based on data trends. Future experiments should expand the sample size to allow for comprehensive statistical analysis.

Future research will focus on elucidating other immune cell populations that may be affected by the loss of Brn-3b. The Brn-3b KO mouse model, particularly in the context of specific immune-vascular dysfunctional diseases such as aneurysms or atherosclerosis, could serve as an ideal model to examine the potential role of Brn-3b in preventing immune-related diseases. Using this model, researchers can compare the expression of various structural vascular proteins between Brn-3b KO and WT controls. Additionally, a deep investigation into the molecular events targeted by Brn-3b in controlling the expression of these proteins in aneurysms or atherosclerosis would be beneficial. This research could aid in the development of drugs targeting Brn-3b to prevent these diseases.

7.3 Concluding remarks

This thesis investigated the potential link between the loss of Brn-3b and immune regulation, and how this might contribute to vascular changes. The data suggest that the loss of Brn-3b may affect normal vascular function by altering the expression trends of key structural vascular proteins in Brn-3b KO mice. However, there was no considerable increase in immune cell infiltration near the vascular wall in these mice. These findings imply that the observed trends in vascular changes may not be directly associated with immune cell infiltration in the Brn-3b KO mouse aorta.

8 REFERENCES

Ackema, K. B., & Charite, J. (2008). Mesenchymal stem cells from different organs are characterized by distinct topographic Hox codes. Stem cells and development, 17(5), 979-992.

Adams, M. L., Grandpre, J., Katz, D. L., & Shenson, D. (2020). Cognitive impairment and cardiovascular disease: a comparison of risk factors, disability, quality of life, and access to health care. Public Health Reports, 135(1), 132-140.

Adcock, I. M., & Caramori, G. (2002). Transcription factors. Asthma and COPD, 315-321.

Adhikari, N., Shekar, K. C., Staggs, R., Win, Z., Steucke, K., Lin, Y. W., ... & Hall, J. L. (2015). Guidelines for the isolation and characterization of murine vascular smooth muscle cells. A report from the International Society of Cardiovascular Translational Research. Journal of cardiovascular translational research, 8(3), 158-163.

Adnan Haider., Adeeb Shehzad., Fazli Wahid., Anuj Kumar., Kummara Madhusudana Rao and Sung Soo Han (2016). The Multi Regulatory Role of Signal Transducer and Activator of Transcription Factor Brn-3a. Journal of Neurology and Neuroscience, 7 (2), 1-j7.

Afewerki, T., Ahmed, S., & Warren, D. (2019). Emerging regulators of vascular smooth muscle cell migration. Journal of muscle research and cell motility, 40, 185-196.

Ai, W., Li, H., Song, N., Li, L., & Chen, H. (2013). Optimal method to stimulate cytokine production and its use in immunotoxicity assessment. International journal of environmental research and public health, 10(9), 3834-3842.

Alberts, B., Johnson, A., Lewis, J., Raff, M., Roberts, K., & Walter, P. (2002). Helper T cells and lymphocyte activation. In Molecular Biology of the Cell. 4th edition. Garland Science.

Alberts, B., Johnson, A., Lewis, J., Raff, M., Roberts, K., & Walter, P. (2002). From RNA to protein. In Molecular Biology of the Cell. 4th edition. Garland Science.

Alberts, B., Johnson, A., Lewis, J., Raff, M., Roberts, K., & Walter, P. (2002). DNA-binding motifs in gene regulatory proteins. In Molecular Biology of the Cell. 4th edition. Garland Science.

Albiero, M., Ciciliot, S., Tedesco, S., Menegazzo, L., D'Anna, M., Scattolini, V., ... & Fadini, G. P. (2019). Diabetes-associated myelopoiesis drives stem cell mobilopathy through an OSM-p66Shc signaling pathway. Diabetes, 68(6), 1303-1314.

Aldo, P. B., Craveiro, V., Guller, S., & Mor, G. (2013). Effect of culture conditions on the phenotype of THP - 1 monocyte cell line (Vol. 70, No. 1, pp. 80-86).

Alexander, R. W. (1995). Oxidative stress and the mediation of arterial inflammatory response: a new perspective. Hypertension, 25, 155-161.

Alfaddagh, A., Martin, S. S., Leucker, T. M., Michos, E. D., Blaha, M. J., Lowenstein, C. J., ... & Toth, P. P. (2020). Inflammation and cardiovascular disease: From mechanisms to therapeutics. American journal of preventive cardiology, 4, 100130.

Altevogt, P., Sammar, M., Hüser, L., & Kristiansen, G. (2021). Novel insights into the function of CD24: A driving force in cancer. International journal of cancer, 148(3), 546-559.

Alves - Bezerra, M., & Cohen, D. E. (2011). Triglyceride metabolism in the liver. Comprehensive Physiology, 8(1), 1-22.

Annual Review of Pathology: Mechanisms of Disease 2006 1:1, 297-329.

Archacki, S., & Wang, Q. (2004). Expression profiling of cardiovascular disease. Human genomics, 1(5), 355.

Aristizábal, B., & González, Á. (2013). Innate immune system. In Autoimmunity: From Bench to Bedside [Internet]. El Rosario University Press.

Armentano, R. L., Graf, S., Barra, J. G., Velikovsky, G., Baglivo, H., Sánchez, R., ... & Levenson, J. (1998). Carotid wall viscosity increase is related to intima-media thickening in hypertensive patients. Hypertension, 31(1), 534-539.

Aronoff, L., Epelman, S., & Clemente-Casares, X. (2018). Isolation and identification of extravascular immune cells of the heart. JoVE (Journal of Visualized Experiments), (138), e58114.

Ashley, E. A., Ashley, E., & Niebauer, J. (2004). Cardiology explained. Chapter 12 Aneurysm and dissection of the aorta. National Library of Medicine. 189

Aslankoohi, E., Rezaei, M. N., Vervoort, Y., Courtin, C. M., & Verstrepen, K. J. (2015). Glycerol production by fermenting yeast cells is essential for optimal bread dough fermentation. PloS one, 10(3).

Aziz, M., Holodick, N. E., Rothstein, T. L., & Wang, P. (2015). The role of B-1 cells in inflammation. Immunologic research, 63(1), 153-166.

Azuaje, F. J., Zhang, L., Devaux, Y., & Wagner, D. R. (2011). Drug-target network in myocardial infarction reveals multiple side effects of unrelated drugs. Scientific reports, 1, 52.

Baaten, B. J., Li, C. R., Deiro, M. F., Lin, M. M., Linton, P. J., & Bradley, L. M. (2010). CD44 regulates survival and memory development in Th1 cells. Immunity, 32(1), 104-115.

Bacakova, L., Travnickova, M., Filova, E., Matějka, R., Stepanovska, J., Musilkova, J., ... & Molitor, M. (2018). The role of vascular smooth muscle cells in the physiology and pathophysiology of blood vessels. Muscle Cell and Tissue-Current Status of Research Field, 1, 13.

Bacher, M., Metz, C. N., Calandra, T., Mayer, K., Chesney, J., Lohoff, M., ... & Bucala, R. (1996). An essential regulatory role for macrophage migration inhibitory factor in T-cell activation. Proceedings of the National Academy of Sciences, 93(15), 7849-7854.

Badran, A., Nasser, S. A., Mesmar, J., El-Yazbi, A. F., Bitto, A., Fardoun, M. M., ... & Eid, A. H. (2020). Reactive oxygen species: modulators of phenotypic switch of vascular smooth muscle cells. International Journal of Molecular Sciences, 21(22), 8764.

Balint, B., Bernstorff, I. G. L., Schwab, T., & Schäfers, H. J. (2023). Age-dependent phenotypic modulation of smooth muscle cells in the normal ascending aorta. Frontiers in Cardiovascular Medicine, 10, 1114355.

Banna, G. L., Friedlaender, A., Tagliamento, M., Mollica, V., Cortellini, A., Rebuzzi, S. E., ... & Addeo, A. (2022). Biological Rationale for Peripheral Blood Cell–Derived Inflammatory Indices and Related Prognostic Scores in Patients with Advanced Non-Small-Cell Lung Cancer. Current Oncology Reports, 24(12), 1851-1862.

Bao, M. H., Li, J. M., Zhou, Q. L., Li, G. Y., Zeng, J., Zhao, J., & Zhang, Y. W. (2016). Effects of miR590 on oxLDLinduced endothelial cell apoptosis: roles of p53 and NFκB. Molecular medicine reports, 13(1), 867-873.

Bathala, L., Mehndiratta, M. M., & Sharma, V. K. (2013). Cerebrovascular ultrasonography: Technique and common pitfalls. Annals of Indian Academy of Neurology, 16(1), 121-127.

Batra, R., Suh, M. K., Carson, J. S., Dale, M. A., Meisinger, T. M., Fitzgerald, M., ... & Baxter, B. T. (2018). IL-1β (interleukin-1β) and TNF-α (tumor necrosis factor-α) impact abdominal aortic aneurysm formation by differential effects on macrophage polarization. Arteriosclerosis, Thrombosis, and Vascular Biology, 38(2), 457-463.

Batty, M., Bennett, M. R., & Yu, E. (2022). The role of oxidative stress in atherosclerosis. Cells, 11(23), 3843.

Baxter, E. W., Graham, A. E., Re, N. A., Carr, I. M., Robinson, J. I., Mackie, S. L., & Morgan, A. W. (2020). Standardized protocols for differentiation of THP-1 cells to macrophages with distinct M (IFNγ+ LPS), M (IL-4) and M (IL-10) phenotypes. Journal of Immunological Methods, 478, 112721.

Bayly, G. R. (2014). Lipids and disorders of lipoprotein metabolism. In Clinical Biochemistry: Metabolic and Clinical Aspects (pp. 702-736). Churchill Livingstone.

Bellows, C. F., Zhang, Y., Simmons, P. J., Khalsa, A. S., & Kolonin, M. G. (2011). Influence of BMI on level of circulating progenitor cells. Obesity, 19(8), 1722-1726.

Ben-Sasson, S. Z., Wang, K., Cohen, J., & Paul, W. E. (2013, January). IL-1β strikingly enhances antigen-driven CD4 and CD8 T-cell responses. In Cold Spring Harbor symposia on quantitative biology (Vol. 78, pp. 117-124). Cold Spring Harbor Laboratory Press.

Berbudi, A., Rahmadika, N., Tjahjadi, A. I., & Ruslami, R. (2020). Type 2 diabetes and its impact on the immune system. Current diabetes reviews, 16(5), 442.

Berg, J. M., Tymoczko, J. L., & Stryer, L. (2002). Section 22.4, fatty acids are synthesized and degraded by different pathways. Biochemistry.

Berliner, J. A., Navab, M., Fogelman, A. M., Frank, J. S., Demer, L. L., Edwards, P. A., ... & Lusis, A. J. (1995). Atherosclerosis: basic mechanisms: oxidation, inflammation, and genetics. Circulation, 91(9), 2488-2496.

Bhandoola, A., von Boehmer, H., Petrie, H. T., & Zúñiga-Pflücker, J. C. (2007). Commitment and developmental potential of extrathymic and intrathymic T cell precursors: plenty to choose from. Immunity, 26(6), 678-689.

Bhat, P., Leggatt, G., Waterhouse, N., & Frazer, I. H. (2017). Interferon-γ derived from cytotoxic lymphocytes directly enhances their motility and cytotoxicity. Cell death & disease, 8(6), e2836-e2836.

Bhatnagar, P., Wickramasinghe, K., Wilkins, E., & Townsend, N. (2016). Trends in the epidemiology of cardiovascular disease in the UK. Heart, 102(24), 1945-1952.

Biglu, M. H., Ghavami, M., & Biglu, S. (2016). Cardiovascular diseases in the mirror of science. Journal of cardiovascular and thoracic research, 8(4), 158.

Bitsi, S., Ali, H., Maskell, L., Ounzain, S., Mohamed-Ali, V., & Budhram-Mahadeo, V. S. (2016). Profound hyperglycemia in knockout mutant mice identifies novel function for POU4F2/Brn-3b in regulating metabolic processes. American Journal of Physiology-Endocrinology and Metabolism, 310(5), E303-E312.

Blue, M. L., Daley, J. F., Levine, H., & Schlossman, S. F. (1985). Coexpression of T4 and T8 on peripheral blood T cells demonstrated by two-color fluorescence flow cytometry. Journal of immunology (Baltimore, Md.: 1950), 134(4), 2281-2286.

Blum, M., Saemann, A., & Wolf, G. (2011). The eye, the kidney and microcirculation.

Bobryshev, Y. V., Ivanova, E. A., Chistiakov, D. A., Nikiforov, N. G., & Orekhov, A. N. (2016). Macrophages and their role in atherosclerosis: pathophysiology and transcriptome analysis. BioMed research international, 2016.

Boes, K. M., & Durham, A. C. (2017). Bone marrow, blood cells, and the lymphoid/lymphatic system. Pathologic basis of veterinary disease, 724.

Bonilla, F. A., & Oettgen, H. C. (2010). Adaptive immunity. Journal of Allergy and Clinical Immunology, 125(2), S33-S40.

Bonomo, A., Monteiro, A. C., Gonçalves-Silva, T., Cordeiro-Spinetti, E., Galvani, R. G., & Balduino, A. (2016). AT cell view of the bone marrow. Frontiers in immunology, 7, 151967.

Bosetti, F., Galis, Z. S., Bynoe, M. S., Charette, M., Cipolla, M. J., del Zoppo, G. J., ... & Lutty, G. A. (2016). "Small Blood Vessels: Big Health Problems?": Scientific Recommendations of the National Institutes of Health Workshop. Journal of the American Heart Association, 5(11), e004389.

Bosshart, H., & Heinzelmann, M. (2016). THP-1 cells as a model for human monocytes. Annals of translational medicine, 4(21).

Botts, S. R., Fish, J. E., & Howe, K. L. (2021). Dysfunctional vascular endothelium as a driver of atherosclerosis: emerging insights into pathogenesis and treatment. Frontiers in pharmacology, 12, 787541.

Brignall, R., Cauchy, P., Bevington, S. L., Gorman, B., Pisco, A. O., Bagnall, J., ... & Paszek, P. (2017). Integration of kinase and calcium signaling at the level of chromatin underlies inducible gene activation in T cells. The Journal of Immunology, 199(8), 2652-2667.

Brignall, R., Cauchy, P., Bevington, S. L., Gorman, B., Pisco, A. O., Bagnall, J., ... & Paszek, P. (2017). Integration of kinase and calcium signaling at the level of chromatin underlies inducible gene activation in T cells. The Journal of Immunology, 199(8), 2652-2667.

Brown, I. A., Diederich, L., Good, M. E., DeLalio, L. J., Murphy, S. A., Cortese-Krott, M. M., ... & Isakson, B. E. (2018). Vascular smooth muscle remodeling in conductive and resistance arteries in hypertension. Arteriosclerosis, thrombosis, and vascular biology, 38(9), 1969-1985.

Brown, S. D. (2021). Advances in mouse genetics for the study of human disease. Human Molecular Genetics, 30(R2), R274-R284.

Brugman, M. H., & Staal, F. J. T. (2016). DNA Barcoding of Human Stem and Progenitor Cells Reveals Differences in Clonal Dynamics of B and T lymphoid Progeny. J Clin Cell Immunol, 7(408), 2.

Buchan, L., St Aubin, C. R., Fisher, A. L., Hellings, A., Castro, M., Al-Nakkash, L., ... & Plochocki, J. H. (2018). High-fat, high-sugar diet induces splenomegaly that is ameliorated with exercise and genistein treatment. BMC Research Notes, 11(1), 1-6.

Budhram-Mahadeo, V. S., Bowen, S., Lee, S., Perez-Sanchez, C., Ensor, E., Morris, P. J., & Latchman, D. S. (2006). Brn-3b enhances the pro-apoptotic effects of p53 but not its induction of cell cycle arrest by cooperating in trans-activation of bax expression. Nucleic acids research, 34(22), 6640-6652.

Budhram-Mahadeo, V. S., Irshad, S., Bowen, S., Lee, S. A., Samady, L., Tonini, G. P., & Latchman, D. S. (2008). Proliferation-associated Brn-3b transcription factor can activate cyclin D1 expression in neuroblastoma and breast cancer cells. Oncogene, 27(1), 145-154.

Budhram-Mahadeo, V. S., Solomons, M. R., & Mahadeo-Heads, E. A. (2021). Linking metabolic dysfunction with cardiovascular diseases: Brn-3b/POU4F2 transcription factor in cardiometabolic tissues in health and disease. Cell Death & Disease, 12(3), 1-13.

Budhram-Mahadeo, V., Fujita, R., Bitsi, S., Sicard, P., & Heads, R. (2014). Co-expression of POU4F2/Brn-3b with p53 may be important for controlling expression of pro-apoptotic genes in cardiomyocytes following ischaemic/hypoxic insults. Cell death & disease, 5(10), e1503-e1503.

Budhram-Mahadeo, V., Moore, A., Morris, P. J., Ward, T., Weber, B., Sassone-Corsi, P., & Latchman, D. S. (2001). The closely related POU family transcription factors Brn-3a and Brn-3b are expressed in distinct cell types in the testis. The international journal of biochemistry & cell biology, 33(10), 1027-1039.

Budhram-Mahadeo, V., Ndisang, D., Ward, T., Weber, B. L., & Latchman, D. S. (1999). The Brn-3b POU family transcription factor represses expression of the BRCA-1 anti-oncogene in breast cancer cells. Oncogene, 18(48), 6684-6691.

Budhram-Mahadeo, V., Parker, M., & Latchman, D. S. (1998). POU transcription factors Brn-3a and Brn-3b interact with the estrogen receptor and differentially

regulate transcriptional activity *via* an estrogen response element. Molecular and Cellular Biology, 18(2), 1029-1041.

Burkholder, B., Huang, R. Y., Burgess, R., Luo, S., Jones, V. S., Zhang, W., ... & Huang, R. P. (2014). Tumor-induced perturbations of cytokines and immune cell networks. Biochimica et Biophysica Acta (BBA)-Reviews on Cancer, 1845(2), 182-201.

Bürkle, A., Niedermeier, M., Schmitt-Gräff, A., Wierda, W. G., Keating, M. J., & Burger, J. A. (2007). Overexpression of the CXCR5 chemokine receptor, and its ligand, CXCL13 in B-cell chronic lymphocytic leukemia. Blood, The Journal of the American Society of Hematology, 110(9), 3316-3325.

Cairns, A. P., Crockard, A. D., McConnell, J. R., Courtney, P. A., & Bell, A. L. (2001). Reduced expression of CD44 on monocytes and neutrophils in systemic lupus erythematosus: relations with apoptotic neutrophils and disease activity. Annals of the rheumatic diseases, 60(10), 950-955.

Cannata-Andía, J. B., Carrillo-López, N., Messina, O. D., Hamdy, N. A., Panizo, S., Ferrari, S. L., & International Osteoporosis Foundation (IOF) Working Group on Bone and Cardiovascular Diseases. (2021). Pathophysiology of vascular calcification and bone loss: Linked disorders of ageing?. Nutrients, 13(11), 3835.

Cano, R. L. E., & Lopera, H. D. E. (2013). Introduction to T and B lymphocytes. In Autoimmunity: from bench to bedside [Internet]. El Rosario University Press.

Cantorna, M. T., & Waddell, A. (2014). The vitamin D receptor turns off chronically activated T cells. Annals of the New York Academy of Sciences, 1317(1), 70-75.

Cao, G., Xuan, X., Hu, J., Zhang, R., Jin, H., & Dong, H. (2022). How vascular smooth muscle cell phenotype switching contributes to vascular disease. Cell Communication and Signaling, 20(1), 180.

Carlberg, C. (2022). Vitamin D and its target genes. Nutrients, 14(7), 1354.

Carlson, N. G., Wieggel, W. A., Chen, J., Bacchi, A., Rogers, S. W., & Gahring, L. C. (1999). Inflammatory cytokines IL-1α, IL-1β, IL-6, and TNF-α impart neuroprotection to an excitotoxin through distinct pathways. The Journal of Immunology, 163(7), 3963-3968.

Carter, C. M. (2018). Alterations in blood components. Comprehensive toxicology, 249.

Casella, S., Bielli, A., Mauriello, A., & Orlandi, A. (2015). Molecular pathways regulating macrovascular pathology and vascular smooth muscle cells phenotype in type 2 diabetes. International journal of molecular sciences, 16(10), 24353-24368.

Cassese, G., Parretta, E., Pisapia, L., Santoni, A., Guardiola, J., & Di Rosa, F. (2007). Bone marrow CD8 cells down-modulate membrane IL-7Rα expression and exhibit increased STAT-5 and p38 MAPK phosphorylation in the organ environment. Blood, The Journal of the American Society of Hematology, 110(6), 1960-1969.

cDNA Synthesis for RT-PCR Protocol https://ccr.cancer.gov/sites/default/files/cdna_synthesis_for_rt-pcr.pdf

Cecchettini, A., Rocchiccioli, S., Boccardi, C., & Citti, L. (2011). Vascular smooth-muscle-cell activation: proteomics point of view. International review of cell and molecular biology, 288, 43-99.

Čejková, S., Králová-Lesná, I., & Poledne, R. (2016). Monocyte adhesion to the endothelium is an initial stage of atherosclerosis development. Cor et Vasa, 58(4), e419-e425.

Celik, M. Ö., Labuz, D., Keye, J., Glauben, R., & Machelska, H. (2020). IL-4 induces M2 macrophages to produce sustained analgesia *via* opioids. JCI insight, 5(4).

Celik, M. Ö., Labuz, D., Keye, J., Glauben, R., & Machelska, H. (2020). IL-4 induces M2 macrophages to produce sustained analgesia *via* opioids. JCI insight, 5(4).

Chaffey, N. (2003). Alberts, B., Johnson, A., Lewis, J., Raff, M., Roberts, K. and Walter, P. Molecular biology of the cell. 4th edn.

Chang, P., Zhang, B., Shao, L., Song, W., Shi, W., Wang, L., ... & Wang, J. (2018). Mesenchymal stem cells over-expressing cxcl12 enhance the radioresistance of the small intestine. Cell death & disease, 9(2), 154.

Chanput, W., Mes, J. J., & Wichers, H. J. (2014). THP-1 cell line: an *in vitro* cell model for immune modulation approach. International immunopharmacology, 23(1), 37-45.

Chatila, T. A. L. A. L., Silverman, L., Miller, R., & Geha, R. (1989). Mechanisms of T cell activation by the calcium ionophore ionomycin. The Journal of Immunology, 143(4), 1283-1289.

Chatterjee, S. Chapter two-oxidative stress, inflammation, and disease. Oxid Stress Biomater. 2016: 35–58.

Chaudhary, N., Nguyen, T. N. Q., Cullen, D., Meade, A., & Wynne, C. (2021). Discrimination of immune cell activation using Ramanmicro-spectroscopy in anin-vitro & ex-vivo model.

Chaussabel, D., Pascual, V., & Banchereau, J. (2010). Assessing the human immune system through blood transcriptomics. BMC biology, 8, 1-14.

Chekol Abebe, E., Asmamaw Dejenie, T., Mengie Ayele, T., Dagnew Baye, N., Agegnehu Teshome, A., & Tilahun Muche, Z. (2021). The role of regulatory B cells in health and diseases: a systemic review. Journal of inflammation research, 75-84.

Chen, C. Y., Yi, L., Jin, X., Zhang, T., Fu, Y. J., Zhu, J. D., ... & Yu, B. (2011). Inhibitory Effect of Delphinidin on Monocyte–Endothelial Cell Adhesion Induced by Oxidized Low-Density Lipoprotein *via* ROS/p38MAPK/NF-κB Pathway. Cell biochemistry and biophysics, 61(2), 337-348.

Chen, L., Deng, H., Cui, H., Fang, J., Zuo, Z., Deng, J., ... & Zhao, L. (2018). Inflammatory responses and inflammation-associated diseases in organs. Oncotarget, 9(6), 7204.

Chen, L., Tuo, B., & Dong, H. (2016). Regulation of intestinal glucose absorption by ion channels and transporters. Nutrients, 8(1), 43.

Chen, P., Wu, B., Ji, L., Zhan, Y., Li, F., Cheng, L., ... & Cheng, Y. (2021). Cytokine Consistency Between Bone Marrow and Peripheral Blood in Patients With Philadelphia-Negative Myeloproliferative Neoplasms. Frontiers in Medicine, 8, 607.

Chen, S., Saeed, A. F., Liu, Q., Jiang, Q., Xu, H., Xiao, G. G., ... & Duo, Y. (2023). Macrophages in immunoregulation and therapeutics. Signal Transduction and Targeted Therapy, 8(1), 207.

Chen, X., Albrecht, S., Cui, W., & Zhang, D. (2020). Increased immature T-cells detected by flow cytometry in post chemotherapeutic patients with acute myeloid

leukemia, a case report and small series study. American Journal of Blood Research, 10(6), 351.

Chen, Z., Huang, A., Sun, J., Jiang, T., Qin, F. X. F., & Wu, A. (2017). Inference of immune cell composition on the expression profiles of mouse tissue. Scientific reports, 7(1), 40508.

Cheng, A. S., Cheng, Y. H., & Chang, T. L. (2012). Scopoletin attenuates allergy by inhibiting Th2 cytokines production in EL-4 T cells. Food & function, 3(8), 886-89.

Cheng, X., Wang, H., Wang, Z., Zhu, B., & Long, H. (2023). Tumor-associated myeloid cells in cancer immunotherapy. Journal of Hematology & Oncology, 16(1), 71.

Cherian, S., Miller, V., McCullouch, V., Dougherty, K., Fromm, J. R., & Wood, B. L. (2018). A novel flow cytometric assay for detection of residual disease in patients with B - lymphoblastic leukemia/lymphoma post anti - CD19 therapy. Cytometry Part B: Clinical Cytometry, 94(1), 112-120.

Chi, H., Pepper, M., & Thomas, P. G. (2024). Principles and therapeutic applications of adaptive immunity. Cell, 187(9), 2052-2078.

Chistiakov, D. A., Orekhov, A. N., & Bobryshev, Y. V. (2016). LOX-1-mediated effects on vascular cells in atherosclerosis. Cellular Physiology and Biochemistry, 38(5), 1851-1859.

Chiu, J. J., & Chien, S. (2011). Effects of disturbed flow on vascular endothelium: pathophysiological basis and clinical perspectives. Physiological reviews, 91(1), 327-387.

Chiu, S., & Bharat, A. (2016). Role of monocytes and macrophages in regulating immune response following lung transplantation. Current opinion in organ transplantation, 21(3), 239.

Christian, S. L. (2022). CD24 as a potential therapeutic target in patients with B-cell leukemia and lymphoma: current insights. OncoTargets and therapy, 15, 1391.

Ciavarella, C., Gallitto, E., Ricci, F., Buzzi, M., Stella, A., & Pasquinelli, G. (2017). The crosstalk between vascular MSCs and inflammatory mediators determines

the pro-calcific remodelling of human atherosclerotic aneurysm. Stem cell research & Therapy, 8(1), 1-13.

Clancy, S. (2008). DNA transcription. Nature education, 1(1), 41.

Cochain, C., Koch, M., Chaudhari, S. M., Busch, M., Pelisek, J., Boon, L., & Zernecke, A. (2015). CD8+ T cells regulate monopoiesis and circulating Ly6Chigh monocyte levels in atherosclerosis in mice. Circulation research, 117(3), 244-253.

Cooper, G. M. (2000). Eukaryotic RNA polymerases and general transcription factors. The Cell: A Molecular Approach.

Corrêa-Silva, S., Alencar, A. P., Moreli, J. B., Borbely, A. U., Lima, L. D. S., Scavone, C., ... & Calderon, I. M. (2018). Hyperglycemia induces inflammatory mediators in the human chorionic villous. Cytokine, 111, 41-48.

Cortazar, M. A., Sheridan, R. M., Erickson, B., Fong, N., Glover-Cutter, K., Brannan, K., & Bentley, D. L. (2019). Control of RNA Pol II speed by PNUTS-PP1 and Spt5 dephosphorylation facilitates termination by a “sitting duck torpedo” mechanism. Molecular cell, 76(6), 896-908.

Corthay, A. (2009). How do regulatory T cells work?. Scandinavian journal of immunology, 70(4), 326-336.

Courtney, J. M., Morris, G. P., Cleary, E. M., Howells, D. W., & Sutherland, B. A. (2021). An automated approach to improve the quantification of pericytes and microglia in whole mouse brain sections. eneuro, 8(6).

Cox, R. A., & García-Palmieri, M. R. (1990). Cholesterol, triglycerides, and associated lipoproteins.

Cuff, C. A., Kothapalli, D., Azonobi, I., Chun, S., Zhang, Y., Belkin, R., ... & Puré, E. (2001). The adhesion receptor CD44 promotes atherosclerosis by mediating inflammatory cell recruitment and vascular cell activation. The Journal of clinical investigation, 108(7), 1031-1040.

Cui, A., Huang, T., Li, S., Ma, A., Pérez, J. L., Sander, C., ... & Hacohen, N. (2024). Dictionary of immune responses to cytokines at single-cell resolution. Nature, 625(7994), 377-384.

Currie, M., Zhu, B., Vashisht, R., Elkin, D., & Huecker, M. R. (2017). Ultrasound intravascular access.

Cyprian, F., Lefkou, E., & Girardi, G. (2019). Immunomodulatory effects of vitamin D in pregnancy and beyond. Frontiers in immunology, 10, 475850.

Czech, M. P. (2017). Insulin action and resistance in obesity and type 2 diabetes. Nature medicine, 23(7), 804-814.

Da Costa Martins, P., García-Vallejo, J. J., van Thienen, J. V., Fernandez-Borja, M., van Gils, J. M., Beckers, C., ... & Zwaginga, J. J. (2007). P-selectin glycoprotein ligand-1 is expressed on endothelial cells and mediates monocyte adhesion to activated endothelium. Arteriosclerosis, thrombosis, and vascular biology, 27(5), 1023-1029.

Dagur, P. K., Sharma, B., Kumar, G., Khan, N. A., Katoch, V. M., Sengupta, U., & Joshi, B. (2010). Mycobacterial antigen (s) induce anergy by altering TCR-and TCR/CD28-induced signalling events: insights into T-cell unresponsiveness in leprosy. Molecular immunology, 47(5), 943-952.

Dal Lin, C., Tona, F., & Osto, E. The crosstalk between the cardiovascular and the immune system. Vasc. Biol. 2019; 1: H83–H88. doi: 10.1530. VB-19-0023.[Europe PMC free article][Abstract][CrossRef][Google Scholar].

Dallagi, A., Girouard, J., Hamelin-Morrissette, J., Dadzie, R., Laurent, L., Vaillancourt, C., ... & Reyes-Moreno, C. (2015). The activating effect of IFN-γ on monocytes/macrophages is regulated by the LIF–trophoblast–IL-10 axis *via* Stat1 inhibition and Stat3 activation. Cellular & molecular immunology, 12(3), 326-341.

Dan, P., Velot, É., Decot, V., & Menu, P. (2015). The role of mechanical stimuli in the vascular differentiation of mesenchymal stem cells. Journal of Cell Science, 128(14), 2415-2422.

Dandona, P., Aljada, A., Chaudhuri, A., Mohanty, P., & Garg, R. (2005). Metabolic syndrome: a comprehensive perspective based on interactions between obesity, diabetes, and inflammation. Circulation, 111(11), 1448-1454

Daniels, T. F., Killinger, K. M., Michal, J. J., Wright Jr, R. W., & Jiang, Z. (2009). Lipoproteins, cholesterol homeostasis and cardiac health. International journal of biological sciences, 5(5), 474.

Daryabor, G., Atashzar, M. R., Kabelitz, D., Meri, S., & Kalantar, K. (2020). The effects of type 2 diabetes mellitus on organ metabolism and the immune system. Frontiers in immunology, 11, 1582.

Davis, R., Pillai, S., Lawrence, N., & Chellappan, S. P. (2012). TNF-α-mediated proliferation of vascular smooth muscle cells involves Raf-1-mediated inactivation of Rb and transcription of E2F1-regulated genes. Cell Cycle, 11(1), 109-118.

Dean, L. (2005). Blood and the cells it contains. Blood groups and red cell antigens, 16.

DeCarvalho, A. C., Cappendijk, S. L., & Fadool, J. M. (2004). Developmental expression of the POU domain transcription factor Brn - 3b (Pou4f2) in the lateral line and visual system of zebrafish. Developmental dynamics: an official publication of the American Association of Anatomists, 229(4), 869-876.

DeFilippis, A. P., Chapman, A. R., Mills, N. L., de Lemos, J. A., Arbab-Zadeh, A., Newby, L. K., & Morrow, D. A. (2019). Assessment and treatment of patients with type 2 myocardial infarction and acute nonischemic myocardial injury. Circulation, 140(20), 1661-1678.

Delprat, V., Tellier, C., Demazy, C., Raes, M., Feron, O., & Michiels, C. (2020). Cycling hypoxia promotes a pro-inflammatory phenotype in macrophages *via* JNK/p65 signaling pathway. Scientific reports, 10(1), 1-13.

Delves, P. J. (2019). Cells of the Immune System. eLS, 1-8.

Delves, P. J., & Roitt, I. M. (1998). Encyclopedia of immunology. Academic Press.

Demers, I. (2015). Detection and Differentiation of Different Monocyte Subsets: Optimalization of a Multiparameter Flowcytometric Assay. MaRBLe, 6.

Dennis, J. H., Budhram-Mahadeo, V., & Latchman, D. S. (2001). The Brn-3b POU family transcription factor regulates the cellular growth, proliferation, and anchorage dependence of MCF7 human breast cancer cells. Oncogene, 20(36), 4961-4971.

Dhingra, R., & Vasan, R. S. (2017). Biomarkers in cardiovascular disease: Statistical assessment and section on key novel heart failure biomarkers. Trends in cardiovascular medicine, 27(2), 123-133.

Di Rosa, F., & Pabst, R. (2005). The bone marrow: a nest for migratory memory T cells. Trends in immunology, 26(7), 360-366.

Diamond, M. S., & Kanneganti, T. D. (2022). Innate immunity: the first line of defense against SARS-CoV-2. Nature immunology, 1-12.

Dimitrov, V., Barbier, C., Ismailova, A., Wang, Y., Dmowski, K., Salehi-Tabar, R., ... & White, J. H. (2021). Vitamin D-regulated gene expression profiles: Species-specificity and cell-specific effects on metabolism and immunity. Endocrinology, 162(2), bqaa218.

Domagała, D., Data, K., Szyller, H., Farzaneh, M., Mozdziak, P., Woźniak, S., ... & Kempisty, B. (2024). Cellular, Molecular and Clinical Aspects of Aortic Aneurysm—Vascular Physiology and Pathophysiology. Cells, 13(3), 274.

Donath, M. Y., & Shoelson, S. E. (2011). Type 2 diabetes as an inflammatory disease. Nature reviews immunology, 11(2), 98-107.

Draper, D. (2018). Nonclinical Studies.

Du, X. J. (2007). Divergence of hypertrophic growth and fetal gene profile: the influence of β - blockers. British journal of pharmacology, 152(2), 169-171.

Dubey, S., Yoon, H., Cohen, M. S., Nagarkatti, P., Nagarkatti, M., & Karan, D. (2018). Withaferin A associated differential regulation of inflammatory cytokines. Frontiers in immunology, 9, 195.

Dunsmore, G., Rosero, E. P., Shahbaz, S., Santer, D. M., Jovel, J., Lacy, P., ... & Elahi, S. (2021). Neutrophils promote T-cell activation through the regulated release of CD44-bound Galectin-9 from the cell surface during HIV infection. PLoS Biology, 19(8), e3001387.

Egashira, K. (2002). Clinical importance of endothelial function in arteriosclerosis and ischemic heart disease. Circulation journal, 66(6), 529-533.

Einarson, T. R., Acs, A., Ludwig, C., & Panton, U. H. (2018). Prevalence of cardiovascular disease in type 2 diabetes: a systematic literature review of scientific evidence from across the world in 2007–2017. Cardiovascular diabetology, 17(1), 1-19.

Eisenreich, A. (2013). Regulation of vascular function on posttranscriptional level. Thrombosis, 2013(1), 948765.

Elghetany, M. T., & Patel, J. (2002). Assessment of CD24 expression on bone marrow neutrophilic granulocytes: CD24 is a marker for the myelocytic stage of development. American journal of hematology, 71(4), 348-349.

Elmas, Ç., Erdogan, D., Take, G., Ozogul, C., Nacar, A., & Koksal, M. (2008). Ultrastructure of the thymus in diabetes mellitus and starvation. Advances in therapy, 25(1), 67-76.

Elmore, S. A. (2006). Enhanced histopathology of the spleen. Toxicologic pathology, 34(5), 648-655.

El-Sheikh, A., Suarez-Pinzon, W. L., Power, R. F., & Rabinovitch, A. (1999). Both CD4+ and CD8+ T cells are required for IFN-γ gene expression in pancreatic islets and autoimmune diabetes development in biobreeding rats. Journal of autoimmunity, 12(2), 109-119.

Elshourbagy, N. A., Meyers, H. V., & Abdel-Meguid, S. S. (2014). Cholesterol: the good, the bad, and the ugly-therapeutic targets for the treatment of dyslipidemia. Medical Principles and Practice, 23(2), 99-111.

Ernst, D. N., Weigle, W. O., Noonan, D. J., McQuitty, D. N., & Hobbs, M. V. (1993). The age-associated increase in IFN-gamma synthesis by mouse CD8+ T cells correlates with shifts in the frequencies of cell subsets defined by membrane CD44, CD45RB, 3G11, and MEL-14 expression. The Journal of Immunology, 151(2), 575-587.

Evans, J. L., Goldfine, I. D., Maddux, B. A., & Grodsky, G. M. (2003). Are oxidative stress− activated signaling pathways mediators of insulin resistance and β-cell dysfunction?. Diabetes, 52(1), 1-8.

Faggin, E., Puato, M., Zardo, L., Franch, R., Millino, C., Sarinella, F., ... & Chiavegato, A. (1999). Smooth muscle-specific SM22 protein is expressed in the adventitial cells of balloon-injured rabbit carotid artery. Arteriosclerosis, thrombosis, and vascular biology, 19(6), 1393-1404.

Fang, P., Li, X., Dai, J., Cole, L., Camacho, J. A., Zhang, Y., ... & Wang, H. (2018). Immune cell subset differentiation and tissue inflammation. Journal of hematology & oncology, 11, 1-22.

Fang, Y., Zhu, Y., Yue, W., Liu, L., & Wang, H. (2022). Protective effects of mitochondrial fission inhibition on ox-LDL induced VSMC foaming *via* metabolic reprogramming. Frontiers in Pharmacology, 3556.

Faries, P. L., Rohan, D. I., Takahara, H., Wyers, M. C., Contreras, M. A., Quist, W. C., ... & LoGerfo, F. W. (2001). Human vascular smooth muscle cells of diabetic origin exhibit increased proliferation, adhesion, and migration. Journal of vascular surgery, 33(3), 601-607.

Farooqui-Kabir, S. R., Diss, J. K., Henderson, D., Marber, M. S., Latchman, D. S., Budhram-Mahadeo, V., & Heads, R. J. (2008). Cardiac expression of Brn-3a and Brn-3b POU transcription factors and regulation of Hsp27 gene expression. Cell Stress and Chaperones, 13(3), 297-312.

Feil, S., Hofmann, F., & Feil, R. (2004). SM22α modulates vascular smooth muscle cell phenotype during atherogenesis. Circulation research, 94(7), 863-865.

Fernandez, G. J., Ramírez-Mejía, J. M., & Urcuqui-Inchima, S. (2022). Vitamin D boosts immune response of macrophages through a regulatory network of microRNAs and mRNAs. The Journal of Nutritional Biochemistry, 109, 109105.

Fernando, N., Sciumè, G., O'Shea, J. J., & Shih, H. Y. (2021). Multi-dimensional gene regulation in innate and adaptive lymphocytes: a view from regulomes. Frontiers in Immunology, 12, 932.

Fest, J., Ruiter, R., Ikram, M. A., Voortman, T., van Eijck, C. H., & Stricker, B. H. (2018). Reference values for white blood-cell-based inflammatory markers in the Rotterdam Study: a population-based prospective cohort study. Scientific reports, 8(1), 10566.

Filali, S., Noack, M., Géloën, A., Pirot, F., & Miossec, P. (2023). Effects of pro-inflammatory cytokines and cell interactions on cell area and cytoskeleton of rheumatoid arthritis synoviocytes and immune cells. European Journal of Cell Biology, 102(2), 151303.

Fiore, P. F., Di Matteo, S., Tumino, N., Mariotti, F. R., Pietra, G., Ottonello, S., ... & Azzarone, B. (2020). Interleukin-15 and cancer: some solved and many unsolved questions. Journal for immunotherapy of cancer, 8(2).

Fishbein, G. A., & Fishbein, M. C. (2009). Arteriosclerosis: rethinking the current classification. Archives of pathology & laboratory medicine, 133(8), 1309-1316.

Fishburn, J., Tomko, E., Galburt, E., & Hahn, S. (2015). Double-stranded DNA translocase activity of transcription factor TFIIH and the mechanism of RNA polymerase II open complex formation. Proceedings of the National Academy of Sciences, 112(13), 3961-3966.

Flammer, J., Konieczka, K., Bruno, R. M., Virdis, A., Flammer, A. J., & Taddei, S. (2013). The eye and the heart. European heart journal, 34(17), 1270-1278.

Foa, R., & Vitale, A. (2002). Towards an integrated classification of adult acute lymphoblastic leukemia. Reviews in clinical and experimental hematology, 6(2), 181-199.

Forester, N. D., Cruickshank, S. M., Scott, D. J. A., & Carding, S. R. (2005). Functional characterization of T cells in abdominal aortic aneurysms. Immunology, 115(2), 262-270.

Frietze, S., & Farnham, P. J. (2011). Transcription factor effector domains. A handbook of transcription factors, 261-277.

Frismantiene, A., Philippova, M., Erne, P., & Resink, T. J. (2018). Smooth muscle cell-driven vascular diseases and molecular mechanisms of VSMC plasticity. Cellular signalling, 52, 48-64.

Frostegård, J. (2013). Immunity, atherosclerosis and cardiovascular disease. BMC medicine, 11(1), 117.

Fujita, R., Ounzain, S., Wang, A. C. Y., Heads, R. J., & Budhram-Mahadeo, V. S. (2011). Hsp-27 induction requires POU4F2/Brn-3b TF in doxorubicin-treated breast cancer cells, whereas phosphorylation alters its cellular localisation following drug treatment. Cell Stress and Chaperones, 16(4), 427-439.

Furlong, S., Coombs, M. R. P., Ghassemi-Rad, J., & Hoskin, D. W. (2018). Thy-1 (CD90) signaling preferentially promotes RORγt expression and a Th17 response. Frontiers in Cell and Developmental Biology, 6, 158.

Furman, D., Campisi, J., Verdin, E., Carrera-Bastos, P., Targ, S., Franceschi, C., ... & Slavich, G. M. (2019). Chronic inflammation in the etiology of disease across the life span. Nature medicine, 25(12), 1822-1832.

Gałąska, R., Kulawiak-Gałąska, D., Dorniak, K., Stróżyk, A., Sabisz, A., Chmara, M., ... & Gruchała, M. (2023). Aortic Wall Thickness as a Surrogate for Subclinical Atherosclerosis in Familial and Nonfamilial Hypercholesterolemia: Quantitative 3D Magnetic Resonance Imaging Study and Interrelations with Computed Tomography Calcium Scores, and Carotid Ultrasonography. Journal of Clinical Medicine, 12(17), 5589.

Galicia-Garcia, U., Benito-Vicente, A., Jebari, S., Larrea-Sebal, A., Siddiqi, H., Uribe, K. B.,& Martín, C. (2020). Pathophysiology of type 2 diabetes mellitus. International journal of molecular sciences, 21(17), 6275.

Galkina, E., & Ley, K. (2009). Immune and inflammatory mechanisms of atherosclerosis. Annual review of immunology, 27.

Gallagher, K. A., Joshi, A., Carson, W. F., Schaller, M., Allen, R., Mukerjee, S., ... & Kunkel, S. L. (2015). Epigenetic changes in bone marrow progenitor cells influence the inflammatory phenotype and alter wound healing in type 2 diabetes. Diabetes, 64(4), 1420-1430.

Gallego, A., Vargas, J. A., Castejon, R., Citores, M. J., Romero, Y., Millan, I., & Durantez, A. (2003). Production of intracellular IL - 2, TNF - α, and IFN - γ by T cells in B - CLL. Cytometry Part B: Clinical Cytometry: The Journal of the International Society for Analytical Cytology, 56(1), 23-29.

Galson, D. L., & Roodman, G. D. (2010). Origins of Osteoclasts. Osteoimmunology: Interactions of the Immune and Skeletal Systems, 7.

Gan, L., Xiang, M., Zhou, L., Wagner, D. S., Klein, W. H. & Nathans, J. 1996. POU domain factor Brn-3b is required for the development of a large set of retinal ganglion cells. Proc Natl Acad Sci U S A, 93, 3920-5.

Gartner, L. P., & Hiatt, J. L. (2010). Concise Histology E-Book. Elsevier Health Sciences.

Gebuhrer, V., Murphy, J. F., Bordet, J. C., Reck, M. P., & McGregor, J. L. (1995). Oxidized low-density lipoprotein induces the expression of P-selectin (GMP140/PADGEM/CD62) on human endothelial cells. Biochemical Journal, 306(1), 293-298.

Genin, M., Clement, F., Fattaccioli, A., Raes, M., & Michiels, C. (2015). M1 and M2 macrophages derived from THP-1 cells differentially modulate the response of cancer cells to etoposide. BMC cancer, 15(1), 1-14.

Ghasemlou, N., Chiu, I. M., Julien, J. P., & Woolf, C. J. (2015). CD11b+ Ly6G− myeloid cells mediate mechanical inflammatory pain hypersensitivity. Proceedings of the National Academy of Sciences, 112(49), E6808-E6817.

Ghebre, Y. T., Yakubov, E., Wong, W. T., Krishnamurthy, P., Sayed, N., Sikora, A. G., & Bonnen, M. D. (2016). Vascular aging: implications for cardiovascular disease and therapy. Translational medicine (Sunnyvale, Calif.), 6(4).

Ghofrani Nezhad, M., Jami, G., Kooshkaki, O., Chamani, S., & Naghizadeh, A. (2023). The role of inflammatory cytokines (Interleukin-1 and interleukin-6) as a potential biomarker in the different stages of COVID-19 (Mild, severe, and critical). Journal of Interferon & Cytokine Research, 43(4), 147-163.

Ginsberg, H. N. (1996). Diabetic dyslipidemia: basic mechanisms underlying the common hypertriglyceridemia and low HDL cholesterol levels. Diabetes, 45(Supplement 3), S27-S30.

Girard, D., & Vandiedonck, C. (2022). How dysregulation of the immune system promotes diabetes mellitus and cardiovascular risk complications. Frontiers in Cardiovascular Medicine, 9, 991716.

Gjurich, B. N., Taghavie-Moghadam, P. L., & Galkina, E. V. (2015). Flow cytometric analysis of immune cells within murine aorta. Methods in Mouse Atherosclerosis, 161-175.

Glaviano, A., Wander, S. A., Baird, R. D., Yap, K. C., Lam, H. Y., Toi, M., ... & Kumar, A. P. (2024). Mechanisms of sensitivity and resistance to CDK4/CDK6 inhibitors in hormone receptor-positive breast cancer treatment. Drug Resistance Updates, 101103.

Gold, D. A., Gates, R. D., & Jacobs, D. K. (2014). The early expansion and evolutionary dynamics of POU class genes. Molecular biology and evolution, 31(12), 3136-3147.

Golle, L., Gerth, H. U., Beul, K., Heitplatz, B., Barth, P., Fobker, M., ... & Brand, M. (2017). Bone marrow-derived cells and their conditioned medium induce

microvascular repair in uremic rats by stimulation of endogenous repair mechanisms. Scientific reports, 7(1), 9444.

Goncalves, I., Zanoli, L., Nilsson, J., & Edsfeldt, A. (2024). Chronic Inflammation in Atherosclerosis and Arteriosclerosis. In Early Vascular Aging (EVA) (pp. 251-260). Academic Press.

Gong, R., Jiang, Z., Zagidullin, N., Liu, T., & Cai, B. (2021). Regulation of cardiomyocyte fate plasticity: a key strategy for cardiac regeneration. Signal Transduction and Targeted Therapy, 6(1), 1-11.

Gong, S., Gao, X., Xu, F., Shang, Z., Li, S., Chen, W., ... & Li, J. (2018). Association of lymphocyte to monocyte ratio with severity of coronary artery disease. Medicine, 97(43).

Goran K. Hansson, Anna-Karin L. Robertson, and Cecilia Söderberg-Nauclér

Gordon, S. (2003). Alternative activation of macrophages. Nature reviews immunology, 3(1), 23-35.

Graham, V. A., Marzo, A. L., & Tough, D. F. (2007). A role for CD44 in T cell development and function during direct competition between CD44+ and CD44– cells. European journal of immunology, 37(4), 925-934.

Grover, A., & Joshi, A. (2015). An overview of chronic disease models: a systematic literature review. Global journal of health science, 7(2), 210.

Groves, D. T., & Jiang, Y. (1995). Chemokines, a family of chemotactic cytokines. Critical Reviews in Oral Biology & Medicine, 6(2), 109-118.

Gruber, S., & Nickel, A. (2023). Toxic or not toxic? The specifications of the standard ISO 10993-5 are not explicit enough to yield comparable results in the cytotoxicity assessment of an identical medical device. Frontiers in Medical Technology, 5, 1195529.

Gu, W., Hong, X., Potter, C., Qu, A., & Xu, Q. (2017). Mesenchymal stem cells and vascular regeneration. Microcirculation, 24(1), e12324.

Guan, H., Nagarkatti, P. S., & Nagarkatti, M. (2009). Role of CD44 in the differentiation of Th1 and Th2 cells: CD44-deficiency enhances the development of Th2 effectors in response to sheep RBC and chicken ovalbumin. The Journal of Immunology, 183(1), 172-180.

Gui, T., Shimokado, A., Sun, Y., Akasaka, T., & Muragaki, Y. (2012). Diverse roles of macrophages in atherosclerosis: from inflammatory biology to biomarker discovery. Mediators of inflammation, 2012(1), 693083.

Guo, L., Urban, J. F., Zhu, J., & Paul, W. E. (2008). Elevating calcium in Th2 cells activates multiple pathways to induce IL-4 transcription and mRNA stabilization. The Journal of Immunology, 181(6), 3984-3993.

Gupta, A. (2022). Chapter 6-direct and indirect actions of insulin: role of insulin receptor, glucose transporters (GLUTs), and sodium-glucose linked transporters (SGLTs). Understanding insulin and insulin resistance, 179-201.

Gurumurthy, C. B., Saunders, T. L., & Ohtsuka, M. (2021). Designing and generating a mouse model: frequently asked questions. Journal of Biomedical Research, 35(2), 76.

Haeryfar, S. M., & Hoskin, D. W. (2004). Thy-1: more than a mouse pan-T cell marker. The Journal of Immunology, 173(6), 3581-3588.

Hagen, M., Pangrazzi, L., Rocamora-Reverte, L., & Weinberger, B. (2023). Legend or truth: Mature CD4+ CD8+ double-positive T cells in the periphery in health and disease. Biomedicines, 11(10), 2702.

Hamon, P., Rodero, M. P., Combadière, C., & Boissonnas, A. (2015). Tracking mouse bone marrow monocytes *in vivo*. JoVE (Journal of Visualized Experiments), (96), e52476.

Han, M., Dong, L. H., Zheng, B., Shi, J. H., Wen, J. K., & Cheng, Y. (2009). Smooth muscle 22 alpha maintains the differentiated phenotype of vascular smooth muscle cells by inducing filamentous actin bundling. Life sciences, 84(13-14), 394-401.

Hansson, G. K., Robertson, A. K. L., & Söderberg-Nauclér, C. (2006). Inflammation and atherosclerosis. Annu. Rev. Pathol. Mech. Dis., 1, 297-329.

Hardy, R. R., & Hayakawa, K. (2001). B cell development pathways. Annual review of immunology, 19(1), 595-621.

Harky, A., Sokal, P. A., Hasan, K., & Papaleontiou, A. (2021). The aortic pathologies: how far we understand it and its implications on thoracic aortic surgery. Brazilian journal of cardiovascular surgery, 36, 535-549.

Harman, J. L., & Jørgensen, H. F. (2019). The role of smooth muscle cells in plaque stability: Therapeutic targeting potential. British journal of pharmacology, 176(19), 3741-3753.

Harrer, C., Otto, F., Radlberger, R. F., Moser, T., Pilz, G., Wipfler, P., & Harrer, A. (2022). The CXCL13/CXCR5 immune axis in health and disease—Implications for intrathecal B cell activities in neuroinflammation. Cells, 11(17), 2649.

Hashemi, R., Morshedi, M., Jafarabadi, M. A., Altafi, D., Hosseini-Asl, S. S., & Rafie-Arefhosseini, S. (2018). Anti-inflammatory effects of dietary vitamin D3 in patients with multiple sclerosis. Neurology genetics, 4(6).

Häusser-Kinzel, S., & Weber, M. S. (2019). The role of B cells and antibodies in multiple sclerosis, neuromyelitis optica, and related disorders. Frontiers in immunology, 10, 201.

Hawkins, L. J., Al-Attar, R., & Storey, K. B. (2018). Transcriptional regulation of metabolism in disease: From transcription factors to epigenetics. PeerJ, 6, e5062.

Haybar, H., Rezaeeyan, H., Shahjahani, M., Shirzad, R., & Saki, N. (2019). T - bet transcription factor in cardiovascular disease: Attenuation or inflammation factor?. Journal of cellular physiology, 234(6), 7915-7922.

Hayday, A. C., & Pennington, D. J. (2007). Key factors in the organized chaos of early T cell development. Nature immunology, 8(2), 137-144.

He, D., Liu, Q., Wu, Y., & Xie, L. (2022). A context-aware deconfounding autoencoder for robust prediction of personalized clinical drug response from cell-line compound screening. Nature Machine Intelligence, 4(10), 879-892.

Heinecke, J. W. (2006). Lipoprotein oxidation in cardiovascular disease: chief culprit or innocent bystander?. The Journal of experimental medicine, 203(4), 813-816.

Hernandes, V. V., Barbas, C., & Dudzik, D. (2017). A review of blood sample handling and pre - processing for metabolomics studies. Electrophoresis, 38(18), 2232-2241.

Hernandez-Garcia, C. M., & Finer, J. J. (2014). Identification and validation of promoters and cis-acting regulatory elements. Plant Science, 217, 109-119.

Herr, W., & Cleary, M. A. (1995). The POU domain: versatility in transcriptional regulation by a flexible two-in-one DNA-binding domain. Genes & development, 9(14), 1679-1693.

Hess, N. J., Turicek, D. P., Riendeau, J., McIlwain, S. J., Contreras Guzman, E., Nadiminti, K., ... & Capitini, C. M. (2023). Inflammatory CD4/CD8 double-positive human T cells arise from reactive CD8 T cells and are sufficient to mediate GVHD pathology. Science Advances, 9(12), eadf0567.

Hiam-Galvez, K. J., Allen, B. M., & Spitzer, M. H. (2021). Systemic immunity in cancer. Nature reviews cancer, 21(6), 345-359.

Himmel, L. E., Hackett, T. A., Moore, J. L., Adams, W. R., Thomas, G., Novitskaya, T., ... & Boyd, K. L. (2018). Beyond the H&E: Advanced technologies for in situ tissue biomarker imaging. Ilar Journal, 59(1), 51-65.

Hirabayashi, Y., Yoon, B. I., Tsuboi, I., Huo, Y., Kodama, Y., Kanno, J., ... & Inoue, T. (2008). The Cell Cycle in Hematopoietic Stem Cells, Lin−/C-kit+/Sca1+ Fraction, Is Regulated by Connexin 32, Specifically Expressed in the Stem Cell Compartment. Blood, 112(11), 4775.

Hong, X., & Gu, W. (2019). Plasticity of vascular resident mesenchymal stromal cells during vascular remodeling. Vascular Biology, 1(1), H67.

Hristozova, T., Konschak, R., Budach, V., & Tinhofer, I. (2012). A simple multicolor flow cytometry protocol for detection and molecular characterization of circulating tumor cells in epithelial cancers. Cytometry Part A, 81(6), 489-495.

Hu, D., Al-Shalan, H. A., Shi, Z., Wang, P., Wu, Y., Nicholls, P. K., ... & Ma, B. (2020). Distribution of nerve fibers and nerve-immune cell association in mouse spleen revealed by immunofluorescent staining. Scientific Reports, 10(1), 9850.

Hu, X., Li, J., Fu, M., Zhao, X., & Wang, W. (2021). The JAK/STAT signaling pathway: from bench to clinic. Signal transduction and targeted therapy, 6(1), 402.

Hu, X., Paik, P. K., Chen, J., Yarilina, A., Kockeritz, L., Lu, T. T., ... & Ivashkiv, L. B. (2006). IFN-γ suppresses IL-10 production and synergizes with TLR2 by regulating GSK3 and CREB/AP-1 proteins. Immunity, 24(5), 563-574.

Huang, L., & Hu, X. (2021). Molecular mechanisms and functions of lncRNAs in the inflammatory reaction of diabetes mellitus. International Journal of Endocrinology, 2021(1), 2550399.

Hung, J. T., Liao, J. H., Lin, Y. C., Chang, H. Y., Wu, S. F., Chang, T. H., ... & Sytwu, H. K. (2005). Immunopathogenic role of TH1 cells in autoimmune diabetes: evidence from a T1 and T2 doubly transgenic non-obese diabetic mouse model. Journal of autoimmunity, 25(3), 181-192.

Idzkowska, E., Eljaszewicz, A., Miklasz, P., Musial, W. J., Tycinska, A. M., & Moniuszko, M. (2015). The role of different monocyte subsets in the pathogenesis of atherosclerosis and acute coronary syndromes. Scandinavian journal of immunology, 82(3), 163-173.

Igarashi, K., Kurosaki, T., & Roychoudhuri, R. (2017). BACH transcription factors in innate and adaptive immunity. Nature Reviews Immunology, 17(7), 437-450.

InformedHealth.org [Internet]. Cologne, Germany: Institute for Quality and Efficiency in Health Care (IQWiG); 2006-. The innate and adaptive immune systems. [Updated 2020 Jul 30]. Available from: https://www.ncbi.nlm.nih.gov/books/NBK279396/

Ingersoll, M. A., Spanbroek, R., Lottaz, C., Gautier, E. L., Frankenberger, M., Hoffmann, R., ... & Habenicht, A. J. (2010). Comparison of gene expression profiles between human and mouse monocyte subsets. Blood, The Journal of the American Society of Hematology, 115(3), e10-e19.

Inukai, S., Kock, K. H., & Bulyk, M. L. (2017). Transcription factor–DNA binding: beyond binding site motifs. Current opinion in genetics & development, 43, 110-119.

Iqbal, A. J., Krautter, F., Blacksell, I. A., Wright, R. D., Austin - Williams, S. N., Voisin, M. B., ... & Cooper, D. (2022). Galectin - 9 mediates neutrophil capture and adhesion in a CD44 and β2 integrin - dependent manner. The FASEB Journal, 36(1), e22065.

Iqbal, J., & Hussain, M. M. (2009). Intestinal lipid absorption. American Journal of Physiology-Endocrinology and Metabolism, 296(6), E1183-E1194.

Irshad, S., Pedley, R. B., Anderson, J., Latchman, D. S., & Budhram-Mahadeo, V. (2004). The Brn-3b transcription factor regulates the growth, behavior, and

invasiveness of human neuroblastoma cells *in vitro* and *in vivo*. Journal of Biological Chemistry, 279(20), 21617-21627.

Israel-Roming, F., Luta, G., Balan, D., Gherghina, E., Cornea, C. P., & Matei, F. (2015). Time and Temperature Stability of Collagenase Produced by Bacillus licheniformis. Agriculture and Agricultural Science Procedia, 6, 579-584.

Italiani, P., & Boraschi, D. (2014). From monocytes to M1/M2 macrophages: phenotypical vs. functional differentiation. Frontiers in immunology, 5, 514.

Iwafuchi - Doi, M. (2019). The mechanistic basis for chromatin regulation by pioneer transcription factors. Wiley Interdisciplinary Reviews: Systems Biology and Medicine, 11(1), e1427.

Jain, M., He, Q., Lee, W. S., Kashiki, S., Foster, L. C., Tsai, J. C., ... & Haber, E. (1996). Role of CD44 in the reaction of vascular smooth muscle cells to arterial wall injury. The Journal of clinical investigation, 97(3), 596-603.

Jain, S., Kaur, I. R., Das, S., Bhattacharya, S. N., & Singh, A. (2009). T helper 1 to T helper 2 shift in cytokine expression: an autoregulatory process in superantigen-associated psoriasis progression?. Journal of Medical Microbiology, 58(2), 180-184.

Jaminon, A., Reesink, K., Kroon, A., & Schurgers, L. (2019). The role of vascular smooth muscle cells in arterial remodeling: focus on calcification-related processes. International journal of molecular sciences, 20(22), 5694.

Janeway CA Jr, Travers P, Walport M, et al. Immunobiology: The Immune System in Health and Disease. 5th edition. New York: Garland Science; 2001. Chapter 8, T Cell-Mediated Immunity. Available from: https://www.ncbi.nlm.nih.gov/books/NBK10762/

Janeway Jr, C. A., Travers, P., Walport, M., & Shlomchik, M. J. (2001). The components of the immune system. In Immunobiology: The Immune System in Health and Disease. 5th edition. Garland Science.

Janeway, C., Travers, P., Walport, M., & Shlomchik, M. (2001). Immunobiology: the immune system in health and disease (Vol. 2, p. 154). New York: Garland Pub..

Jaskuła, K., Sacharczuk, M., Gaciong, Z., & Skiba, D. S. (2021). Cardiovascular effects mediated by hmmr and cd44. Mediators of Inflammation, 2021(1), 4977209.

Javadifar, A., Rastgoo, S., Banach, M., Jamialahmadi, T., Johnston, T. P., & Sahebkar, A. (2021). Foam cells as therapeutic targets in atherosclerosis with a focus on the regulatory roles of non-coding RNAs. International journal of molecular sciences, 22(5), 2529.

Jenkins, S. J., Ruckerl, D., Cook, P. C., Jones, L. H., Finkelman, F. D., Van Rooijen, N., ... & Allen, J. E. (2011). Local macrophage proliferation, rather than recruitment from the blood, is a signature of TH2 inflammation. science, 332(6035), 1284-1288.

Jennette, J. C., & Stone, J. R. (2014). Diseases of medium-sized and small vessels. In Cellular and Molecular Pathobiology of Cardiovascular Disease (pp. 197-219). Academic Press.

Jiang, W., Agrawal, D. K., & Boosani, C. S. (2018). Cellspecific histone modifications in atherosclerosis. Molecular medicine reports, 18(2), 1215-1224.

Johnson, J., Jaggers, R. M., Gopalkrishna, S., Dahdah, A., Murphy, A. J., Hanssen, N. M., & Nagareddy, P. R. (2022). Oxidative stress in neutrophils: implications for diabetic cardiovascular complications. Antioxidants & redox signaling, 36(10), 652-666.

Johnston, J. A., Bacon, C. M., Riedy, M. C., & O'Shea, J. J. (1996). Signaling by IL - 2 and related cytokines: JAKs, STATs, and relationship to immunodeficiency. Journal of leukocyte biology, 60(4), 441-452.

Kamalov, G., Bhattacharya, S. K., & Weber, K. T. (2010). Congestive heart failure: where homeostasis begets dyshomeostasis. Journal of cardiovascular pharmacology, 56(3), 320.

Kany, S., Vollrath, J. T., & Relja, B. (2019). Cytokines in inflammatory disease. International journal of molecular sciences, 20(23), 6008.

Karlmark, K., Tacke, F., & Dunay, I. (2012). Monocytes in health and disease—Minireview. European Journal of Microbiology and Immunology, 2(2), 97-102.

Kassi, E., Adamopoulos, C., Basdra, E. K., & Papavassiliou, A. G. (2013). Role of vitamin D in atherosclerosis. Circulation, 128(23), 2517-2531.

Kathiriya, I. S., Nora, E. P., & Bruneau, B. G. (2015). Investigating the transcriptional control of cardiovascular development. Circulation research, 116(4), 700-714.

Katsiari CG, Bogdanos DP, Sakkas LI. Inflammation and cardiovascular disease. World J Transl Med 2019; 8(1): 1-8 [DOI: 10.5528/wjtm.v8.i1.1]

Katsiari, C.G., Bogdanos, D.P & Sakkas, L.I (2019). Inflammation and cardiovascular disease. World J Transl Med 2019 January 31; 8(1): 1-8.

Kattoor, A. J., Goel, A., & Mehta, J. L. (2019). LOX-1: Regulation, Signaling and Its Role in Atherosclerosis. Antioxidants, 8(7), 218.

Kaur, J., & Bachhawat, A. K. (2009). A modified Western blot protocol for enhanced sensitivity in the detection of a membrane protein. Analytical Biochemistry, 384(2), 348-349.

Kawano, Y., Petkau, G., Stehle, C., Durek, P., Heinz, G. A., Tanimoto, K., ... & Melchers, F. (2018). Stable lines and clones of long-term proliferating normal, genetically unmodified murine common lymphoid progenitors. Blood, The Journal of the American Society of Hematology, 131(18), 2026-2035.

Kelly, B. B., & Fuster, V. (Eds.). (2010). Promoting cardiovascular health in the developing world: a critical challenge to achieve global health. National Academies Press.

Kerr, M. W. A., Magalhães-Gama, F., Ibiapina, H. N. S., Hanna, F. S. A., Xabregas, L. A., Alves, E. B., ... & Malheiro, A. (2021). Bone marrow soluble immunological mediators as clinical prognosis biomarkers in b-cell acute lymphoblastic leukemia patients undergoing induction therapy. Frontiers in Oncology, 11, 696032.

Khalaf, H., Jass, J., & Olsson, P. E. (2010). Differential cytokine regulation by NF-κB and AP-1 in Jurkat T-cells. BMC immunology, 11(1), 1-12.

Kim, C. S., Park, S., & Kim, J. (2017). The role of glycation in the pathogenesis of aging and its prevention through herbal products and physical exercise. Journal of exercise nutrition & biochemistry, 21(3), 55.

Kim, N. H., & Kang, P. M. (2010). Apoptosis in cardiovascular diseases: mechanism and clinical implications. Korean circulation journal, 40(7), 299-305.

Klinge, C. M. (2001). Estrogen receptor interaction with estrogen response elements. Nucleic acids research, 29(14), 2905-2919.

Koju, N., Taleb, A., Zhou, J., Lv, G., Yang, J., Cao, X., ... & Ding, Q. (2019). Pharmacological strategies to lower crosstalk between nicotinamide adenine dinucleotide phosphate (NADPH) oxidase and mitochondria. Biomedicine & Pharmacotherapy, 111, 1478-1498.

Kologrivova, I. V., Suslova, T. E., Koshelskaya, O. A., Vinnizkaya, I. V., & Popov, S. V. (2016). T-helper-1, T-helper-17, T-regulatory lymphocytes in hypertensive patients with diabetes mellitus type 2 or impaired glucose tolerance: association with clinical and metabolic parameters in a case control study. Translational Medicine Communications, 1(1), 1-11.

Krajewska, M., Witkowska-Sędek, E., & Rumińska, M. (2022). Vitamin D effects on selected anti-inflammatory and pro-inflammatory markers of obesity-related chronic inflammation. Frontiers in Endocrinology, 13, 920340.

Krampera, M., Sartoris, S., Liotta, F., Pasini, A., Angeli, R., Cosmi, L., ... & Annunziato, F. (2007). Immune regulation by mesenchymal stem cells derived from adult spleen and thymus. Stem cells and development, 16(5), 797-810.

Kraus, R. F., & Gruber, M. A. (2021). Neutrophils—from bone marrow to first-line defense of the innate immune system. Frontiers in immunology, 12, 767175.

Krausgruber, T., Fortelny, N., Fife-Gernedl, V., Senekowitsch, M., Schuster, L. C., Lercher, A., ... & Bock, C. (2020). Structural cells are key regulators of organ-specific immune responses. Nature, 583(7815), 296-302.

Kroeze, E., Loeffen, J. L., Poort, V. M., & Meijerink, J. P. (2020). T-cell lymphoblastic lymphoma and leukemia: different diseases from a common premalignant progenitor?. Blood advances, 4(14), 3466-3473.

Krueger, A., & von Boehmer, H. (2007). Identification of a T lineage-committed progenitor in adult blood. Immunity, 26(1), 105-116.

Ku, H. C., & Cheng, C. F. (2020). Master regulator activating transcription factor 3 (ATF3) in metabolic homeostasis and cancer. Frontiers in Endocrinology, 11, 552603.

Kuang, J., Yan, X., Genders, A. J., Granata, C., & Bishop, D. J. (2018). An overview of technical considerations when using quantitative real-time PCR

analysis of gene expression in human exercise research. PloS one, 13(5), e0196438.

Kwartler, C., Zhou, P., Kuang, S. Q., Duan, X. Y., Gong, L., & Milewicz, D. (2016). Vascular smooth muscle cell isolation and culture from mouse aorta. Bio Protoc, 6, e2045.

L Ramos, T., Sánchez-Abarca, L. I., Muntión, S., Preciado, S., Puig, N., López-Ruano, G., ... & del Cañizo, C. (2016). MSC surface markers (CD44, CD73, and CD90) can identify human MSC-derived extracellular vesicles by conventional flow cytometry. Cell Communication and Signaling, 14(1), 1-14.

Lacolley, P., Regnault, V., & Laurent, S. (2020). Mechanisms of arterial stiffening: from mechanotransduction to epigenetics. Arteriosclerosis, thrombosis, and vascular biology, 40(5), 1055-1062.

Lai, S. L., Marín Juez, R., & Stainier, D. Y. (2018). Immune responses in cardiac repair and regeneration: a comparative.

Lalu, M. M., Montroy, J., Begley, C. G., Bubela, T., Hunniford, V., Ripsman, D., ... & Fergusson, D. A. (2020). Identifying and understanding factors that affect the translation of therapies from the laboratory to patients: a study protocol. F1000Research, 9.

Lamb, F. S., Choi, H., Miller, M. R., & Stark, R. J. (2020). TNFα and reactive oxygen signaling in vascular smooth muscle cells in hypertension and atherosclerosis. American journal of hypertension, 33(10), 902-913.

Lancrin, C., Schneider, E., Lambolez, F., Arcangeli, M. L., Garcia-Cordier, C., Rocha, B., & Ezine, S. (2002). Major T cell progenitor activity in bone marrow–derived spleen colonies. The Journal of experimental medicine, 195(7), 919-929.

Laporte, B., Petit, D., Rocha, D., Boussaha, M., Grohs, C., Maftah, A., & Petit, J. M. (2012). Characterization of bovine FUT7 furthers understanding of FUT7 evolution in mammals. BMC genetics, 13(1), 74.

Lara-Pezzi, E., Dopazo, A., & Manzanares, M. (2012). Understanding cardiovascular disease: a journey through the genome (and what we found there). Disease models & mechanisms, 5(4), 434-443.

Larkin, J., Renukaradhya, G. J., Sriram, V., Du, W., Gervay-Hague, J., & Brutkiewicz, R. R. (2006). CD44 differentially activates mouse NK T cells and conventional T cells. The Journal of Immunology, 177(1), 268-279.

Lee, J. U., Kim, L. K., & Choi, J. M. (2018). Revisiting the concept of targeting NFAT to control T cell immunity and autoimmune diseases. Frontiers in immunology, 9, 2747.

Lee, S. A., Ndisang, D., Patel, C., Dennis, J. H., Faulkes, D. J., D'Arrigo, C., ... & Budhram-Mahadeo, V. S. (2005). Expression of the Brn-3b transcription factor correlates with expression of HSP-27 in breast cancer biopsies and is required for maximal activation of the HSP-27 promoter. Cancer research, 65(8), 3072-3080.

Lee, S. J., Lee, I. K., & Jeon, J. H. (2020). Vascular calcification—new insights into its mechanism. International journal of molecular sciences, 21(8), 2685.

Lee, T. I., & Young, R. A. (2013). Transcriptional regulation and its misregulation in disease. Cell, 152(6), 1237-1251.

Leitschuh, M., & Chobanian, A. (1987). Vascular changes in hypertension. The Medical clinics of North America, 71(5), 827-841.

Lent-Schochet, D., & Jialal, I. (2019). Biochemistry, Lipoprotein Metabolism. In StatPearls [Internet]. StatPearls Publishing.

Leon, B. M., & Maddox, T. M. (2015). Diabetes and cardiovascular disease: Epidemiology, biological mechanisms, treatment recommendations and future research. World journal of diabetes, 6(13), 1246.

Leopold, J. A., & Loscalzo, J. (2008). Oxidative mechanisms and atherothrombotic cardiovascular disease. Drug Discovery Today: Therapeutic Strategies, 5(1), 5-13.

Levy, E., & Slavov, N. (2018). Single cell protein analysis for systems biology. Essays in biochemistry, 62(4), 595-605.

Lewis, S. M., Williams, A., & Eisenbarth, S. C. (2019). Structure and function of the immune system in the spleen. Science immunology, 4(33), eaau6085.

Lhoták, Š., Gyulay, G., Cutz, J. C., Al - Hashimi, A., Trigatti, B. L., Richards, C. D., ... & Austin, R. C. (2016). Characterization of proliferating lesion - resident

cells during all stages of atherosclerotic growth. Journal of the American Heart Association, 5(8), e003945.

Li, H., & Tsokos, G. C. (2021). Double-negative T cells in autoimmune diseases. Current opinion in rheumatology, 33(2), 163-172.

Li, H., Zou, X., Baatrup, A., Lind, M., & Bünger, C. (2005). Cytokine profiles in conditioned media from cultured human intervertebral disc tissue. Implications of their effect on bone marrow stem cell metabolism. Acta Orthopaedica, 76(1).

Li, L., Leid, M., & Rothenberg, E. V. (2010). An early T cell lineage commitment checkpoint dependent on the transcription factor Bcl11b. Science, 329(5987), 89-93.

Li, L., Miano, J. M., Cserjesi, P., & Olson, E. N. (1996). SM22α, a marker of adult smooth muscle, is expressed in multiple myogenic lineages during embryogenesis. Circulation research, 78(2), 188-195.

Li, S. L., Reddy, M. A., Cai, Q., Meng, L., Yuan, H., Lanting, L., & Natarajan, R. (2006). Enhanced proatherogenic responses in macrophages and vascular smooth muscle cells derived from diabetic db/db mice. Diabetes, 55(9), 2611-2619.

Li, Y., Liu, Y., Liu, S., Gao, M., Wang, W., Chen, K., ... & Liu, Y. (2023). Diabetic vascular diseases: molecular mechanisms and therapeutic strategies. Signal transduction and targeted therapy, 8(1), 152.

Li, Y., Liu, Z., Han, X., Liang, F., Zhang, Q., Huang, X., ... & He, B. (2024). Dynamics of Endothelial Cell Generation and Turnover in Arteries During Homeostasis and Diseases. Circulation, 149(2), 135-154.

Li, Z., Zhao, H., & Wang, J. (2021). Metabolism and chronic inflammation: the links between chronic heart failure and comorbidities. Frontiers in Cardiovascular Medicine, 8, 650278.

Liao, W., Schones, D. E., Oh, J., Cui, Y., Cui, K., Roh, T. Y., ... & Leonard, W. J. (2008). Priming for T helper type 2 differentiation by interleukin 2–mediated induction of interleukin 4 receptor α-chain expression. Nature immunology, 9(11), 1288-1296.

Lillycrop, K. A., Budrahan, V. S., Lakin, N. D., Terrenghi, G., Wood, J. N., Polak, J. M., & Latchman, D. S. (1992). A novel POU family transcription factor is closely

related to Brn-3 but has a distinct expression pattern in neuronal cells. Nucleic Acids Research, 20(19), 5093-5096.

Lima, J. E., Moreira, N. C., & Sakamoto-Hojo, E. T. (2022). Mechanisms underlying the pathophysiology of type 2 diabetes: From risk factors to oxidative stress, metabolic dysfunction, and hyperglycemia. Mutation Research/Genetic Toxicology and Environmental Mutagenesis, 874, 503437.

Linton, M. F., Yancey, P. G., Davies, S. S., Jerome, W. G., Linton, E. F., Song, W. L., ... & Vickers, K. C. (2019). The role of lipids and lipoproteins in atherosclerosis. In Endotext [Internet]. MDText. com, Inc..

Liu, T., Zhang, L., Joo, D., & Sun, S. C. (2017). NF-κB signaling in inflammation. Signal transduction and targeted therapy, 2(1), 1-9.

Liu, X., & Quan, N. (2015). Immune cell isolation from mouse femur bone marrow. Bio-protocol, 5(20), e1631-e1631.

Li-Weber, M., & Krammer, P. H. (2003). Regulation of IL4 gene expression by T cells and therapeutic perspectives. Nature Reviews Immunology, 3(7), 534-543.

Locher, R., Brandes, R. P., Vetter, W., & Barton, M. (2002). Native LDL induces proliferation of human vascular smooth muscle cells *via* redox-mediated activation of ERK 1/2 mitogen-activated protein kinases. Hypertension, 39(2), 645-650.

Lohoff, M., Giaisi, M., Köhler, R., Casper, B., Krammer, P. H., & Li-Weber, M. (2010). Early growth response protein-1 (Egr-1) is preferentially expressed in T helper type 2 (Th2) cells and is involved in acute transcription of the Th2 cytokine interleukin-4. Journal of Biological Chemistry, 285(3), 1643-1652.

Lopez-Castejon, G., & Brough, D. (2011). Understanding the mechanism of IL-1β secretion. Cytokine & growth factor reviews, 22(4), 189-195.

Lopez, E. O., Ballard, B. D., & Jan, A. (2023). Cardiovascular disease. In StatPearls [Internet]. StatPearls Publishing.

Lu, H., Wu, Y., Shao, X., Zhou, S., Jiang, Y., Chen, R., ... & Su, Z. (2018). ANG II facilitated CD11+ Ly6Chi cells reprogramming into M1 - like macrophage through Erk1/2 or p38 - Stat3 pathway and involved in EAM. Journal of Leukocyte Biology, 103(4), 719-730.

Luca DC. Monocytes. PathologyOutlines.com website. https://www.pathologyoutlines.com/topic/bonemarrowmonocytematuration.html.

Luche, H., Ardouin, L., Teo, P., See, P., Henri, S., Merad, M., ... & Malissen, B. (2011). The earliest intrathymic precursors of CD8 α + thymic dendritic cells correspond to myeloid - type double - negative 1c cells. European journal of immunology, 41(8), 2165-2175.

Ludwig, W. D., Matutes, E., Orfao, A., & van't Veer, M. B. (1995). Proposals for the immunological classification of acute leukemia. Leukemia, 9(10), 1783-1786.

Luo, C., Ruan, Y., Sun, P., Wang, H., Yang, W., Gong, Y., & Wang, D. (2022). The role of transcription factors in coronary artery disease and myocardial infarction. Frontiers in Bioscience-Landmark, 27(12), 329.

Ma, J., Li, Y., Yang, X., Liu, K., Zhang, X., Zuo, X., ... & Chen, X. (2023). Signaling pathways in vascular function and hypertension: molecular mechanisms and therapeutic interventions. Signal transduction and targeted therapy, 8(1), 168.

Ma, W. T., Gao, F., Gu, K., & Chen, D. K. (2019). The role of monocytes and macrophages in autoimmune diseases: a comprehensive review. Frontiers in immunology, 10, 1140.

Mak, T. W., & Saunders, M. E. (2005). The immune response: basic and clinical principles. Academic Press.

Mantovani, A., Sica, A., Sozzani, S., Allavena, P., Vecchi, A., & Locati, M. (2004). The chemokine system in diverse forms of macrophage activation and polarization. Trends in immunology, 25(12), 677-686.

Marchio, P., Guerra-Ojeda, S., Vila, J. M., Aldasoro, M., Victor, V. M., & Mauricio, M. D. (2019). Targeting early atherosclerosis: A focus on oxidative stress and inflammation. Oxidative medicine and cellular longevity, 2019.

Marshall, J. S., Warrington, R., Watson, W., & Kim, H. L. (2018). An introduction to immunology and immunopathology. Allergy, Asthma & Clinical Immunology, 14, 1-10.

Martinez, F. O., & Gordon, S. (2014). The M1 and M2 paradigm of macrophage activation: time for reassessment. F1000prime reports, 6.

Masenga, S. K., & Kirabo, A. (2023). Hypertensive heart disease: risk factors, complications and mechanisms. Frontiers in Cardiovascular Medicine, 10, 1205475.

Maskell, L. J., Mahadeo, A. V., & Budhram-Mahadeo, V. S. (2018). POU4F2/Brn-3b transcription factor is associated with survival and drug resistance in human ovarian cancer cells. Oncotarget, 9(95), 36770.

Maskell, L. J., Qamar, K., Babakr, A. A., Hawkins, T. A., Heads, R. J., & Budhram-Mahadeo, V. S. (2017). Essential but partially redundant roles for POU4F1/Brn-3a and POU4F2/Brn-3b transcription factors in the developing heart. Cell death & disease, 8(6), e2861.

Mathew, J., Sankar, P., & Varacallo, M. (2018). Physiology, blood plasma.

Matsumori, A. (2023). Nuclear factor-κB is a prime candidate for the diagnosis and control of inflammatory cardiovascular disease. European Cardiology Review, 18.

Mazurek, R., Dave, J. M., Chandran, R. R., Misra, A., Sheikh, A. Q., & Greif, D. M. (2017). Vascular cells in blood vessel wall development and disease. Advances in Pharmacology, 78, 323-350.

Mazurek, R., Dave, J. M., Chandran, R. R., Misra, A., Sheikh, A. Q., & Greif, D. M. (2017). Vascular cells in blood vessel wall development and disease. Advances in Pharmacology, 78, 323-350.

Mele, L., Maskell, L. J., Stuckey, D. J., Clark, J. E., Heads, R. J., & Budhram-Mahadeo, V. S. (2019). The POU4F2/Brn-3b transcription factor is required for the hypertrophic response to angiotensin II in the heart. Cell death & disease, 10(8), 1-18.

Mendis S, Puska P, Norrving B (2011). Global Atlas on Cardiovascular Disease Prevention and Control (PDF). World Health Organization in collaboration with the World Heart Federation and the World Stroke Organization. pp. 3–18. ISBN 978-92-4-156437-3. Archived (PDF) from the original on 2014-08-17.

Menzel, A., Samouda, H., Dohet, F., Loap, S., Ellulu, M. S., & Bohn, T. (2021). Common and novel markers for measuring inflammation and oxidative stress ex vivo in research and clinical practice—which to use regarding disease outcomes?. Antioxidants, 10(3), 414.

Mills, C. D., & Ley, K. (2014). M1 and M2 macrophages: the chicken and the egg of immunity. Journal of innate immunity, 6(6), 716-726.

Mills, C. D. (2015). Anatomy of a discovery: m1 and m2 macrophages. Frontiers in immunology, 6, 212.

Minta, J., Yun, J. J., & Bernard, R. S. (2010). Microarray analysis of ox - LDL (oxidized low - density lipoprotein) - regulated genes in human coronary artery smooth muscle cells. Cell biology international reports, 17(2), 33-45.

Mishra, M. N., Chandavarkar, V., Sharma, R., & Bhargava, D. (2019). Structure, function and role of CD44 in neoplasia. Journal of Oral and Maxillofacial Pathology, 23(2), 267-272.

Miteva, K., Madonna, R., De Caterina, R., & Van Linthout, S. (2018). Innate and adaptive immunity in atherosclerosis. Vascular Pharmacology, 107, 67-77.

Mitsis, T., Efthimiadou, A., Bacopoulou, F., Vlachakis, D., Chrousos, G. P., & Eliopoulos, E. (2020). Transcription factors and evolution: an integral part of gene expression. World Academy of Sciences Journal, 2(1), 3-8.

Moganti, K., Li, F., Schmuttermaier, C., Riemann, S., Klüter, H., Gratchev, A., ... & Kzhyshkowska, J. (2017). Hyperglycemia induces mixed M1/M2 cytokine profile in primary human monocyte-derived macrophages. Immunobiology, 222(10), 952-959.

Mohmmad - Rezaei, M., Arefnezhad, R., Ahmadi, R., Abdollahpour - Alitappeh, M., Mirzaei, Y., Arjmand, M. H., ... & Bagheri, N. (2021). An overview of the innate and adaptive immune system in atherosclerosis. Iubmb Life, 73(1), 64-91.

Molnar, C., & Gair, J. (2013). 15.1 Digestive Systems. Concepts of Biology-1st Canadian Edition.

Monaghan, K. L., Zheng, W., Hu, G., & Wan, E. C. (2019). Monocytes and monocyte-derived antigen-presenting cells have distinct gene signatures in experimental model of multiple sclerosis. Frontiers in immunology, 10, 499553.

Montano, M. (2014). Translational biology in medicine. Elsevier.

Montecino-Rodriguez, E., & Dorshkind, K. (2012). B-1 B cell development in the fetus and adult. Immunity, 36(1), 13-21.

Mooradian, A. D. (2009). Dyslipidemia in type 2 diabetes mellitus. Nature Reviews Endocrinology, 5(3), 150-159.

Moore, A. J., Sarmiento, J., Mohtashami, M., Braunstein, M., Zúñiga-Pflücker, J. C., & Anderson, M. K. (2012). Transcriptional priming of intrathymic precursors for dendritic cell development. Development, 139(2), 373-384.

Moraes, D. (2018). What the relationship between CD90 e CD44 in Mesenchymal Stem Cells?. Cytotherapy, 20(5), S47.

Moraes, D. A., Sibov, T. T., Pavon, L. F., Alvim, P. Q., Bonadio, R. S., Da Silva, J. R., ... & Oliveira, D. M. (2016). A reduction in CD90 (THY-1) expression results in increased differentiation of mesenchymal stromal cells. Stem cell research & therapy, 7(1), 1-14.

MSDcytokineassay https://www.mesoscale.com/~/media/files/product%20inserts/proinflammatory%20panel%201%20mouse%20insert.pdf

Müller-Graff, F. T., Fitzner, B., Jaster, R., Vollmar, B., & Zechner, D. (2018). Impact of hyperglycemia on autoimmune pancreatitis and regulatory T-cells. World Journal of Gastroenterology, 24(28), 3120.

Mussbacher, M., Schossleitner, K., Kral-Pointner, J. B., Salzmann, M., Schrammel, A., & Schmid, J. A. (2022). More than just a monolayer: the multifaceted role of endothelial cells in the pathophysiology of atherosclerosis. Current atherosclerosis reports, 24(6), 483-492.

Nagareddy, P. R., Murphy, A. J., Stirzaker, R. A., Hu, Y., Yu, S., Miller, R. G., ... & Goldberg, I. J. (2013). Hyperglycemia promotes myelopoiesis and impairs the resolution of atherosclerosis. Cell metabolism, 17(5), 695-708.

Nagasawa, T. (2006). Microenvironmental niches in the bone marrow required for B-cell development. Nature Reviews Immunology, 6(2), 107-116.

Narayan, R. (2018). Encyclopedia of biomedical engineering. Elsevier.

Nedosugova, L. V., Markina, Y. V., Bochkareva, L. A., Kuzina, I. A., Petunina, N. A., Yudina, I. Y., & Kirichenko, T. V. (2022). Inflammatory Mechanisms of Diabetes and Its Vascular Complications. Biomedicines, 10(5), 1168.

Netea, M. G., Schlitzer, A., Placek, K., Joosten, L. A., & Schultze, J. L. (2019). Innate and adaptive immune memory: an evolutionary continuum in the host's response to pathogens. Cell host & microbe, 25(1), 13-26.

Newland, P. K., Lunsford, V., & Flach, A. (2017). The interaction of fatigue, physical activity, and health-related quality of life in adults with multiple sclerosis (MS) and cardiovascular disease (CVD). Applied Nursing Research, 33, 49-53.

Ngai, P., McCormick, S., Small, C., Zhang, X., Zganiacz, A., Aoki, N., & Xing, Z. (2007). Gamma interferon responses of CD4 and CD8 T-cell subsets are quantitatively different and independent of each other during pulmonary Mycobacterium bovis BCG infection. Infection and immunity, 75(5), 2244-2252.

N'Guessan, P. D., Riediger, F., Vardarova, K., Scharf, S., Eitel, J., Opitz, B., ... & Suttorp, N. (2009). Statins control oxidized LDL-mediated histone modifications and gene expression in cultured human endothelial cells. Arteriosclerosis, thrombosis, and vascular biology, 29(3), 380-386.

Nikolajczyk, B. S., Jagannathan-Bogdan, M., Shin, H., & Gyurko, R. (2011). State of the union between metabolism and the immune system in type 2 diabetes. Genes & Immunity, 12(4), 239-250.

Nikolov, D. B., & Burley, S. K. (1997). RNA polymerase II transcription initiation: a structural view. Proceedings of the National Academy of Sciences, 94(1), 15-22.

Nojima, I., Eikawa, S., Tomonobu, N., Hada, Y., Kajitani, N., Teshigawara, S., ... & Wada, J. (2020). Dysfunction of CD8+ PD-1+ T cells in type 2 diabetes caused by the impairment of metabolism-immune axis. Scientific reports, 10(1), 14928.

Nordén, R. (2013). Herpesvirus-induced glycans.

Nothelfer, K., Sansonetti, P. J., & Phalipon, A. (2015). Pathogen manipulation of B cells: the best defence is a good offence. Nature Reviews Microbiology, 13(3), 173-184.

Nurminen, V., Neme, A., Ryynänen, J., Heikkinen, S., Seuter, S., & Carlberg, C. (2015). The transcriptional regulator BCL6 participates in the secondary gene regulatory response to vitamin D. Biochimica et Biophysica Acta (BBA)-Gene Regulatory Mechanisms, 1849(3), 300-308.

O'Connell, K. E., Mikkola, A. M., Stepanek, A. M., Vernet, A., Hall, C. D., Sun, C. C., ... & Brown, D. E. (2015). Practical murine hematopathology: a comparative review and implications for research. Comparative medicine, 65(2), 96-113.

O'Donnell, C. J., & Elosua, R. (2008). Cardiovascular risk factors. Insights from framingham heart study. Revista Española de Cardiología (English Edition), 61(3), 299-310.

Oguntibeju, O. O. (2019). Type 2 diabetes mellitus, oxidative stress and inflammation: examining the links. International journal of physiology, pathophysiology and pharmacology, 11(3), 45.

Oh, E. S., You, Z., Nowak, K. L., & Jovanovich, A. J. (2022). Association of Monocyte Count and Monocyte/Lymphocyte Ratio with the Risk of Cardiovascular Outcomes in Patients with CKD. Kidney360, 3(4), 657.

Oh, S., Liu, X., Berzins, S. P., Naik, S. H., Gray, D. H., & Chong, M. M. (2023). Distinct subpopulations of DN1 thymocytes exhibit preferential γδ T lineage potential. Frontiers in immunology, 14, 1106652.

Ohnmacht, J., May, P., Sinkkonen, L., & Krüger, R. (2020). Missing heritability in Parkinson's disease: the emerging role of non-coding genetic variation. Journal of Neural Transmission, 127, 729-748.

Okeke, E. B., & Uzonna, J. E. (2019). The pivotal role of regulatory T cells in the regulation of innate immune cells. Frontiers in immunology, 10, 680.

Ong, S. B., Hernández-Reséndiz, S., Crespo-Avilan, G. E., Mukhametshina, R. T., Kwek, X. Y., Cabrera-Fuentes, H. A., & Hausenloy, D. J. (2018). Inflammation following acute myocardial infarction: multiple players, dynamic roles, and novel therapeutic opportunities. Pharmacology & therapeutics, 186, 73-87.

Orth, M., & Bellosta, S. (2012). Cholesterol: its regulation and role in central nervous system disorders. Cholesterol, 2012.

Ounzain, S., Bowen, S., Patel, C., Fujita, R., Heads, R. J., & Budhram-Mahadeo, V. S. (2011). Proliferation-associated POU4F2/Brn-3b transcription factor expression is regulated by oestrogen through ERα and growth factors *via* MAPK pathway. Breast Cancer Research, 13(1), R5.

Overgaard, N. H., Jung, J. W., Steptoe, R. J., & Wells, J. W. (2015). CD4+/CD8+ double-positive T cells: more than just a developmental stage?. Journal of Leucocyte Biology, 97(1), 31-38.

Pabst, R., & Westermann, J. (1991). The unique role of the spleen and its compartments in lymphocyte migration. Research in immunology, 142(4), 339-342.

Palasubramaniam, J., Wang, X., & Peter, K. (2019). Myocardial infarction—From atherosclerosis to thrombosis: Uncovering new diagnostic and therapeutic approaches. Arteriosclerosis, thrombosis, and vascular biology, 39(8), e176-e185.

Pan, L., Yang, Z., Feng, L., & Gan, L. (2005). Functional equivalence of Brn3 POU-domain transcription factors in mouse retinal neurogenesis. Development, 132(4), 703-712.

Panagiotou, E., Syrigos, N. K., Charpidou, A., Kotteas, E., & Vathiotis, I. A. (2022). CD24: a novel target for cancer immunotherapy. Journal of Personalized Medicine, 12(8), 1235.

Parameswaran, N., & Patial, S. (2010). Tumor necrosis factor-α signaling in macrophages. Critical Reviews™ in Eukaryotic Gene Expression, 20(2).

Park, C. W., Kim, K. S., Bae, S., Son, H. K., Myung, P. K., Hong, H. J., & Kim, H. (2009). Cytokine secretion profiling of human mesenchymal stem cells by antibody array. International journal of stem cells, 2(1), 59.

Park, J. B., & Avolio, A. (2023). Arteriosclerosis and atherosclerosis assessment in clinical practice: Methods and significance. Pulse, 11(1), 1-8.

Pasumarthi, K. B., & Field, L. J. (2002). Cardiomyocyte cell cycle regulation. Circulation research, 90(10), 1044-1054.

Patel, A. A., Ginhoux, F., & Yona, S. (2021). Monocytes, macrophages, dendritic cells and neutrophils: an update on lifespan kinetics in health and disease. Immunology, 163(3), 250-261.

Patel, H., & Davidson, D. (2014). Control of pro-inflammatory cytokine release from human monocytes with the use of an interleukin-10 monoclonal antibody. In Cytokine Bioassays (pp. 99-106). Humana Press, New York, NY.

Perry, S. S., Welner, R. S., Kouro, T., Kincade, P. W., & Sun, X. H. (2006). Primitive lymphoid progenitors in bone marrow with T lineage reconstituting potential. The Journal of Immunology, 177(5), 2880-2887.

Petrie, H. T., & Kincade, P. W. (2005). Many roads, one destination for T cell progenitors. The Journal of experimental medicine, 202(1), 11-13.

Pettengill, M. A., van Haren, S. D., & Levy, O. (2014). Soluble mediators regulating immunity in early life. Frontiers in immunology, 5, 110462.

Phillips, T. & Hoopes, L. (2008) Transcription factors and transcriptional control in eukaryotic cells. Nature Education 1(1):119

Picot, T., Aanei, C. M., Flandrin Gresta, P., Noyel, P., Tondeur, S., Tavernier Tardy, E., ... & Campos Catafal, L. (2018). Evaluation by flow cytometry of mature monocyte subpopulations for the diagnosis and follow-up of chronic myelomonocytic leukemia. Frontiers in oncology, 8, 109.

Pinto, S. M., Kim, H., Subbannayya, Y., Giambelluca, M. S., Bösl, K., Ryan, L., ... & Kandasamy, R. K. (2021). Comparative proteomic analysis reveals varying impact on immune responses in phorbol 12-myristate-13-acetate-mediated THP-1 monocyte-to-macrophage differentiation. Frontiers in Immunology, 2241.

Pinzone, J. J., Hall, B. M., Thudi, N. K., Vonau, M., Qiang, Y. W., Rosol, T. J., & Shaughnessy Jr, J. D. (2009). The role of Dickkopf-1 in bone development, homeostasis, and disease. Blood, The Journal of the American Society of Hematology, 113(3), 517-525.

Pober, J. S., & Tellides, G. (2012). Participation of blood vessel cells in human adaptive immune responses. Trends in immunology, 33(1), 49-57.

Polak-Iwaniuk, A., Harasim-Symbor, E., Gołaszewska, K., & Chabowski, A. (2019). How hypertension affects heart metabolism?. Frontiers in Physiology, 10, 435.

Pollack, R. M., Donath, M. Y., LeRoith, D., & Leibowitz, G. (2016). Anti-inflammatory agents in the treatment of diabetes and its vascular complications. Diabetes care, 39(Supplement_2), S244-S252.

Ponnusamy, M., Li, P. F., & Wang, K. (2017). Understanding cardiomyocyte proliferation: an insight into cell cycle activity. Cellular and Molecular Life Sciences, 74(6), 1019-1034.

Popko, K., Gorska, E., Stelmaszczyk-Emmel, A., Plywaczewski, R., Stoklosa, A., Gorecka, D., ... & Demkow, U. (2010). Proinflammatory cytokines Il-6 and TNF-α and the development of inflammation in obese subjects. European journal of medical research, 15(2), 1-3.

Porritt, H. E., Rumfelt, L. L., Tabrizifard, S., Schmitt, T. M., Zúñiga-Pflücker, J. C., & Petrie, H. T. (2004). Heterogeneity among DN1 prothymocytes reveals multiple progenitors with different capacities to generate T cell and non-T cell lineages. Immunity, 20(6), 735-745.

Prasad, C., Davis, K. E., Imrhan, V., Juma, S., & Vijayagopal, P. (2019). Advanced glycation end products and risks for chronic diseases: intervening through lifestyle modification. American Journal of Lifestyle Medicine, 13(4), 384-404.

Price, P. W., & Cerny, J. (1999). Characterization of CD4+ T cells in mouse bone marrow. I. Increased activated/memory phenotype and altered TCR Vβ repertoire. European journal of immunology, 29(3), 1051-1056.

Prinz, I., Sansoni, A., Kissenpfennig, A., Ardouin, L., Malissen, M., & Malissen, B. (2006). Visualization of the earliest steps of γδ T cell development in the adult thymus. Nature immunology, 7(9), 995-1003.

Pugsley, M. K., & Tabrizchi, R. (2000). The vascular system: An overview of structure and function. Journal of pharmacological and toxicological methods, 44(2), 333-340.

Pulugulla, S. H., Packard, T. A., Galloway, N. L., Grimmett, Z. W., Doitsh, G., Adamik, J., ... & Auron, P. E. (2018). Distinct mechanisms regulate IL1B gene transcription in lymphoid CD4 T cells and monocytes. Cytokine, 111, 373-381.

Qin, Y., Guan, J., & Zhang, C. (2014). Mesenchymal stem cells: mechanisms and role in bone regeneration. Postgraduate Medical Journal, 90(1069), 643-647.

Queiroz, L. A., Assis, J. B., Guimarães, J., Sousa, E. S., Milhomem, A. C., Sunahara, K. K., ... & Martins, J. O. (2021). Endangered lymphocytes: The effects of alloxan and streptozotocin on immune cells in type 1 induced diabetes. Mediators of Inflammation, 2021.

Rachubik, P., Szrejder, M., Audzeyenka, I., Rogacka, D., Rychłowski, M., Angielski, S., & Piwkowska, A. (2020). The PKGIα/VASP pathway is involved in

insulin-and high glucose-dependent regulation of albumin permeability in cultured rat podocytes. The journal of biochemistry, 168(6), 575-588.

Rafieian-Kopaei, M., Setorki, M., Doudi, M., Baradaran, A., & Nasri, H. (2014). Atherosclerosis: process, indicators, risk factors and new hopes. International journal of preventive medicine, 5(8), 927.

Rahman, M. S., Hossain, K. S., Das, S., Kundu, S., Adegoke, E. O., Rahman, M. A., ... & Pang, M. G. (2021). Role of insulin in health and disease: an update. International journal of molecular sciences, 22(12), 6403.

Raife, T. J., Lager, D. J., Kemp, J. D., & Dick, F. R. (1994). Expression of CD24 (BA-1) predicts monocytic lineage in acute myeloid leukemia. American journal of clinical pathology, 101(3), 296-299.

Rajasagi, M., Vitacolonna, M., Benjak, B., Marhaba, R., & Zöller, M. (2009). CD44 promotes progenitor homing into the thymus and T cell maturation. Journal of Leucocyte Biology, 85(2), 251-261.

Rakebrandt, N., & Joller, N. (2019). Infection history determines susceptibility to unrelated diseases. BioEssays, 41(6), 1800191.

Ralston, A., & Shaw, K. (2008). Gene expression regulates cell differentiation. Nat Educ, 1(1), 127-131.

Ramakrishnan, P., Kahn, D. A., & Baltimore, D. (2011). Anti-apoptotic effect of hyperglycemia can allow survival of potentially autoreactive T cells. Cell Death & Differentiation, 18(4), 690-699.

Ramalho, A. S., Beck, S., Farinha, C. M., Clarke, L. A., Heda, G. D., Steiner, B., ... & Tzetis, M. (2004). Methods for RNA extraction, cDNA preparation and analysis of CFTR transcripts. Journal of Cystic Fibrosis, 3, 11-15.

Ramasamy, S. K. (2017). Structure and functions of blood vessels and vascular niches in bone. Stem cells international, 2017.

Rask-Madsen, C., & King, G. L. (2013). Vascular complications of diabetes: mechanisms of injury and protective factors. Cell metabolism, 17(1), 20-33.

Ratajczak, M. Z., & Kucia, M. (2022). Hematopoiesis and innate immunity: an inseparable couple for good and bad times, bound together by an hormetic relationship. Leukemia, 36(1), 23-32.

Rattan, S., & Ali, M. (2015). Role of SM22 in the differential regulation of phasic vs. tonic smooth muscle. American Journal of Physiology-Gastrointestinal and Liver Physiology, 308(7), G605-G612.

Ray-Jones, H., & Spivakov, M. (2021). Transcriptional enhancers and their communication with gene promoters. Cellular and Molecular Life Sciences, 78(19-20), 6453-6485.

Ray, P., Krishnamoorthy, N., Oriss, T. B., & Ray, A. (2010). Signaling of c - kit in dendritic cells influences adaptive immunity. Annals of the New York Academy of Sciences, 1183(1), 104-122.

Reali, E., Ferrando-Martinez, S., & Catalfamo, M. (2021). The interplay between immune activation and cardiovascular disease during infection, autoimmunity and aging: The role of T cells. Frontiers in Immunology, 12, 719517.

Reddy, M. A., Das, S., Zhuo, C., Jin, W., Wang, M., Lanting, L., & Natarajan, R. (2016). Regulation of vascular smooth muscle cell dysfunction under diabetic conditions by miR-504. Arteriosclerosis, thrombosis, and vascular biology, 36(5), 864-873.

Redhu, N. S., Saleh, A., Halayko, A. J., Ali, A. S., & Gounni, A. S. (2011). Essential role of NF-κB and AP-1 transcription factors in TNF-α-induced TSLP expression in human airway smooth muscle cells. American Journal of Physiology-Lung Cellular and Molecular Physiology, 300(3), L479-L485.

Reijrink, M., van Ark, J., Lexis, C. P. H., Visser, L. M., Lodewijk, M. E., van der Horst, I. C. C., ... & Hillebrands, J. L. (2022). Increased frequency of proangiogenic tunica intima endothelial kinase 2 (Tie2) expressing monocytes in individuals with type 2 diabetes mellitus. Cardiovascular Diabetology, 21(1), 1-16.

Rengarajan, A., Goldblatt, H. E., Beebe, D. J., Virumbrales-Muñoz, M., & Boeldt, D. S. (2024). Immune cells and inflammatory mediators cause endothelial dysfunction in a vascular microphysiological system. Lab on a Chip, 24(6), 1808-1820.

Rhein, P., Mitlohner, R., Basso, G., Gaipa, G., Dworzak, M. N., Kirschner-Schwabe, R., ... & Ratei, R. (2010). CD11b is a therapy resistance–and minimal residual disease–specific marker in precursor B-cell acute lymphoblastic

leukemia. Blood, The Journal of the American Society of Hematology, 115(18), 3763-3771.

Riaz, S. (2015). Study of protein biomarkers of diabetes mellitus type 2 and therapy with vitamin B1. Journal of diabetes research, 2015.

Riekstina, U., Cakstina, I., Parfejevs, V., Hoogduijn, M., Jankovskis, G., Muiznieks, I., ... & Ancans, J. (2009). Embryonic stem cell marker expression pattern in human mesenchymal stem cells derived from bone marrow, adipose tissue, heart and dermis. Stem Cell Reviews and Reports, 5(4), 378-386.

Rinschen, M. M., Ivanisevic, J., Giera, M., & Siuzdak, G. (2019). Identification of bioactive metabolites using activity metabolomics. Nature Reviews Molecular Cell Biology, 20(6), 353-367.

Rizzoni, D., De Ciuceis, C., Szczepaniak, P., Paradis, P., Schiffrin, E. L., & Guzik, T. J. (2022). Immune system and microvascular remodeling in humans. Hypertension, 79(4), 691-705.

RNA Isolation with TRIzol (Invitrogen) and Qiagen RNAeasy https://www.cancer.gov/ccg/research/structural-genomics/target/using-target-data/nbl-rna-prep-trizol.pdf

Robert, P. A., Kunze-Schumacher, H., Greiff, V., & Krueger, A. (2021). Modeling the dynamics of T-cell development in the thymus. Entropy, 23(4), 437.

Robinson, M. W., Harmon, C., & O'Farrelly, C. (2016). Liver immunology and its role in inflammation and homeostasis. Cellular & molecular immunology, 13(3), 267-276.

Rocamonde, B., Carcone, A., Mahieux, R., & Dutartre, H. (2019). HTLV-1 infection of myeloid cells: from transmission to immune alterations. Retrovirology, 16, 1-12.

Röder, P. V., Wu, B., Liu, Y., & Han, W. (2016). Pancreatic regulation of glucose homeostasis. Experimental & molecular medicine, 48(3), e219-e219.

Rodewald, H. R., Kretzschmar, K., Takeda, S., Hohl, C., & Dessing, M. (1994). Identification of pro - thymocytes in murine fetal blood: T lineage commitment can precede thymus colonization. The EMBO journal, 13(18), 4229-4240.

Rodig, S. J., Shahsafaei, A., Li, B., & Dorfman, D. M. (2005). The CD45 isoform B220 identifies select subsets of human B cells and B-cell lymphoproliferative disorders. Human pathology, 36(1), 51-57.

Romagnani, S. (1992). Type 1 T helper and type 2 T helper cells: functions, regulation and role in protection and disease. International Journal of Clinical and Laboratory Research, 21(2), 152-158.

Rotondo, F., Ho-Palma, A. C., Remesar, X., Fernández-López, J. A., del Mar Romero, M., & Alemany, M. (2017). Glycerol is synthesized and secreted by adipocytes to dispose of excess glucose, *via* glycerogenesis and increased acyl-glycerol turnover. Scientific reports, 7(1), 1-14.

Roy, A. L. (2019). Transcriptional regulation in the immune system: one cell at a time. Frontiers in immunology, 10, 1355.

Rudijanto, A. (2007). The role of vascular smooth muscle cells on the pathogenesis of atherosclerosis. Acta Med Indones, 39(2), 86-93.

Rui, L. (2011). Energy metabolism in the liver. Comprehensive physiology, 4(1), 177-197.

Rumfelt, L. L., Zhou, Y., Rowley, B. M., Shinton, S. A., & Hardy, R. R. (2006). Lineage specification and plasticity in CD19− early B cell precursors. The Journal of experimental medicine, 203(3), 675-687.

Saba, A., & Oridupa, O. (2012). Lipoproteins and cardiovascular diseases. Lipoproteins-role in health and diseases, 197-222.

Sadofsky, L. R., Hayman, Y. A., Vance, J., Cervantes, J. L., Fraser, S. D., Wilkinson, H. N., ... & Morice, A. H. (2019). Characterisation of a new human alveolar macrophage-like cell line (Daisy). Lung, 197, 687-698.

Salari, V., Mengoni, F., Del Gallo, F., Bertini, G., & Fabene, P. F. (2020). The anti-inflammatory properties of mesenchymal stem cells in epilepsy: Possible treatments and future perspectives. International Journal of Molecular Sciences, 21(24), 9683.

Samady, L., Dennis, J. J., Budhram-Mahadeo, V., & Latchman, D. S. (2004). Activation of CDK4 gene expression in human breast cancer cells by the Brn-3b POU family transcription factor. Cancer Biology & Therapy, 3(3), 317-323.

Samady, L., Faulkes, D. J., Budhram - Mahadeo, V., Ndisang, D., Potter, E., Brabant, G., & Latchman, D. S. (2006). The Brn - 3b POU family transcription factor represses plakoglobin gene expression in human breast cancer cells. International journal of cancer, 118(4), 869-878.

Samanthi, (2018). Difference Between General and Specific Transcription Factors. (2018 January 26). Retrieved (date), from http://differencebetween.com/difference-betweengeneral-and-vs-specific-transcription-factors/

Saran, N., Łyszkiewicz, M., Pommerencke, J., Witzlau, K., Vakilzadeh, R., Ballmaier, M., ... & Krueger, A. (2010). Multiple extrathymic precursors contribute to T-cell development with different kinetics. Blood, The Journal of the American Society of Hematology, 115(6), 1137-1144.

Saran, N., Pommerencke, J., Witzlau, K., Regelin, M., & Krueger, A. (2012). Extra-thymic physiological T lineage progenitor activity is exclusively confined to cells expressing either CD127, CD90, or high levels of CD117. Plos one, 7(2), e30864.

Sauls, R. S., McCausland, C., & Taylor, B. N. (2018). Histology, T-cell lymphocyte.

Schäfer, S., & Zernecke, A. (2020). CD8+ T cells in atherosclerosis. Cells, 10(1), 37.

Schirrmacher, V. (2023). Bone marrow: The central immune system. Immuno, 3(3), 289-329.

Schnoegl, D., Hiesinger, A., Huntington, N. D., & Gotthardt, D. (2023). AP-1 transcription factors in cytotoxic lymphocyte development and antitumor immunity. Current Opinion in Immunology, 85, 102397.

Schnoor, M., Buers, I., Sietmann, A., Brodde, M. F., Hofnagel, O., Robenek, H., & Lorkowski, S. (2009). Efficient non-viral transfection of THP-1 cells. Journal of immunological methods, 344(2), 109-115.

Schofield, J. D., Liu, Y., Rao-Balakrishna, P., Malik, R. A., & Soran, H. (2016). Diabetes dyslipidemia. Diabetes therapy, 7(2), 203-219.

Schubert, W., Frank, P. G., Razani, B., Park, D. S., Chow, C. W., & Lisanti, M. P. (2001). Caveolae-deficient endothelial cells show defects in the uptake and transport of albumin *in vivo*. Journal of Biological Chemistry, 276(52), 48619-48622.

Schumann, J., Stanko, K., Schliesser, U., Appelt, C., & Sawitzki, B. (2015). Differences in CD44 surface expression levels and function discriminates IL-17 and IFN-γ producing helper T cells. PLoS One, 10(7), e0132479.

Schürch, C. M., Caraccio, C., & Nolte, M. A. (2021). Diversity, localization, and (patho) physiology of mature lymphocyte populations in the bone marrow. Blood, The Journal of the American Society of Hematology, 137(22), 3015-3026.

Schwartz, D. M., Burma, A. M., Kitakule, M. M., Luo, Y., & Mehta, N. N. (2020). T cells in autoimmunity-associated cardiovascular diseases. Frontiers in Immunology, 11, 588776.

Schwende, H., Fitzke, E., Ambs, P., & Dieter, P. (1996). Differences in the state of differentiation of THP - 1 cells induced by phorbol ester and 1, 25 - dihydroxyvitamin D3. Journal of leukocyte biology, 59(4), 555-561.

Seder, R. A., & Ahmed, R. (2003). Similarities and differences in CD4+ and CD8+ effector and memory T cell generation. Nature immunology, 4(9), 835-842.

Selimoglu-Buet, D., Wagner-Ballon, O., Saada, V., Bardet, V., Itzykson, R., Bencheikh, L., ... & Solary, E. (2015). Characteristic repartition of monocyte subsets as a diagnostic signature of chronic myelomonocytic leukemia. Blood, The Journal of the American Society of Hematology, 125(23), 3618-3626.

Seo, I. H., & Lee, Y. J. (2022). Usefulness of complete blood count (CBC) to assess cardiovascular and metabolic diseases in clinical settings: a comprehensive literature review. Biomedicines, 10(11), 2697.

Serrano-Lopez, J., Hegde, S., Kumar, S., Serrano, J., Fang, J., Wellendorf, A. M., ... & Cancelas, J. A. (2021). Inflammation rapidly recruits mammalian GMP and MDP from bone marrow into regional lymphatics. Elife, 10, e66190.

Shah, D. K. (2014). T - cell development in the thymus. BiteSized Immunology, British Society for Immunology.

Shaheen, M., & Broxmeyer, H. E. (2018). Cytokine/receptor families and signal transduction. In Hematology: Basic principles and practice (pp. 163-175). Elsevier Inc.

Shao, D., & Tian, R. (2015). Glucose transporters in cardiac metabolism and hypertrophy. Comprehensive Physiology, 6(1), 331.

Shen, Jianbin, Donghong Ju, Shichao Wu, Jiawei Zhao, Lucynda Pham, Alejandro Ponce, Maozhou Yang et al. "SM22α deficiency: promoting vascular fibrosis *via* SRF-SMAD3-mediated activation of Col1a2 transcription following arterial injury." Research Square (2024).

Sheng, J., Chen, Q., Soncin, I., Ng, S. L., Karjalainen, K., & Ruedl, C. (2017). A discrete subset of monocyte-derived cells among typical conventional type 2 dendritic cells can efficiently cross-present. Cell reports, 21(5), 1203-1214.

Shi, C., & Pamer, E. G. (2011). Monocyte recruitment during infection and inflammation. Nature reviews immunology, 11(11), 762-774.

Shifera, A. S., Leong, D., & Hardin, J. A. (2010). Vitamin D does not modulate NF-κB activity in Jurkat T cells. Immunology letters, 131(2), 151-158.

Shihan, M. H., Novo, S. G., Le Marchand, S. J., Wang, Y., & Duncan, M. K. (2021). A simple method for quantitating confocal fluorescent images. Biochemistry and biophysics reports, 25, 100916.

Shimizu, I., & Minamino, T. (2016). Physiological and pathological cardiac hypertrophy. Journal of molecular and cellular cardiology, 97, 245-262.

Shiraz, A. K., Panther, E. J., & Reilly, C. M. (2022). Altered germinal-center metabolism in B cells in autoimmunity. Metabolites, 12(1), 40.

Simmons, D. (2008). Epigenetic influence and disease. Nature Education, 1(1), 6.

Singh, A. K., & Cancelas, J. A. (2020). Gap junctions in the bone marrow lympho-hematopoietic stem cell niche, leukemia progression, and chemoresistance. International journal of molecular sciences, 21(3), 796.

Sixt, M., & Lämmermann, T. (2020). T cells: bridge-and-channel commute to the white pulp. Immunity, 52(5), 721-723.

Skordos, I., Demeyer, A., & Beyaert, R. (2021). Analysis of T cells in mouse lymphoid tissue and blood with flow cytometry. STAR protocols, 2(1), 100351.

Smolen, K. K., Plotkin, A. L., Shannon, C. P., Idoko, O. T., Pak, J., Darboe, A., ... & EPIC Consortium. (2021). Ontogeny of plasma cytokine and chemokine concentrations across the first week of human life. Cytokine, 148, 155704.

Song, W., Zhang, C. L., Gou, L., He, L., Gong, Y. Y., Qu, D., ... & Huang, Y. (2019). Endothelial TFEB (transcription factor EB) restrains IKK (IκB kinase)-p65 pathway to attenuate vascular inflammation in diabetic db/db mice. Arteriosclerosis, thrombosis, and vascular biology, 39(4), 719-730

Sorokin, V., Vickneson, K., Kofidis, T., Woo, C. C., Lin, X. Y., Foo, R., & Shanahan, C. M. (2020). Role of vascular smooth muscle cell plasticity and interactions in vessel wall inflammation. Frontiers in immunology, 11, 599415.

Spagnoli, L. G., Bonanno, E., Sangiorgi, G., & Mauriello, A. (2007). Role of inflammation in atherosclerosis. Journal of nuclear medicine, 48(11), 1800-1815.

Spivakov, M. (2014). Spurious transcription factor binding: non - functional or genetically redundant?. Bioessays, 36(8), 798-806.

Sprague, A. H., & Khalil, R. A. (2009). Inflammatory cytokines in vascular dysfunction and vascular disease. Biochemical pharmacology, 78(6), 539-552.

Srikakulapu, P., & McNamara, C. A. (2017). B cells and atherosclerosis. American Journal of Physiology-Heart and Circulatory Physiology, 312(5), H1060-H1067.

Srikakulapu, P., & McNamara, C. A. (2020). B lymphocytes and adipose tissue inflammation. Arteriosclerosis, Thrombosis, and Vascular Biology, 40(5), 1110-1122.

Staats, J., Divekar, A., McCoy, J. P., & Maecker, H. T. (2019). Guidelines for gating flow cytometry data for immunological assays. Immunophenotyping: Methods and Protocols, 81-104.

Stagg, A. J., Burke, F., Hill, S., & Knight, S. C. (2001). Isolation of mouse spleen dendritic cells. In Dendritic Cell Protocols (pp. 9-22). Humana Press.

Stenmark, K. R., Yeager, M. E., El Kasmi, K. C., Nozik-Grayck, E., Gerasimovskaya, E. V., Li, M., ... & Frid, M. G. (2013). The adventitia: essential

regulator of vascular wall structure and function. Annual review of physiology, 75(1), 23-47.

Sticka, K. D., Schnurr, T. M., Jerome, S. P., Dajles, A., Reynolds, A. J., Duffy, L. K., ... & Dunlap, K. L. (2018). Exercise increases glucose transporter-4 levels on peripheral blood mononuclear cells. Medicine and science in sports and exercise, 50(5), 938.

Stone, W. L., Basit, H., & Burns, B. (2021). Pathology, inflammation. In StatPearls [Internet]. StatPearls Publishing.

Stukenborg, J. B., Kjartansdóttir, K. R., Reda, A., Colon, E., Albersmeier, J. P., & Söder, O. (2014). Male germ cell development in humans. Hormone research in paediatrics, 81(1), 2-12.

Stylianou, I. M., Bauer, R. C., Reilly, M. P., & Rader, D. J. (2012). Genetic basis of atherosclerosis: insights from mice and humans. Circulation research, 110(2), 337-355.

Sudheendran, S., Chang, C. C., & Deckelbaum, R. J. (2010). N-3 vs. saturated fatty acids: effects on the arterial wall. Prostaglandins, Leukotrienes and Essential Fatty Acids (PLEFA), 82(4-6), 205-209.

Sulkava, M., Raitoharju, E., Levula, M., Seppälä, I., Lyytikäinen, L. P., Mennander, A., ... & Klopp, N. (2017). Differentially expressed genes and canonical pathway expression in human atherosclerotic plaques–Tampere Vascular Study. Scientific reports, 7(1), 1-10.

Summers, M. E., Richmond, B. W., Kropski, J. A., Majka, S. A., Bastarache, J. A., Hatzopoulos, A. K., ... & Majka, S. M. (2021). Balanced Wnt/Dickkopf-1 signaling by mesenchymal vascular progenitor cells in the microvascular niche maintains distal lung structure and function. American Journal of Physiology-Cell Physiology, 320(1), C119-C131.

Summers, M. E., Richmond, B. W., Menon, S., Sheridan, R. M., Kropski, J. A., Majka, S. A., ... & Majka, S. M. (2020). Resident mesenchymal vascular progenitors modulate adaptive angiogenesis and pulmonary remodeling via regulation of canonical Wnt signaling. The FASEB Journal, 34(8), 10267-10285.

Sun, B., Chen, H., Xue, J., Li, P., & Fu, X. (2023). The role of GLUT2 in glucose metabolism in multiple organs and tissues. Molecular biology reports, 50(8), 6963-6974.

Sun, L., Su, Y., Jiao, A., Wang, X., & Zhang, B. (2023). T cells in health and disease. Signal Transduction and Targeted Therapy, 8(1), 235.

Sun, L., Wang, X., Saredy, J., Yuan, Z., Yang, X., & Wang, H. (2020). Innate-adaptive immunity interplay and redox regulation in immune response. Redox biology, 37, 101759.

Sun, D., Luo, T., Dong, P., Zhang, N., Chen, J., Zhang, S., ... & Zhang, S. (2020). CD86+/CD206+ tumor-associated macrophages predict prognosis of patients with intrahepatic cholangiocarcinoma. PeerJ, 8, e8458.

Sun, W., & Hu, Z. W. (2013). Making T cells functional: a new solution for the athymic BMT recipients. Acta Pharmacologica Sinica, 34(2), 189-190.

Tabas, I., & Lichtman, A. H. (2017). Monocyte-macrophages and T cells in atherosclerosis. Immunity, 47(4), 621-634.

Tachikawa, S., Kawamura, T., Kawamura, H., Kanda, Y., Fujii, Y., Matsumoto, H., & Abo, T. (2008). Appearance of B220low autoantibody-producing B-1 cells at neonatal and older stages in mice. Clinical & Experimental Immunology, 153(3), 448-455.

Talukdar, P. D., & Chatterji, U. (2023). Transcriptional co-activators: emerging roles in signaling pathways and potential therapeutic targets for diseases. Signal Transduction and Targeted Therapy, 8(1), 427.

Tan, C., Taylor, A. A., Coburn, M. Z., Marino, J. H., Van De Wiele, C. J., & Teague, T. K. (2011). Ten-color flow cytometry reveals distinct patterns of expression of CD124 and CD126 by developing thymocytes. BMC immunology, 12, 1-9.

Tan, F., Cao, Y., Zheng, L., Wang, T., Zhao, S., Chen, J., ... & Chi, X. (2022). Diabetes exacerbated sepsis-induced intestinal injury by promoting M1 Macrophage Polarization *via* miR-3061/Snail1 signaling.

Tan, W. C. C., Nerurkar, S. N., Cai, H. Y., Ng, H. H. M., Wu, D., Wee, Y. T. F., ... & Lim, T. K. H. (2020). Overview of multiplex

immunohistochemistry/immunofluorescence techniques in the era of cancer immunotherapy. Cancer Communications, 40(4), 135-153.

Tan, Y., Cheong, M. S., & Cheang, W. S. (2022). Roles of reactive oxygen species in vascular complications of diabetes: therapeutic properties of medicinal plants and food. Oxygen, 2(3), 246-268.

Tang, Z., Wang, A., Yuan, F., Yan, Z., Liu, B., Chu, J. S., ... & Li, S. (2012). Differentiation of multipotent vascular stem cells contributes to vascular diseases. Nature communications, 3(1), 875.

Tarfi, S., Harrivel, V., Dumezy, F., Guy, J., Roussel, M., Mimoun, A., ... & Groupe Francophone des Myélodysplasies (GFM). (2018). Multicenter validation of the flow measurement of classical monocyte fraction for chronic myelomonocytic leukemia diagnosis. Blood Cancer Journal, 8(11), 114.

Taylor, C. A., Shawlot, W., Ren, J. X., & Mukhopadhyay, S. (2019). Generation and Validation of Tissue - Specific Knockout Strains for Toxicology Research. Current protocols in toxicology, 81(1), e86.

Tchilian, E. Z., Dawes, R., Hyland, L., Montoya, M., Le Bon, A., Borrow, P., ... & Beverley, P. C. (2004). Altered CD45 isoform expression affects lymphocyte function in CD45 Tg mice. International immunology, 16(9), 1323-1332.

Teixeira, L. K., Fonseca, B. P., Vieira-de-Abreu, A., Barboza, B. A., Robbs, B. K., Bozza, P. T., & Viola, J. P. (2005). IFN-γ production by CD8+ T cells depends on NFAT1 transcription factor and regulates Th differentiation. The Journal of Immunology, 175(9), 5931-5939.

Tellides, G., & Pober, J. S. (2015). Inflammatory and immune responses in the arterial media. Circulation research, 116(2), 312-322.

Thapa, P., & Farber, D. L. (2019). The role of the thymus in the immune response. Thoracic surgery clinics, 29(2), 123-131.

Theobalt, N., Hofmann, I., Fiedler, S., Renner, S., Dhom, G., Feuchtinger, A., ... & Blutke, A. (2021). Unbiased analysis of obesity related, fat depot specific changes of adipocyte volumes and numbers using light sheet fluorescence microscopy. Plos one, 16(3), e0248594.

Thomas, A. M., Dong, Y., Beskid, N. M., García, A. J., Adams, A. B., & Babensee, J. E. (2020). Brief exposure to hyperglycemia activates dendritic cells *in vitro* and *in vivo*. Journal of cellular physiology, 235(6), 5120-5129.

Tiwari, A., Elgrably, B., Saar, G., & Vandoorne, K. (2022). Multi-scale imaging of vascular pathologies in cardiovascular disease. Frontiers in Medicine, 8, 754369.

Tompa, A., & Faresjö, M. (2023). Shift in the B cell subsets between children with type 1 diabetes and/or celiac disease. Clinical and Experimental Immunology, uxad136.

Tong, X., Gu, J., Song, R., Wang, D., Sun, Z., Sui, C., ... & Liu, Z. (2019). Osteoprotegerin inhibit osteoclast differentiation and bone resorption by enhancing autophagy *via* AMPK/mTOR/p70S6K signaling pathway *in vitro*. Journal of Cellular Biochemistry, 120(2), 1630-1642.

Torres-Castro, I., Arroyo-Camarena, Ú. D., Martínez-Reyes, C. P., Gómez-Arauz, A. Y., Dueñas-Andrade, Y., Hernández-Ruiz, J., ... & Escobedo, G. (2016). Human monocytes and macrophages undergo M1-type inflammatory polarization in response to high levels of glucose. Immunology letters, 176, 81-89.

Trop-Steinberg, S., & Azar, Y. (2017). AP-1 expression and its clinical relevance in immune disorders and cancer. The American journal of the medical sciences, 353(5), 474-483.

Tsioufis, P., Theofilis, P., Tsioufis, K., & Tousoulis, D. (2022). The impact of cytokines in coronary atherosclerotic plaque: current therapeutic approaches. International Journal of Molecular Sciences, 23(24), 15937.

Tune, J. D., Goodwill, A. G., Sassoon, D. J., & Mather, K. J. (2017). Cardiovascular consequences of metabolic syndrome. Translational Research, 183, 57-70.

Tylutka, A., Walas, Ł., & Zembron-Lacny, A. (2024). Level of IL-6, TNF, and IL-1β and age-related diseases: a systematic review and meta-analysis. Frontiers in Immunology, 15, 1330386.

Ubanako, P., Xelwa, N., & Ntwasa, M. (2019). LPS induces inflammatory chemokines *via* TLR-4 signalling and enhances the Warburg Effect in THP-1 cells. PloS one, 14(9), e0222614.

Umare, V., Pradhan, V., Nadkar, M., Rajadhyaksha, A., Patwardhan, M., Ghosh, K. K., & Nadkarni, A. H. (2014). Effect of proinflammatory cytokines (IL-6, TNF-α, and IL-1β) on clinical manifestations in Indian SLE patients. Mediators of inflammation, 2014.

Vaeth, M., & Feske, S. (2018). NFAT control of immune function: New frontiers for an abiding trooper. F1000Res. 7: 260. Journal Article Review Competing interests: SF is a co-founder of CalciMedica. MV declares that he has no competing interests. No competing interests were disclosed. No competing interests were disclosed. https://doi. org/10, 12688, f1000research.

Vale, A. M., & Schroeder Jr, H. W. (2010). Clinical consequences of defects in B-cell development. Journal of Allergy and Clinical Immunology, 125(4), 778-787.

van de Schans, V. A., Smits, J. F., & Blankesteijn, W. M. (2008). The Wnt/frizzled pathway in cardiovascular development and disease: friend or foe?. European journal of pharmacology, 585(2-3), 338-345.

Van Den Eeckhout, B., Huyghe, L., Van Lint, S., Burg, E., Plaisance, S., Peelman, F., ... & Tavernier, J. (2021). Selective IL-1 activity on CD8+ T cells empowers antitumor immunity and synergizes with neovasculature-targeted TNF for full tumor eradication. Journal for Immunotherapy of Cancer, 9(11).

Van Niekerk, G., Davis, T., Patterton, H. G., & Engelbrecht, A. M. (2019). How Does Inflammation - Induced Hyperglycemia Cause Mitochondrial Dysfunction in Immune Cells?. BioEssays, 41(5), 1800260.

van Vlerken-Ysla, L., Tyurina, Y. Y., Kagan, V. E., & Gabrilovich, D. I. (2023). Functional states of myeloid cells in cancer. Cancer Cell, 41(3), 490-504.

Vanessa Fiorentino, T., Prioletta, A., Zuo, P., & Folli, F. (2013). Hyperglycemia-induced oxidative stress and its role in diabetes mellitus related cardiovascular diseases. Current pharmaceutical design, 19(32), 5695-5703.

Vats, D., Mukundan, L., Odegaard, J. I., Zhang, L., Smith, K. L., Morel, C. R., ... & Chawla, A. (2006). Oxidative metabolism and PGC-1β attenuate macrophage-mediated inflammation. Cell metabolism, 4(1), 13-24.

Verrills, N. M. (2006). Clinical proteomics: present and future prospects. Clinical Biochemist Reviews, 27(2), 99.

Villa-Bellosta, R., & Hamczyk, M. R. (2015). Isolation and culture of aortic smooth muscle cells and *in vitro* calcification assay. In Methods in Mouse Atherosclerosis (pp. 119-129). Humana Press, New York, NY.

Villarino, A. V., Kanno, Y., Ferdinand, J. R., & O'Shea, J. J. (2015). Mechanisms of Jak/STAT signaling in immunity and disease. The Journal of Immunology, 194(1), 21-27.

Vinci, M. C., Gambini, E., Bassetti, B., Genovese, S., & Pompilio, G. (2020). When good guys turn bad: bone marrow's and hematopoietic stem cells' role in the pathobiology of diabetic complications. International Journal of Molecular Sciences, 21(11), 3864.

Vinson, C., Chatterjee, R., & Fitzgerald, P. (2011). Transcription factor binding sites and other features in human and Drosophila proximal promoters. A Handbook of Transcription Factors, 205-222.

Volarevic, V., Al-Qahtani, A., Arsenijevic, N., Pajovic, S., & Lukic, M. L. (2010). Interleukin-1 receptor antagonist (IL-1Ra) and IL-1Ra producing mesenchymal stem cells as modulators of diabetogenesis. Autoimmunity, 43(4), 255-263.

Wacleche, V. S., Tremblay, C. L., Routy, J. P., & Ancuta, P. (2018). The biology of monocytes and dendritic cells: contribution to HIV pathogenesis. Viruses, 10(2), 65.

Wager, L., & Wormley, F. L. (2014). Classical versus alternative macrophage activation: the Ying and the Yang in host defense against pulmonary fungal infections. Mucosal immunology, 7(5), 1023-1035.

Wagner, R. J., Martin, K. A., Powell, R. J., & Rzucidlo, E. M. (2010). Lovastatin induces VSMC differentiation through inhibition of Rheb and mTOR. American Journal of Physiology-Cell Physiology, 299(1), C119-C127.

Walker, J. A., & McKenzie, A. N. (2018). TH2 cell development and function. Nature Reviews Immunology, 18(2), 121-133.

Walsh, M. J., Ali, L. R., Lenehan, P., Kureshi, C. T., Kureshi, R., Dougan, M., ... & Dougan, S. K. (2023). Blockade of innate inflammatory cytokines TNF α, IL-1 β, or IL-6 overcomes virotherapy-induced cancer equilibrium to promote tumor regression. Immunotherapy Advances, 3(1), ltad011.

Wang, F., Zhang, S., Jeon, R., Vuckovic, I., Jiang, X., Lerman, A., ... & Herrmann, J. (2018). Interferon gamma induces reversible metabolic reprogramming of M1 macrophages to sustain cell viability and pro-inflammatory activity. EBioMedicine, 30, 303-316.

Wang, L., Li, J., & Di, L. J. (2022). Glycogen synthesis and beyond, a comprehensive review of GSK3 as a key regulator of metabolic pathways and a therapeutic target for treating metabolic diseases. Medicinal Research Reviews, 42(2), 946-982.

Wang, X. F., Ye, Z. X., Chen, J. Y., Yang, S. L., & Wang, Y. F. (2018). Roles of Nitric Oxide Signaling Pathway in Atherosclerosis. Atheroscler Open Access, 3(120), 2.

Wang, Y. C., Hsieh, C. C., Kuo, H. F., Tsai, M. K., Yang, S. N., Kuo, C. H., ... & Hung, C. H. (2014). Effect of vitamin D3 on monocyte chemoattractant protein 1 production in monocytes and macrophages. Acta Cardiologica Sinica, 30(2), 144.

Wang, Y., Bai, Y., Qin, L., Zhang, P., Yi, T., Teesdale, S. A., ... & Tellides, G. (2007). Interferon-γ induces human vascular smooth muscle cell proliferation and intimal expansion by phosphatidylinositol 3-kinase–dependent mammalian target of rapamycin raptor complex 1 activation. Circulation research, 101(6), 560-569.

Wang, Y., Nunna, B. B., Talukder, N., Etienne, E. E., & Lee, E. S. (2021). Blood plasma self-separation technologies during the self-driven flow in microfluidic platforms. Bioengineering, 8(7), 94.

Wang, Y., Yan, X., Mi, S., Li, Z., Wang, Y., Zhu, H., ... & Ge, J. (2017). Naoxintong attenuates Ischaemia/reperfusion injury through inhibiting NLRP 3 inflammasome activation. Journal of Cellular and Molecular Medicine, 21(1), 4-12.

Watson, K. E., Peters Harmel, A. L., & Matson, G. (2003). Atherosclerosis in type 2 diabetes mellitus: the role of insulin resistance. Journal of cardiovascular pharmacology and therapeutics, 8(4), 253-260.

Weathington, N. M., Kanth, S. M., Gong, Q., Londino, J., Hoji, A., Rojas, M., ... & Mallampalli, R. K. (2017). IL-4 induces IL17Rb gene transcription in monocytic cells with coordinate autocrine IL-25 signaling. American journal of respiratory cell and molecular biology, 57(3), 346-354.

WHO, 2021. https://www.who.int/news-room/fact-sheets/detail/cardiovascular-diseases-(cvds)

Wiejak, J., Murphy, F. A., Maffia, P., & Yarwood, S. J. (2023). Vascular smooth muscle cells enhance immune/vascular interplay in a 3-cell model of vascular inflammation. Scientific Reports, 13(1), 15889.

Wilkinson, A. C., & Göttgens, B. (2013). Transcriptional regulation of haematopoietic stem cells. Transcriptional and Translational Regulation of Stem Cells, 187-212.

Willerson, J. T., & Ridker, P. M. (2004). Inflammation as a cardiovascular risk factor. Circulation, 109(21_suppl_1), II-2.

Williams, H. J., Fisher, E. A., & Greaves, D. R. (2012). Macrophage differentiation and function in atherosclerosis: opportunities for therapeutic intervention?. Journal of innate immunity, 4(5-6), 498-508.

Williams, M. L., Menon, G. K., & Hanley, K. P. (1992). HMG-CoA reductase inhibitors perturb fatty acid metabolism and induce peroxisomes in keratinocytes. Journal of lipid research, 33(2), 193-208.

Willows, J. W., Blaszkiewicz, M., & Townsend, K. L. (2022). A clearing-free protocol for imaging intact whole adipose tissue innervation in mice. STAR protocols, 3(1), 101109

Wissinger, E., & London, I. C. (2017). CD8+ T cells. British Society for Immunology| Bite-Sized Immunology. Br. Soc. Immunol.

Wolf, A. A., Yáñez, A., Barman, P., & Goodridge, H. S. (2019). The ontogeny of monocyte subsets. Frontiers in immunology, 10, 1642Yang, V. W. (1998). Eukaryotic transcription factors: identification, characterization and functions. The Journal of nutrition, 128(11), 2045-2051.

Wu, J., Huang, Y., Zhou, X., Xiang, Z., Yang, Z., Meng, D., ... & Yang, J. (2022). ATF3 and its emerging role in atherosclerosis: a narrative review. Cardiovascular Diagnosis and Therapy, 12(6), 926.

Wu, Z., Zheng, Y., Sheng, J., Han, Y., Yang, Y., Pan, H., & Yao, J. (2022). CD3+ CD4-CD8-(Double-negative) T cells in inflammation, immune disorders and cancer. Frontiers in Immunology, 13, 816005.

Xia, C., Rao, X., & Zhong, J. (2017). Role of T lymphocytes in type 2 diabetes and diabetes-associated inflammation. Journal of diabetes research, 2017.

Xiang, M., Zhou, L., Peng, Y. W., Eddy, R. L., Shows, T. B., & Nathans, J. (1993). Brn-3b: a POU domain gene expressed in a subset of retinal ganglion cells. Neuron, 11(4), 689-701.

Xiang, M., Zhou, L., Macke, J. P., Yoshioka, T., Hendry, S. H., Eddy, R. L., ... & Nathans, J. (1995). The Brn-3 family of POU-domain factors: primary structure, binding specificity, and expression in subsets of retinal ganglion cells and somatosensory neurons. Journal of Neuroscience, 15(7), 4762-4785.

Xin, Y., Zhang, Z., Lv, S., Xu, S., Liu, A., Li, H., ... & Liu, Y. (2024). Elucidating VSMC phenotypic transition mechanisms to bridge insights into cardiovascular disease implications. Frontiers in Cardiovascular Medicine, 11, 1400780.

Xiong, J., Parker, B. L., & Yankee, T. M. (2014). The combined loss of Gads and CD127 reveals a novel function of Gads prior to TCRβ expression. Immunologic research, 60, 77-84.

Xu, Y. (2014). Transcriptional regulation of endothelial dysfunction in atherosclerosis: an epigenetic perspective. Journal of biomedical research, 28(1), 47.

Yan, Z. Q., & Hansson, G. K. (2007). Innate immunity, macrophage activation, and atherosclerosis. Immunological reviews, 219(1), 187-203.

Yáñez, A., Coetzee, S. G., Olsson, A., Muench, D. E., Berman, B. P., Hazelett, D. J., ... & Goodridge, H. S. (2017). Granulocyte-monocyte progenitors and monocyte-dendritic cell progenitors independently produce functionally distinct monocytes. Immunity, 47(5), 890-902.

Yang, J., Park, Y., Zhang, H., Gao, X., Wilson, E., Zimmer, W., ... & Zhang, C. (2009). Role of MCP-1 in tumor necrosis factor-α-induced endothelial dysfunction in type 2 diabetic mice. American Journal of Physiology-Heart and Circulatory Physiology, 297(4), H1208-H1216.

Yang, J., Zhan, X. Z., Malola, J., Li, Z. Y., Pawar, J. S., Zhang, H. T., & Zha, Z. G. (2020). The multiple roles of Thy-1 in cell differentiation and regeneration. Differentiation, 113, 38-48.

Yang, J., Zhang, L., Yu, C., Yang, X. F., & Wang, H. (2014). Monocyte and macrophage differentiation: circulation inflammatory monocyte as biomarker for inflammatory diseases. Biomarker research, 2(1), 1-9.

Yang, X., Liu, S., & Yan, Q. (2013). Role of fucosyltransferase IV in epithelial–mesenchymal transition in breast cancer cells. Cell death & disease, 4(7), e735-e735.

Yao, B. C., Meng, L. B., Hao, M. L., Zhang, Y. M., Gong, T., & Guo, Z. G. (2019). Chronic stress: a critical risk factor for atherosclerosis. Journal of International Medical Research, 47(4), 1429-1440.

Yi, P., Cao, P., Yang, M., Xiong, F., Jiang, J., Mei, Y., ... & Lu, Q. (2023). Overexpressed CD44 is associated with B-cell activation *via* the HA-CD44-AIM2 pathway in lupus B cells. Clinical Immunology, 255, 109710.

Ying, W., Cheruku, P. S., Bazer, F. W., Safe, S. H., & Zhou, B. (2013). Investigation of macrophage polarization using bone marrow derived macrophages. JoVE (Journal of Visualized Experiments), (76), e50323.

Yoganathan, K., Yan, A., Rocha, J., Trotman-Grant, A., Mohtashami, M., Wells, L., ... & Anderson, M. K. (2022). Regulation of the signal-dependent e protein HEBAlt through a YYY motif is required for progression through T cell development. Frontiers in Immunology, 13, 848577.

Yogendran, V., Mele, L., Prysyazhna, O., & Budhram-Mahadeo, V. S. (2023). Vascular dysfunction caused by loss of Brn-3b/POU4F2 transcription factor in aortic vascular smooth muscle cells is linked to deregulation of calcium signalling pathways. Cell Death & Disease, 14(11), 770.

Young, C., & Brink, R. (2021). The unique biology of germinal center B cells. Immunity, 54(8), 1652-1664.

Yu, H., Lin, L., Zhang, Z., Zhang, H., & Hu, H. (2020). Targeting NF-κB pathway for the therapy of diseases: mechanism and clinical study. Signal transduction and targeted therapy, 5(1), 209.

Yu, K. C. W., Chen, W., & Cooper, A. D. (2001). LDL receptor–related protein mediates cell-surface clustering and hepatic sequestration of chylomicron remnants in LDLR-deficient mice. The Journal of clinical investigation, 107(11), 1387-1394.

Yu, Y. R. A., O'Koren, E. G., Hotten, D. F., Kan, M. J., Kopin, D., Nelson, E. R., ... & Gunn, M. D. (2016). A protocol for the comprehensive flow cytometric analysis of immune cells in normal and inflamed murine non-lymphoid tissues. PloS one, 11(3), e0150606.

Yuan, S. M., & Wu, N. (2018). Aortic α-smooth muscle actin expressions in aortic disorders and coronary artery disease: An immunohistochemical study. Anatolian Journal of Cardiology/Anadolu Kardiyoloji Dergisi, 19(1).

Yuan, T., Yang, T., Chen, H., Fu, D., Hu, Y., Wang, J., ... & Xie, X. (2019). New insights into oxidative stress and inflammation during diabetes mellitus-accelerated atherosclerosis. Redox biology, 20, 247-260.

Yuan, X., Mitsis, A., & Nienaber, C. A. (2022). Current understanding of aortic dissection. Life, 12(10), 1606.

Zanoli, L., Briet, M., Empana, J. P., Cunha, P. G., Mäki-Petäjä, K. M., Protogerou, A. D., ... & Boutouyrie, P. (2020). Vascular consequences of inflammation: a position statement from the ESH Working Group on Vascular Structure and Function and the ARTERY Society. Journal of hypertension, 38(9), 1682-1698.

Zaqout, S., Becker, L. L., & Kaindl, A. M. (2020). Immunofluorescence staining of paraffin sections step by step. Frontiers in neuroanatomy, 14, 582218.

Zernecke, A., Winkels, H., Cochain, C., Williams, J. W., Wolf, D., Soehnlein, O., ... & Ley, K. (2020). Meta-analysis of leukocyte diversity in atherosclerotic mouse aortas. Circulation research, 127(3), 402-426.

Zhang, B., Yang, Y., Yi, J., Zhao, Z., & Ye, R. (2021). Hyperglycemia modulates M1/M2 macrophage polarization *via* reactive oxygen species overproduction in ligature - induced periodontitis. Journal of Periodontal Research, 56(5), 991-1005.

Zhang, D. D., Song, Y., Kong, P., Xu, X., Gao, Y. K., Dou, Y. Q., ... & Han, M. (2021). Smooth muscle 22 alpha protein inhibits VSMC foam cell formation by supporting normal LXRα signaling, ameliorating atherosclerosis. Cell Death & Disease, 12(11), 982.

Zhang, G., Zhang, H., Liu, Y., He, Y., Wang, W., Du, Y., ... & Gao, F. (2014). CD44 clustering is involved in monocyte differentiation. Acta Biochim Biophys Sin, 46(7), 540-547.

Zhang, H., Park, Y., Wu, J., Chen, X. P., Lee, S., Yang, J., ... & Zhang, C. (2009). Role of TNF-α in vascular dysfunction. Clinical science, 116(3), 219-230.

Zhang, J. (2007). Yin and yang interplay of IFN-γ in inflammation and autoimmune disease. The Journal of clinical investigation, 117(4), 871-873.

Zhang, J. M., & An, J. (2007). Cytokines, inflammation, and pain. International anesthesiology clinics, 45(2), 27-37.

Zhang, Y., Carreras, D., & de Bold, A. J. (2003). Discoordinate re-expression of cardiac fetal genes in N ω-nitro-l-arginine methyl ester (l-NAME) hypertension. Cardiovascular research, 57(1), 158-167.

Zhang, Y., Yang, X., Bian, F., Wu, P., Xing, S., Xu, G., ... & Wu, D. (2014). TNF-α promotes early atherosclerosis by increasing transcytosis of LDL across endothelial cells: crosstalk between NF-κB and PPAR-γ. Journal of molecular and cellular cardiology, 72, 85-94.

Zhao, E., Xu, H., Wang, L., Kryczek, I., Wu, K., Hu, Y., ... & Zou, W. (2012). Bone marrow and the control of immunity. Cellular & molecular immunology, 9(1), 11-19.

Zhao, S. L., Mo, Z. H., He, H. H., Zhao, L. L., & Xie, Y. H. (2018). Imbalance of T-helper 1/T-helper 2 cytokines and impaired glucose tolerance among patient with acute coronary syndrome. Journal of Cancer Research and Therapeutics, 14(9), 480.

Zheng, W., Du, J., Mary, V. R., Anna, N., & Rong, L. (2023). Lineage tracking to reveal the fate of hematopoietic stem cells influenced by Flk2− multipotent progenitors after transplantation. Experimental and Molecular Medicine, 55, 1-10.

Zhou, H., Li, N., Yuan, Y., Jin, Y. G., Guo, H., Deng, W., & Tang, Q. Z. (2018). Activating transcription factor 3 in cardiovascular diseases: a potential therapeutic target. Basic research in cardiology, 113, 1-13.

Zhou, X., Jiang, Y., Lu, L., Ding, Q., Jiao, Z., Zhou, Y., ... & Chou, K. Y. (2007). MHC class II transactivator represses human IL - 4 gene transcription by interruption of promoter binding with CBP/p300, STAT6 and NFAT1 *via* histone hypoacetylation. Immunology, 122(4), 476-485.

Zhou, Y., Yoshida, S., Kubo, Y., Yoshimura, T., Kobayashi, Y., Nakama, T., ... & Ishibashi, T. (2017). Different distributions of M1 and M2 macrophages in a

mouse model of laser-induced choroidal neovascularization. Molecular medicine reports, 15(6), 3949-3956.

Zhou, Y., Zhang, Y., Han, J., Yang, M., Zhu, J., & Jin, T. (2020). Transitional B cells involved in autoimmunity and their impact on neuroimmunological diseases. Journal of translational medicine, 18(1), 131.

Zhao, Y., Xiong, W., Li, C., Zhao, R., Lu, H., Song, S., ... & Ge, J. (2023). Hypoxia-induced signaling in the cardiovascular system: pathogenesis and therapeutic targets. Signal transduction and targeted therapy, 8(1), 431.

Zhu, X., & Zhu, J. (2020). CD4 T helper cell subsets and related human immunological disorders. International Journal of Molecular Sciences, 21(21), 8011.

(https://www.aatbio.com/resources/buffer-preparations-and-recipes/ack-lysis-buffer).

APPENDIX 1 – LIST OF MATERIALS NEEDED FOR THE EXPERIMENT AND THE SUPPLIERS.

Table 16: List of materials' suppliers and catalogue numbers used for the experiments in this project.

Materials	Supplier/provider	Catalog number
Cell culture		
RPMI 1640 Medium	Gibco	21875034
RPMI-1640 Medium	Sigma-Aldrich	R8758
Fetal Bovine Serum, qualified, heat inactivated, Brazil	Gibco	10500064
Penicillin-Streptomycin	Sigma-Aldrich	P4333
2-Mercapethanol	Gibco	21985023
HEPES buffer solution	Gibco	11560496
Sodium Pyruvate 100Mm	Gibco	12539059
D-Glucose Solution	Gibco	15384895
Cell lines		
THP-1 cells	Human monocytes were derived from acute leukaemia patients	
Jurkat cells	Human T lymphocytes were derived from T cell leukaemia patient	
Cytokine array		
V-PLEX Custom Mouse Biomarkers (1 plate)	Meso Scale Diagnostics (MSD) LLC	K152A0H-1

Proinflammatory Panel1 (mouse)		
Blocker™ BSA	ThermoFisher	37520
Western blotting		
PBS tablets	Gibco/Life Technologies	18912-014
Protein Ladder, Color Prestained Protein Standard, Broad Range (10-250 kDa)	New England Biolabs	P7719
30% Acrylamide/Bis Solution	Bio-Rad	1610156
Ammonium persulfate	Honeywell	215589
TEMED	Bio-Rad	1610800
Tween 20	Sigma-Aldrich	T8787
Pierce BCA Protein Assay Kit	ThermoFisher	23225
Nonfat dried milk powder	ITW Reagents	A0830
Goat Anti-Rabbit Immunoglobulins/HRP (affinity isolated)	Agilent Dako	P0448
Goat Anti-Mouse Immunoglobulins/HRP (affinity isolated)	Agilent Dako	P0447
Clarity Western ECL Substrate	Bio-Rad	1705061
Flow cytometry		
EDTA (0.5 M), pH 8.0, RNase-free	Invitrogen	AM9260G

Paraformaldehyde Solution, 4% in PBS	ThermoScientific Chemicals	J19943.K2
LIVE/DEAD™ Fixable Blue Dead Cell Stain Kit, for UV excitation	Invitrogen	L23105
ACK Lysing Buffer	Gibco	A1049201
Accustain Solution	Nano Enstek	ADK-1000
Accuchip 4X	Nano Enstek	AD4K-200
Ammonium Chloride	BDH	10017
Ethylenediaminetetraacetic acid disodium salt dihydrate (EDTA)	Sigma-Aldrich	E5513
Potassium Hydrogen Carbonate	BDH	10206
Immunofluorescence		
DAPI	Sigma Aldrich	D9542-1MG
CD11b Monoclonal Antibody (M1/70.15)	Invitrogen	MA1-80091
CD3 Monoclonal Antibody (17A2),	eBioscience™	14-0032-82
CD45R (B220) Monoclonal Antibody (RA3-6B2)	eBioscience™	14-0452-82
CD44 Monoclonal Antibody (IM7)	eBioscience™	14-0441-82
Brn-3b Polyclonal Antibody	BIOSS	BS-6985R
Anti-alpha smooth muscle Actin antibody [1A4]	Abcam	ab7817
Anti-TAGLN/Transgelin antibody (SM22)	Abcam	ab14106

Ki67/MKI67 Antibody - BSA Free	Novus Biological	NB110-89717
Goat anti-Rat IgG (H+L) Cross-Adsorbed Secondary Antibody, Alexa Fluor™ 488	Invitrogen	A-11006
Goat anti-Rat IgG (H+L) Cross-Adsorbed Secondary Antibody, Alexa Fluor™ 647	Invitrogen	A-21247
Goat anti-Rabbit IgG (H+L) Highly Cross-Adsorbed Secondary Antibody, Alexa Fluor 555	Invitrogen	A-21429
Goat anti-Mouse IgG (H+L) Cross-Adsorbed Secondary Antibody, Rhodamine Red™-X	ThermoScientific Chemicals	R6393
MTT assay		
Thiazolyl Blue Tetrazolium Bromide	Sigma-Aldrich	M5655-100MG
Corning® 250 mL DMSO (Dimethyl Sulfoxide)	Corning	25-950-CQC
Genotyping PCR		
DirectPCR Lysis Reagent (Mouse Tail)	VIAGEN Biotech	102-T
Proteinase K Solution	meridian BIOSCIENCE	BIO-37084
UltraPure™ DNase/RNase-Free Distilled Water	Invitrogen™	11538646
UltraPure Agarose	Invitrogen™	16500500

Brn3-b primers (150bp)	Forward primer: 5’ GAGAGAGCGCTCACAATTCC 3’ Reverse primer: 5’ ATGGTGGTGGTGGCTCTTAC 3’	
Neomycin primers (250bp)	Forward primer: 5’ AGACAATCGGCTGCTCTGAT 3’ Reverse primer: 5’ ATACTTTCTCGGCAGGAGCA 3’	
Antibodies		
Brn-3b Rabbit Anti-POU Class 4 Homeobox 2 antibody, Polyclonal	Biobyt	orb576708
GAPDH	Santa Cruz	sc-32233
BD Horizon™ BV421 Rat Anti-Mouse CD44	BD Bioscience	563970
BD Horizon BUV395 rat anti-mouse CD4 (clone GK1 5)	BD Bioscience	563790
BD horizon BV786 rat anti-mouse CD8a (clone:53-6.7)	BD Bioscience	563332
Brilliant Violet 711™ anti-mouse/human CD11b Antibody	BioLegend	101241
CD45R (B220) Monoclonal Antibody (RA3-6B2), eBioscience™	ThermoScientific Chemicals	14-0452-82

Alexa Fluor® 488 anti-mouse/human CD45R/B220 Antibody	BioLegend	103225
Mouse CD90/ Thy-1 Alexa Fluor® 647-conjugated Antibody	R&D System	FAB7335R
PE anti-mouse CD25 Antibody	BioLegend	101904
APC anti-mouse TCR β chain Recombinant Antibody	BioLegend	159708
Brilliant Violet 711™ anti-mouse CD117 (cKIT) Antibody	BioLegend	105841
PE/Cyanine7 anti-mouse CD90.2 (Thy-1.2) Antibody	BioLegend	140310
FITC anti-mouse CD24 Antibody	BioLegend	101805
PE anti-mouse CD25 Antibody	BioLegend	101904
BD Pharmingen™ Purified Rat Anti-Mouse CD16/CD32 (Mouse BD Fc Block™)	BD Bioscience	553141

APPENDIX 2 – VALIDATION OF BRN-3B KO TISSUES

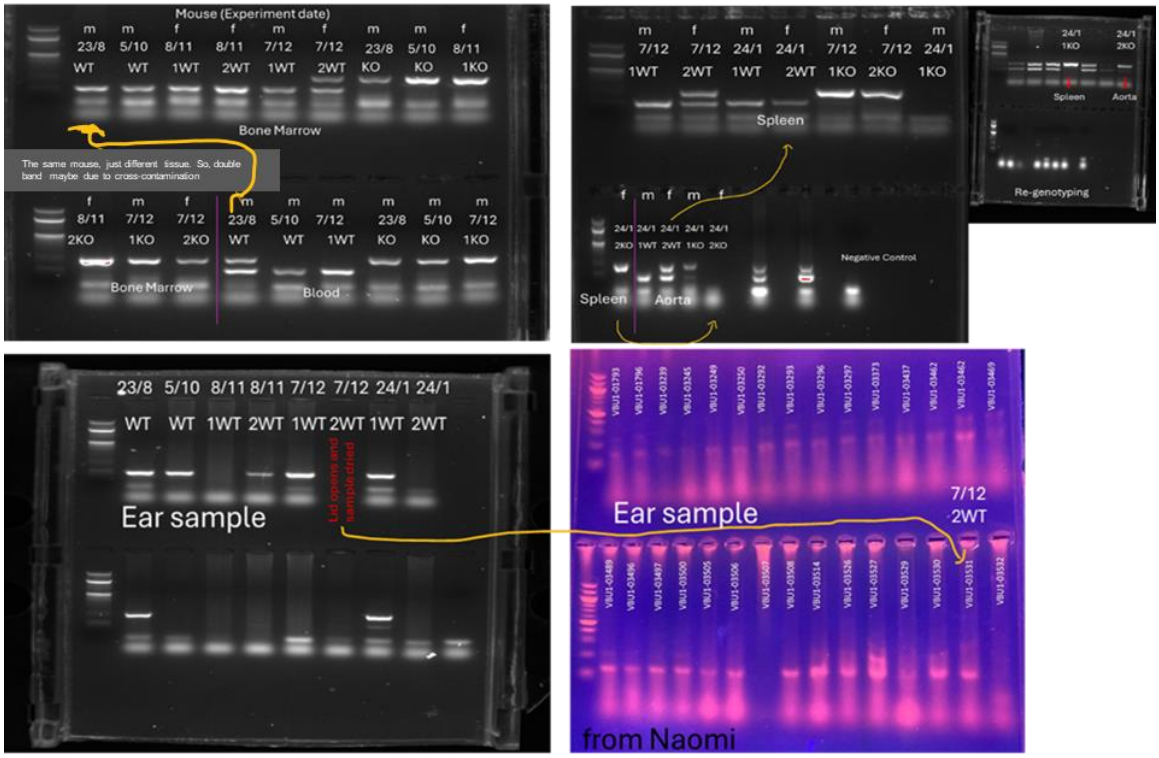

Figure 89: The PCR gel electrophoresis images. The genotyping of the mouse has been conducted before the experiment and validating the Brn-3b KO after the experiments. The PCR genotyping has been conducted to screen the mouse phenotype using ear sample by the lab member. The confirmation of the samples including bone marrow, blood, spleen aorta and ear samples has been conducted after the experiments. Some of the WT sample from the same mouse expressing the neomycin cassette band due to the sample spill over/cross contamination between nearby well. However, this cross-contamination has been confirmed by comparing the sample genotype with the other tissue from the same mouse and referring based on the ear sample genotyping result. (m = male, f = female, WT = Wild Type, KO = Knock-out).

APPENDIX 3 – EXAMPLE OF PROTEIN MARKERS EXPRESSION

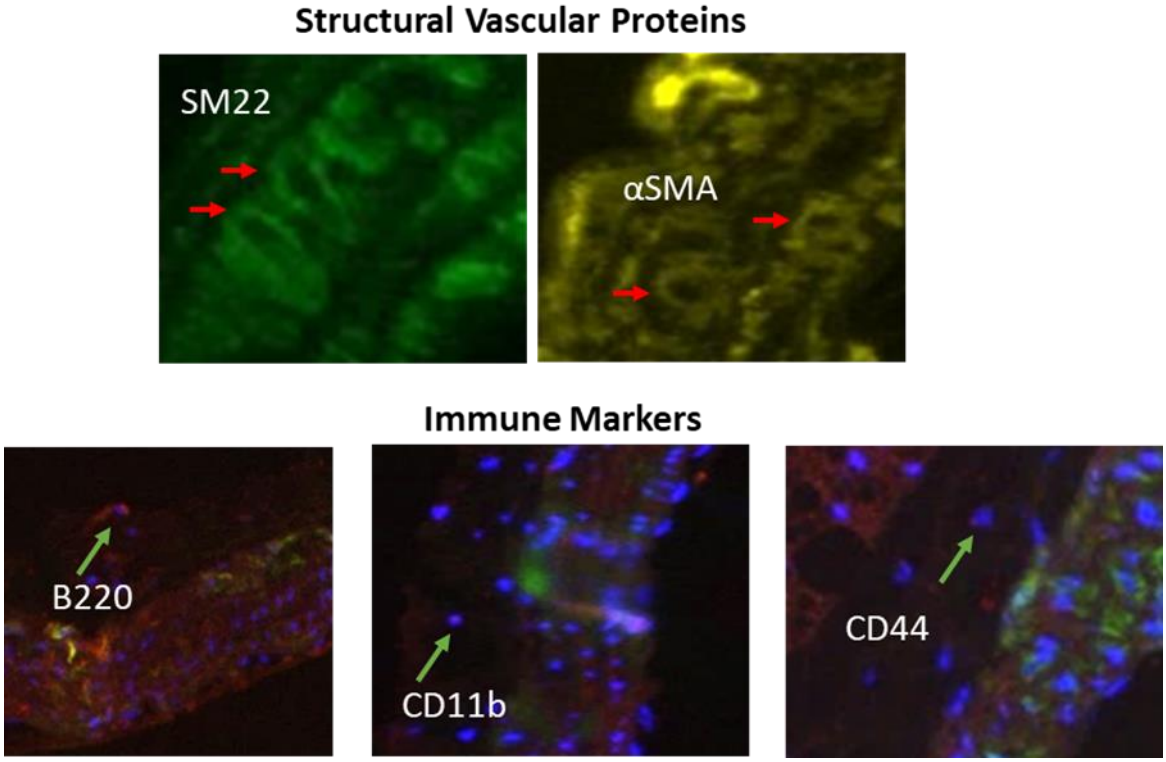

Figure 90: The expression signal of SM22, αSMA, B220, CD11b and CD44 markers. The example of the fluorescent expression signal of structural vascular protein (Smooth Muscle -22 (SM22) and alpha- Smooth Muscle Actin (αSMA)), and immune marker (CD45R/B220 (B220), CD11b) and immune/Mesenchymal like-CD44 in the longitudinal cut section of aorta. These signals were detected by QuPath software following the subtraction of the background threshold signal.

APPENDIX 4 – REGION OF INTEREST (ROI) FOR AORTIC WALL

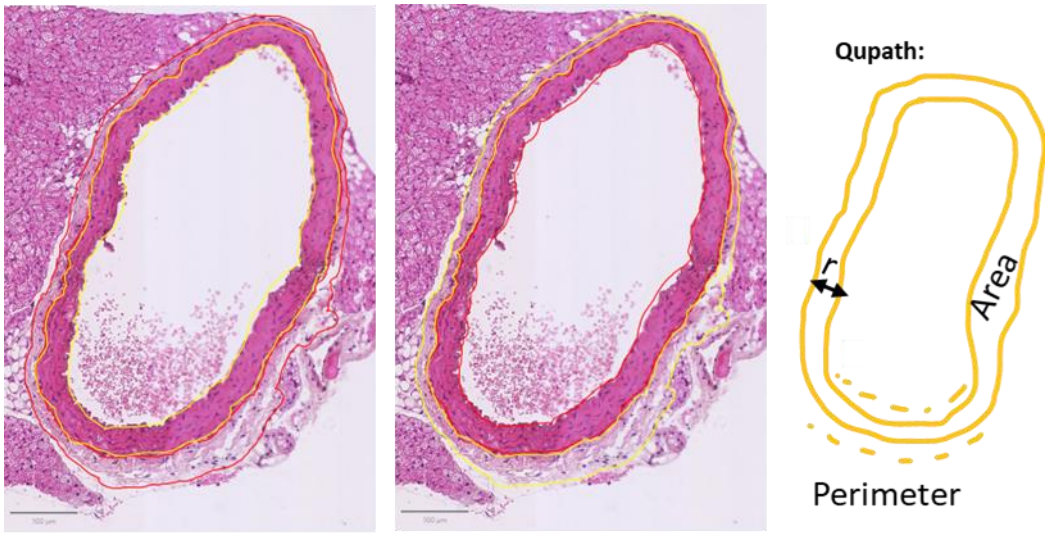

Figure 91: Region of Interest (ROI) for aortic wall drawn for analysis. The ROI of Tunica Media (TM) and Tunica Intima (TI), and Tunica Adventitia (TA) was drawn using the annotation (**in yellow**) in Qupath 0.4.3 software. The approximate aortic wall thickness (r) TI, TM and TA were measured by dividing the TI and TM area or TA area by the average of the inner and outer contour lengths (perimeter). The area and perimeter of the aortic wall and TA were automatically generated by QuPath software (Galaska et al., 2023).